Spectroscopic Investigations of Oligopeptides from Aquatic Cyanobacteria

Characterisation of New Oligopeptides, Development of Microcystin Quantification Tools and Investigations into Microcystin Production

A thesis

submitted in fulfilment

of the requirements for the degree

of

Doctor of Philosophy in Chemistry

at

The University of Waikato

by

Jonathan Puddick

THE UNIVERSITY OF
WAIKATO
Te Whare Wānanga o Waikato

2013

Abstract

Cyanobacteria (blue-green algae) are a group of ancient prokaryotic organisms which have become synonymous with water quality deterioration. An array of compounds is produced by aquatic cyanobacteria, the largest group being the oligopeptides. A major class of cyanobacterial oligopeptides are the microcystins; cyclic heptapeptides which contain the unique amino acid Adda (3-amino-9-methoxy-2,6,8-trimethyl-10-phenyldeca-4,6-dienoic acid). Due to their ability to inhibit protein phosphatases 1 and 2A and as they are concentrated in the liver, microcystins can be highly toxic to animals.

Anabaenopeptins are cyclic hexapeptides which contain a carbonyl-linked sidechain amino acid and a ring which is cyclised through the sidechain amine of the position two D-lysine. Matrix-assisted laser desorption/ionisation-time of flight mass spectrometry (MALDI-TOF MS) analysis of a cyanobacterial bloom sample from Lake Wiritoa (Manawatu, New Zealand) led to the identification of a new anabaenopeptin. The putative structure for anabaenopeptin 906 was constructed using tandem MS (MS/MS) data, in conjunction with the sequences of the known anabaenopeptins.

A *Microcystis* species (CYN06) isolated from Lake Hakanoa (Huntly, New Zealand) was investigated as it produced a large number of microcystin congeners. Liquid chromatography-MS/MS analysis was used to identify seventeen known microcystin congeners and to characterise ten new variants. Two of the new microcystins, MC-FA and MC-WA, were structurally characterised using amino acid analysis and nuclear magnetic resonance (NMR) spectroscopy. The other new congeners included MC-FAba, MC-WAba, MC-FL, MC-WL as well as [Asp^3] analogues of MC-FA, MC-WA, and [Asp^3] analogues of two known congeners; MC-RA and MC-RAba. A review of the number of microcystin congeners produced by reported cyanobacterial strains placed CYN06 in the upper ten percentile. However, CYN06 differed from the other strains as it showed relaxed substrate specificity at position two and four and simultaneously produced microcystin congeners which contained no arginine residues, one arginine residue and two arginine residues.

Abstract

Microcystis CYN06 also contained an unidentified microcystin with a mass of 1014.5 Da. Structural characterisation by NMR spectroscopy indicated that it was an analogue of MC-WA which contained *N*-formylkynurenine at position two. As *N*-formylkynurenine is a known oxidation product of tryptophan it was proposed that further unidentified microcystins from CYN06 contained two other oxidation products of tryptophan; kynurenine and oxindolyalanine. This is the first report of the presence of oxidised tryptophan residues in microcystins.

Analysis of a cyanobacterial hydroterrestrial mat sample collected from Miers Valley in Eastern Antarctica indicated the presence of fourteen new oligopeptides. A combination of MS/MS and amino acid analysis was used to characterise eight new microcystins which each contained a position one glycine. A recently-developed thiol derivatisation technique indicated that the position seven amino acid in each of the microcystins was very likely dehydrobutyrine. Different combinations of variable modifications at positions two, four and five resulted in eight unique structures. These included four microcystins with Adda moieties which possessed an *O*-acetyl group (ADMAdda) instead of the conventional C9 methoxy. As well as being the first report of microcystins containing a position one glycine, this is the first report of ADMAdda-containing microcystins in the southern hemisphere. The putative structures of six new Antarctic linear peptides were determined through a combination of mass spectrometric techniques. The compounds contained an N-terminus with the molecular formula $C_9H_{14}NO_2$ linked to isoleucine, two aromatic amino acids and an ester-linked hydroxyphenyllactic acid. The hydroxyphenyllactic acid C-terminus and the unidentified N-terminus suggest that these new compounds are a novel class of cyanobacterial oligopeptide.

Seven different sample preparation techniques for the quantitative analysis of microcystins by MALDI-TOF MS were assessed for signal reproducibility and sensitivity using a cost-effective internal standard (angiotensin I). The sensitivity of six of the preparations was acceptable, as was the reproducibility for two thin-layer preparations performed on a polished steel target. Both thin-layer preparations could be used with a MALDI-TOF mass spectrometer which automatically acquires data. The thin-layer-spot preparation could also be used in an automated sample preparation work-flow. Further investigation using this

preparation demonstrated that linear quantification of three different microcystin congeners ([Dha^7] MC-LR, MC-RR and MC-YR) was possible. Use of this MALDI sample preparation will allow large numbers of microcystin-containing samples to be analysed rapidly and at low cost.

A batch culture experiment using *Microcystis* CYN06 exhibited a decreased abundance of arginine-containing microcystins as nitrate concentrations decreased. Linear regression of the relationship between $\log_{10}$ microcystin content and nitrate concentration revealed slopes which were dependent upon the number of arginine residues present in the compound. During this experiment the abundance of congeners with a single arginine residue at position two did not change ($p > 0.05$), whilst the abundance of the congeners with a position four arginine decreased significantly ($p \leq 0.001$). This suggests that there could be an element of selectivity in regards to which arginine in the microcystin structure is modulated and could explain why congener modulation in response to nitrogen concentration has not been observed previously. Whilst it was not proven that nitrogen supply was the causative factor for the congener modulation, the results from this experiment warrant further study in this area.

This research has significantly expanded our knowledge of oligopeptide diversity, improved an existing method of quantifying microcystins and shed new light on the regulation of the abundance of microcystin congeners. The identification of eighteen new microcystins is a 16% increase upon the 111 presently characterised. Also reported was the identification of nine oxidised analogues of tryptophan-containing microcystins from *Microcystis* CYN06. The presence of oxidised Trp residues in microcystins has not been reported previously and will allow researchers working with samples of Trp-containing microcystins to now assign the oxidised analogues. Seven new cyanobacterial oligopeptides were characterised during this study, six of which may belong to a novel class of linear peptides. A sample preparation designed for the quantification of microcystins by MALDI-TOF MS gave comparative performance to the previously reported method but was compatible with automated high-throughput sample preparation and data acquisition. For the first time, a culturing experiment showed a relationship between the abundance of arginine-containing microcystins and nitrogen supply.

Acknowledgements

First and foremostly, I would like to thank my supervisors Dr. Michèle Prinsep, Prof. David Hamilton and Prof. Craig Cary. Also, huge thanks go to Dr. Susie Wood from the Cawthron Institute, who has worked closely with me on all of my research and acted in the capacity of a supervisor. Thank you all for the inspiration, the advice, the direction and the benefit of your years of experience.

Thank you to the University of Waikato and the School of Science and Engineering for providing study grants to assist me in this endeavour. To the New Zealand Foundation for Research, Science and Technology (C01X0306), whose funding has contributed to portions of this research. And to Antarctica New Zealand for providing logistical support to other researchers who have provided me with samples from Antarctica.

To everyone from the Chemistry Department, thank you for the comradery, for the good times and for the hallway conversations which have led to breakthroughs (or otherwise). To my lab mates from the Natural Products Research Laboratory, thank you for putting up with my pedantic behaviours, for being fantastic company and for the shared trials. My immense gratitude goes out to Prof. Alistair Wilkins for his assistance with my NMR and to Assoc. Prof. Merilyn Manley-Harris for her sage advice with my HPLC. Thank you to the technical staff from the Department who are always happy to assist and to provide wisdom; Annie Barker, Steve Cameron, Pat Gread, Wendy Jackson, John Little, Jenny Stockdill and Amu Upreti. Special thanks to Wendy who has been my Mass Spec. companion for such a duration of time that the thought of not seeing you each day seems strange.

Thank you the staff and students in the Thermophile Research Unit, in particular the technical staff; Lynne Parker and Colin Monk. Thank you to Bruce Patty and Louise Stewart for their assistance with my nutrient analyses. Thank you to Dr. Charles Lee and Eric Bottos for collecting cyanobacterial samples during their Antarctic expeditions. And I’m extremely grateful to have wonderful friends in the Protein and Microbes, and the Molecular Genetics Laboratories who have

made me feel at home when visiting their labs and shared in some very good times over the years.

My research has relied heavily on the use of scientific instruments, to which I'm very grateful for the extremely skilled Instrument Support Team of Peter Jarman and Steve Hardy here at the University of Waikato. To Ken Jackson and Clive Seymour from Science Directions, thank you for going above and beyond to make sure our mass spectrometer problems are resolved. Similarly, thank you to Jan Streller, Matthias Pelzing and Matthais Keller from Bruker Daltonics for assisting with our trouble-shooting and method development.

To the unsung heroes in the office; Jacqui MacKenzie from Chemistry, Vicki Smith, Gloria Edwards and Gillian Dufty from Biology, thank you for taking care of all those behind-the-scenes jobs which keeps the research world turning.

Throughout this research I've been able to collaborate with some fantastic researchers who have been so giving of their time, knowledge and experience. Thank you to the entire staff at the Cawthron Institute for creating a wonderful environment where it is always a pleasure to visit. To the Phytoplankton and Biotoxin Laboratories, thank you for having me in your spaces during my visits. Thank you particularly to Janet Adamson, Andy Selwood, Dr. Pat Holland Dr. Doug Mountfort and Paul McNabb. Thank you to Barry Gilliland from Horizons Regional Council for collecting cyanobacterial blooms samples for my research. Thank you to Brent Copp and Jiayi Wang for assisting me with polarimetry for my compounds. Thank you to Dr. Chris Miles from the Norwegian Veterinary Institute and Prof. Frode Rise from the University of Oslo for collecting NMR data on MC-NfkA. I was especially lucky to be able to work with Chris, as our conversations and his insights have been invaluable for my research.

Something I've come to realise during my PhD is that conducting the research is only half of the job; presenting your research is just as important. So thank you to everyone who has attended my talks and supplied me with feedback to help improve my presentation skills. Thank you to Jenny Oldham, Susie and my

supervisors for all the proof reading of my writing and for the direction of how to develop each piece.

And to Eddie, my family and friends, thank you for the support you've given me during my PhD and for understanding why you haven't heard much from me during my writeup. Without that external network of support I would not have been able to make it through to the end.

Table of Contents

List of Figures

List of Figures

List of Tables

List of Appendices

List of Appendices

List of Abbreviations Used

HOAc	Acetic acid
ACN	Acetonitrile
ADMAdda	9-Acetoxy-3-amino-2,6,8-trimethyl-10-phenyldeca-4,6-dienoic acid
Ac	Acetyl
ACP	Acyl carrier protein
AT	Acyltransferase
ATP	Adenosine-5'-triphosphate
Ala	Alanine
CHCA	Alpha-cyano-hydroxycinnamic acid
AA	Amino acid
A	Aminoacyl adenylation domain
Aba	2-Aminobutanoic acid
Aib	2-Amino-*iso*-butanoic acid
Ahda	3-Amino-2-hydroxy-decanoic acid
Ahnya	3-Amino-2-hydroxy-non-8-ynoic acid
DMAdda	3-Amino-9-hydroxy-2,6,8-trimethyl-10-phenyldeca-4,6-dienoic acid
Adda	3-amino-9-methoxy-2,6,8-trimethyl-10-phenyldeca-4,6-dienoic acid
Apa	Aminopropanoic acid
AMT	Aminotransferase
NH_3	Ammonia
ANOVA	Analysis of variance
α	Angle of rotation
Arg	Arginine
Asp	Aspartic acid
b	Base(s)
KS	Beta-ketoacyl synthase
br	Broad signal
CO_2	Carbon dioxide
CO	Carbon monoxide
Choi	2-Carboxy-6-hydroxyoctahydroindole
c	Centi (10^{-2})
δ	Chemical shift

List of Abbreviations Used

ca.	Circa or approximately
CM	*C*-methyltransferase
R^2	Coefficient of determination
CV	Coefficient of variation
CoA	Coenzyme A
CID	Collision-induced dissociation
c	Concentration
C	Condensation domain
COSY	Correlation spectroscopy
J	Coupling constant
Da	Dalton(s)
°C	Degrees Celsius
K	Degrees Kelvin
Dha	Dehydroalanine
Dhb	Dehydrobutyrine
DH	Dehydrotase
DNA	Deoxyribonucleic acid
DCM	Dichloromethane
Δ	Difference
FFDNB	1,5-Difluoro-2,4-dinitrobenzene
FDAA	1-Difluoro-2,4-dinitrophenyl-5-alanine amide
FDLA	1-Difluoro-2,4-dinitrophenyl-5-leucine amide
DOI	Digital object identifier
DEPT	Distortionless enhancement by polarisation transfer
Ein	Einstein (one mole of photons)
Ω	Electrical resistance or ohm(s)
eV	Electronvolt(s)
ESI	Electrospray ionisation
ELISA	Enzyme-linked immunosorbent assay
EP	Epimerisation domain
Masp	Erythro-beta-methylaspartic acid
EtOH	Ethanol
EDTA	Ethylenediaminetetraacetic acid
f	Femto (10^{-15})
FA	Formic acid
Glu	Glutamic acid or glutamate
Gly	Glycine
m	Gradient of a linear regression equation
g	Gram(s)

$t_{½}$	Half-life
IC_{50}	Half-maximal inhibitory concentration
Hz	Hertz
HMBC	Heteronuclear multiple-bond correlation spectroscopy
HSQC	Heteronuclear single-quantum correlation spectroscopy
HPLC	High performance liquid chromatography
HRMS	High resolution mass spectrometry
Har	Homoarginine
Hil	Homoisoleucine
Hph	Homophenylalanine
Hty	Homotyrosine
h	Hour(s)
HCl	Hydrochloric acid
pH	Hydrogen ion concentration
HPLA	Hydroxyphenyllactic acid
CPAi	Inhibition of carboxypeptidase-A
CHYi	Inhibition of chymotrypsin
ELAi	Inhibition of elatase
TRPi	Inhibition of trypsin
PPi	Inhibition of protein phosphatases 1 & 2A
IS	Internal standard
Ile	Isoleucine
IPA	Isopropyl alcohol
KR	Ketoacyl reductase
k	Kilo (10^3)
Kyn	Kynurenine
Lan	Lanthionine
Leu	Leucine
LOQ	Limit of quantitation
LC	Liquid chromatography
L	Litre(s)
log	Logarithm
Lys	Lysine
MS	Mass spectrometry
m/z	Mass-to-charge ratio
MALDI	Matrix-assisted laser desorption/ionisation
max	Maximum
LD_{50}	Median lethal dose
M	Mega (10^6)

List of Abbreviations Used

m.p.	Melting point
MeOH	Methanol
CD_3OH	Methanol-d_3
CD_3OD	Methanol-d_4
Met	Methionine
MDL	Method detection limit
Mpla	Methoxyphenyllactic acid
Me	Methyl
MC	Microcystin
Mcy	Microcystin synthase enzyme
mcy	Microcystin synthase gene
min	Minute(s)
µ	Micro (10^{-6})
m	Milli (10^{-3}) or metre(s)
ε	Molar absorption coefficient
M	Molar or moles per litre
n	Nano (10^{-9})
NZ$	New Zealand dollars
Nfk	*N*-formylkynurenine
N/C	Nitrogen:carbon ratio
Mdha	*N*-methyldehydroalanine
NM	*N*-methyltransferase
NRPS	Non-ribosomal peptide synthetase
nd	Not detected
NMR	Nuclear magnetic resonance
C_{18}	Octadecyl carbon chain
OM	*O*-methyltransferase
1D	One-dimensional
Orn	Ornithine
Oia	Oxindolyalanine
ppm	Parts per million
PHR	Peak height ratio
Phe	Phenylalanine
PDA	Photo-diode array
PKS	Polyketide synthase
PSD	Post-source decay
PPIA	Protein phosphatase inhibition assay
RC	Racemase
Ref.	Reference(s)

rcf	Relative centrifugal force
M_r	Relative molecular mass
rNEc	Relaxation of norepine-induced contraction
RT	Retention time
rpm	Revolutions per minute
ROESY	Rotating-frame nuclear Overhauser effect spectroscopy
SAM	*S*-adenosyl-L-methionine
n	Sample size
s	Second(s)
Ser	Serine
s	Standard deviation
MS/MS	Tandem mass spectrometry
(H_4)Tyr	Tetrahydrotyrosine
TE	Thioesterase
TOF	Time of flight
TOCSY	Total correlation spectroscopy
NO_x	Total oxidised nitrogen species
TFA	Trifluoroacetic acid
Trp	Tryptophan
Tyr	Tyrosine
2D	Two-dimensional
UV	Ultraviolet
Val	Valine
vs.	Versus
V	Volt(s)
v/v	Volume per volume ratio
H_2O	Water
W	Watt
w/v	Weight per volume ratio
λ	Wavelength
b	*y*-intercept of a linear regression equation

CHAPTER 1

Introduction

1.1 CYANOBACTERIA

The phylum Cyanobacteria are a group of ancient prokaryotic organisms originating between three and four billion years ago.[1] They consist of oxygenic photosynthetic prokaryotes which harness energy from the sun using chlorophyll-*a* with water as the reductant.[2] Cyanobacteria primarily use carbon dioxide as a carbon source, making their need for nutrients minimal and consequently have been reported in a wide range of environments, including extreme habitats such as geothermal springs, desert soils and the Polar regions.[3]

The five orders of cyanobacteria; Chroococcales, Pleurocapsales, Stigonematales, Nostocales and Oscillatoriales, are distinguished by the physical characteristics shared by the members of each order. Chroococcales and Pleurocapsales are unicellular cyanobacteria which may form colonies (aggregates of cells held together by an exopolysaccharide secretion), but never form true filaments.[2,4] Whilst Chroococcales reproduce by binary fission, reproduction in Pleurocapsales occurs by multiple internal fissions.[2] Stigonematales are filaments with a sheath and truely branched trichomes which may produce heterocysts (pale cells specialised in nitrogen fixation which usually have a well differentiated cell wall) under certain conditions.[2,3] Cyanobacteria from the order Nostocales form filaments with a sheath and heterocysts, but without truely branched trichomes.[2] Oscillatoriales are arranged in the form of filaments without true-branching, heterocysts or akinetes (dormant cells with a thickened wall).[2,5]

Since the anthropogenic euthrophication of lakes, ponds and oceans, cyanobacteria have become synonymous with water quality issues.[4] Cyanobacterial blooms can cause foul tastes and odours,[6] but some species can also produce toxic secondary metabolites (cyanotoxins) which can be harmful to humans and animals (Table 1.1).

Table 1.1: Cyanotoxins produced by freshwater cyanobacteria.

Cyanotoxin	Primary Target in Mammals	Structural Characteristics	Reference
Anatoxin-a	Nerve synapse; Agonists of nicotinic acetylcholine receptors	Bicyclic secondary amine	7
Anatoxin-a(s)	Nerve synapse; Acetylcholinesterase inhibitors	Organophosphate alkaloid	7
Aplysiatoxins	Skin irritant; Carcinogen	Phenolic bislactone	8
Cylindrospermopsins	Liver; Protein synthesis inhibitors	Tricyclic alkaloid with attached uracil	9
Lipopolysaccharides	Irritant of all exposed tissue	Lipopolysaccharide	10
Microcystins	Liver; Protein phosphatase inhibitors	Cyclic heptapeptide	11
Nodularins	Liver; Protein phosphatase inhibitors	Cyclic pentapeptide	11
Saxitoxins	Nerve axon; Blockage of voltage-gated sodium channels	Tricyclic alkaloid	7

Adapted from Table 3.1 of Reference 12.

Aside from toxic compounds, a multitude of secondary metabolites have been reported from cyanobacteria which possess a diverse range of bioactivities.[13] The bioactivities of these metabolites have made them of interest to researchers as potential drug candidates and for other beneficial purposes. A high proportion of cyanobacterial compounds are wholly peptidic or possess peptidic substructures.[14] Cyanobacterial oligopeptides, in particular the microcystins (MCs), will be the focus of the remainder of this thesis.

1.2 FRESHWATER CYANOBACTERIAL OLIGOPEPTIDES

Freshwater cyanobacterial oligopeptides are structurally diverse with linear chains, rings, multiply cyclised rings, polyketide moieties and a plethora of structural modifications reported.[14] These oligopeptides have been shown, or are assumed, to be produced by large multi-enzyme complexes called non-ribosomal peptide synthetases (NRPS) or hybrid NRPS/polyketide synthases (PKS).[14] The eight major classes of freshwater cyanobacterial oligopeptides are reviewed in this section.

1.2.1 *Aeruginosins*

Aeruginosins are linear peptides containing four amino acids. As observed in aeruginosin 103-A (**1**),[15] they contain a hydroxyphenyllactic acid (Hpla) N-terminus, 2-carboxy-6-hydroxyoctahydroindole (Choi) in position three and an arginine derivative as the C-terminus. The position two amino acid varies, but is often in the D-configuration and, at times, can be glycosylated.[16] The position one Hpla can be acetylated,[17] brominated,[18] chlorinated[19] or sulphonated.[16,20] Chlorinated[16] and sulphonated[19] variants of Choi have also been observed. The C-terminus is always an arginine derivative which can take on a variety of structures.[15-20] Members of this class of cyanobacterial peptides are also referred to as microcins and spumigins.[14]

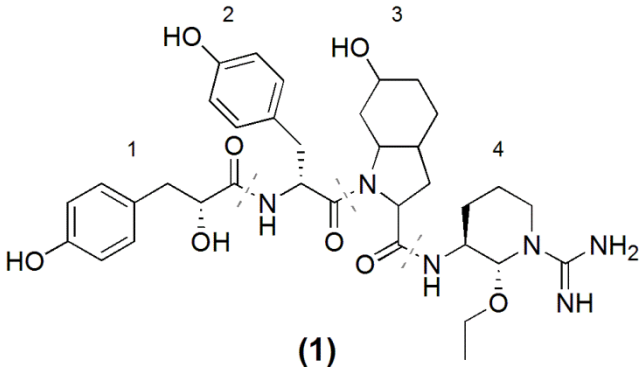

(1)

1.2.2 *Anabaenopeptins*

Anabaenopeptins are cyclic peptides containing six amino acids. As in anabaenopeptin A (**2**),[21] the ring is comprised of five amino acids and a D-lysine is always present in position two. The sidechain amine of the lysine forms a secondary peptide bond with the position five carboxyl group which encloses the ring. The lysine also has a ureido bond to a carbonyl-linked sidechain amino acid in position one. This carbonyl-linked sidechain and the ring amino acids vary, however, an aromatic amino acid has been consistently observed in position four and the position five amino acid is always *N*-methylated.[14] Members of this class of oligopeptides are also referred to as ferintoic acids, lyngbyaureidamides, oscillamides, nodulapeptins and schizpeptins.[14,22]

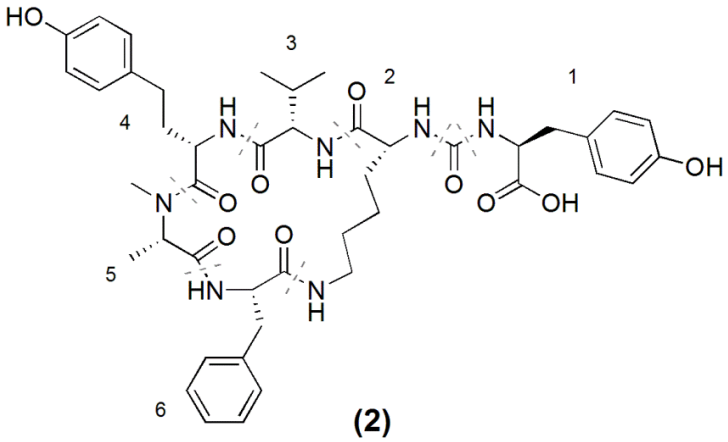

(2)

1.2.3 *Cyanopeptolins*

Cyanopeptolins are cyclic peptides with six ring amino acids and a sidechain of variable length. As observed in cyanopeptolin A (**3**),[23] the ring is cyclised by an ester bond between the sidechain hydroxyl of the position one threonine and the carboxyl group of the position six amino acid. Position three of the cyanopeptolins is always occupied by 3-amino-6-hydroxy-2-piperidone and an *N*-methylated aromatic amino acid is always present in position five. The position two amino acid is highly variable and a selection of structurally different amino acids have been incorporated.[14] The sidechain of the cyanopeptolins can contain Hpla, glyceric acid or an aliphatic fatty acid as the N-terminus. The N-terminus can be attached to either a single amino acid, a dipeptide chain, or directly to the position one amino acid. All of the amino acids in the cyanopeptolins are present in the L-configuration. The cyanopeptolins are referred to by many different synonyms including aeruginopeptin, microcystilide micropeptin, nostocyclin, oscillapeptin.[14]

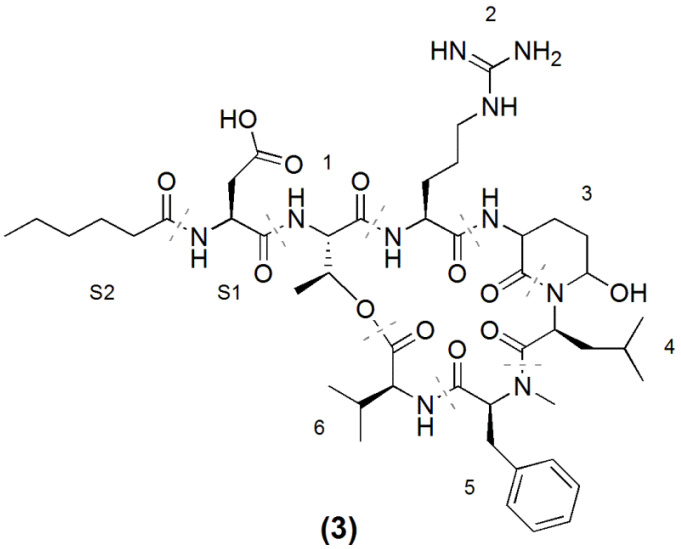

(3)

1.2.4 *Cyclamides*

The cyclamides are cyclic hexapeptides containing thiazole and oxazole moieties. As observed in aerucyclamide B (**4**),[24] each heterocycle unit (positions one, three and five) typically alternates with an amino acid (positions two, four and six). The thiazole and oxazole moieties are thought to be formed by dehydration and reduction of serine, threonine and cysteine residues.[14] This class of oligopeptides are also referred to as aerucyclamides, dendroamides, microcyclamides, nostocyclamides, raocyclamides, ulongamides, tenuecyclamides and westiellamides.[14]

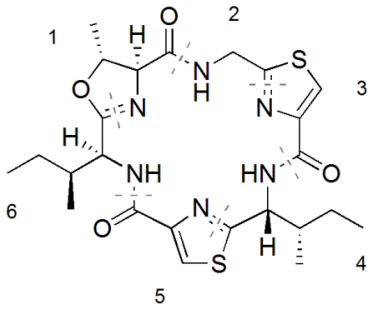

(4)

1.2.5 *Microginins*

Microginins are linear peptides containing four to six amino acids. As observed in microginin FR1 (**5**),[25] they contain a 3-amino-2-hydroxy-decanoic acid (Ahda) N-terminus, whilst the rest of the chain is comprised of more conventional amino acids. The Ahda in position one can be chlorinated[26] or *N*-methylated.[27] The position two amino acid is highly variable, whilst the positions four to six amino acids are often tyrosine related residues.[14] *N*-methylation of the positions three and four amino acids is commonly observed[14] and, at times, an additional tyrosine residue has been incorporated as a sixth amino acid.[26,27] The members of this class of cyanobacterial peptides have also been referred to as cyanostatins, oscillaginins and nostoginins.[14]

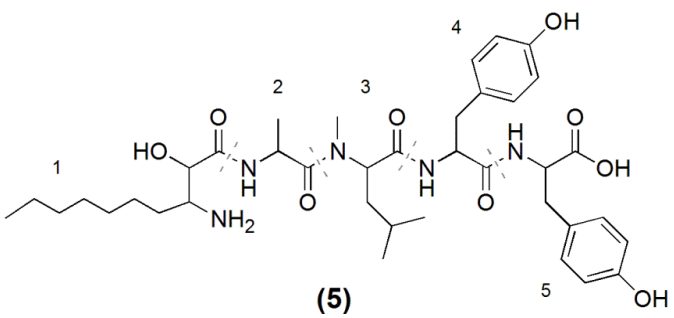

(5)

1.2.6 *Microviridins*

The microviridins are tricyclic peptides comprised of fourteen proteinogenic L-amino acids. As observed in microviridin A (**6**),[28] the primary sidechain consists of the positions one to three amino acids with an acetic acid N-terminus. The first ring is cyclised by an ester bond between the sidechain hydroxyl group of the position four threonine and the sidechain carboxylic acid of the position ten aspartic acid. The second ring is formed through another ester bond between the sidechains of the position nine serine and position twelve glutamic acid. The final ring is formed with a secondary peptide bond between the sidechain amine of the position six lysine and the sidechain carboxylic acid of the amino acid at position thirteen. The secondary sidechain consists of the position fourteen aromatic amino acid. Most of the structural variability in the microviridins is observed in the primary sidechain, where a variety of amino acids have been utilised.[14] Evidence suggests that microviridins are produced ribosomally as a pro-peptide and then processed by tailoring enzymes to form the tricyclic structure.[29,30] To date, no members of this class of cyanobacterial oligopeptide have been named under synonyms.[14]

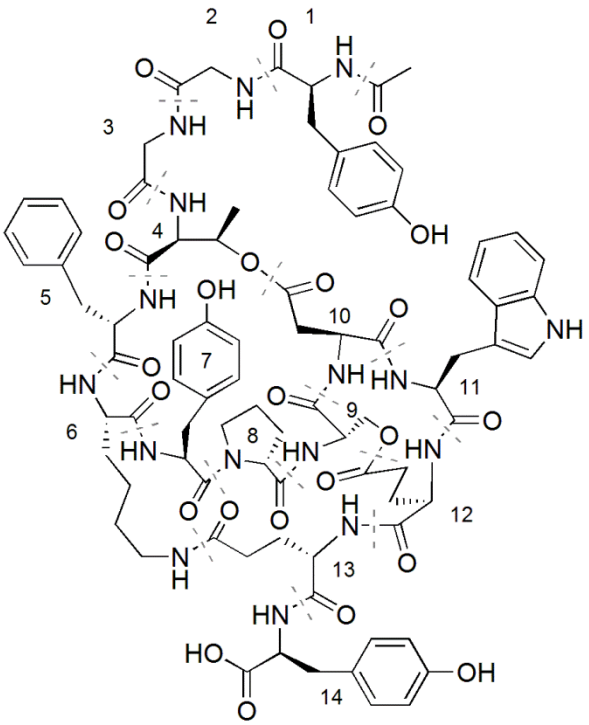

(6)

1.2.7 *Microcystins*

The microcystins are cyclic heptapeptides which can be toxic to terrestrial and aquatic animals. As observed in MC-LR (**7**),[31] position five of the microcystins is occupied by the β-amino acid, Adda (3-amino-9-methoxy-2,6,8-trimethyl-10-phenyldeca-4,6-dienoic acid). Microcystins generally contain two conventional D-amino acids in positions one and six, as well as D-erythro-β-methylaspartic acid (Masp) in position three. The positions two and four amino acids are occupied by variable L-amino acids, whilst position seven is often *N*-methyldehydroalanine (Mdha). The microcystins were originally called cyanoginosins,[31,32] however since the 1980s, no other synonyms have been used.

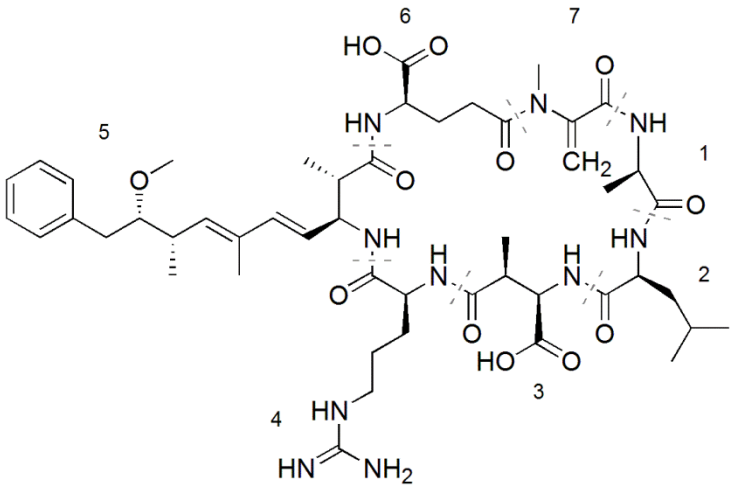

(7)

To date, there have been at least 111 different microcystin congeners characterised (**7**-**118**; Table 1.2 and Appendix A), mostly due to substitutions of the variable L-amino acids in positions two and four, although modifications have been reported for all of the amino acids.[33] Each microcystin congener is named according to the single letter code of the amino acids incorporated at positions two and four; for example, MC-LR contains leucine (L) in position two and arginine (R) in position four. Modifications of the other amino acids are included in brackets prior to the congener name; for example, the desmethyl-Mdha variant of MC-LR is named [Dha^{7}] MC-LR.

Table 1.2: Structures of the known microcystins.

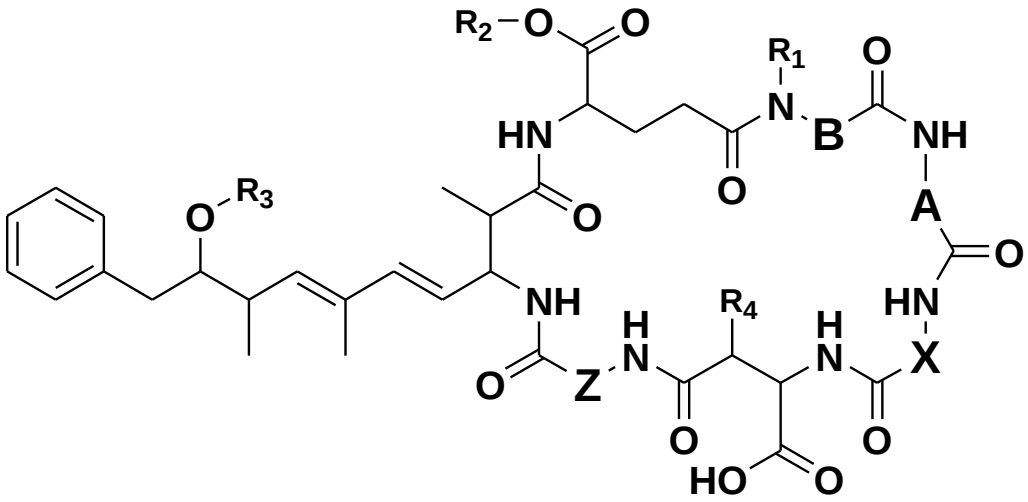

Compound	X	Z	A	B	R_1	R_2	R_3	R_4	Reference
7	Leu	Arg	Ala	Dha	CH_3	H	CH_3	CH_3	31
8	Leu	Ala	Ala	Dha	CH_3	H	CH_3	H	34
9	Leu	Ala	Ala	Dha	CH_3	H	CH_3	CH_3	32
10	Leu	Aba	Ala	Dha	CH_3	CH_3	CH_3	H	35
11	Leu	Aba	Ala	Dha	CH_3	H	CH_3	CH_3	36
12	Leu	Val	Ala	Dha	CH_3	H	CH_3	CH_3	37
13	Leu	Leu	Ala	Dha	CH_3	H	CH_3	H	34
14	Leu	Leu	Ala	Dha	CH_3	H	CH_3	CH_3	37
15	Ala	Arg	Ala	Dha	CH_3	H	CH_3	CH_3	38
16	Arg	Ala	Ala	Dha	CH_3	H	CH_3	CH_3	39
17	Tyr	Ala	Ala	Dha	CH_3	H	CH_3	CH_3	31
18	Ala	Har	Ala	Dha	CH_3	H	CH_3	CH_3	40
19	Arg	Aba	Ala	Dha	CH_3	H	CH_3	CH_3	41
20	Leu	Arg	Ala	Dha	H	H	CH_3	H	42
21	Glu	Glu(OMe)	Ala	Dha	H	H	CH_3	H	43
22	Leu	Met	Ala	Dha	CH_3	H	CH_3	CH_3	37
23	Leu	Phe	Ala	Dha	CH_3	H	CH_3	H	44
24	Val	Phe	Ala	Dha	CH_3	H	CH_3	CH_3	45
25	Leu	Tyr	Ala	Dha	H	H	CH_3	H	41
26	Tyr	Aba	Ala	Dha	CH_3	H	CH_3	CH_3	41
27	Val	Arg	Ala	Dha	CH_3	H	CH_3	CH_3	46
28	Arg	Val	Ala	Dha	CH_3	H	CH_3	CH_3	41
29	Arg	Apa	Ala	Dha	CH_3	H	CH_3	CH_3	41
30	Leu	Arg	Ala	Dha	CH_3	H	CH_3	H	47
31	Leu	Arg	Ala	Dhb	H	H	CH_3	H	48
32	Leu	Arg	Ala	Dha	CH_3	H	H	CH_3	38
33	Leu	Arg	Ala	Dha	H	H	CH_3	CH_3	42
34	Ala	Trp	Ala	Dha	CH_3	H	CH_3	CH_3	49
35	Glu	Glu(OMe)	Ala	Dha	H	H	CH_3	CH_3	43
36	Glu(OMe)	Glu(OMe)	Ala	Dha	H	H	CH_3	H	43
37	Leu	Phe	Ala	Dha	CH_3	H	CH_3	CH_3	37
38	Leu	Tyr	Ala	Dha	CH_3	H	CH_3	H	41
39	Hil	Arg	Ala	Dhb	H	H	CH_3	H	50
40	Leu	Arg	Ala	Dha	CH_3	CH_3	CH_3	H	51

Compound	X	Z	A	B	R_1	R_2	R_3	R_4	Reference
41	Arg	Leu	Ala	Dha	CH_3	H	CH_3	CH_3	41
42	Leu	Arg	Ala	Dha	CH_3	H	CH_3	CH_3	52
43	Glu(OMe)	Glu(OMe)	Ala	Dha	H	H	CH_3	CH_3	43
44	Leu	Arg	Ala	Ser	H	H	CH_3	CH_3	53
45	Hil	Tyr	Ala	Dha	CH_3	H	CH_3	H	41
46	Glu(OMe)	Glu(OMe)	Ala	Ser	H	H	CH_3	H	43
47	Glu	Glu(OMe)	Ala	Ser	H	H	CH_3	CH_3	43
48	Leu	Tyr	Ala	Dha	CH_3	H	CH_3	CH_3	45
49	Tyr	Leu	Ala	Dha	CH_3	H	CH_3	CH_3	35
50	Leu	Tyr	Ala	Ser	CH_3	H	CH_3	H	41
51	Leu	Arg	Ala	Dhb	H	H	$COCH_3$	H	54
52	Leu	Arg	Ala	Dha	CH_3	H	$COCH_3$	H	55
53	Leu	Arg	Ala	Dha	CH_3	CH_3	CH_3	CH_3	51
54	Leu	Arg	Ala	Dhb	CH_3	H	CH_3	CH_3	56
55	Hil	Arg	Ala	Dha	CH_3	H	CH_3	CH_3	57
56	Arg	Arg	Ala	Dha	H	H	CH_3	H	47
57	Leu	Trp	Ala	Dha	CH_3	H	CH_3	H	44
58	Leu	Arg	Ala	Ser	CH_3	H	CH_3	CH_3	38
59	Phe	Arg	Ala	Dha	CH_3	H	CH_3	H	58
60	Phe	Arg	Ala	Dha	H	H	CH_3	CH_3	59
61	Arg	Phe	Ala	Dha	CH_3	H	CH_3	H	41
62	Glu(OMe)	Glu(OMe)	Ala	Ser	H	H	CH_3	CH_3	43
63	Arg	Tyr	Ala	Dha	H	H	CH_3	H	41
64	Tyr	Met	Ala	Dha	CH_3	H	CH_3	CH_3	35
65	Leu	Har	Ala	Dha	CH_3	H	$COCH_3$	H	56
66	Leu	Arg	Ala	Dha	CH_3	H	$COCH_3$	CH_3	55
67	Arg	Arg	Ala	Dha	CH_3	H	CH_3	H	60
68	Arg	Arg	Ala	Dhb	H	H	CH_3	H	61
69	Arg	Arg	Ala	Dha	H	H	CH_3	CH_3	62
70	Leu	Trp	Ala	Dha	CH_3	H	CH_3	CH_3	45
71	Met(O)	Arg	Ala	Dha	CH_3	H	CH_3	CH_3	38
72	Phe	Arg	Ala	Dha	CH_3	H	CH_3	CH_3	38
73	Arg	Phe	Ala	Dha	CH_3	H	CH_3	CH_3	41
74	Hph	Arg	Ala	Dha	H	H	CH_3	CH_3	63
75	Tyr	Arg	Ala	Dha	CH_3	H	CH_3	H	64
76	Tyr	Arg	Ala	Dha	H	H	CH_3	CH_3	65
77	Hty	Arg	Ala	Dha	H	H	CH_3	H	63
78	Arg	Tyr	Ala	Dha	CH_3	H	CH_3	H	66
79	Arg	Tyr	Ala	Dha	H	H	CH_3	CH_3	41
80	Leu	Tyr(OMe)	Ala	Dha	CH_3	H	CH_3	CH_3	41
81	Tyr	Met(O)	Ala	Dha	CH_3	H	CH_3	CH_3	67
82	Leu	Arg	Leu	Dha	CH_3	H	CH_3	CH_3	68
83	Hil	Arg	Ala	Dha	CH_3	H	$COCH_3$	CH_3	69
84	Leu	Har	Ala	Dha	CH_3	H	$COCH_3$	CH_3	55
85	Arg	Arg	Ala	Dha	CH_3	H	CH_3	CH_3	70
86	Tyr	Tyr	Ala	Dha	CH_3	H	CH_3	H	41
87	Arg	Arg	Ala	Dha	CH_3	CH_3	CH_3	H	71
88	Arg	Arg	Ala	Dha	CH_3	H	CH_3	CH_3	52
89	Leu	Arg	Ser	Dha	CH_3	H	$COCH_3$	CH_3	72

Compound	X	Z	A	B	R_1	R_2	R_3	R_4	Reference
90	Leu	Arg	Ala	Ser	CH_3	H	$COCH_3$	CH_3	72
91	Arg	Arg	Ala	Ser	CH_3	H	CH_3	H	73
92	Arg	Arg	Ala	Ser	H	H	CH_3	CH_3	53
93	Hty	Arg	Ala	Dhb	H	H	CH_3	H	48
94	Hty	Arg	Ala	Dha	H	H	CH_3	CH_3	63
95	Hty	Arg	Ala	Dha	CH_3	H	CH_3	H	74
96	Tyr	Arg	Ala	Dha	CH_3	H	CH_3	CH_3	31
97	Arg	Tyr	Ala	Dha	CH_3	H	CH_3	CH_3	66
98	Arg	Tyr	Ala	Ser	CH_3	H	CH_3	H	41
99	Tyr	Arg	Ala	Ser	H	H	CH_3	CH_3	75
100	(H_4)Tyr	Arg	Ala	Dha	CH_3	H	CH_3	CH_3	57
101	Hty	Tyr	Ala	Dhb	H	H	CH_3	H	76
102	Arg	Arg	Ala	Dhb	H	H	$COCH_3$	H	54
103	Leu	Arg	Ala	Dha	CH_3	C_3H_6OH	CH_3	CH_3	38
104	Trp	Arg	Ala	Dha	CH_3	H	CH_3	H	58
105	Hty	Arg	Ala	Dha	CH_3	H	CH_3	CH_3	74
106	Hty	Arg	Ala	Ser	H	H	CH_3	CH_3	63
107	Tyr	Arg	Ala	Ser	CH_3	H	CH_3	CH_3	77
108	Arg	Tyr	Ala	Ser	CH_3	H	CH_3	CH_3	41
109	Har	Har	Ala	Dha	CH_3	H	CH_3	CH_3	78
110	Hty	Hty	Ala	Dhb	H	H	CH_3	H	76
111	Arg	Arg	Ala	Dha	CH_3	H	$COCH_3$	CH_3	79
112	Trp	Arg	Ala	Dha	CH_3	H	CH_3	CH_3	38
113	Hty	Arg	Ala	Dha	CH_3	H	$COCH_3$	H	80
114	Hty	Arg	Ala	Dhb	H	H	$COCH_3$	H	54
115	Arg	Tyr(OMe)	Ala	Dha	CH_3	H	CH_3	CH_3	41
116	(H_4)Tyr	Arg	Ala	Dha	CH_3	H	$COCH_3$	CH_3	69
117	Leu	Arg	Ala	Lan	CH_3	H	CH_3	CH_3	57

Whilst at least 111 microcystins have been reported, the level of structural characterisation which has been performed on each congener varies. Many of the microcystins listed in Table 1.2 have been characterised solely by tandem mass spectrometry (MS/MS) which provides no information on the stereochemistry of the amino acids present. Furthermore, the configuration of the unique amino acid; Adda (2*S*,3*S*,8*S*,9*S*; as observed in **7**), has only been elucidated on a single occasion.[81] To the best of my knowledge, in all subsequent reports, the stereochemistry of Adda has been assumed to be the same due to similar coupling constants being observed by nuclear magnetic resonance (NMR) spectroscopy. This was also the case for microcystins that contained the *O*-acetyl-modification of Adda (ADMAdda).[55]

The different microcystin congeners range in toxicity from non-toxic to highly toxic ([(6*Z*)-Adda[5]] MC-LR, LD_{50} > 1,200 µg/kg; MC-LR, LD_{50} = 50 µg/kg),[33] according to their ability to inhibit the important eukaryotic regulatory enzymes; serine/threonine protein phosphatases 1 and 2A.[82] Microcystins predominantly affect the liver cells of mammals as they are not able to translocate the membranes of most tissues but are actively transported into the hepatocytes.[83] Inhibition of the protein phosphatases in these cells then results in excessive signalling due to a lack of regulation via the phosphatases. This may lead to cellular disruption due to actin filaments of the cytoskeleton becoming hyperphosphorylated,[84] or cell proliferation and tumour promotion.[85]

1.2.8 *Nodularins*

The nodularins are cyclic peptides that are very similar to the microcystins, but contain only five amino acids. As in nodularin-R (**118**), the β-amino acid Adda observed in the microcystins is present, as well as Masp and D-glutamic acid. The position two amino acid is a variable L-amino acid and the position five *N*-methyldehydrobutyrine moiety is similar to the Mdha found in microcystins. Like the microcystins, nodularins can also be potent protein phosphatase 1 and 2A inhibitors,[82] promote tumours of the liver[86] and be lethal to mammals.[87]

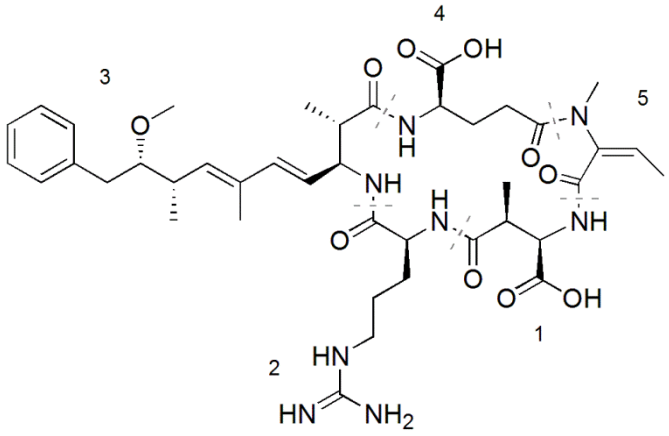

(118)

1.3 MICROCYSTIN PRODUCTION

1.3.1 Biosynthesis of Microcystins

The ability to synthesise microcystins is dependent on the presence of specific NRPS and PKS genes. To date, microcystins have been reported to be produced by many cyanobacterial genera including; *Anabaena*,[74] *Anabaenopsis*,[88] *Aphanizomenon*,[89] *Aphanocapsa*,[90] *Arthrospira*,[91] *Cylindrospermopsis*,[92] *Fisherella*,[93] *Hapalosiphon*,[94] *Microcystis*,[31] *Nostoc*,[72] *Oscillatoria*,[48] *Phormidium*,[95] *Planktothrix*,[71] *Radiocystis*,[96] *Synechocystis*[97] and *Woronichinia*.[98]

In *Microcystis*, the genes required for synthesis of microcystins (*mcyA-J*) are located in two operons (*mcyA-C* and *mcyD-J*) orientated in opposite directions and separated by a 750 base pair promoter region.[99-101] These genes produce a multi-enzyme complex consisting of both peptide synthetase and polyketide synthase modules which sequentially add onto phenylacetate to produce a peptide chain, which is then condensed to form a cyclic ring.[99-101] In other microcystin-producing genera, the arrangement of the open reading frames within the gene cluster differs slightly.[102,103]

The biosynthesis mechanism of MC-LR was elucidated through a series of feeding experiments, genetic mutational studies and sequence comparison with known NRPS and PKS.[99-106] The biosynthesis begins with the addition of phenylacetate onto the thiolation domain of McyG (Figure 1.1A) and the consecutive addition of four acetates from malonyl-CoA (Figure 1.1B-E).[99] The surplus carbonyl oxygens are reduced to hydroxyl groups and dehydrated, forming the C4 and C6 alkenes. The methylations at C17-19 are facilitated by *C*-methyltransferases (CM) and *S*-adenosyl-L-methionine (SAM).[99,105] The C20 methoxyl group is added by an *O*-methyltransferase (OM; McyJ) after reduction of the C9 carbonyl (Figure 1.1B). Finally, an aminotransferase (AMT) adds an amino group onto the C3, from what is likely to be a glutamate (Figure 1.1E).[99]

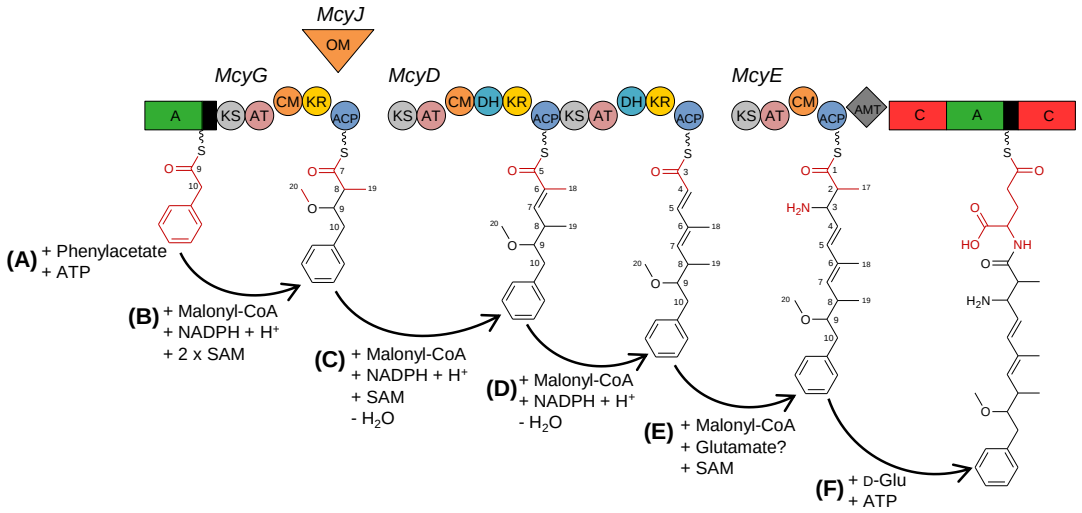

Figure 1.1: Proposed biosynthetic mechanism for the Adda portion of MC-LR. Each rectangle, circle, triangle and diamond represents an enzymatic domain. Aminoacyl adenylation domain (A); Acyl carrier protein (ACP); Aminotransferase (AMT); Acyltransferase (AT); Condensation domain (C); *C*-methyltransferase (CM); Dehydratase (DH); Ketoacyl reductase (KR); β-ketoacyl synthase (KS); *O*-methyltransferase (OM). Adapted from Reference 99.

The remainder of the peptide chain is built up from the position six glutamic acid by consecutive condensation, adenylation and thiolation domains. Each amino acid is recognised by the adenylation domain and loaded onto the thiolation domain, while the condensation domain forms the peptide bond with the previous amino acid (Figure 1.2).[99] The Mdha in position seven is incorporated as a serine, *N*-methylated by a *N*-methyltransferase (NM), then dehydrated by McyI (Figure 1.2A-B).[99] The position one D-alanine is synthesised from the L-amino acid by an epimerisation domain (EP) located within McyA2. The leucine and arginine incorporated into positions two and four remain in the L-configuration (Figure 1.2C & E). The D-Masp incorporated into position three is produced by the racemase McyF (RC).[107] Feeding studies using labelled precursors suggest that the Masp incorporated into microcystins is synthesised from acetyl-CoA and pyruvic acid,[105] as opposed to the rearrangement of glutamic acid observed in other bacteria.[108] The racemase responsible for the isomerisation of the D-glutamic acid incorporated into position six has been suggested to be located outside of the *mcy* cluster.[107]

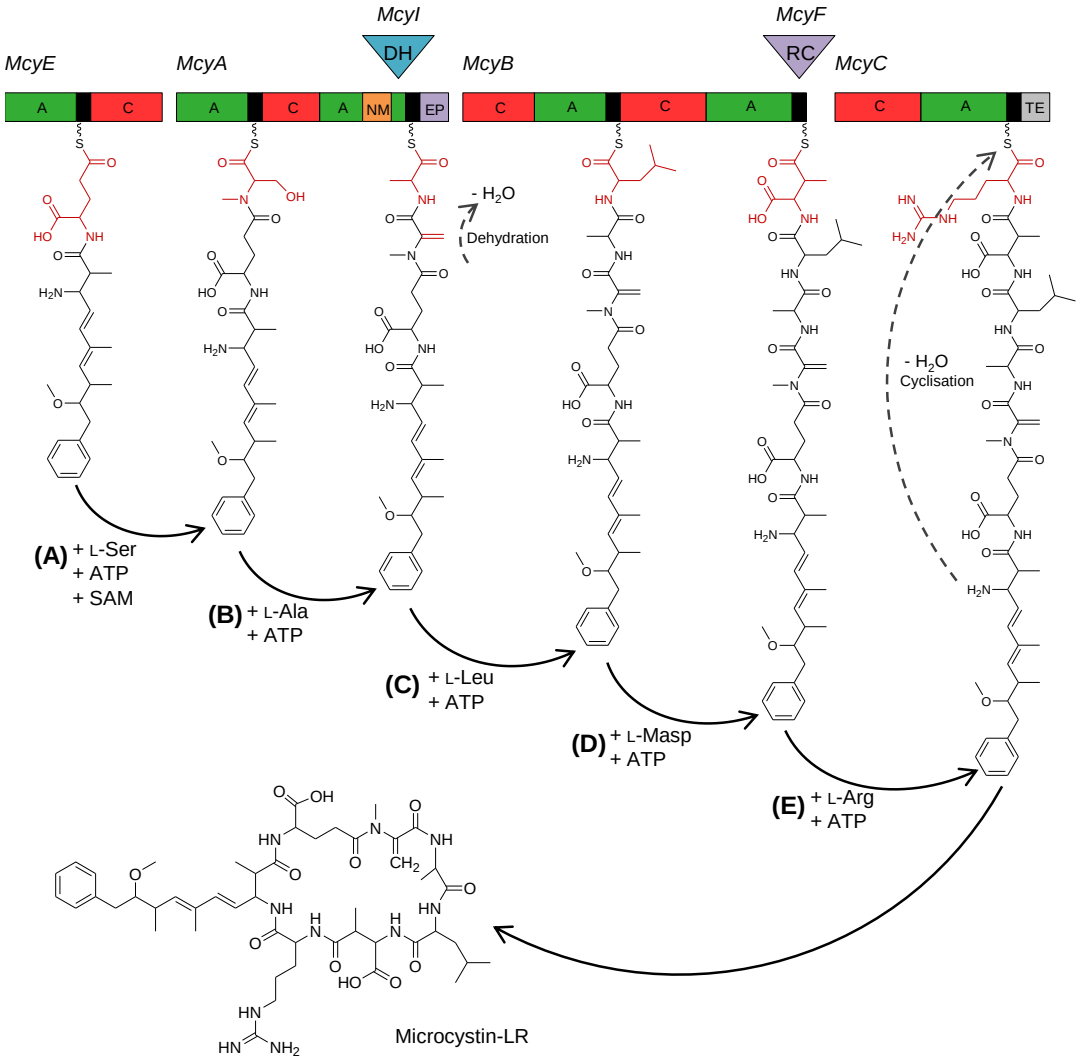

Figure 1.2: Proposed biosynthetic mechanism for the peptidic portion of MC-LR. Each rectangle and triangle represents an enzymatic domain. Aminoacyl adenylation domain (A); Condensation domain (C); Dehydratase (DH); Epimerisation (EP); *N*-methyltransferase (NM); Racemase (RC); Thioesterase (TE). Adapted from Reference 99.

The *mcyH* gene included in the *mcy* cluster is not directly involved in the synthesis of microcystins and resembles an ABC-A_1 transporter protein.[99] Deletion of this gene has been shown to disrupt microcystin production.[109] A phosphopantetheine transferase gene, not located within the *mcy* cluster, is also required to transfer the essential cofactor 4-phosphopantetheine onto the acyl carrier proteins of the complex.[99]

1.3.2 Structural Diversity of Microcystins

There have been at least 111 microcystin congeners characterised to date (Table 1.2 and Appendix A) and modifications have been reported at each amino acid present in the cyclic peptide. This is due to differences in the coding of the microcystin synthase genes of different cyanobacterial strains.

The amino acids incorporated into microcystins are dependent upon the substrate specificity of the adenylation domain responsible for loading the amino acid onto the microcystin synthase module.[110] The substrate specificity of the position two and four adenylation domains (McyB1 and McyC) is varied, as fifteen different amino acids have been incorporated at position two and thirteen at position four (Table 1.2 and Appendix A).

Whilst substrate variability is common at McyB1 and McyC, it is less common in the other adenylation domains. The position one alanine is more highly conserved, with only substitutions for serine and leucine having been reported.[68,72,111] The position three amino acid is also highly conserved, as only Masp and aspartic acid have been shown to be present. Glutamic acid has been incorporated into position six of every microcystin characterised, although esterified variants have also been observed.[35,43,57,71] Whether these modifications occurred prior to incorporation of the glutamic acid residue, were due to an additional transferase domain or were an artefact of the purification, remains to be elucidated.

Mdha or dehydroalanine (Dha) are commonly observed at position seven of microcystins (Table 1.2 and Appendix A). The Dha variant has been observed alongside Mdha-containing microcystins,[112] which indicates that the McyA *N*-methyltransferase was not working at full efficiency in these instances. Dha-containing microcystins have also been observed in the absence of position seven *N*-methylated variants,[42,43,63] which could suggest that the McyA *N*-methyltransferase was not present. However, sequencing of the *mcy* gene cluster of one of these cyanobacterial strains (*Microcystis aeruginosa* K-139) showed that the *N*-methyltransferase domain of McyA was still present,[42,100] suggesting that the enzyme was not functional.

Mdha and Dha are produced by dehydration of *N*-methylated and non-methylated serine residues, respectively.[99] In some cases, dehydrobutyrine (Dhb) has been observed at position seven, which is proposed to be the result of threonine being incorporated instead of serine.[48,61] *N*-methylated and non-methylated serine residues have been observed at position seven, but in each case their Mdha or Dha counterpart was also present.[38,43,57,63,72,73,77] This suggests that the serine analogues were the biosynthetic precursors of the Mdha- and Dha-containing microcystins and that the McyI dehydrogenase was not functioning at full efficiency.

The occurrence of *seco*[Asp^3] MC-RR (**119**),[71] a linear microcystin with a pyruvate present in position seven, was attributed to hydrolytic cleavage of Mdha. The researchers eliminated the possibility of this modification being an artefact of the isolation protocol,[71] but whether the cleavage was enzyme-catalysed or due to the conditions inside the cell was not determined.

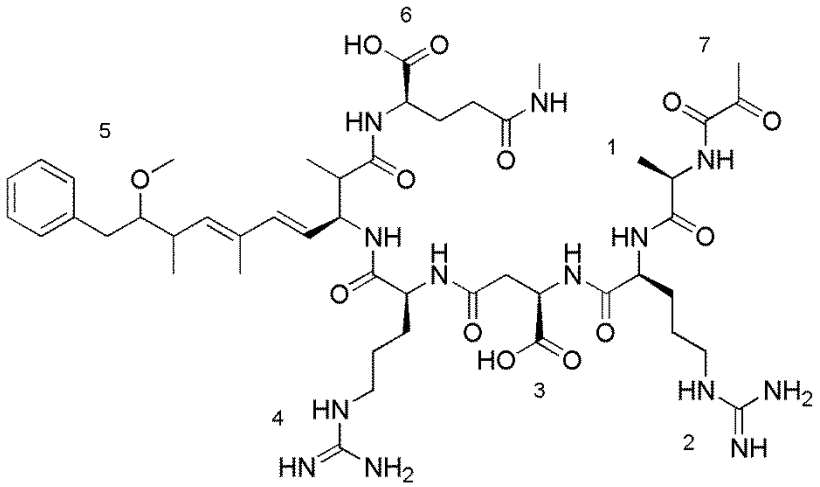

(119)

Structural diversity of the Adda moiety has been limited to changes in the configuration of the C4 and C6 alkenes, and the group present on the C9 oxygen. Isomerisation of the C4 and C6 double bonds is thought to be due to ultraviolet (UV) irradiation rather than a product of the biosynthesis.[113] Generally, a methoxyl group is present at C9, however, substitution for an acetyl group (ADMAdda) and the desmethyl variant (DMAdda) have been observed (Table 1.2 and Appendix A). The ADMAdda modification indicates that, in some instances, the *O*-methyltransferase McyJ could have relaxed substrate specificity and utilise acetyl groups instead of methyl groups. The single report of a DMAdda

microcystin congener,[38] may indicate that McyJ does not always function at full efficiency. However, the presence of this microcystin should be regarded carefully, as it has been observed that the *O*-acetyl group in ADMAdda was readily hydrolysed,[54] which produces the respective DMAdda microcystin.

A single strain of cyanobacteria can often produce more than one microcystin congener, which could suggest the presence of multiple microcystin synthases. However, knockout of a single *mcy* gene has been shown to render a cyanobacterium usually capable of producing multiple microcystin congeners, incapable of producing any microcystins.[99-101,104] This demonstrates that a single microcystin synthase was responsible for the production of all of the congeners. Multiple microcystin congeners being produced by a single cyanobacterial strain are generally due to an adenylation domain possessing relaxed substrate specificity, due to the amino acid sequence in the binding pocket.[110,114] This results in a single adenylation domain being able to act upon different amino acids, giving rise to multiple microcystin congeners from a single microcystin synthase. As discussed, in regards to the position seven amino acid, an inefficient transferase or dehydrogenase could also result in multiple microcystin congeners being produced by a single cyanobacterial strain.

As mentioned previously, the structural variations observed in microcystins can have a marked effect on the toxicity of the compound (Appendix A). The most harmful microcystin reported to date is MC-LR (LD_{50} = 50 μg/kg)[115] and since many of the structural analogues of MC-LR have toxicity data available, inferences can be made on the effect of different structural modifications. One caveat is that much of the published toxicity data comes from different studies, performed using a range of methodologies and undertaken in different laboratories.

The most dramatic change in toxicity results from isomerisation of the diene system present in Adda. Generally, both of the double bonds are in the *E*-configuration (MC-LR, LD_{50} = 50 μg/kg).[115] When the C6 double bond is isomerised to the *Z*-configuration, the microcystin becomes non-toxic ([(6*Z*)Adda^5] MC-LR, LD_{50} > 1,200 μg/kg).[52] A similar decrease in toxicity can be produced by modifying the carboxylic acid group of the position six glutamic acid, (for example [Glu(OMe)^6] MC-LR, LD_{50} > 1,000 μg/kg).[33] Changes to the

C9 methoxyl group of Adda do not cause large differences in microcystin toxicity as [ADMAdda^5] MC-LR has an LD_{50} of ca. 60 µg/kg[56] and the desmethyl variation of MC-LR, [DMAdda^5] MC-LR, has half the potency (LD_{50} = 90-100 µg/kg).[38]

When Dhb or *N*-methylserine are present at position seven, the toxicity is still relatively high ([Asp^3, Dhb^7] MC-LR, LD_{50} = 70 µg/kg;[48,61] [MeSer^7] MC-LR, LD_{50} = 150 µg/kg).[57] During the binding of MC-LR to protein phosphatases, a covalent bond is formed between the terminal alkene of Mdha and a cysteine residue of the protein.[116,117] This bond stabilises the binding of the toxin, therefore, the high toxicity of [MeSer^7] MC-LR and [Asp^3, Dhb^7] MC-LR suggests that a similar interaction may occur with a position seven serine or Dhb. However, the incorporation of lanthionine (a large amino acid composed of two alanine residues crosslinked through the β-carbon atoms by a thioether linkage)[118] at position seven causes a large decrease in toxicity ([MeLan^7] MC-LR, LD_{50} = 1,000 µg/kg).[57]

The presence of a position two arginine residue in MC-RR lowers the toxicity of the microcystin by approximately one order of magnitude (LD_{50} = 500-600 µg/kg).[119,120] As with MC-LR, isomerisation of the Adda C6 alkene also renders the MC-RR congener non-toxic ([(6*Z*)Adda^5] MC-RR, LD_{50} > 1,200 µg/kg).[52,121] Incorporation of other large amino acids at position two also lowers the toxicity relative to MC-LR, although not as dramatically as observed with MC-RR (for example, MC-WR, LD_{50} = 150-200 µg/kg[38] and MC-FR, LD_{50} = 250 µg/kg)[38] However, the tyrosine-containing microcystin; MC-YR, has a very similar toxicity to MC-LR (LD_{50} = 68 µg/kg).[120] Incorporation of the slightly larger amino acid; homoisoleucine, has a small effect on toxicity (MC-HilR, LD_{50} = 100 µg/kg)[57] and interestingly, incorporation of the smaller amino acid alanine at position two causes a fivefold reduction in potency (MC-AR, LD_{50} = 250 µg/kg).[38] This observation suggests that when microcystin binds to protein phosphatases, the position two amino acid has a hydrophobic interaction which enhances binding. The crystal structure of MC-LR bound to protein phosphatase 2A supports this, as van der Waals interactions are present between the position two leucine of MC-LR and the cysteine-266 and arginine-268 of the enzyme.[116]

Toxicity data for a microcystin lacking a position four arginine has only been reported once. This microcystin; MC-YM(O), had a potency very similar to that of MC-LR (LD_{50} = 56 μg/kg).[67] However, little can be inferred from such limited information.

In general, the toxicity of microcystins is most dramatically affected by isomerisation of the diene system of Adda and esterification of the carboxylic acid group of the position six glutamic acid. Incorporation of a large amino acid at position seven also interferes with protein phosphatase binding. The incorporation of an amino acid at position two which is smaller than leucine causes a slight decrease in toxicity. In general, the incorporation of larger amino acids at position two adversely affects protein phosphatase binding and lowers the toxicity of the compound. The influence of the commonly observed position four arginine (Table 1.2 and Appendix A) on microcystin toxicity, is difficult to assess given the limited data available.

1.3.3 Environmental Factors Affecting Microcystin Production

Although the biosynthetic pathway for microcystins has been deduced, there is still uncertainty surrounding the transcriptional and post-translational regulation of the microcystin synthase. Microcystins were initially thought to be feeding deterrents for predators, and studies showing increased microcystin content in cyanobacteria exposed to predators supported this theory.[122,123] However, the genes responsible for microcystin synthesis predate the eukaryotic lineage.[124] Furthermore, cyanobacteria often produce other non-toxic oligopeptides and regulate their production in response to the stimuli which cause increased microcystin production.[125-127] It has been suggested that strains which are not capable of producing microcystins may mimic their effect using other oligopeptides.[125]

Cyanobacteria have been shown to respond to varying environmental parameters in both laboratory and field situations, by altering their production of microcystins.[128] In order to determine the regulatory mechanisms controlling microcystin production, many experiments manipulating cyanobacterial cultures have been performed (Appendix B).

In general, the laboratory studies presented in Appendix B, indicate that factors which influence cell growth also affect microcystin production.[129] Microcystin concentrations are maximal around 20-25 °C and decreases at higher and lower temperatures.[130-136] A similar parabolic response was observed in studies investigating the response to light intensity.[130-132,134,136-138] Increased phosphorus and nitrogen concentrations in general caused higher microcystin levels,[131,134,136,137,139] although several experiments showed contradictory results.[131,135] Zinc was shown to be essential for microcystin production,[140] whilst investigations into the response to iron levels yielded conflicting results.[135,139-141]

Although microcystins are not essential for photosynthesis, a *Microcystis aeruginosa* mutant lacking *mcyB* showed altered levels of photosynthetic pigments,[142] suggesting some involvement in the photosystem. This corresponds well with other studies showing that microcystin production is correlated with chlorophyll-*a* production[143,144] and that microcystins are embedded in the thylakoid membrane.[145]

Several culturing experiments have resulted in a change in the proportion of the microcystin congeners present. An investigation of how microcystin production alters during different stages of the cell cycle found that the relative abundance of the microcystin congeners shifted significantly.[146] The strain of *Microcystis viridis* studied produced three microcystin congeners; MC-LR, MC-YR and MC-RR, which are present at a ratio of ca. 23:67:10 during the stationary phase.[147] This microcystin composition was consistent during the pre-mitotic phase,[146] however, cells in the DNA synthetic phase had increased levels of MC-LR/MC-YR and reduced levels of MC-RR. Cells in the mitotic phase showed a rectification of the microcystin composition, with an increase in MC-RR and a decrease in MC-LR/MC-YR. The researchers did not allude to what might be causing the significant shift in microcystin congeners over the different phases of the cell cycle.

Increased photon irradiation has been shown to increase microcystin production, up to a point.[130-132,134,136-138] A strain of *Planktothrix agardhii* which produced [Asp^3] congeners of both MC-LR and MC-RR has been shown to exhibit increased levels of MC-LR with increased irradiation.[148] The implication of this

finding is that MC-LR is an order of magnitude more toxic than MC-RR (Appendix A), so the resulting phenotype from increased light intensity was more toxic. Another study using batch culture and a natural population of *Microcystis aeruginosa* found that at a moderate temperature (20 °C) the microcystin content would switch from being predominantly MC-LR to a less toxic phenotype that was predominantly MC-RR.[135] At a higher temperature (28 °C), this did not occur and the levels of MC-LR and MC-RR remained constant. A similar observation was noted in another study using *Microcystis viridis*, where higher proportions of MC-RR were reported at lower temperatures (15-20 °C).[149]

The microcystin MC-RR contains two of the nitrogen-rich amino acid, arginine, whereas MC-LR contains only one. An assessment of whether the levels of free leucine and arginine in the culture medium would alter the levels of the microcystin congeners showed this to be apparent.[150] When leucine was supplied to a strain of *Planktothrix agardhii*, the ratio of MC-LR/MC-RR increased. When arginine was supplied, the opposite effect was observed, however, the response was not as pronounced. The researchers further experimented with the level of nitrogen in the culture medium,[150] hypothesising that a shift from high nitrogen to low nitrogen would cause an increase in the MC-LR/MC-RR ratio. This was not the case during the time course of their study, as the microcystin proportion did not shift over 25 days. The researchers theorised that this could be due to the phycocyanin pigments, which are utilised in times of nitrogen shortage, not being fully depleted over the period of the experiment. Another study using *Microcystis viridis* had similar findings; that the level of nitrogen in the medium did not have a significant effect on the abundance of microcystin congeners during the study.[146]

An experiment which assessed whether different nitrogen/carbon ratios (N/C) affected the relative abundance of microcystin congeners had similar results.[151] The levels of three microcystin congeners (MC-LR, MC-YR and MC-RR) in a *Microcystis aeruginosa* strain were analysed in respect of the N/C ratio supplied, and also under light limitation in the presence of excess N/C. Whilst manipulating the N/C ratio did not substantially alter the abundance of the different microcystin congeners, supplying excess N/C and limiting light caused an increase in MC-RR and MC-YR with no significant change to MC-LR levels. Whether this was due to the level of nitrogen, the level of carbon or the light limitation is unknown,

however, low light intensities have been previously shown to sustain higher levels of MC-RR.[148]

1.4 METHODS OF MICROCYSTIN ANALYSIS

Due to the health risk posed by microcystins, the World Health Organisation has recommended a 'safe level' for drinking waters of 1 µg/L of MC-LR.[152] In the past, the brine shrimp (*Artemia salina*) bioassay and mouse bioassay were used to detect the presence of toxic compounds in cyanobacterial blooms.[153] However, apart from the symptoms exhibited in the mouse bioassay, these methods gave no indication of which toxic compound/s were present.[154] Nowadays, microcystin levels in environmental samples are generally determined by protein phosphatase inhibition assay (PPIA), enzyme-linked immunosorbent assay (ELISA), high performance liquid chromatography with UV detection (HPLC-UV) or HPLC coupled to mass spectrometry detection (LC-MS).[155,156]

1.4.1 Protein Phosphatase Inhibition Assay

The PPIA utilises the ability of microcystins to inhibit protein phosphatases in order to determine the quantity of microcystin present in a sample. The amount of microcystin is determined by comparison with a standard curve constructed using microcystin at known concentrations and assayed in the same manner. In the past, this technique was limited by the commercial unavailability of the protein phosphatase enzyme and the radioactively-labelled substrate.[155] Nowadays, colorimetric (*p*-nitrophenyl phosphate)[82] and fluorescent (4-methylumbelliferyl phosphate)[157] substrates are available instead of the unstable and hazardous ^{32}P-labelled alternative. High quality protein phosphatase enzyme is also available from several sources.

This technique is very sensitive (low picomolar region),[157] but cannot distinguish between microcystins and other protein phosphatase inhibitors, such as okadaic acid.[158] It also gives no indication of the microcystin congeners present in the sample, however, an estimate of the overall toxicity is given by the strength of protein phosphatase inhibition.[82]

1.4.2 Adda-Specific Enzyme-Linked Immunosorbent Assay

ELISA exploits the specific binding of an antibody with the antigen it was raised against in order to determine the quantity of antigen in a sample.[159] Monoclonal and polyclonal antibodies have been raised against a variety of microcystin congeners[160-163] and Adda-haptens.[164] These antibodies have shown varied cross-reactivity, some reacted uniformly with different microcystin congeners,[160] whilst others reacted poorly to certain congeners.[163]

A direct competitive ELISA for microcystin analysis involves attaching an Adda-specific antibody to a solid phase, for example, a microtitre plate.[165] This is incubated with a mixture of samples/standards and a microcystin-peroxidase conjugate which competes for the binding sites of the antibody. After removing unbound microcystin and incubation with a peroxidase substrate, an inverse response is observed and a high level of colour formation is taken to indicate a low level of microcystin in the sample.

Modern ELISA protocols have sensitivity comparable with the PPIA (low picomolar region),[164] but are specific for Adda-containing compounds. As ELISA gives no indication of the microcystin congeners present, it provides no information on the toxicity of the sample.

1.4.3 High Performance Liquid Chromatography-Ultraviolet Detection

A microcystin-containing extract or water sample can be separated by HPLC in order to determine the microcystin congeners present and their concentration. Generally a reversed-phase C_{18} column with an acidic buffer is utilised.[166] When coupled to a photo-diode array detector, the congeners present can be determined, to some degree, by the retention time on a C_{18} column and the UV spectrum.[167] However, this relies on the appropriate microcystin standard being available for comparison. Most microcystin congeners exhibit a UV maximum of 238 nm due to the conjugated diene group of the Adda moiety, although tryptophan-containing congeners also have a maximum at 222 nm.[153] The quantity of microcystin present in a sample is determined by comparison of the UV absorbance (at 238 nm) of the microcystin peaks with a standard curve.[167]

The sensitivity of this method of microcystin analysis is in the moderate nanomolar range.[168] One disadvantage of HPLC quantification of microcystins is the long duration of both sample handling and analytical procedures, and the method has also been shown to be susceptible to matrix-effects from co-eluting extract components[169] and plasticisers.[170]

1.4.4 Liquid Chromatography-Mass Spectrometry Detection

Liquid chromatography in combination with MS is the most robust of current methods used for microcystin analysis. It gives definitive information on the congeners present according to their retention time on a C_{18} column and their mass-to-charge ratio (*m/z*).[166] Mass spectrometers equipped to perform MS/MS can further clarify any ambiguous identifications. Multiple reaction monitoring methods, which utilise MS/MS capabilities are often used to improve the selectivity and sensitivity of the method.[171] Here, a target ion is isolated and fragmented, then the resulting fragments ions are used for quantification purposes. With microcystin analysis, the *m/z* 135 Adda sidechain fragment ion is commonly utilised, as it is seldom observed in other compounds.[172] Due to a fast scan rate, mass spectrometers equipped with a triple quadrupole mass analyser are able to analyse multiple target ions within a given segment of an HPLC chromatogram, whereas ion trap mass spectrometers, which have a slower scan rate, can only manage several target ions. Despite the enhanced selectivity and sensitivity, the major limitation of MS detection is the high capital and running costs of the instrumentation.

This method of microcystin analysis has a sensitivity in the low nanomolar range.[157] As with HPLC-UV analysis, matrix effects are apparent and lengthy procedures can be a hindrance. However, recent advances in small particle and monolithic silica columns have decreased instrument run-times significantly from those achieved using conventional HPLC.[173,174]

1.4.5 Matrix-Assisted Laser Desorption/Ionisation-Time of Flight Mass Spectrometry

Matrix-assisted laser desorption/ionisation-time of flight (MALDI-TOF) MS produces ions from laser irradiation of a sample co-crystallised with a matrix. The laser energy is absorbed by the matrix and passed to the analyte molecules.[175] This

method of ionisation predominantly produces singly protonated ions to approximately *m/z* 5000 and allows complex mixtures to be analysed from a minute amount of sample without prior separation.[176]

For qualitative analyses of microcystins, MALDI MS gives comparable information to LC-MS. By separating sample ions according to their *m/z*, it allows for the identification of most microcystin congeners. Instruments equipped to analyse post-source decay have the ability to further clarify any ambiguous identifications.[176] Analysis times on a MALDI mass spectrometer are shorter than with LC-MS since sample components do not need to be separated on a C_{18} column and sample preparation is minimal. MALDI MS is also highly suited to automated high-throughput sample preparation and data acquisition,[177] making it an ideal technology for analysing large numbers of samples quickly.

Whilst MALDI MS has frequently been used for qualitative detection of microcystins in cyanobacterial samples,[44,178-183] it has only recently been used as a quantitative tool.[184] The low 'spot-to-spot' and 'shot-to-shot' reproducibility of MALDI MS analyses are the main impediments to its quantitative use.[185-187] To overcome this, an internal standard is commonly added to the sample and to standard solutions prior to preparation of the MALDI target.[188-192] The signal for the analyte is then assessed against the signal for the internal standard. An internal standard used for quantitative MALDI MS needs to have similar chemical properties to the target analyte, be separated in mass, ionise with a similar efficiency and, preferably, be commercially available.[193]

Howard and Boyer[184] investigated the suitability of four potential internal standards; angiotensin I, cyclosporine A, nodularin and ^{15}N-MC-YR, for quantitative MALDI MS analyses of microcystins. Angiotensin I, cyclosporine A and nodularin are commercially available, however nodularin is considerably more expensive than the other alternatives (ca. 50-400 times). A stable isotope labelled internal standard is often the recommended choice of many researchers,[194,195] however the ^{15}N-MC-YR utilised in this study had to be prepared in-house. Of the four internal standards tested by Howard and Boyer,[184] nodularin gave the best quantitative performance.

Detection limits in the low micromolar region were achieved using this technique.[184] However, ionisation suppression effects were observed when microcystins were analysed in a sample matrix which contained contaminating compounds,[184] a problem which would need to be overcome or better understood before this technique could be used for routine analyses. Another drawback of the method is that the existing protocol is not well suited for automated sample preparation or for use in an instrument automatically acquiring data. In order for this emerging technique to reach its full potential, different protocols are required to allow automated sample preparation and data acquisition.

1.5 STRUCTURAL CHARACTERISATION OF OLIGOPEPTIDES

Multiple structural characterisation techniques were utilised during this study in order to acquire as much information as possible on the oligopeptides investigated. A short description of the techniques and the structural information they can supply is provided in this section.

1.5.1 Mass Spectrometry

Mass spectrometry involves the assessment of ions in the gas phase in order to determine their *m/z*. Deconvolution from the determined *m/z* can provide the mass of the analyte. Mass spectrometers consist of a method of sample introduction, an ion source to ionise sample component and a mass analyser which separates ions according to their *m/z*.[196]

Mass spectrometers with multiple mass analysers in series (MS/MS) and ion-trap mass analysers can provide structural information on a compound. The first mass analyser is used to isolate the ion of interest, which is broken apart (generally through collision with an inert, heavy gas) and the *m/z* of the resulting fragments are assessed using the second mass analyser.[197] The *m/z* of the fragment ions indicate how the parent compound was put together. In an ion-trap mass analyser, the ion of interest is trapped whilst the other ions are filtered out, the trap is then flooded with a collision gas, causing fragmentation of the parent ion and the *m/z* of the resulting fragments are assessed.[197] Furthermore, the resulting fragment ions can be trapped and broken apart to provide additional structural information (MS^n).

The ionisation techniques utilised during this study were MALDI and electrospray ionisation (ESI). Both are relatively 'soft', providing intact molecular ions for labile compounds such as peptides.[198] As discussed in Section 1.4.5, MALDI produces ions from laser irradiation of a sample co-crystallised with a matrix.[175] This method of ionisation produces predominantly singly protonated ions and allows complex mixtures to be analysed without prior separation.[176] ESI produces ions by passing a sample in solution through a charged capillary, from which it acquires a charge. As the solution exits the capillary, it is nebulised into a desolvation chamber where solvent is removed from the ionised analyte.[199] This method of ionisation is pH dependent and requires complex mixtures first be separated by HPLC. It also has a propensity towards multiply charged ions when multiple ionisation points are available on a single compound.[200]

These ionisation techniques were utilised in three different mass spectrometers; MALDI directly coupled to a TOF mass analyser (Bruker AutoFlex II), an LC-MS with HPLC coupled to ESI with an ion-trap mass analyser (Bruker AmaZon X) and ESI orthogonally coupled to a TOF mass analyser (Bruker MicrOTOF).

1.5.2 Advanced Marfey's Amino Acid Analysis

In 1984, it was found that derivatisation of an amino acid with FDAA (1-difluoro-2,4-dinitrophenyl-5-alanine amide) allowed for the separation of the D- and L-stereoisomers by conventional reversed-phase HPLC.[201] However, the lack of standards for non-proteinogenic amino acids posed a problem for the analysis of cyanobacterial oligopeptides. To overcome this, two measures were undertaken; racemisation of the sample and coupling with MS, this technique was termed Advanced Marfey's amino acid analysis.[202]

Racemisation of the sample amino acids produces a mixture of both the D- and L-stereoisomers. When the derivatives of this mixture were compared to a non-racemised mixture of the sample amino acids, the configuration of the original amino acid could be determined. Racemisation of the sample amino acids was later replaced by derivatisation with D- and L-FDAA which facilitated the identification of the stereoisomer present in the sample.[203,204] Coupling with MS allowed the mass of unconventional amino acids to be determined. For this, a

heavier derivatisation reagent (1-difluoro-2,4-dinitrophenyl-5-leucine amide; FDLA) was utilised, as it produced a more intense MS signal.[202,205]

Advanced Marfey's amino acid analysis of a cyanobacterial peptide is generally conducted on a pure sample which has been hydrolysed into its constituent amino acids. After derivatisation with L-FDLA or DL-FDLA, the products are analysed by LC-UV-MS.[205] Comparison of the L-FDLA derivatives with those of standard amino acids allows the identification and determination of the configuration of some amino acids. Comparison of the L-FDLA derivatives of the sample hydrolysate with the DL-FDLA derivatives, indicates the configuration of the unconventional amino acids.

1.5.3 Nuclear Magnetic Resonance Spectroscopy

Nuclear magnetic resonance spectroscopy exploits the phenomenon where magnetic nuclei (such as ^{1}H and ^{13}C) absorb electromagnetic radiation at a frequency specific to the isotope.[206] Modern NMR spectrometers use helium-cooled superconducting magnets to generate a magnetic field which the sample is placed inside.[206] Sample nuclei are simultaneously excited by a short, high-powered radio frequency pulse. The time of the resulting decay signals are measured and Fourier transform is used to convert the signals into a readable spectrum measured as a frequency (chemical shift).[207] As the position of the resulting chemical shift is dependent upon the strength of the applied magnetic field, the frequency of the signal is often expressed as dimensionless numbers (δ or ppm) relative to a reference signal.

Shielding by the electron cloud of a nucleus causes a single isotope to resonate at different frequencies.[206,208] The presence of nearby electronegative environments draws the electron cloud away from the nucleus and causes it to become deshielded. The resulting chemical shifts are indicative of the chemical environment the nuclei are in and hence give an indication of the structural elements present in a compound. Coupling (*J*) between adjacent magnetic nuclei is observed in NMR spectra as splitting of the signals, the multiplicity of a signal therefore indicates the number of adjacent magnetic isotopes.[206,209] Carbon spectra are generally acquired decoupled and each ^{13}C nucleus in an unique chemical environment resonates as a single peak.[206] Two-dimensional NMR experiments

plot data on two axes and show correlations between two magnetic nuclei.[206] Two-dimensional NMR experiments can allow correlations between different isotopes to be detected and give an indication of the proximity of other magnetic nuclei.

1.6 OBJECTIVES, SCOPE AND OUTPUTS OF THIS RESEARCH

This study had three distinct objectives:

- To identify and characterise new microcystins, as well as other new cyanobacterial oligopeptides.
- To improve an existing technique for the quantification of microcystins.
- To examine how nitrogen supply can affect the abundance of different microcystin congeners.

Chapter 2 of this thesis describes the MS/MS characterisation of a new anabaenopeptin from a New Zealand cyanobacterial bloom sample. This chapter is based on the article: Puddick, J. & Prinsep, M.R. MALDI-TOF mass spectrometry of cyanobacteria: A global approach to the discovery of novel secondary metabolites. *Chemistry in New Zealand*, **2008**, *72*, 68-71.

Characterisation of 27 conventional microcystin congeners from a *Microcystis* strain isolated from Lake Hakanoa (Huntly, New Zealand) is described in Chapter 3. Ten of these microcystins have not been reported previously. This chapter is being written up as two papers; one article will detail the full structural characterisation of two of the new microcystins, the other will present the MS/MS characterisation of the remaining new variants and discuss the abundance of microcystin congeners produced by CYN06. Microcystins which contained oxidised tryptophan residues were also identified in this cyanobacterial strain and this is the first report of oxidised tryptophan residues in microcystins. This work is presented in Chapter 4 and is currently being developed into a scientific publication.

Chapter 1

The structural characterisation of eight new microcystins and six novel linear peptides from an Antarctic cyanobacterial sample is described in Chapter 5. Portions of this chapter are based on the publication: Wood, S.A., Mountfort, D., Selwood, A.I., Holland, P.T., Puddick, J. and Cary, S.C. Widespread distribution and identification of eight novel microcystins in Antarctic cyanobacterial mats. *Appl. Environ. Microbiol.*, **2008**, *74*, 7243-7251. This was the first report of microcystins which contain a position one glycine, as well as the first report of ADMAdda-containing microcystins from the Southern Hemisphere. The additional characterisation work presented in this chapter will be written up as a scientific publication.

Chapter 6 of the thesis is based on the publication: Puddick, J., Prinsep, M.R., Wood, S.A., Cary S.C. and Hamilton, D.P. Enhanced sample preparation for quantitation of microcystins by matrix-assisted laser desorption/ionisation-time of flight mass spectrometry. *Phytochemical Analysis*, **2012**, *23*, 285-291. Here, the development of a sample preparation for use with quantitative MALDI-TOF analysis of microcystins is described.

A preliminary investigation of microcystin congener abundance in response to nitrogen availability is presented in Chapter 7. This is the first study to show that microcystin congener abundance is affected by nitrogen supply and opens new research avenues for investigating the regulation of microcystin production.

CHAPTER 2

Tandem Mass Spectrometry Characterisation of a New Anabaenopeptin from a New Zealand *Microcystis* Species

2.1 INTRODUCTION

Anabaenopeptins are cyclic peptides containing six amino acids. Each contains a D-lysine (Lys) in position two with a ureido bond to a carbonyl-linked sidechain amino acid in position one. The D-Lys also forms a secondary peptide bond which encloses the ring, as in anabaenopeptin A (**2**).[21] The CO-linked sidechain and the ring amino acids vary, as does their degree of methylation, resulting in 39 different anabaenopeptin structures being observed to date (**2**,**120**-**157**; Table 2.1).

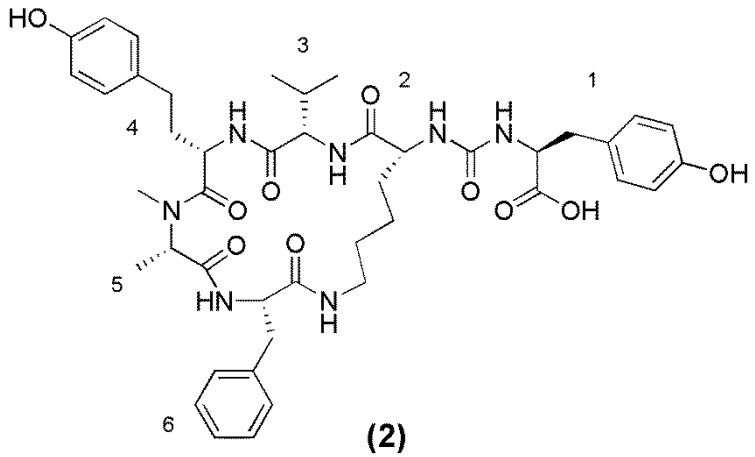

(2)

Anabaenopeptins are produced by a non-ribosomal peptide synthetase module similar to that of the microcystin synthase discussed in Section 1.3.1. The multi-enzyme complex is genetically coded by a 32.5-kb gene cluster consisting of five open reading frames.[210] The enzyme complex builds the structure from the position one sidechain amino acid by consecutive addition of amino acids via condensation, adenylation and thiolation domains. The ring is cyclised by condensation of the carboxyl group of the position six amino acid with the sidechain amine of the position two Lys. An epimerisation domain facilitates

Table 2.1: Amino acid sequence, molecular masses and bioactivity data on the known anabaenopeptins.[a]

Anabaenopeptin	M_r (Da)[b]	1	3	4	5	6	Biological Activities[d]	References
Anabaenopeptin A (**2**)	843.4	Tyr	Val	Hty	*N*-MeAla	Phe	rNEc	21
Anabaenopeptin B (**120**)	836.5	Arg	Val	Hty	*N*-MeAla	Phe	rNEc	21,211,212
Anabaenopeptin B1 (**121**) [c]	850.5	Har	Val	Hty	MeAla	Phe		213
Anabaenopeptin C (**122**)	808.4	Lys	Val	Hty	*N*-MeAla	Phe		214
Anabaenopeptin D (**123**)	827.4	Phe	Val	Hty	*N*-MeAla	Phe		214
Anabaenopeptin E (**124**)	850.5	Arg	Val	Hty(OMe)	*N*-MeAla	Phe		212,215
Anabaenopeptin F (**125**)	850.5	Arg	Ile	Hty	*N*-MeAla	Phe	PPi	212,215,216
Anabaenopeptin F1 (**126**) [c]	864.5	Har	Ile	Hty	MeAla	Phe		213
Anabaenopeptin G (**127**) [c]	908.5	Arg	Ile	Hty	MeLeu	Tyr		181
Anabaenopeptin G* (**128**)	929.5	Tyr	Ile	Hty	*N*-MeHty	Ile	CPAi	212,217
Anabaenopeptin H (**129**)	922.5	Arg	Ile	Hty	*N*-MeHty	Ile	CPAi	212,217
Anabaenopeptin I (**130**)	759.5	Ile	Val	Hty	*N*-MeAla	Leu	CPAi	212
Anabaenopeptin J (**131**)	793.4	Ile	Val	Hty	*N*-MeAla	Phe	CPAi	212
Anabaenopeptin T (**132**)	865.5	Ile	Val	Hty	*N*-MeHty	Ile	CPAi	212,218
Anabaenopeptin HU892 (**133**)	892.5	Arg	Val	Hph	*N*-MeHty	Ile		219
Anabaenopeptin KT864 (**134**)	864.5	Har	Ile	Hty	*N*-MeAla	Phe		220
Anabaenopeptin MM823 (**135**)	823.4	Glu(OMe)	Val	Hty	*N*-MeAla	Phe	CHYi, ELAi	221
Anabaenopeptin MM850 (**136**)	850.5	Arg(OMe)	Val	Hty	*N*-MeAla	Phe	TRPi, CHYi, ELAi	221
Anabaenopeptin MM913 (**137**)	913.5	Tyr	Ile	Hph	*N*-MeHty	Ile		221
Anabaenopeptin NZ825 (**138**)	825.4	Phe	Ile	Hph	*N*-MeGly	Hph		222

Anabaenopeptin NZ841 (**139**)	841.4	Phe	Ile	Hty	*N*-MeGly	Hph		222
Anabaenopeptin NZ857 (**140**)	857.4	Phe	Ile	Hty	*N*-MeGly	Hty		222
Anabaenopeptin 820 (**141**) [c]	820.5	Arg	Val	Hph	MeAla	Phe		183
Anabaenopeptin 908 (**142**)	908.5	Arg	Val	Hty	*N*-MeHty	Ile	CPAi	223
Anabaenopeptin 915 (**143**)	915.5	Tyr	Val	Hty	*N*-MeHty	Ile		223
Ferintoic Acid A (**144**)	866.4	Trp	Val	Hty	*N*-MeAla	Phe		224
Ferintoic Acid B (**145**)	880.4	Trp	Ile	Hty	*N*-MeAla	Phe		224
Lyngbyaureidamide A (**146**)	855.5	Phe	Ile	Hty	*N*-MeAla	Hph		22
Lyngbyaureidamide B (**147**)	841.4	Phe	Ile	Hty	*N*-MeAla	Phe		22
Nodulapeptin A (**148**)	929.4	Ile	Met(O_2)	Hph	*N*-MeHty	Ser(OAc)		225
Nodulapeptin B (**149**)	913.4	Ile	Met(O)	Hph	*N*-MeHty	Ser(OAc)		225
Nodulapeptin 899 (**150**)	899.4	Phe	Val	Hph	*N*-MeHty	Met		226
Nodulapeptin 901 (**151**)	901.4	Phe	Val	Hph	*N*-MeHty	Met(O)		226
Nodulapeptin 917 (**152**)	917.4	Phe	Val	Hph	*N*-MeHty	Ser(OAc)		226
Oscillamide B (**153**)	868.4	Arg	Met	Hty	*N*-MeAla	Phe	PPi	216
Oscillamide C (**154**)	956.5	Arg	Ile	Hty	*N*-MeHty	Phe	PPi	216
Oscillamide H (**155**)	929.5	Tyr	*N*-MeIle	Hty	Hty	Ile		227
Oscillamide Y (**156**)	857.4	Tyr	Ile	Hty	*N*-MeAla	Phe	CHYi	216,228
Schizopeptin 791 (**157**)	791.5	Ile	Ile	Hph	*N*-MeAla	Phe	TRPi	229

[a] Amino acid numbering is as indicated in Anabaenopeptin A (**2**); D-Lys is omitted as it is always present in position two. [b] Masses are rounded to one decimal place. [c] Reported structure is based on tandem mass spectrometry data so identity of some amino acids is putative. [d] rNEc = Relaxation of norepinephrine-induced contraction; CPAi = Inhibition of carboxypeptidase-A; PPi = Inhibition of protein phosphatases 1 & 2A; TRPi = Inhibition of trypsin; CHYi = Inhibition of chymotrypsin; ELAi = Inhibition of elastase.

isomerisation of L-Lys to D-Lys, whilst the presence of methyltransferase domains allows for the methylated variants sometimes observed.[29,210] As with microcystin biosynthesis, the substrate specificity of the various adenylation domains determines which amino acid is incorporated at each position and a lack of specificity at a certain domain results in multiple anabaenopeptins being produced by a single cyanobacterial strain.

To date, anabaenopeptins have been found in multiple cyanobacterial genera including; *Anabaena*,[21] *Aphanizomenon*,[212] *Lyngbya*,[22] *Microcystis*,[219] *Nodularia*,[225] *Oscillatoria*[215] and *Schizothrix*.[229] The varied structures of the anabaenopeptins, listed in Table 2.1, also have varied biological activities including; relaxation of norepinephrine-induced contraction,[21] protein phosphatase inhibition,[216] carboxypeptidase-A inhibition[217] and protease inhibition.[228]

Compounds structurally related to anabaenopeptins have been found in marine cyanobacteria[230] and sponges,[231-235] as well as terrestrial cyanobacteria.[236] The structures are similar to that of an anabaenopeptin as they are D-Lys mediated cyclic pentapeptides which contain a CO-linked amino acid sidechain, as in mozamide A (**158**).[233] However, they regularly contain modified tryptophan residues and almost all contain a leucine in position four instead of an aromatic amino acid. The presence of these compounds in sponges is assumed to be due to a symbiotic relationship with cyanobacteria.[231-235] This assumption is supported by observations that the cyclic peptides patellamides A and C,[237] which were initially isolated from an ascidian, were actually produced by its cyanobacterial symbiont *Prochloron didemni*.

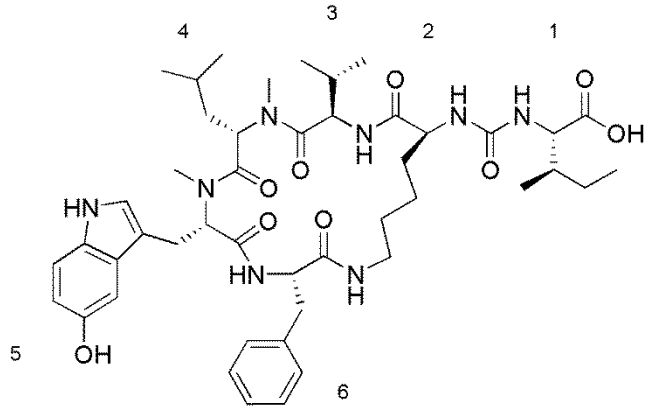

(158)

This chapter details the partial characterisation of a new anabaenopeptin, found in an environmental sample collected from Lake Wiritoa (Manawatu, New Zealand) using matrix-assisted laser desorption/ionisation-time of flight mass spectrometry (MALDI-TOF MS).

2.2 RESULTS

The positive ion MALDI-TOF mass spectrum of the Lake Wiritoa sample (Figure 2.1) showed multiple peaks relating to the masses of various known oligopeptides including several anabaenopeptins (Table 2.2). Analysis of the daughter ion spectra collected by MALDI post source decay (PSD) confirmed these identifications and indicated the presence of an unknown metabolite with *m/z* 907.

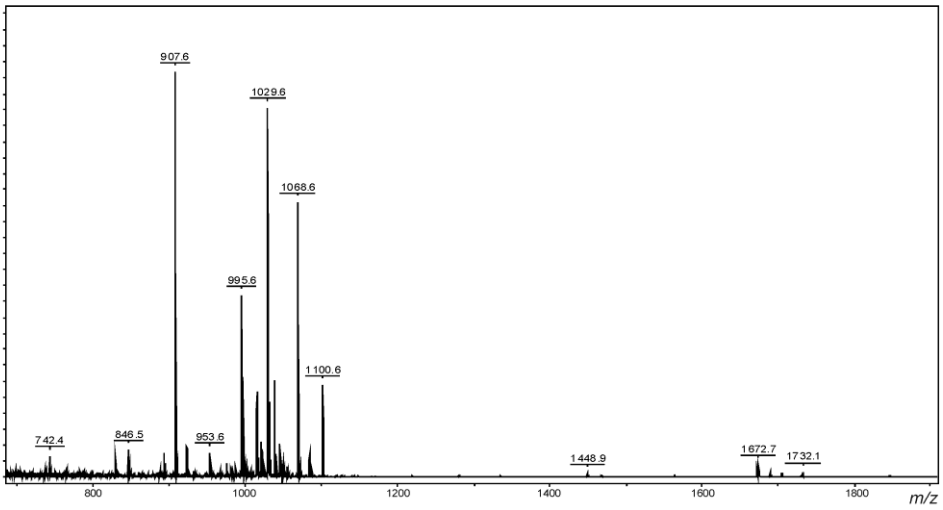

Figure 2.1: Positive ion MALDI-TOF mass spectrum of a methanol extract of the Lake Wiritoa sample.

Table 2.2: Assignment of the ions observed in the MALDI-TOF mass spectrum of the Lake Wiritoa sample.

m/z	Assignment	*m/z*	Assignment
742.4	Nostoginin BN741[238]	828.5	Anabaenopeptin D[214]
846.5	Unknown compound	887.6	Microginin 299-A[239]
893.5	Anabaenopeptin HU892[219]	907.6	**New Anabaenopeptin 906**
923.6	Anabaenopeptin H[217]	953.6	MC-AR[38]
975.6	Unknown compound	987.6	Micropeptin A[240] or K139[241]
995.6	MC-LR[31]	1015.6	Desmethyl MC-FR[58,59]
1021.6	Unknown compound	1029.6	MC-FR[38]
1038.6	MC-RR[70]	1045.6	MC-YR[31]
1049.6	MC-(H_4)YR[57]	1054.6	Desmethyl MC-WR[58]
1068.6	MC-WR[38]	1084.6	Unknown microcystin
1100.6	Unknown microcystin	1448.9	Unknown compound
1672.7	Unknown compound	1732.1	Unknown compound

The MALDI PSD spectrum of the *m/z* 907 ion (Figure 2.2), in conjunction with the sequences of the presently known anabaenopeptins (Table 2.1), allowed for the postulation of the structure of the new anabaenopeptin 906 (**159**). The PSD spectrum showed the loss of a 200 Da fragment, which is diagnostic of an anabaenopeptin possessing an arginine (Arg) sidechain.[181] The low *m/z* species (Table 2.3) indicated the presence of Arg (*m/z* 129), Lys (*m/z* 84), isoleucine (Ile; *m/z* 86), methylleucine (MeLeu; *m/z* 100), and methylhomotyrosine (MeHty; *m/z* 107, 164). Thus, five of the six amino acids present in the anabaenopeptin were identified and the missing mass entity correlated with that of a phenylalanine (Phe) residue.

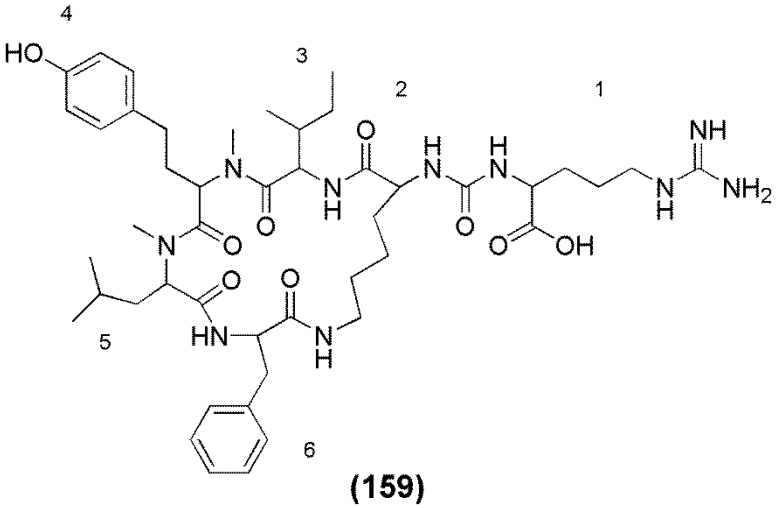

(159)

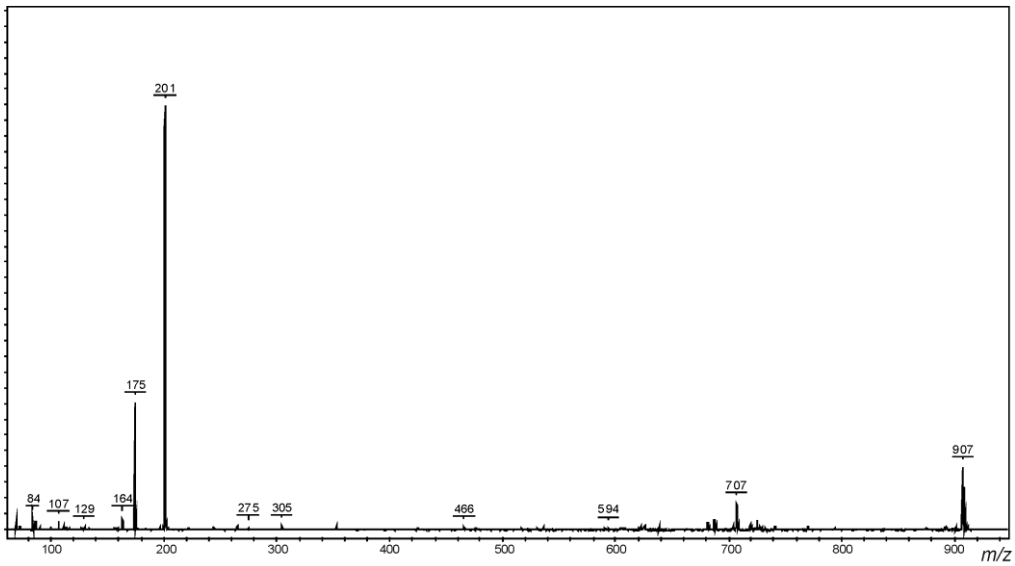

Figure 2.2: Tandem mass spectrum of anabaenopeptin 906. Fragmentation induced by matrix-assisted laser desorption/ionisation post-source decay.

Table 2.3: Tandem mass spectrometry fragment ions for anabaenopeptin 906 observed by matrix-assisted laser desorption/ionisation post-source decay.

m/z	Fragment Assignment	*m/z*	Fragment Assignment
84	Lys fragment	86	Ile immonium
100	MeLeu immonium	107	Tyr sidechain
112	Arg fragment	129	Arg immonium
164	MeHty immonium	175	Arg + 2H
201	CO-Arg	275	MeLeu-Phe + H
305	Ile-MeHty + H	449	Arg-CO-Lys-Phe − CO + 2H
466	MeHty-MeLeu-Phe + H	579	Ile-MeHty-MeLeu-Phe + H
594	Lys-Phe-MeLeu-MeHty + 2H	603	Arg-CO-Lys-Phe-MeLeu + H
707	Lys-Ile-MeHty-MeLeu-Phe + 2H	907	M + H

The fragment ions which characterise the CO-linked Arg sidechain are displayed in Figure 2.3A.[181] As well as being attached to the Arg sidechain, the Lys at position two is also attached to the positions three and six ring amino acids. The *m/z* 449 fragment showed that Phe was one of these amino acids, however, the fragment could represent Phe attached to the sidechain amine of Lys (Figure 2.3A), or to the backbone amine of Lys (Figure 2.3B).

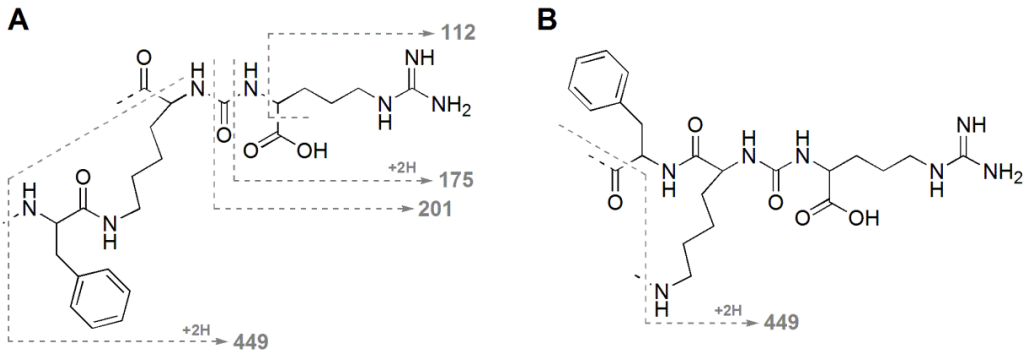

Figure 2.3: Fragment ions observed from the sidechain of anabaenopeptin 906 with phenylalanine present in position six **(A)** and position three **(B)**.

The higher mass fragments provide the sequence of the ring amino acids in anabaenopeptin 906 (Table 2.3). The *m/z* 275 fragment indicated that Phe was joined to MeLeu (Figure 2.4) and the *m/z* 449 fragment showed that Phe was also attached to Lys, placing it in either position three or six. The *m/z* 466 fragment therefore, showed that MeHty was attached to MeLeu since Phe was already attached to both Lys and MeLeu. This gave a final ring sequence of

Ile-MeHty-MeLeu-Phe, and supported the presence of the Ile-MeHty fragment at *m/z* 305.

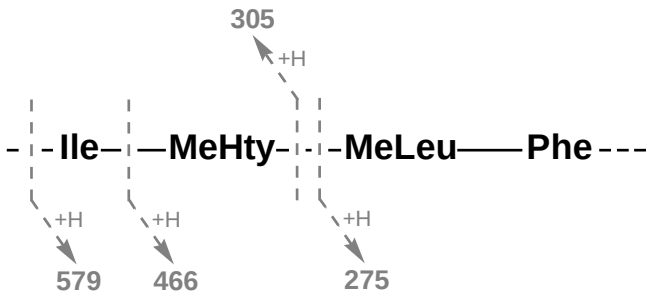

Figure 2.4: Tandem mass spectrometry fragment ions which indicate the ring amino acid sequence in anabaenopeptin 906.

Although none of the observed fragments confirmed the order in which the amino acids were present in the ring or the identity of the Leu/Ile and MeLeu/MeIle residues present in positions three and five, the proposed structure **159** was constructed using the fragments listed in Table 2.3 in conjunction with the sequences of the presently known anabaenopeptins (Table 2.1). Here, Phe is commonly seen at position six and never in position three. Also, an aromatic amino acid, such as Hty, has always been present at position four. These observations suggested that the order of the ring amino acids is most likely Ile-MeHty-MeLeu-Phe instead of in the opposite order. According to the tandem MS (MS/MS) data, the position three amino acid could be either an Ile or a Leu, as these amino acids have an identical mass. However Ile is commonly observed in this position and Leu has never been reported. Similarly, MeLeu has been reported in position five once, but MeIle has not.

2.3 DISCUSSION

The proposed structure for anabaenopeptin 906 was constructed using MS/MS data and the amino acid sequences of the presently known anabaenopeptins. Whilst the MS/MS data indicated the amino acids present in anabaenopeptin 906 and the order of these amino acids, it does not indicate their position in the structure. The presently known anabaenopeptin sequences provide a strong indication that Ile is more likely to be in position three than Phe, which enabled a sequence of Arg-Lys-Ile-MeHty-MeLeu-Phe to be postulated.

The MS/MS data cannot confirm whether the extra 14 Da mass on two of the amino acids (MeHty and MeLeu) was an *N*-methylation of the amine in the backbone of the amino acid chain or an additional methylene in the branching arm of the amino acid sidechain. However, in the case of the MeHty in position four, the methylation cannot be attributed to an *O*-methylation of the hydroxyl group of the sidechain, as this would cause the observed Tyr sidechain fragment ion (*m/z* 107; Table 2.3) to be 14 Da heavier.

Leu and Ile, which have identical masses, can in some cases be differentiated by MS/MS. The use of high-energy, collision-induced dissociation (CID) can yield sufficiently intense fragmentation that a portion of the Leu/Ile sidechain breaks off.[242,243] As a result, the d- or w-fragment ions for Leu would be 42 Da less than the corresponding a- or z-ions, whilst those for Ile would show a reduction of 28 Da (Figure 2.5).[242,243] Neither of these fragment ions were observed in the MS/MS spectrum. The likely reason for their absence was the low abundance of these ions, combined with the "LIFT" technology used in this particular MALDI mass spectrometer. When MS/MS analyses are performed on an instrument operating without "LIFT", multiple fragment ion spectra would be collected over different *m/z* ranges to obtain the complete spectrum. A consequential benefit of this is that a particular *m/z* region, where the fragment ions of interest were expected to be, can be focused upon and as a result, enhance the spectrum. Using an instrument equipped with "LIFT" technology, all the fragment ions were assessed simultaneously and a single region could not be focused on.

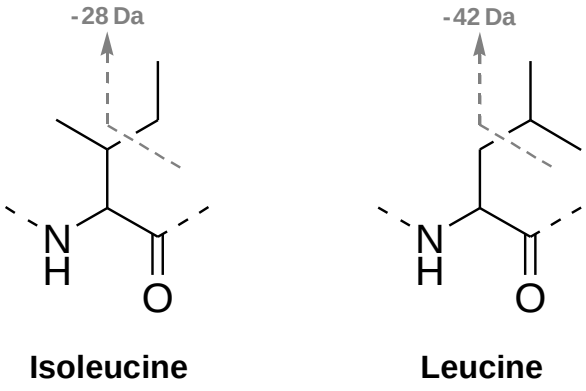

Figure 2.5: Sidechain fragmentation of the amino acids isoleucine and leucine by high-energy, collision-induced dissociation.

As discussed in Section 2.1, various anabaenopeptins have been reported to have several different bioactivities including; relaxation of norepinephrine-induced contraction,[21] protein phosphatase inhibition,[216] carboxypeptidase inhibition[217] and protease inhibition.[228] Utilising the structures and bioactivities of the known anabaenopeptins (Table 2.1) and comparing them with the proposed structure of anabaenopeptin 906, the potential activities of this new compound can be postulated. Several anabaenopeptins inhibit carboxypeptidase-A, however it is unlikely that anabaenopeptin 906 would prove an effective inhibitor, since anabaenopeptins possessing an Arg sidechain have been shown to be ineffective or less effective inhibitors of the enzyme.[212] Anabaenopeptin 906 could inhibit protein phosphatases 1 and 2A, as an Arg sidechain has been shown to be important for inhibition of this enzyme.[216] However, an *N*-MeHty in position five was shown to enhance this inhibition and this amino acid is absent in anabaenopeptin 906. Only two anabaenopeptins (anabaenopeptins A and B) have been assessed for relaxation of norepinephrine-induced contraction.[21] Given that anabaenopeptin 906 shows some structural similarity to anabaenopeptin B, it could possibly exhibit the same effect.

Since the putative structure of anabaenopeptin 906 was determined from a small environmental sample (≈ 0.5 mg), there was insufficient material to proceed with purification and further characterisation. In the following year, cyanobacterial blooms at Lake Wiritoa were monitored by MALDI-TOF MS for the presence of anabaenopeptin 906, but it was not observed. This study illustrates the power, and the limitations of characterising cyanobacterial secondary metabolites by MALDI-TOF MS. Whilst a putative structure was pieced together quickly from a small amount of sample, the identity of several of the amino acids present could not be confirmed and their stereochemistry would never be deduced by this technique. Ultimately, full characterisation of this novel compound would require purification of a larger sample and the use of other techniques such as nuclear magnetic resonance spectroscopy and amino acid analysis.

2.4 CONCLUSIONS

A putative structure for anabaenopeptin 906 was constructed from MALDI MS/MS data, in conjunction with the sequences of the presently known anabaenopeptins. However, the identity and position of several amino acids cannot be stated with absolute certainty without the use of additional techniques. Unfortunately, the sample size did not allow for this, illustrating both the power, and the limitations of using such a sensitive technique for structural characterisation.

CHAPTER 3

Structural Characterisation of New Microcystins from *Microcystis* CYN06

3.1 INTRODUCTION

Microcystins (MCs) are cyclic heptapeptides which can be toxic to mammals. They are generally composed of the unique β-amino acid Adda (3-amino-9-methoxy-2,6,8-trimethyl-10-phenyldeca-4,6-dienoic acid), D-glutamic acid (Glu), *N*-methyldehydroalanine (Mdha), D-alanine (Ala), D-erythro-β-methylaspartic acid (Masp) and two variable L-amino acids. To date, there have been at least 111 different microcystin congeners characterised (Appendix A), mostly due to substitutions of the variable L-amino acids in positions two and four, although modifications have been reported for all of the amino acids.[33]

The different microcystin congeners range in toxicity according to their ability to inhibit the important eukaryotic regulatory enzymes, serine/threonine protein phosphatases 1 and 2A.[82] Microcystins predominantly affect the liver cells of mammals, where inhibition of the protein phosphatases in these cells results in excessive signalling due to a lack of regulation via the phosphatases (see Section 1.2.7).[244]

Microcystins have been reported to be produced by numerous cyanobacterial genera when the necessary microcystin synthase genes are present. These non-ribosomal peptide synthetase (NRPS) and polyketide synthase (PKS) genes produce a multi-enzyme complex which sequentially adds onto phenylacetate to produce a peptide chain which is condensed to form the cyclic microcystin (see Section 1.3.1).[99-101]

The occurrence of different microcystin congeners is due to differences in the coding of the microcystin synthase genes of different cyanobacterial strains. At times, the McyA1 *N*-methyltransferase domain can be inefficient or inactive,

which results in a position seven desmethyl variant. The amino acid specificity of the various adenylation domains is dependent upon their sequence. Changes to this sequence can cause the domains to be specific for a different amino acid or to recognise more than one amino acid.[110] The substrate specificity of many of the adenylation domains is relatively conserved, whilst the substrate specificity of the position two and four adenylation domains are varied (see Section 1.3.2).

A single strain of cyanobacteria can often produce more than one microcystin congener. This is mainly due to at least one adenylation domain possessing relaxed substrate specificity and being able to incorporate different amino acids into the structure.[110,114] A cyanobacterial strain will generally produce around four microcystin congeners, in most cases; MC-LR, MC-RR and desmethyl analogues of each (Appendix C). Whilst uncommon, cyanobacterial strains which produce up to 47 microcystin congeners have been reported.[245]

A *Microcystis* species (CYN06) isolated from Lake Hakanoa (Huntly, New Zealand) in 2005[246] was investigated as it produced a large number of microcystin congeners, including ten new variants. As modern mass spectrometry (MS) based techniques for microcystin detection rely upon previous knowledge of the compounds (see Section 1.4), the structural characterisation of these new microcystins was conducted.

3.2 RESULTS

3.2.1 Oligopeptide Diversity of *Microcystis* CYN06

A methanol extract of *Microcystis* CYN06 was analysed by matrix-assisted laser desorption/ionisation-time of flight (MALDI-TOF) MS. The resulting spectrum contained multiple ions spanning a mass range of 600-1,800 Da (Figure 3.1). Further investigation of these ions by MALDI post source decay (PSD), indicated the presence of linear, cyclic and tricyclic oligopeptides including; aeruginosins, microcystins, microviridins and a group of unknown metabolites with molecular weights of approximately 1,500 Da.

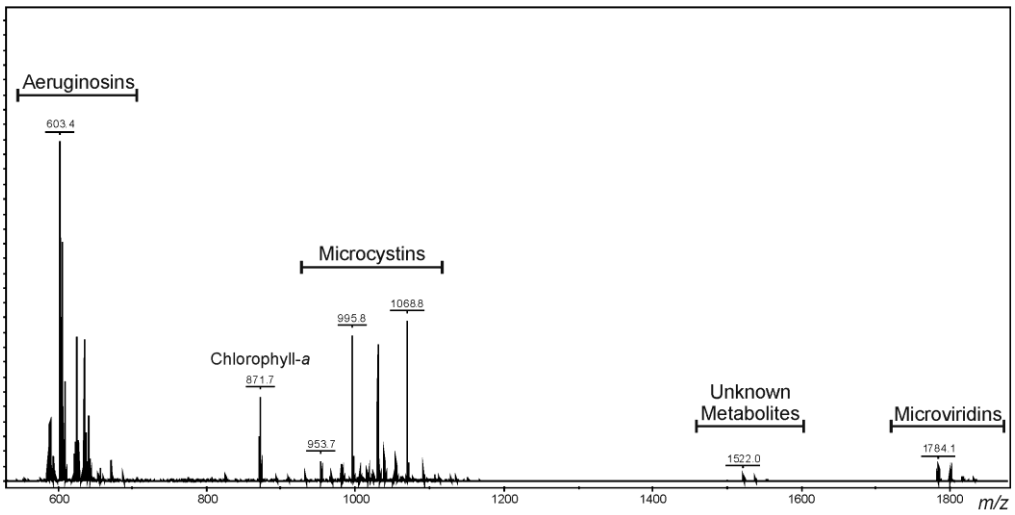

Figure 3.1: Positive ion MALDI-TOF mass spectrum of a methanol extract of CYN06.

The aeruginosins produced by CYN06 included the known aeruginosin 602,[183] as well as several new aeruginosin analogues with masses of 604, 616, 618, 620, 634 and 660 Da. The microviridins present may include the known microviridin I,[247] however the tandem MS (MS/MS) analysis could not confirm this. Several new microviridins with masses of 1779, 1745, 1780, 1759 and 1791 Da were also present in the extract. No attempt was made in the present study to purify and characterise the new aeruginosins and microviridins, but characterisation of these compounds form the basis of the current research in our group.

The MALDI-TOF MS and MS/MS analysis of CYN06 also indicated the presence of a plethora of arginine-containing microcystins (Figure 3.2A). This included a new analogue of MC-RA with a position three aspartic acid (Asp; [Asp^3] MC-RA; **160**). Since microcystins which do not contain an arginine residue have a low ionisation efficiency using MALDI,[184] the microcystin diversity of CYN06 was further investigated using high performance liquid chromatography (HPLC) with electrospray ionisation (ESI) MS. The LC-MS analysis (Figure 3.2B) revealed the presence of fifteen microcystin congeners which were not evident from the MALDI-TOF MS analysis. In total, 27 microcystin congeners were detected, ten of which were new (**160**-**169**; Table 3.1). These microcystins ranged in polarity from hydrophilic (MC-RR) to slightly hydrophobic (MC-WL) and in size from 895.5 Da ([Asp^3] MC-LA) to 1067.5 Da (MC-WR). CYN06 also contained oxidised tryptophan microcystin congeners which are described in Chapter 4 of this thesis.

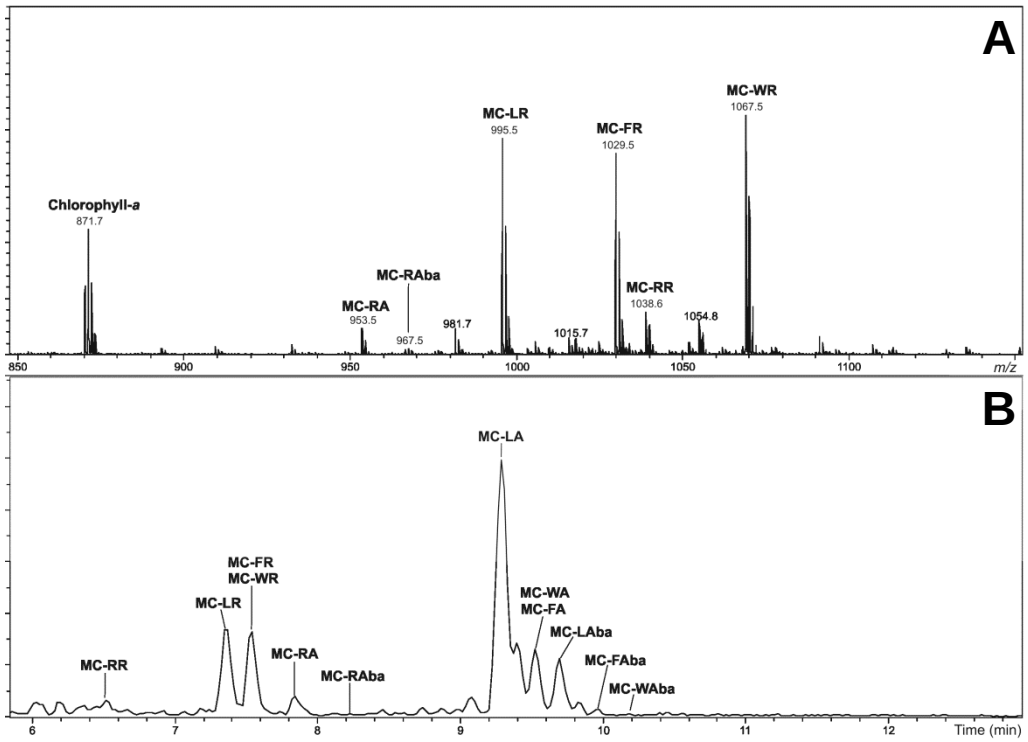

Figure 3.2: Positive ion MALDI-TOF mass spectrum of the microcystin-containing region (*m/z* 850-1,150; **A**) and a liquid chromatography-mass spectrometry basepeak chromatogram (negative ion; *m/z* 850-1,150; **B**) of a methanol extract of CYN06.

A microcystin containing a terminal alkene, as is found in Mdha and dehydroalanine (Dha), will readily react with β-mercaptoethanol under alkaline conditions.[41] When dehydrobutyrine (Dhb) is present, this reaction rate is hundreds of times slower.[248] A β-mercaptoethanol derivatisation of the CYN06 extract underwent rapid reaction ($t_{½}$ < 18 min) and all of the congeners were fully derivatised within four hours (see Appendix D.2). This indicated that each of the microcystins identified contained Dha or Mdha. Tandem MS analysis of each congener showed that an 83 Da moiety was present at position seven (Appendix E); therefore, each congener was designated as containing Mdha.

The microcystin congeners produced by CYN06 show variability of the amino acids at both positions two and four. This indicates that the microcystin synthase in CYN06 has relaxed substrate specificity at McyB1 as well as at McyC (see Section 1.3.2). The presence of [Asp^3] desmethyl congeners indicates that the adenylation domain of McyB2 recognises both Masp and Asp. This results in approximately 2.5% of each microcystin congener containing an Asp in position three. As the various substitutions occur at different levels, not all of the possible

Table 3.1: Structures, molecular masses and retention times of the microcystins observed in CYN06.

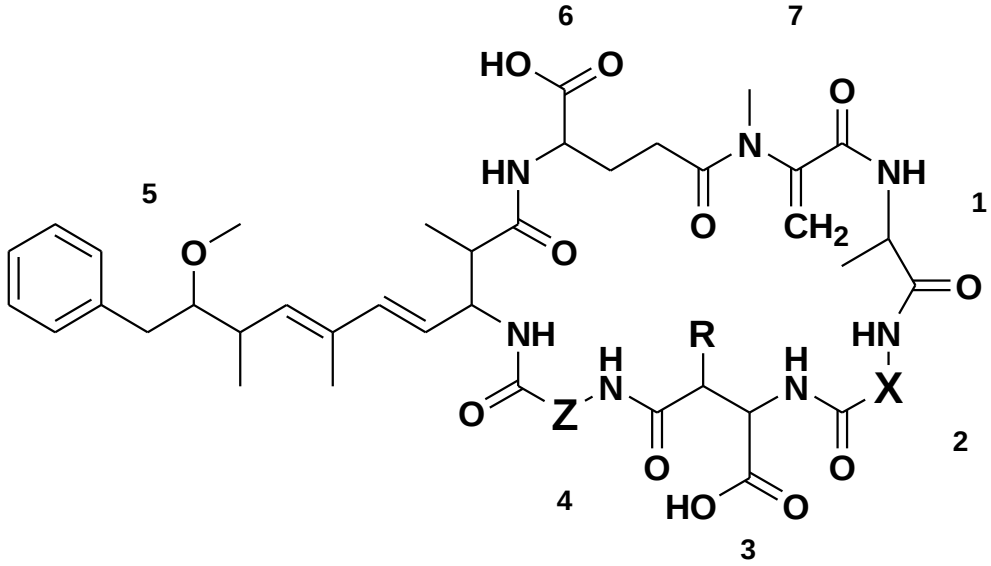

	Microcystin	M_r [a] (Da)	RT [b] (min)	X	Z	R	References
MC-RRs	[Asp^3] MC-RR (**67**)	1023.6	6.32	Arg	Arg	H	60
	MC-RR (**85**)	1037.6	6.45	Arg	Arg	CH_3	70,119,120
MC-XRs	MC-YR (**97**)	1044.5	7.20	Tyr	Arg	CH_3	31
	[Asp^3] MC-LR (**30**)	980.5	7.32	Leu	Arg	H	47,74
	MC-LR (**7**)	994.5	7.35	Leu	Arg	CH_3	31,82
	[Asp^3] MC-FR (**59**)	1014.5	7.52	Phe	Arg	H	58
	MC-FR (**72**)	1028.5	7.54	Phe	Arg	CH_3	38
	[Asp^3] MC-WR (**105**)	1053.5	7.56	Trp	Arg	H	58
	MC-WR (**113**)	1067.5	7.60	Trp	Arg	CH_3	38
MC-RZs	[Asp^3] MC-RA (**160**)	938.5	7.80	Arg	Ala	H	This Study
	MC-RA (**16**)	952.5	7.84	Arg	Ala	CH_3	39,41
	[Asp^3] MC-RAba (**161**)	952.5	8.16	Arg	Aba	H	This Study
	MC-RAba (**19**)	966.5	8.18	Arg	Aba	CH_3	41
	MC-RL (**41**)	994.5	8.35	Arg	Leu	CH_3	41
MC-XAs	MC-YA (**17**)	959.5	9.01	Tyr	Ala	CH_3	31
	[Asp^3] MC-LA (**8**)	895.5	9.12	Leu	Ala	H	34
	MC-LA (**9**)	909.5	9.29	Leu	Ala	CH_3	32
	[Asp^3] MC-FA (**162**)	929.5	9.46	Phe	Ala	H	This Study
	MC-FA (**163**)	943.5	9.52	Phe	Ala	CH_3	This Study
	[Asp^3] MC-WA (**164**)	968.5	9.48	Trp	Ala	H	This Study
	MC-WA (**165**)	982.5	9.54	Trp	Ala	CH_3	This Study
MC-XAbas	MC-LAba (**11**)	923.5	9.69	Leu	Aba	CH_3	34,35,249
	MC-FAba (**166**)	957.5	9.97	Phe	Aba	CH_3	This Study
	MC-WAba (**167**)	996.5	10.24	Trp	Aba	CH_3	This Study
MC-XLs	MC-LL (**14**)	951.5	10.50	Leu	Leu	CH_3	37
	MC-FL (**168**)	985.5	10.71	Phe	Leu	CH_3	This Study
	MC-WL (**169**)	1024.5	10.77	Trp	Leu	CH_3	This Study

[a] Molecular weights are rounded to one decimal place. [b] RT = Retention time on a C_{18} column as per Table 9.3.

congeners have been observed in the present study, namely [Asp^3] analogues of -RL, the -XAba, -XL and -YZ microcystin congeners. Tyrosine-containing analogues of the -XAba and -XL congeners were also not observed.

On account of the difference in abundance of the various microcystins produced by CYN06, not all of the new microcystins were purified in adequate amounts to be fully characterised. MC-FA and MC-WA were isolated in sufficient quantities to undertake analysis by nuclear magnetic resonance (NMR) spectroscopy, MS and amino acid analysis. The other microcystins were present at lower levels and only MS characterisation could be performed. Whilst the characterisation of the known microcystins produced by CYN06 is not detailed in this chapter, the MS/MS characterisation of each microcystin listed in Table 3.1 can be found in Appendix E.

3.2.2 Structural Characterisation of MC-FA from CYN06

The presence and stereochemistry of several of the amino acids present in MC-FA (**163**) were determined by Advanced Marfey's amino acid analysis.[204,205] Derivatisation of amino acids with L-FDLA allowed for the separation of both stereoisomers by reversed-phase C_{18} HPLC. LC-MS analysis of the L-FDLA derivatives of hydrolysed MC-FA indicated it comprised seven amino acids (Figure 3.3). The presence of D-Glu (*m/z* 440; 14.3 min), L-Ala (*m/z* 382; 15.8 min), D-Ala (*m/z* 382; 18.6 min) and L-phenylalanine (Phe; *m/z* 458; 21.3 min) was determined by comparison with standard amino acids. The identities of the remaining peaks were determined by comparison with the L-FDLA derivatives of hydrolysed MC-LR (Appendix F.3). This indicated the presence of D-Masp (*m/z* 440; 15.9 min), *N*-methylamine (*m/z* 324; 19.6 min) and the methanol-loss product of 3(*S*)-Adda (*m/z* 592; 32.9 min). *N*-methylamine is produced during the breakdown of the Mdha or *N*-methyldehydrobutyrine observed in microcystins.[250]

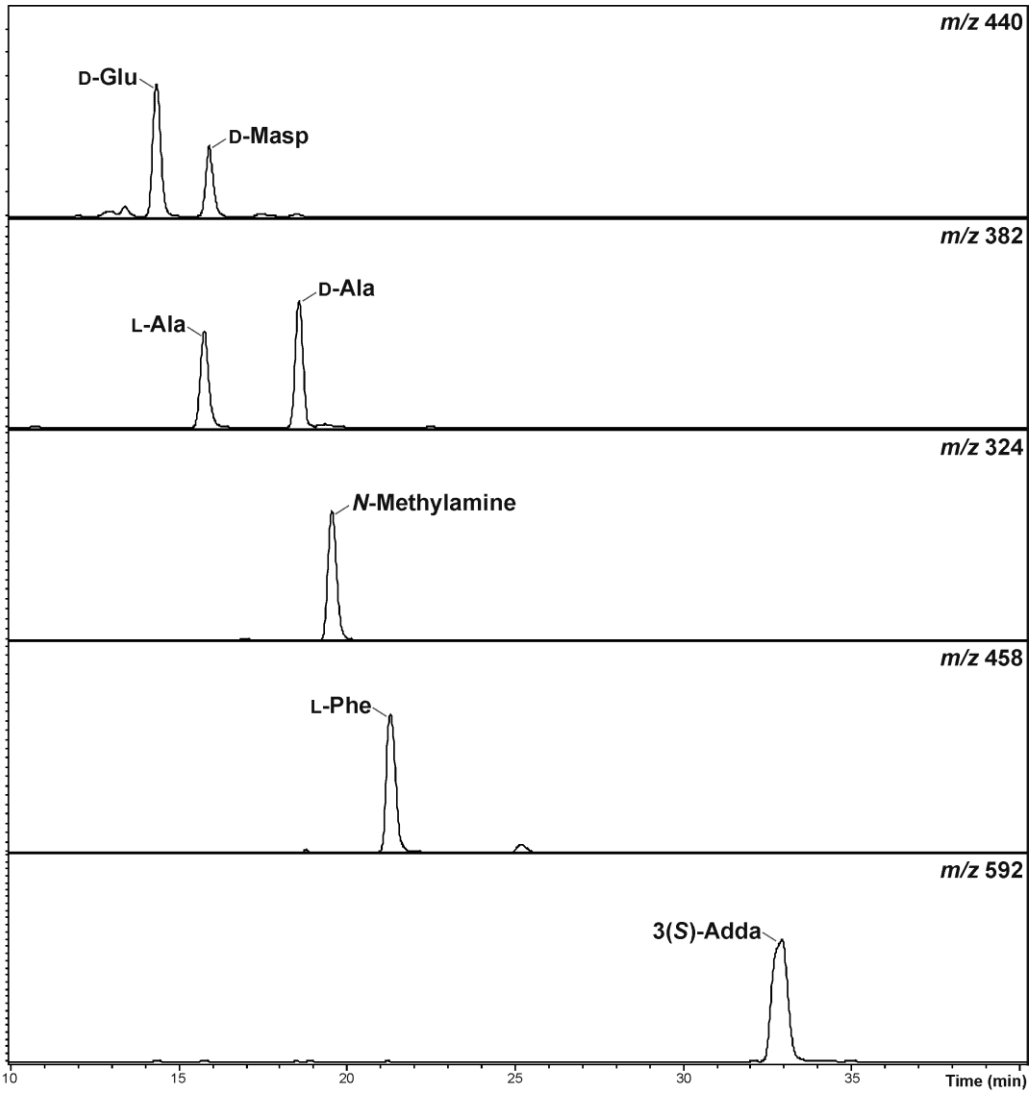

Figure 3.3: Advanced Marfey's amino acid analysis of MC-FA. Extracted ion chromatograms of hydrolysed MC-FA derivatised with L-FDLA.

The high resolution MS (HRMS) analysis of **163** yielded a *m/z* of 966.4550, consistent with the sodium adduct ion of a cyclic peptide containing the six amino acids indicated by amino acid analysis (L-Ala, D-Ala, Glu, Masp, Phe, Adda) and Mdha ($C_{49}H_{65}N_7O_{12}Na$, *m/z* 966.4583, Δ −3.41 ppm).

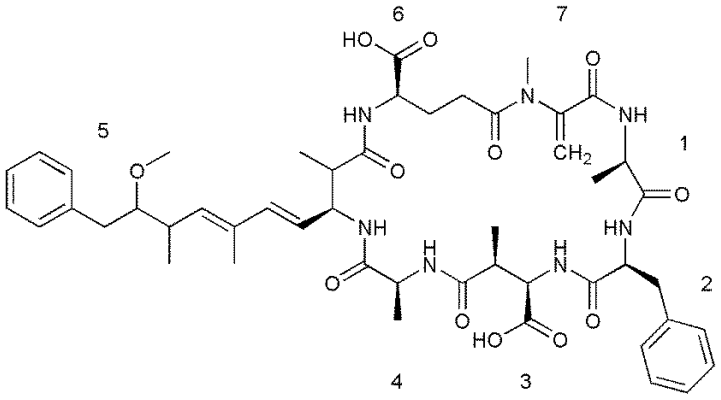

(163)

The MS/MS spectrum of **163** (Figure 3.4) indicated that it was a microcystin with a structure similar to the majority of those previously characterised (Appendix A). The presence of Adda was indicated by the loss of 134 Da (*m/z* 810) and 313 Da (*m/z* 631).[34] These fragments represented the loss of a portion of the Adda sidechain and the entire amino acid respectively (Figure 3.4). The mass difference between other fragment ions indicated the position of the amino acids in the structure (Table 3.2).

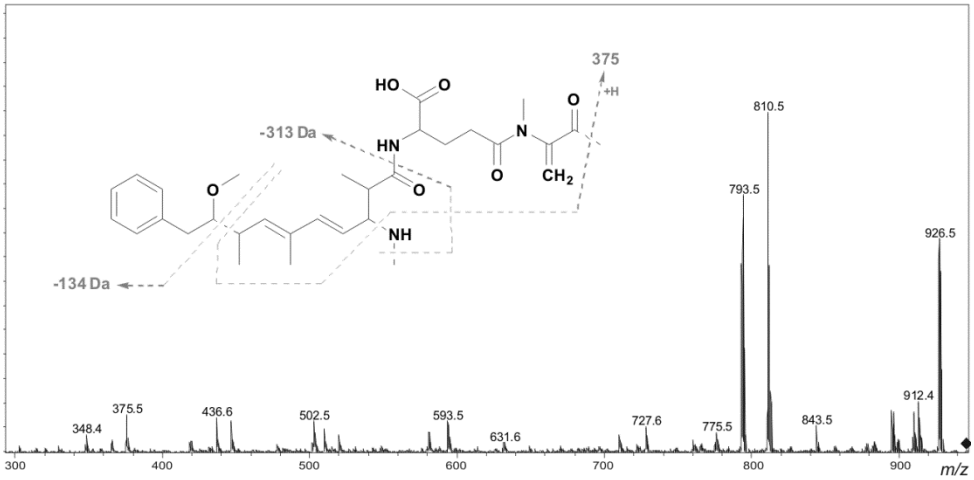

Figure 3.4: Tandem mass spectrum of MC-FA and fragments commonly observed from the generic microcystin structure. Fragmentation induced by electrospray ionisation collision-induced dissociation.

Table 3.2: Tandem mass spectrometry fragment ions for MC-FA observed by electrospray ionisation collision-induced dissociation.

m/z	Fragment Assignment [a]	*m/z*	Fragment Assignment [a]
348	Ala-Phe-Masp + H	365	Phe-Masp-Ala + NH_4
375	Adda'-Glu-Mdha + H	419	Ala-Phe-Masp-Ala + H
436	Ala-Phe-Masp-Ala + NH_4	446	Adda'-Glu-Mdha-Ala + H
502	Mdha-Ala-Phe-Masp-Ala + H	509	Adda-Glu-Mdha – NH_3 + H
519	Mdha-Ala-Phe-Masp-Ala + NH_4	580	Adda-Glu-Mdha-Ala – NH_3 + H
593	Adda'-Glu-Mdha-Ala-Phe + H	631	Glu-Mdha-Ala-Phe-Masp-Ala + H
727	Adda-Glu-Mdha-Ala-Phe – NH_3 + H	856	Adda-Glu-Mdha-Ala-Phe-Masp – NH_3 + H
792	M – Adda sidechain – H_2O + H	810	M – Adda sidechain + H
843	M – Mdha – H_2O + H	926	M – H_2O + H
944	M + H		

[a] Adda' = Adda minus NH_2 and the sidechain ($C_9H_{11}O$).

The Adda'-Glu-Mdha fragment ion (*m/z* 375) commonly observed in microcystins[35,78] was extended to include Ala and Phe (Figure 3.5A). This sequence was supported by a similar ion series containing Adda minus NH_3

(*m/z* 509, 580, 727) and was extended to include Masp (Figure 3.5B). The fragment ion series which began with Phe-Masp-Ala (*m/z* 348) and extended in the opposite direction to include the second Ala residue, gave the complete amino acid sequence of Adda-Glu-Mdha-Ala-Phe-Masp-Ala. A fragment where Mdha and water were lost from the compound (*m/z* 843; Table 3.2) indicated that Adda and the second Ala residue were adjacent and that the structure was cyclic.

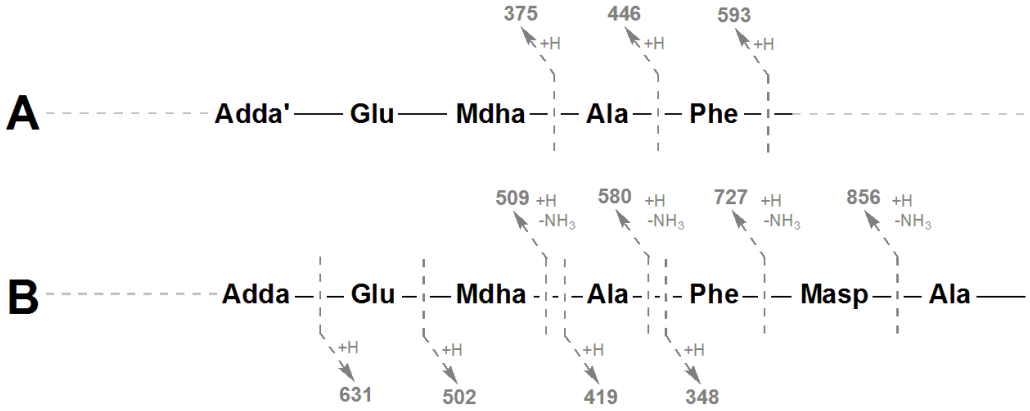

Figure 3.5: Tandem mass spectrometry fragment ions indicating the amino acid sequence in MC-FA.

The structures of several of the amino acids present in microcystins can only be confirmed by NMR spectroscopy. Interpretation of COSY, TOCSY, HSQC and HMBC spectra allowed for the assignment of the ^{1}H and ^{13}C NMR signals (Table 3.3). Several of the ^{1}H signals overlapped in the spectrum acquired at 400 MHz and the peak patterns had to be resolved using selective TOCSY experiments. Nuclear magnetic resonance spectra for MC-FA are presented in Appendix G.

Table 3.3: Nuclear magnetic resonance spectroscopy assignment of MC-FA at 400 MHz in CD_3OD.

AA[a]	^{13}C	^{1}H	Mult.[b] (*J* in Hz)	AA[a]	^{13}C	^{1}H	Mult.[b] (*J* in Hz)
D-Ala-1				**Adda**-5 cont.			
1	173.8	-		5	138.8	6.26	d (15.9)
2	49.1[c]	4.45	q (7.3)[d]	6	134.0	-	
3	18.0	1.30	d (7.3)	7	137.1	5.45	d (11.6)[d]
				8	37.8	2.59	m
L-Phe-2				9	88.5	3.26	dt (5.9, 6.7)[d]
1	178.9	-		10	39.1	2.67	dd (7.2, 14.0)
2	59.7	4.35[c]	m			2.82	dd (4.7, 14.0)
3	37.9	3.19 (2H)	m	11	140.7	-	
4	139.5	-		12 & 16	130.7	7.18[c]	d (7.8)
5 & 9	130.4	7.37	d (7.8)	13 & 15	129.3	7.25[c]	dd (7.3, 7.8)
6 & 8	129.5	7.24	dd (6.8, 7.8)[d]	14	127.1	7.16[c]	t (7.3)
7	127.7	7.17	t (6.8)[d]	17	16.4	1.06	d (6.8)[d]
				18	13.0	1.63	s
D-Masp-3				19	16.7	1.02	d (6.8)
1	nd	-		20	58.8	3.24	s
2	57.9	4.41[c]	d (3.9)				
3	41.6	3.13	m	**D-Glu**-6			
4	179.1	-		1	nd	-	
5	15.7	1.05	d (7.3)[d]	2	55.3	4.33[c]	m
				3	29.5	1.96	m
L-Ala-4						2.22	m
1	175.1	-		4	33.6	2.55 (2H)	m
2	49.3[c]	4.56	q (7.3)[d]	5	177.3	-	
3	17.5	1.25	d (7.3)				
				Mdha-7			
Adda-5				1	165.9	-	
1	176.8	-		2	146.6	-	
2	45.5	2.97	m	3	114.4	5.45	s[d]
3	56.7	4.59	dd (9.7, 10.9)			5.89	s
4	126.7	5.44	dd (10.9, 15.9)[d]	*N*-CH_3	38.5	3.30[c]	s

[a] AA = Amino acid (number indicates the position in the structure); nd = Not detected. [b] Mult. = Multiplicity of the proton signal; *J* = Coupling constant. [c] Signals were overlapped so chemical shifts were determined using correlations observed in 2D HSQC spectra. [d] Multiplicity and coupling constants were determined using 1D-selective TOCSY experiments.

NMR Characterisation of the Adda residue in MC-FA

The Adda residue in MC-FA was characterised by NMR spectroscopy through analysis of the results of ^{1}H, ^{13}C, DEPT, COSY, HSQC and HMBC experiments. The residue gave rise to sixteen proton signals; two singlets at 1.63 and 3.24 ppm, five doublets at 1.02, 1.06, 5.45, 6.26 and 7.18 ppm, a triplet at 7.16 ppm, five doublets of doublets at 2.67, 2.82, 4.59, 5.44 and 7.25 ppm, a doublet of triplets at 3.26 ppm, and two multiplets at 2.59 and 2.97 ppm (Figure 3.6 and Table 3.3). The HSQC spectrum correlated these signals with fifteen carbon signals and indicated that the 2.67 and 2.82 ppm protons were both attached to a carbon atom which resonated at 39.1 ppm. The DEPT-135 indicated that this carbon was the only methylene present in the residue.

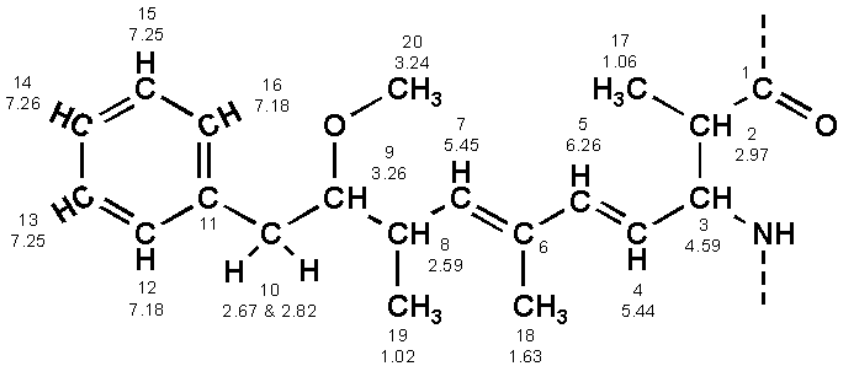

Figure 3.6: Structure of the Adda residue in MC-FA. Atoms are numbered according to Reference 111 and proton chemical shifts are indicated.

The chemical shift and multiplicity of the doublet at 1.06 ppm (H17) indicated it was a methyl adjacent to a methine. This was coupled to a multiplet at 2.97 ppm (H2; Figure 3.7A) which, due to its chemical shift, was likely to be adjacent to a carbonyl and another carbon. This was reinforced by a correlation in the HMBC spectrum between the H17 signal and a carbonyl at 176.8 ppm (C1; Figure 3.7B).

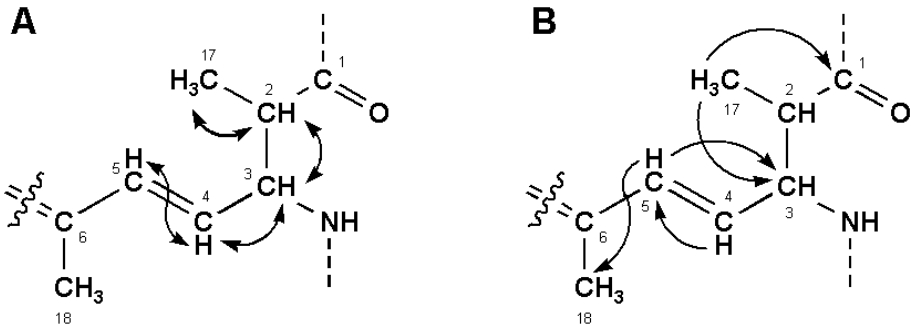

Figure 3.7: COSY **(A)** and HMBC **(B)** correlations for the C1-C6 portion of the Adda residue in MC-FA.

The C2 methine was also coupled to the 4.59 ppm resonance (H3; Figure 3.7A), which was coupled to the signal at 5.44 ppm (H4), also coupled to the proton signal at 6.26 (H5). The downfield chemical shifts of the H4 and H5 signals indicated that they were part of an alkene. The slightly downfield chemical shift of the H3 signal suggested that it was adjacent to two electron-withdrawing environments (an amine and an alkene). The multiplicity of the H5 doublet indicated that it was adjacent to a quaternary carbon. These pieces of information were used to build up the substructure in Figure 3.7. HMBC correlations were observed between H17-C3 and H5-C3 (Figure 3.7B) which supports that substructure if ^{3}J correlations were being observed.

The C6 quaternary terminated the COSY coupling beyond the C5 methine, however, multiple HMBC correlations to the C6 carbon re-established connectivity within the amino acid. HMBC ^{3}J correlations were observed from the H4 signal, as well as from a multiplet at 2.59 ppm (H8; Figure 3.8B). HMBC ^{2}J correlations were also observed from the H5 signal and a doublet at 5.45 ppm (H7). The downfield resonance of the H7 doublet indicated that it was part of an alkene and a COSY coupling to the multiplet at 2.59 ppm (Figure 3.8A; H8) indicated the double bond was shared with the C6 quaternary (since the chemical shift of the H8 proton was too upfield to be part of an alkene).

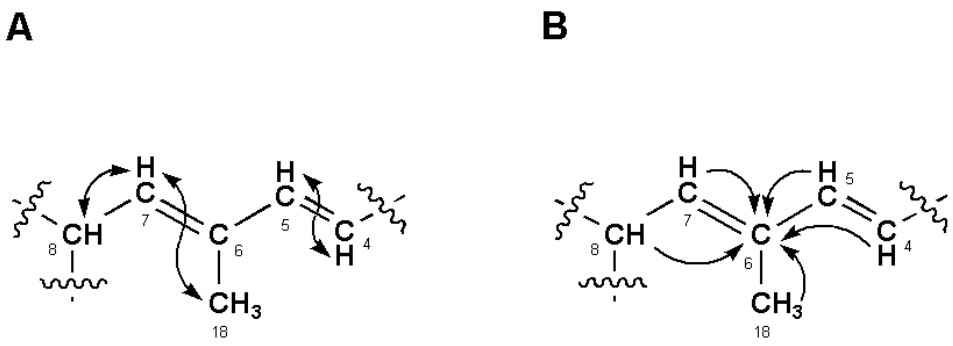

Figure 3.8: COSY **(A)** and selected HMBC **(B)** correlations for C4-C8 portion of the Adda residue in MC-FA.

An HMBC correlation to the C6 quaternary carbon was also observed from a singlet at 1.63 ppm (H18; Figure 3.8B). The HSQC spectrum indicated that it was attached to a carbon which resonated at 13 ppm, a signal which H5 showed an HMBC correlation to (Figure 3.7B). As the H18 signal was not split by any other protons, it was designated as a methyl attached to the C6 quaternary. The slightly downfield resonance was due to the double bond attached to the C6 carbon. The only COSY coupling observed for this signal was a ^{4}J coupling with the H7 doublet (Figure 3.8A).

The H8 multiplet was also coupled to a doublet at 1.02 ppm (H19) and a doublet of triplets at 3.26 ppm (H9; Figure 3.9A). The H19 doublet was a methyl attached to the H8 methine. The HSQC spectrum correlated the H9 proton signal with a carbon which resonated at 88.5 ppm, which the DEPT analysis assigned as a methine. The COSY spectrum indicated that it was adjacent to the methylene with diastereotopic protons (C10), but the downfield chemical shift of the signal suggested that it was also adjacent to an electron-withdrawing environment.

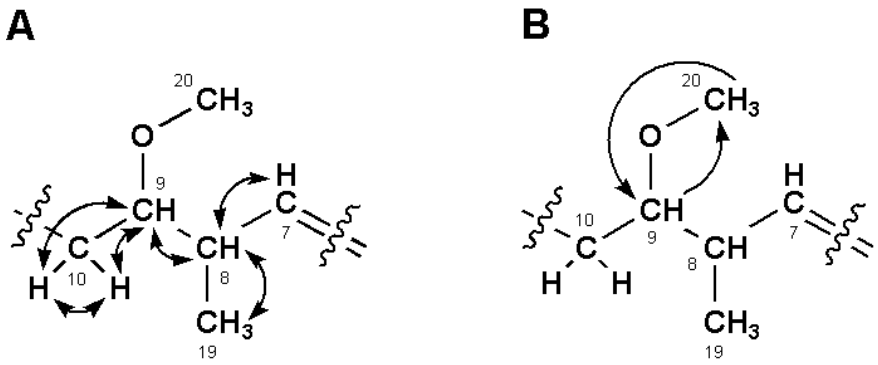

Figure 3.9: COSY **(A)** and selected HMBC **(B)** correlations for the C7-C10 portion of the Adda residue in MC-FA.

A proton singlet at 3.24 ppm (H20) was shown to be attached to a carbon at 58.8 ppm by the HSQC spectrum. The DEPT analysis designated it as a methyl and the downfield chemical shift indicated that it was adjacent to an electron-withdrawing environment. HMBC correlations between it and the C9 methine showed that they were attached to the same electron-withdrawing environment (Figure 3.9B). This chemical environment was likely an oxygen, as the 3.24 ppm signal was a sharp peak indicating that there was no exchange of protons/deuterium with the solvent (which would be the case if it were a secondary amine).

As the Adda aromatic proton signals overlapped with those of the Phe residue, resolved HSQC and HMBC experiments were required to assign the signals (Figure 3.10). The HMBC correlations were then used to assign the aromatic portion of the Adda residue.

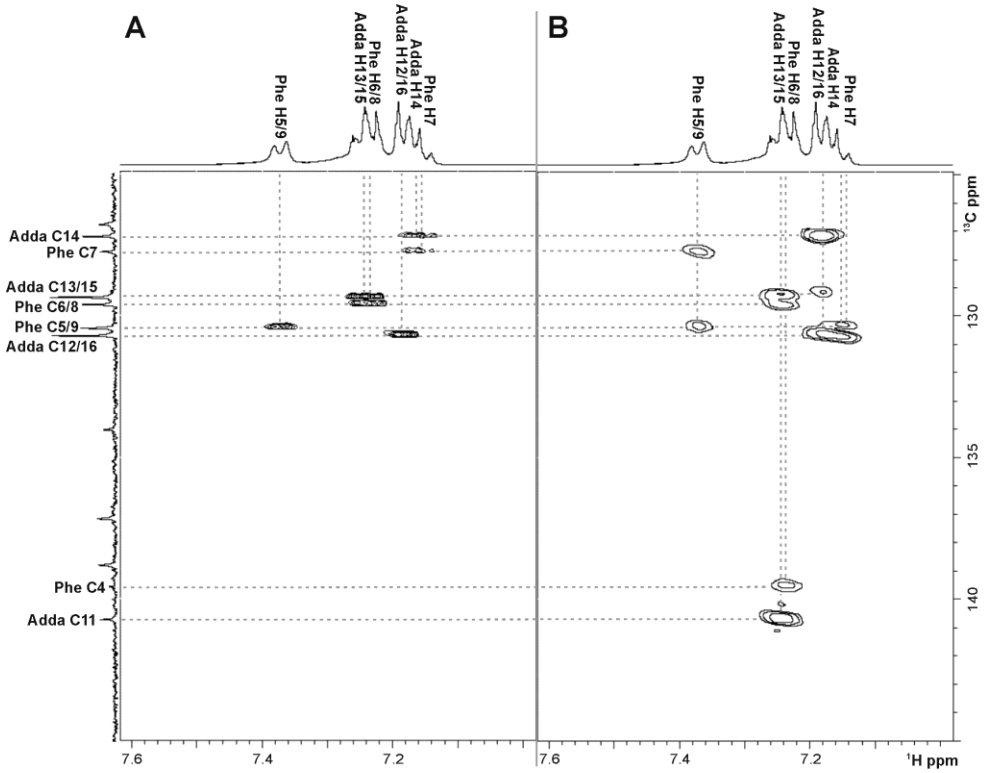

Figure 3.10:HSQC **(A)** and HMBC **(B)** spectra of the MC-FA aromatic region.

Both of the H10 methylene signals showed HMBC correlations with a quaternary carbon at 140.7 ppm (C11), as well as a carbon at 130.7 ppm (C12/16; Figure 3.11). The HSQC spectrum correlated the C12/16 signal with a proton doublet at 7.18 ppm which showed an HMBC correlation to a carbon at 127.1 ppm (Figure 3.10A & B). As the HMBC correlation (in an aromatic ring) was likely to be a ^{3}J coupling, this signal was assigned as the *para*-position (C14; Figure 3.11). The C14 signal was correlated with the proton triplet at 7.16 ppm by HSQC. This assignment was reinforced by the HMBC correlation observed between the doublet of doublets at 7.25 ppm (H13/15) and the C11 quaternary. Again assuming a ^{3}J coupling, that would attribute this signal to the *meta*-position on the ring.

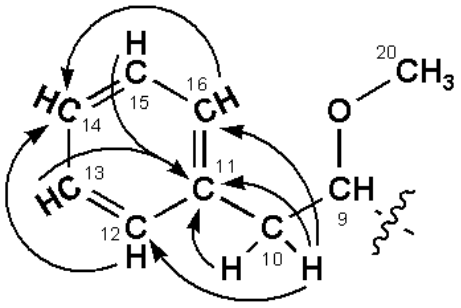

Figure 3.11: Selected HMBC correlations for the aromatic portion of the Adda residue in MC-FA.

The ROESY spectrum of MC-FA showed many correlations throughout the Adda moiety (Figure 3.12), which indicated that there was a great deal of flexibility within the structure. The Adda residue contains two double bonds, the stereochemistry of which is important for the toxicity of the microcystin.[52,121] Generally the double bonds are both in the *E*-configuration, however exposure to ultraviolet light has been shown to isomerise the second double bond to the *Z*-configuration.[113] The large coupling constant observed between the H4 and H5 protons (15.9 Hz; Table 3.3) indicated that the C4 double bond was in the *E*-configuration. The C6 double bond was also determined to be in the *E*-configuration due to a correlation between the H5 and H7 signals in the ROESY spectrum. If it were in the *Z*-configuration, a correlation would have been observed between the H5 and H8 protons.[52]

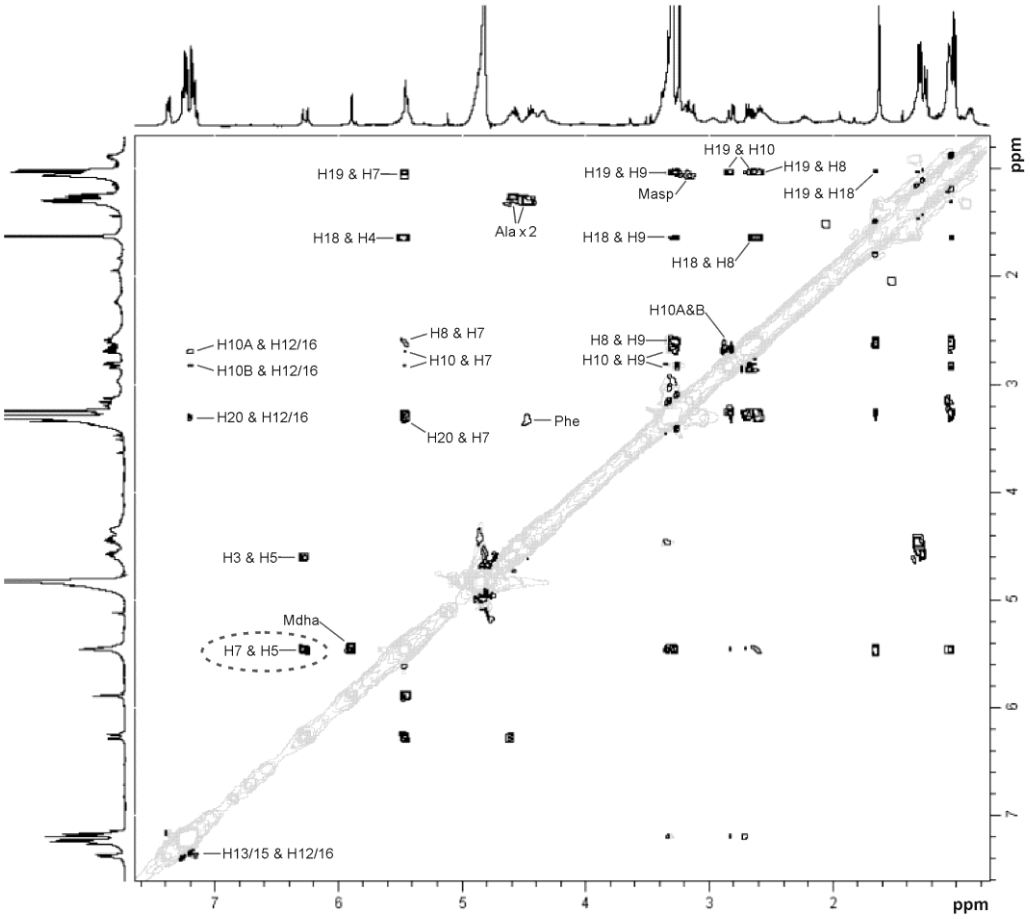

Figure 3.12: ROESY spectrum of MC-FA. Correlations for the Adda residue are indicated.

NMR Characterisation of the Mdha residue in MC-FA

The Mdha residue in MC-FA gave rise to three proton singlets at 3.30, 5.45 and 5.89 ppm (Table 3.3). The HSQC spectrum indicated that the 5.45 and 5.89 ppm protons were attached to a methylene carbon that resonated at 114.4 ppm. This and the downfield chemical shifts of these signals indicated that they were geminal alkene protons

The COSY spectrum showed coupling between these two protons (Figure 3.13A), but no others. HMBC ^{2}J correlations from each of the H3 proton signals indicated that they were attached to a quaternary carbon which resonated at 146.6 ppm (C2; Figure 3.13B). The HMBC spectrum also showed a ^{3}J correlation between the H3 protons and another quaternary carbon at 165.9 ppm (C1). Whilst this chemical shift was lower than expected for a carbonyl, conjugation with the nearby alkene has been shown to lower the chemical shift of a carbonyl by approximately 10 ppm,[206] which has been commonly observed in the Mdha residue of microcystins.[32,52,111,251]

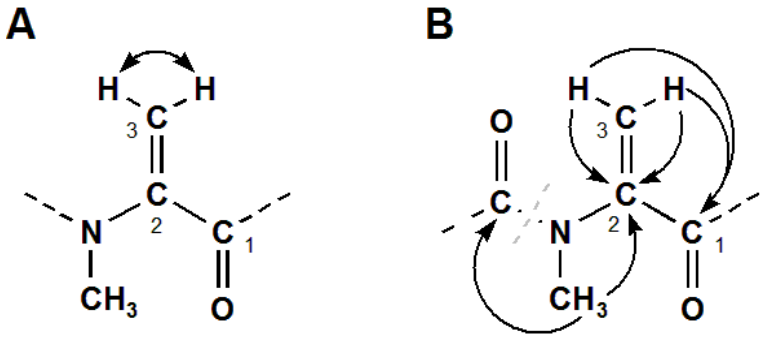

Figure 3.13: COSY **(A)** and HMBC **(B)** correlations for the *N*-methyl dehydroalanine residue in MC-FA.

The HSQC spectrum indicated that the 3.30 ppm proton was attached to a carbon at 38.5 ppm. The DEPT analysis indicated it was a methyl carbon and the downfield chemical shift suggested it was attached to an electron-withdrawing environment. An HMBC correlation to C2 showed that both carbons were attached to the same environment (Figure 3.13B) and therefore this was assigned as the *N*-methylation observed in Mdha.[32,52,111,251] The 3.30 ppm *N*-methyl signal also showed an HMBC correlation to the C5 carbonyl of Glu (Figure 3.13B).

NMR Characterisation of the Masp residue in MC-FA

The Masp residue in MC-FA gave rise to three proton signals; a doublet at 1.05 ppm and two multiplets at 3.13 and 4.41 ppm (Table 3.3). The COSY spectrum indicated that these protons were on three adjacent carbons (Figure 3.14A); the doublet at 1.05 ppm being coupled to the multiplet at 3.13 ppm, which was in turn coupled to the doublet at 4.41 ppm. The HSQC spectrum correlated each of these signals with methyl or methine carbons at 15.7, 41.6 and 57.9 ppm, respectively.

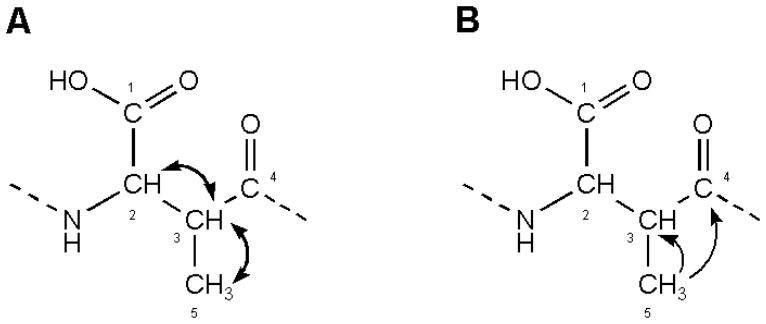

Figure 3.14: COSY **(A)** and HMBC **(B)** correlations for the methylaspartic acid residue in MC-FA.

The doublet at 1.05 ppm (H5) was a methyl adjacent to a methine. The slightly downfield chemical shift of this 3.13 ppm methine (H3) indicated it was adjacent to an electron-withdrawing environment. An HMBC correlation between the H5 doublet and a carbon that resonated at 179.1 ppm (C4; Figure 3.14B) indicated that this environment was a carbonyl. Since the doublet at 4.41 ppm (H2) was already adjacent to the C3 methine, it could not be adjacent to any other protons. The chemical shift indicated it was most likely adjacent to two electronegative environments, an amine and a carboxylic acid, as would be observed in *iso*-Masp. However, no HMBC correlations to the carboxylic acid (C1) were observed.

Masp contains two chiral centres at the C2 and C3 positions. Amino acid analysis indicated MC-FA contained D-Masp, demonstrating that the C2 carbon was in the *R*-configuration (Figure 3.15A). The rotational constriction of being part of a cyclic peptide then allowed the stereochemistry of the C3 asymetric carbon to be deduced by NMR spectroscopy. The small coupling constant observed in the H2 doublet (3.9 Hz; Table 3.3) indicated that the H3 proton was *syn* to the H2 proton (Figure 3.15B), or in the β-configuration commonly observed in microcystins.[14]

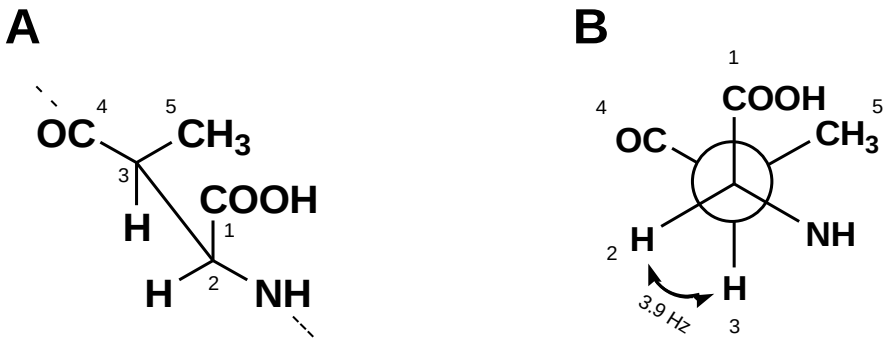

Figure 3.15: Staggered sawhorse **(A)** and Newman **(B)** projections of the methylaspartic acid residue in MC-FA.

NMR Characterisation of the Proteinogenic Amino Acids in MC-FA

Amino acid analysis of MC-FA indicated the presence of L-Ala, D-Ala, L-Phe and D-Glu. As these amino acids were confirmed by comparison with standard amino acids, the NMR characterisation of these amino acids will only be discussed briefly. The chemical shifts, coupling patterns and HMBC correlations matched those reported previously,[32,50,206,226]

Both alanine residues each gave rise to two proton signals; a doublet (≈ 1.3 ppm) and a quartet (≈ 4.5 ppm; Table 3.3). The multiplicity of the signals and a COSY coupling (Figure 3.16A) indicated that they were adjacent to each other and no other protons. The chemical shift of the methine indicated that it was close to electronegative nuclei, consistent with the carbonyl and amine groups of an intact peptide bond. HMBC correlations to a carbon with a downfield resonance (≈ 174 ppm; Figure 3.16B) confirmed the presence of the carbonyl.

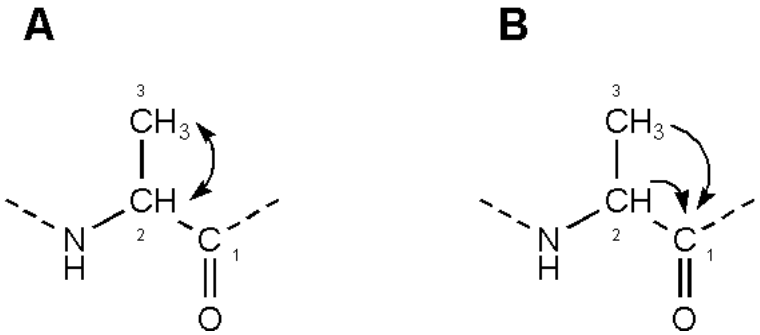

Figure 3.16: COSY **(A)** and HMBC **(B)** correlations for the alanine residues in MC-FA.

Comparison of the proton NMR spectrum of MC-FA with that of MC-LR facilitated assignment of the signals to each Ala residue. MC-LR contains one Ala residue located in position one. The methyl protons of the Ala in MC-LR resonated at 1.35 ppm (Figure 3.17A), slightly downfield from the methyl signals observed in MC-FA. Therefore, the more downfield signal in the spectrum of MC-FA (Figure 3.17B) was assigned as the position one Ala, and the upfield signal was assigned as the position four Ala. This was in accordance with previous NMR studies of microcystins in CD_3OD, where the position one Ala methyl group frequently resonated around 1.3 ppm.[48,50,54,61] Amino acid analysis of MC-FA indicated the presence of D- and L-Ala and since a D-amino acid has consistently been observed in position one of the microcystins,[31,32,68,72] the D-Ala was assigned to position one and the L-Ala to position four.

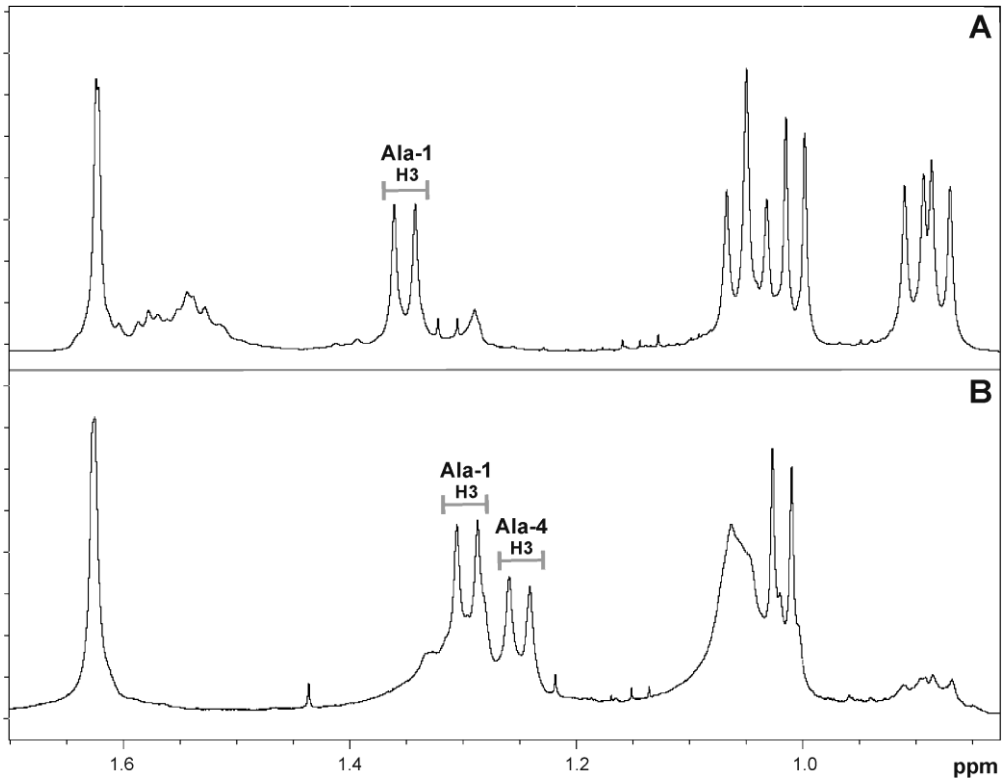

Figure 3.17: Proton nuclear magnetic resonance spectra of the methyl regions for MC-LR **(A)** and MC-FA **(B)**.

The Phe residue in MC-FA gave rise to five proton signals; a doublet at 7.37 ppm, a doublet of doublets at 7.24 ppm, a triplet at 7.17 ppm and two multiplets at 3.19 and 4.35 ppm (Table 3.3). The H3 methylene (3.19 ppm) showed a COSY coupling to the H2 methine (4.35 ppm; Figure 3.18A). The chemical shift of the H2 signal indicated that it was most likely adjacent to a carbonyl and an amine

group, which was reinforced by an HMBC correlation to a carbon that resonated at 178.9 ppm (C1; Figure 3.18B).

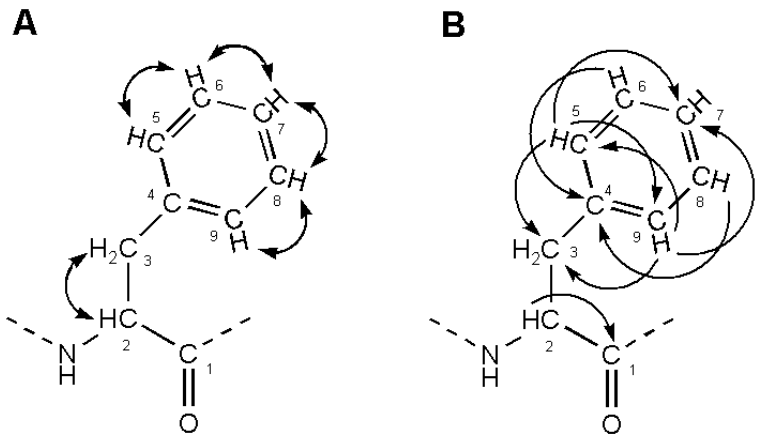

Figure 3.18: COSY **(A)** and HMBC **(B)** correlations for the phenylalanine residue in MC-FA.

The remaining proton signals (7.17, 7.24 and 7.37 ppm) were aromatic. Due to the multiplicity of the 7.37 ppm doublet and an HMBC correlation to the C3 methylene (Figure 3.18B), it was attributed to the H5/9 protons of the aromatic ring. The 7.37 ppm doublet showed an HMBC correlation to the C7 carbon, to which the 7.17 ppm proton was attached. This was assigned to the *para*-position as a ^{3}J correlation was likely to be observed. The remaining proton signal (7.24 ppm) was assigned as the H6/8 signal, which was supported by an HMBC correlation to a quaternary carbon at 139.5 ppm (Figure 3.18B). A selective TOCSY experiment with variable mixing times confirmed these proton assignments (Appendix G.9).

The Glu residue in MC-FA gave rise to four proton multiplets at 1.96, 2.22, 2.55 and 4.33 ppm (Table 3.3). A combination of HSQC and DEPT analysis indicated that the 4.33 ppm proton was part of a methine (C2), that the 1.96 and 2.22 ppm protons were attached to the same methylene carbon (C3) and that the 2.55 ppm multiplet was attached to a different methylene carbon (C4). The COSY spectrum showed that these three carbon atoms were adjacent (Figure 3.19A). An HMBC correlation was observed from the Mdha *N*-methyl proton to a carbon signal at 177.3 ppm, which was assigned as the C5 carbonyl of the Glu residue (Figure 3.19B). The chemical shift of the C2 methine indicated that it was

adjacent to an amine and a carboxylic acid, but no HMBC correlations to the carboxylic acid (C1) were observed.

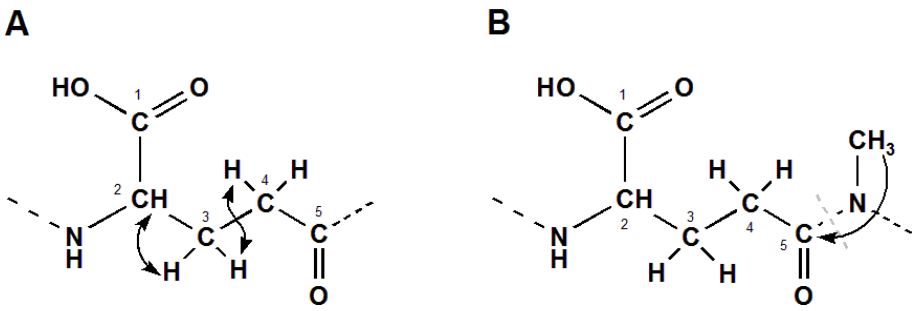

Figure 3.19: COSY **(A)** and HMBC **(B)** correlations for the glutamic acid residue in MC-FA.

Structural Characterisation of [Asp^3] MC-FA

A microcystin with a similar reversed-phase C_{18} retention time to MC-FA but 14 Da lower in mass (929.5 Da; Table 3.1) was present at low levels. The MS/MS spectrum of the *m/z* 930.5 ion (Figure 3.20) attributed this to Asp being present in position three instead of Masp. Assignment of the MS/MS spectrum showed that each fragment ion which contained Masp in MC-FA exhibited a loss of 14 Da in [Asp^3] MC-FA (**162**; Appendix E.4). This modification is commonly observed in microcystins (Appendix A).

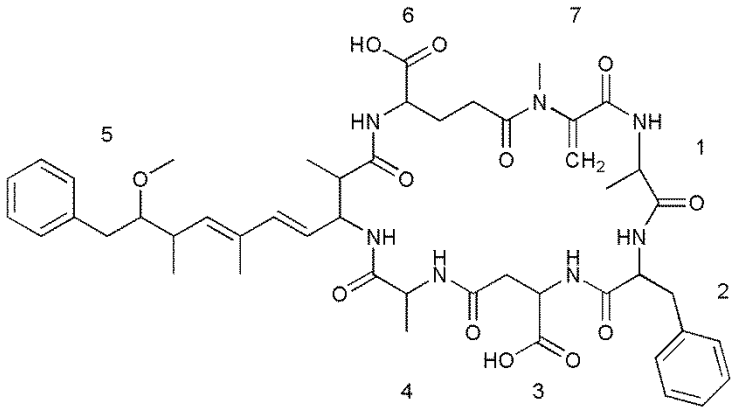

(162)

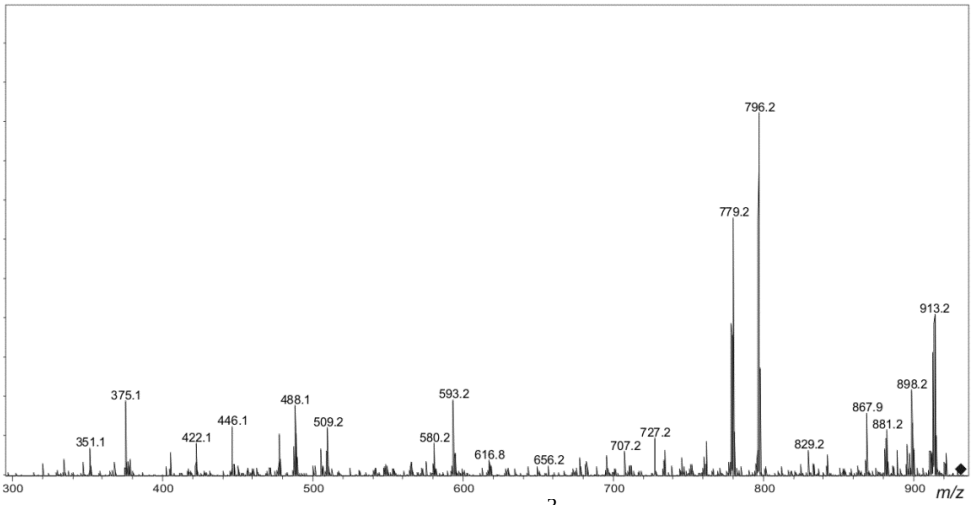

Figure 3.20: Tandem mass spectrum of [Asp^3] MC-FA. Fragmentation induced by electrospray ionisation collision-induced dissociation.

MC-FA (**163**) was characterised by a combination of amino acid analysis, MS and NMR spectroscopy. Amino acid analysis of **163** indicated the presence of L-Ala, D-Ala, D-Glu, D-Masp, L-Phe, *N*-methylamine and (3*S*)-Adda. MS/MS analysis suggested that the *N*-methylamine observed in the amino acid analysis was due to the breakdown of Mdha. The MS/MS also arranged the seven amino acids as a cyclic peptide with the sequence: Ala-Phe-Masp-Ala-Adda-Glu-Mdha. Nuclear magnetic resonance spectroscopy confirmed the structure of each of the amino acids indicated by amino acid analysis. It was also utilised to determine that the D-Masp was in the β-configuration and that both of the double bonds in Adda were in the *E*-configuration. The chemical shifts, coupling constants and correlation patterns observed for MC-FA were consistent with those observed for other microcystins characterised by NMR spectroscopy.[32,38,50-54] Using MS/MS, a minor component **162** with 14 Da lower mass was determined to be [Asp^3] MC-FA. Neither **162** or **163** have been reported previously.

4.2.3 Structural Characterisation of MC-WA from CYN06

The presence and stereochemistry of several of the amino acids present in MC-WA (**165**) were determined by Advanced Marfey's amino acid analysis. LC-MS analysis of the L-FDLA derivatives of hydrolysed MC-WA indicated the presence of six amino acids (Figure 3.21). The presence of D-Glu (*m/z* 440; 14.3 min), L-Ala (*m/z* 382; 15.8 min) and D-Ala (18.6 min), was determined by comparison with standard amino acids. Identification of D-Masp (*m/z* 440; 15.9 min), 3(*S*)-Adda (*m/z* 592; 32.9 min) and *N*-methylamine (*m/z* 324;

19.6 min) was facilitated by comparison with the L-FDLA derivatives of hydrolysed MC-LR (Appendix F.3).

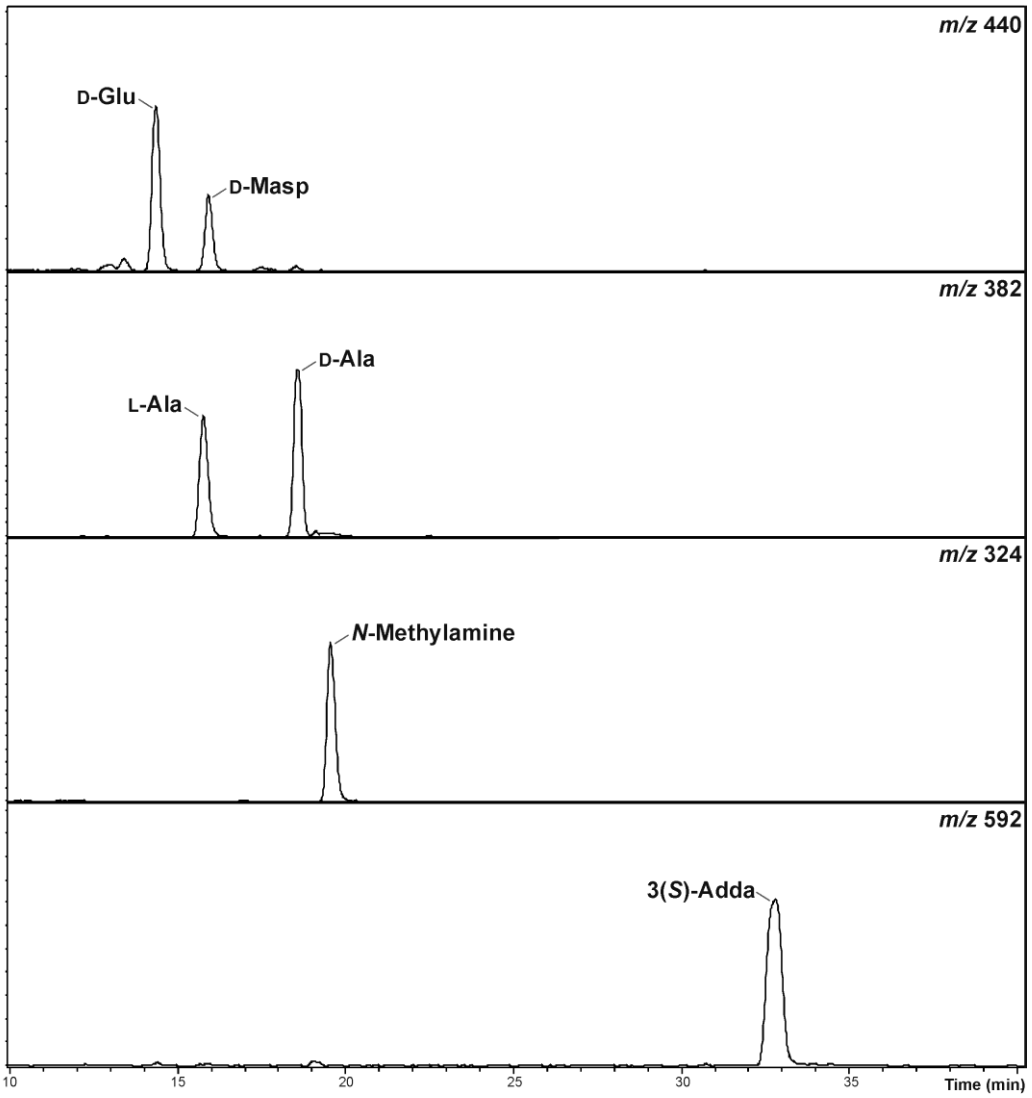

Figure 3.21: Advanced Marfey's amino acid analysis of MC-WA. Extracted ion chromatograms of hydrolysed MC-WA derivatised with L-FDLA.

The HRMS for **165** yielded a *m/z* of 1005.4650, consistent with the sodium adduct ion of a cyclic peptide containing L-Ala, D-Ala, Glu, Masp, Mdha, Adda and a tryptophan (Trp; $C_{51}H_{66}N_8O_{12}Na$, *m/z* 1005.4692, Δ -4.25 ppm). As Trp residues break down during acid hydrolysis, it was not detected by amino acid analysis.[38]

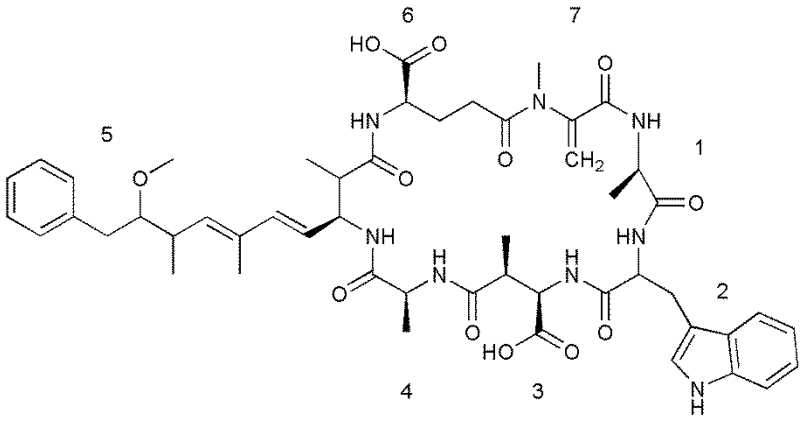

(165)

The MS/MS spectrum for **165** (Figure 3.22) indicated that it was a microcystin with a structure similar to MC-FA but with a Trp residue in position two. The presence of Adda was indicated by the loss of 134 Da (*m/z* 849) and 313 Da (*m/z* 670). The mass difference between the other fragment ions indicated the position of the remaining amino acids in the compound (Table 3.4).

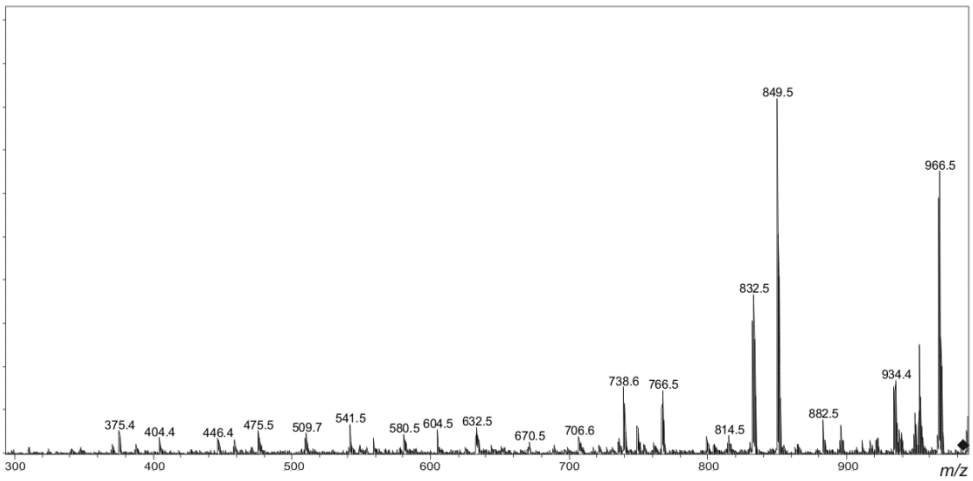

Figure 3.22: Tandem mass spectrum of MC-WA. Fragmentation induced by electrospray ionisation collision-induced dissociation.

Table 3.4: Tandem mass spectrometry fragment ions for MC-WA observed by electrospray ionisation collision-induced dissociation.

m/z	Fragment Assignment [a]	*m/z*	Fragment Assignment [a]
387	Ala-Trp-Masp + H	404	Trp-Masp-Ala + NH_4
375	Adda'-Glu-Mdha + H	458	Ala-Trp-Masp-Ala + H
475	Ala-Trp-Masp-Ala + NH_4	446	Adda'-Glu-Mdha-Ala + H
541	Mdha-Ala-Trp-Masp-Ala + H	509	Adda-Glu-Mdha – NH_3 + H
558	Mdha-Ala-Trp-Masp-Ala + NH_4	580	Adda-Glu-Mdha-Ala – NH_3 + H
632	Adda'-Glu-Mdha-Ala-Trp + H	670	Glu-Mdha-Ala-Trp-Masp-Ala + H
766	Adda-Glu-Mdha-Ala-Trp – NH_3 + H	895	Adda-Glu-Mdha-Ala-Trp-Masp – NH_3 + H
831	M – Adda sidechain – H_2O + H	849	M – Adda sidechain + H
882	M – Mdha – H_2O + H	965	M – H_2O + H
944	M + H		

[a] Adda' = Adda minus NH_2 and the sidechain ($C_9H_{11}O$).

The fragment ion series starting with Adda'-Glu-Mdha (*m/z* 375) was extended to include Ala and Trp (Figure 3.23A). This sequence was supported by the ion series containing Adda minus NH_3 (*m/z* 509, 580, 766) which was extended to include Masp (Figure 3.23B). A fragment ion series which began with Trp-Masp-Ala (*m/z* 387; Figure 3.23B) and extended in the opposite direction to include a second Ala residue, gave the complete amino acid sequence of Adda-Glu-Mdha-Ala-Trp-Masp-Ala. A fragment where Mdha and water were lost from the compound (*m/z* 882; Table 3.4) indicated that Adda and the second Ala residue were joined and that the structure was cyclic.

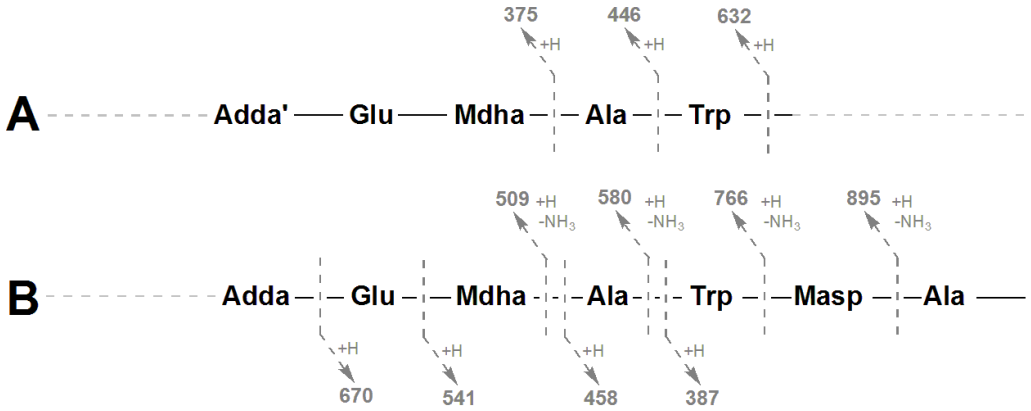

Figure 3.23: Tandem mass spectrometry fragment ions indicating the amino acid sequence in MC-WA.

NMR spectroscopy was utilised for confirmation of the structure indicated by MS and amino acid analysis. Interpretation of COSY, TOCSY, HSQC and HMBC spectra allowed for the assignment of the ^{1}H and ^{13}C signals (Table 3.5). Several

of the ^{1}H signals overlapped at 400 MHz and the peak patterns were resolved using selective TOCSY experiments. Nuclear magnetic resonance spectra for MC-WA are presented in Appendix H.

Table 3.5: Nuclear magnetic resonance spectroscopy assignment of MC-WA at 400 MHz in CD_3OD.

AA[a]	^{13}C	^{1}H	Mult.[b] (*J* in Hz)	AA[a]	^{13}C	^{1}H	Mult.[b] (*J* in Hz)
D-Ala-1				**Adda**-5 cont.			
1	174.0	-		3	56.5	4.63	m
2	49.1[c]	4.49	q (7.7)[d]	4	126.9	5.46[c]	m
3	18.0	1.31	d (7.7)[d]	5	138.7	6.29	d (16.1)
				6	134.0	-	
Trp-2				7	137.1	5.46[c]	d (10.4)[d]
1	nd	-		8	37.8	2.60	m
2	58.2	4.47	m	9	88.5	3.26	m
3	28.0	3.31	dd (1.7, 3.3)[d]	10	39.1	2.68	dd (7.5, 14.0)
		3.38	m			2.83	dd (4.6, 14.0)
4	111.5	-		11	140.7	-	
5	138.2	-		12 & 16	130.7	7.19[c]	d (8.1)
6	112.3	7.31	d (8.7)	13 & 15	129.3	7.25	dd (7.4, 8.1)
7	122.3	7.07	dd (7.4, 8.7)	14	127.2	7.17[c]	t (7.4)
8	119.8	7.00	dd (7.4, 8.4)	17	16.2	1.08	d (6.7)[d]
9	119.1	7.67	d (8.4)	18	13.0	1.64	s
10	128.3	-		19	16.6	1.03	d (6.7)
11	125.7	7.29	s	20	58.9	3.25	s
D-Masp-3				**D-Glu**-6			
1	nd	-		1	nd	-	
2	58.8	4.36[c]	d (4.0)	2	55.9	4.32	m
3	41.5	3.15	m	3	30.5	1.89	m
4	179.1	-				2.23	m
5	16.3	1.07	d (7.7)[d]	4	33.8	2.55 (2H)	m
				5	177.4	-	
L-Ala-4							
1	175.0	-		**Mdha**-7			
2	49.0[c]	4.60	q (7.7)[d]	1	166.0	-	
3	17.4	1.23	d (7.7)[d]	2	146.4	-	
				3	113.8	5.45[c]	s[d]
Adda-5						5.87	s
1	176.7	-		*N*-CH_3	38.3	3.30[c]	s
2	45.3	2.98	m				

[a] AA = Amino acid (number indicates position in the structure); nd = Not detected. [b] Mult. = Multiplicity of the proton signal; *J* = Coupling constant. [c] Signals were overlapped so chemical shifts were determined using correlations observed in 2D HSQC spectra. [d] Multiplicity and coupling constants were determined using 1D-selective TOCSY experiments.

A large proportion of the structure of MC-WA is the same as that of MC-FA, and as a result, very similar chemical shifts and coupling constants were observed (Tables 3.3 and 3.5). The COSY coupling patterns and HMBC correlations observed in each of the common amino acids were also the same as those described for MC-FA, therefore only the NMR characteristics of the position two

Trp have been described. As with MC-FA, the Ala residue with the downfield methyl proton resonance was assigned to position one and designated as the D-Ala.

NMR Characterisation of the Tryptophan Residue in MC-WA

The Trp residue in MC-WA gave rise to eight proton signals; one singlet at 7.29 ppm, two doublets at 7.31 and 7.67 ppm, two doublets of doublets at 7.00 and 7.07 ppm, and three multiplets at 3.31, 3.38 and 4.47 ppm (Table 3.5). The HSQC spectrum indicated that the 3.31 and 3.38 ppm protons were attached to a single carbon that resonated at 28.0 ppm, which the DEPT-135 designated as a methylene (C3). These proton signals showed a COSY coupling to the 4.47 ppm multiplet (H2; Figure 3.24) which, due to its chemical shift, was adjacent to two electron-withdrawing environments. These were presumably a carbonyl and an amine, however, no HMBC correlations were detected between the H2 or H3 protons and what was assumed to be the C1 carbonyl.

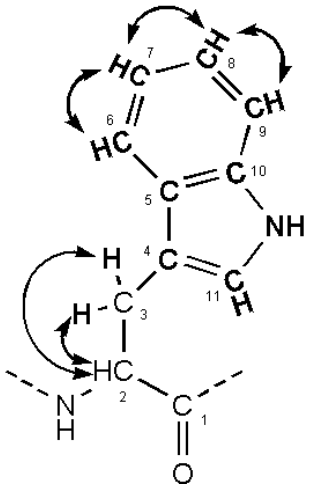

Figure 3.24: COSY correlations for the tryptophan residue in MC-WA.

Unlike MC-FA, the signals from the aromatic region of MC-WA showed little overlap and were resolved in an HSQC experiment. The three Adda aromatic signals at 7.17, 7.19 and 7.25 ppm and five downfield signals from the Trp residue were evident in the HSQC spectrum (Figure 3.25A).

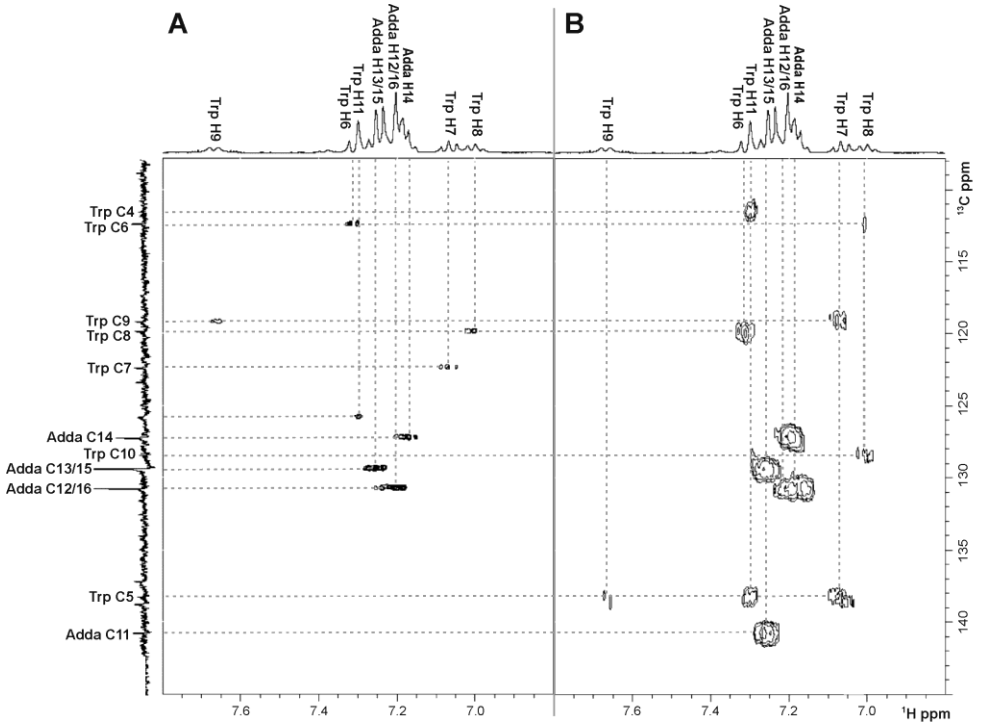

Figure 3.25: HSQC **(A)** and HMBC **(B)** spectra of the MC-WA aromatic region.

The doublet at 7.67 ppm (H9) showed a COSY coupling to a doublet of doublets at 7.00 ppm (H8), which was in turn coupled to a doublet of doublets at 7.07 ppm (H7), coupled to a doublet at 7.31 ppm (H6; Figure 3.26). Each of the Trp aromatic protons were in unique chemical environments, which indicated asymmetric substitution of the aromatic ring.

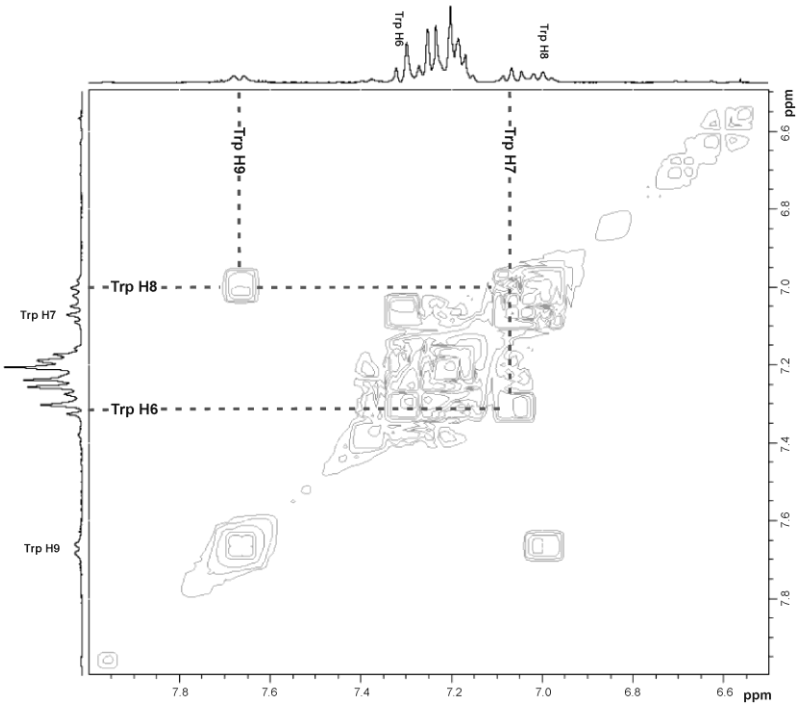

Figure 3.26: COSY spectrum displaying the aromatic region of MC-WA. Lines indicate proton coupling within the tryptophan residue.

The H6 and H8 protons showed HMBC ^{3}J correlations to a quaternary carbon that resonated at 128.3 ppm (C10; Figure 3.27) and the H7 and H9 protons showed correlations to another quaternary carbon at 138.2 ppm (C5). The singlet at 7.29 ppm (H11) also showed an HMBC correlation to the C5 quaternary carbon, as well as to a third quaternary carbon which resonated at 111.5 ppm (C4). This pattern of correlations between the H7, H9 and H11 protons and the C5 quaternary carbon suggested that the H11 proton had a ^{3}J correlation to the C5 quaternary and a ^{2}J correlation to the C4 quaternary (Figure 3.27). The downfield chemical shift of the H11 signal indicated that it was in a very electron-withdrawing environment, which would be accounted for by being part of a double bond and adjacent to an amine, as observed in the indole ring of a tryptophan.[206]

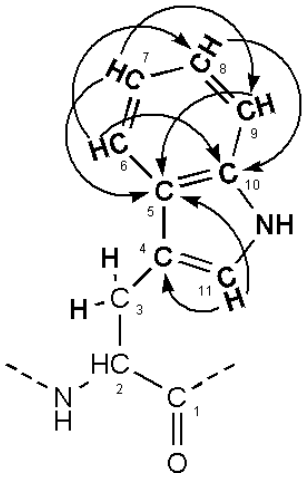

Figure 3.27: HMBC correlations for the tryptophan residue in MC-WA.

Structural Characterisation of [Asp^{3}] MC-WA

A microcystin with a similar reversed-phase C_{18} retention time to MC-WA, but with 14 Da lower mass (968.5 Da; Table 3.1) was present in CYN06. The MS/MS spectrum of the *m/z* 969.5 ion (Figure 3.28) attributed the 14 Da mass difference to Asp being present in position three instead of Masp ([Asp^{3}] MC-WA; **164**; Appendix E.4).

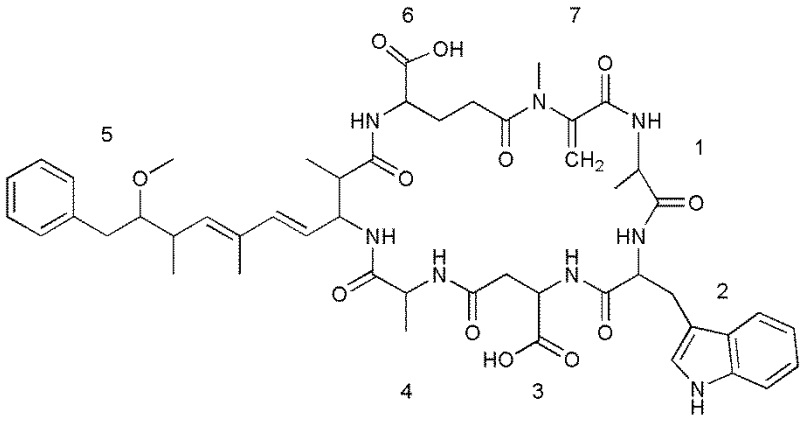

(164)

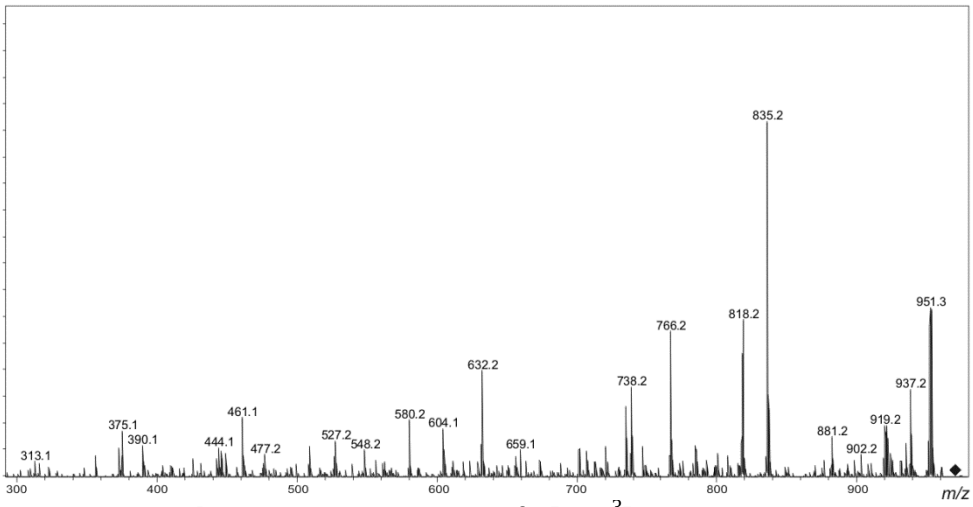

Figure 3.28: Tandem mass spectrum of [Asp^3] MC-WA. Fragmentation induced by electrospray ionisation collision-induced dissociation.

MC-WA (**165**) was characterised by a combination of amino acid analysis, MS and NMR spectroscopy. Amino acid analysis of **165** indicated the presence of L-Ala, D-Ala, D-Glu, D-Masp, *N*-methylamine and (3*S*)-Adda. Tandem MS analysis suggested that the *N*-methylamine was due to the breakdown of Mdha and that the compound also contained a Trp residue. The MS/MS arranged the seven amino acids as a cyclic peptide with the sequence: Ala-Trp-Masp-Ala-Adda-Glu-Mdha. As with MC-FA, NMR spectroscopy was used to confirm the structure and some of the stereochemistry of several of the amino acids in MC-WA. The signals and coupling patterns observed in the position two residue confirmed it was Trp, however, no connectivity was observed between the backbone and the sidechain portions. A minor component **164** with 14 Da less mass, was determined to be [Asp^3] MC-WA using MS/MS. Both **164** and **165** are new microcystin congeners.

3.2.4 Structural Characterisation of the -RZ Microcystins from CYN06

The -RZ microcystin congeners observed in CYN06 were MC-RA, [Asp^3] MC-RA, MC-RAba, [Asp^3] MC-RAba and MC-RL (Table 3.1). Only [Asp^3] MC-RA and [Asp^3] MC-RAba are new microcystin congeners, however, they were only present in sufficient quantities to conduct MS/MS analysis. Therefore, amino acid analysis of MC-RA and MC-RAba was conducted to facilitate the characterisation of the [Asp^3] analogues.

Structural Characterisation of MC-RA

As with MC-FA and MC-WA, the presence and stereochemistry of the amino acids in MC-RA (**16**) were determined by Advanced Marfey's amino acid analysis. LC-MS analysis of the L-FDLA derivatives of hydrolysed MC-RA indicated the presence of seven amino acids (Figure 3.29). The presence of D-Glu (*m/z* 440; 14.3 min), L-Ala (*m/z* 382; 15.8 min) and D-Ala (18.6 min), was

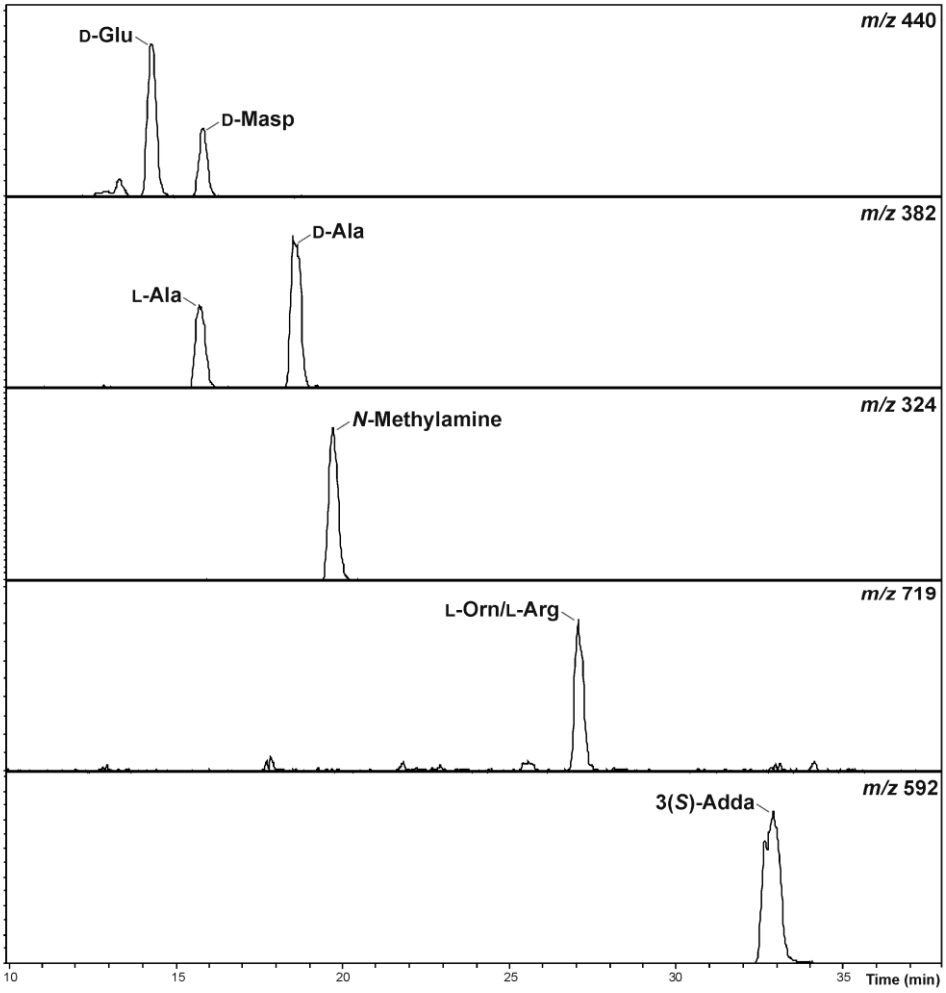

Figure 3.29: Advanced Marfey's amino acid analysis of MC-RA. Extracted ion chromatograms of hydrolysed MC-RA derivatised with L-FDLA.

determined by comparison with standard amino acids. The D-Masp (*m/z* 440; 15.9 min), *N*-methylamine (*m/z* 324; 19.6 min) and 3(*S*)-Adda (*m/z* 592; 32.9 min) derivatives observed in MC-LR (Appendix F.3) were also present.

A peak was present at 27.2 min with *m/z* 719, which could be indicative of an ornithine (Orn) bonded to two FDLA.[205] However, it could also represent an arginine (Arg) residue which has lost the guanidinium group from the sidechain and become an Orn. This was consistently observed using standard Arg and the protocol followed during this work (Appendix F.2). Comparison of the retention time of the Orn/Arg derivative from MC-RA with standard L-Arg derivatised with L-FDLA did indicate that the Orn/Arg present in MC-RA was in the L-configuration.

The HRMS for **16** yielded a *m/z* of 953.5122, consistent with the protonated ion of a cyclic peptide consisting of the amino acids indicated by the amino acid analysis (L-Ala, D-Ala, Glu, Masp, Mdha, Adda) and an Arg residue ($C_{46}H_{69}N_{10}O_{12}$, *m/z* 953.5091, Δ +3.28 ppm).

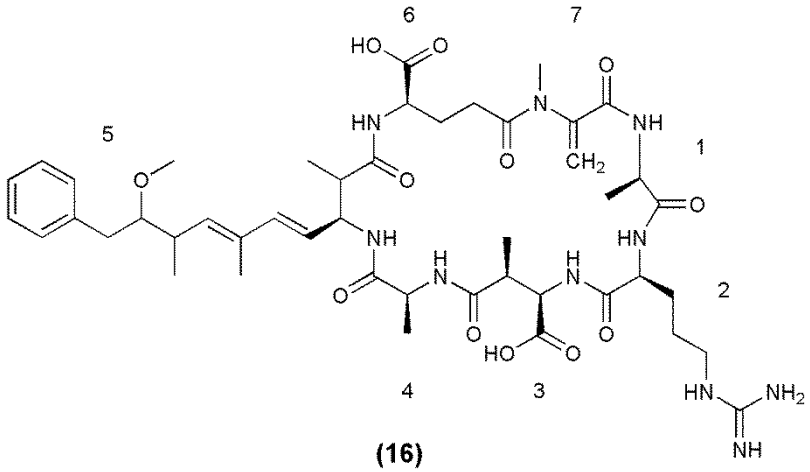

(16)

The major ionisation point on an Arg-containing microcystin is the guanidinium group of the Arg residue, so an alteration of the position in the structure dramatically altered the MS/MS fragment ions observed. Where the *m/z* 599 ion (Arg-Adda-Glu)[78] is one of the major fragment ions in a -XR microcystin congener, a *m/z* 440 ion (Glu-Mdha-Ala-Arg and Mdha-Ala-Arg-Masp) was present in the -RZ congeners.[66]

Due to the presence of an Arg residue, MC-RA ionised very efficiently by MALDI, therefore, MALDI PSD was also utilised for the MS/MS characterisation. For MC-RA (and other arginine-containing microcystins), both the MALDI PSD and ESI CID produced similar fragment ion series, however MALDI PSD produced lower mass fragment ions whilst ESI CID yielded information on the higher mass fragments. The MS/MS spectra for MC-RA (Figure 3.30) indicated that it was a microcystin which possessed the unusual mass spectrometric characteristics described previously. The presence of Adda was indicated by loss of the 134 Da sidechain fragment (*m/z* 819), the protonated Adda sidechain (*m/z* 135) and the *m/z* 163 fragment ion (Adda'). The mass difference between the other fragment ions indicated the position of the remaining amino acids in the compound (Table 3.6).

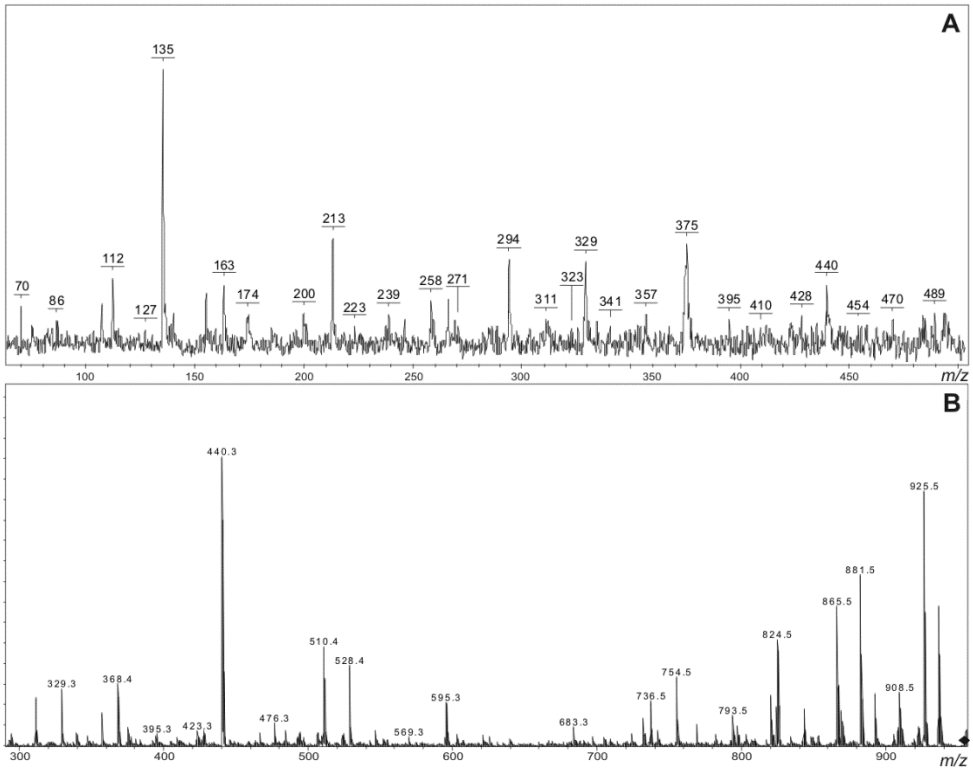

Figure 3.30: Tandem mass spectra of MC-RA. Fragmentation induced by matrix-assisted laser desorption ionisation post-source decay **(A)** and electrospray ionisation collision-induced dissociation **(B)**.

Table 3.6: Tandem mass spectrometry fragment ions for MC-RA observed by matrix-assisted laser desorption ionisation post-source decay and electrospray ionisation collision-induced dissociation.

m/z	**Fragment Assignment** [a]	*m/z*	**Fragment Assignment** [a]
70	Arg fragment	84	Arg fragment
112	Arg fragment	135	Adda sidechain
155	Mdha-Ala + H	201	Masp-Ala + H
163	Adda' + H	213	Glu-Mdha + H
311	Mdha-Ala-Arg + H	329	Arg-Masp-Ala – CO + H
357	Arg-Masp-Ala + H	368	Glu-Mdha-Ala-Arg – $CH_2NHCN_2H_3$ + H
368	Mdha-Ala-Arg-Masp – $CH_2NHCN_2H_3$ + H	375	Adda'-Glu-Mdha + H
395	Glu-Mdha-Ala-Arg – COOH + H	423	Mdha-Ala-Arg-Masp – NH_3 + H
428	Ala-Arg-Masp-Ala + H	440	Glu-Mdha-Ala-Arg + H
440	Mdha-Ala-Arg-Masp + H	466	Mdha-Ala-Arg-Masp-Ala – COOH + H
494	Mdha-Ala-Arg-Masp-Ala – NH_3 + H	510	Mdha-Ala-Arg-Masp-Ala – H_2O + NH_4
511	Mdha-Ala-Arg-Masp-Ala + H	528	Mdha-Ala-Arg-Masp-Ala + NH_4
819	M – Adda sidechain + H	824	M – Glu or Masp + H
881	M – $CH_2NHCN_2H_3$ + H	882	M – Ala + H
908	M – COOH + H	935	M – H_2O + H
953	M + H		

[a] Adda' = Adda minus NH_2 and the sidechain ($C_9H_{11}O$); $CH_2NHCN_2H_3$ is a fragment of the Arg sidechain.

A fragment ion series beginning with Mdha-Ala (*m/z* 155; Figure 3.31A) which extended to include Arg, Masp and Ala indicated much of the amino acid sequence. Another ion series which extended in the opposite direction supported this partial sequence of Mdha-Ala-Arg-Masp-Ala. A Glu-Mdha fragment (*m/z* 213; Figure 3.31B) showed that Glu was attached to Mdha. The *m/z* 375 fragment (Adda'-Glu-Mdha) commonly observed in Adda-containing microcystins, showed that Adda was attached to Glu, which yielded the complete amino acid sequence of Adda-Glu-Mdha-Ala-Arg-Masp-Ala. The peptide was shown to be cyclic by the loss of Glu or Masp (*m/z* 824; Table 3.6), which indicated that Adda was attached to Ala.

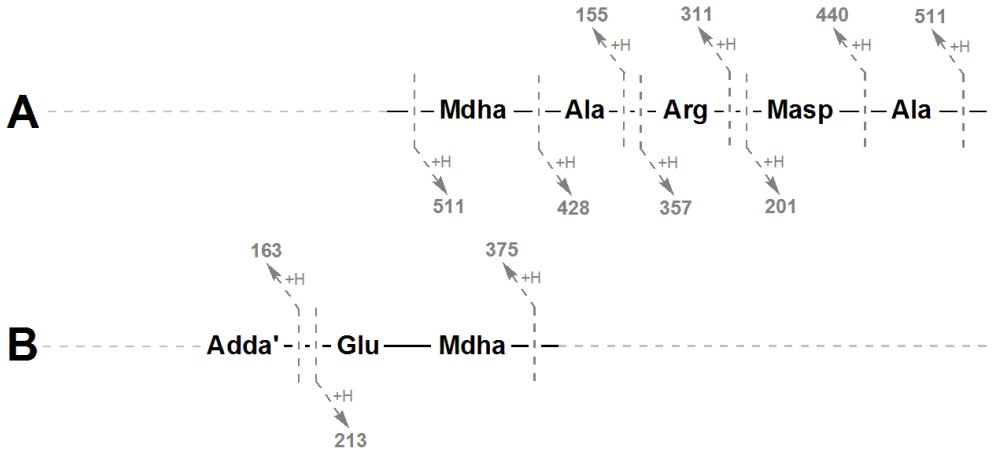

Figure 3.31: Tandem mass spectrometry fragment ions indicating the amino acid sequence in MC-RA.

Structural Characterisation of [Asp^3] MC-RA

The reversed-phase C_{18} retention time of [Asp^3] MC-RA (**160**) was similar to MC-RA (Table 3.1), but the compound was 14 Da lower in mass (938.5 Da). The MS/MS spectra of **160** (Figure 3.32) attributed this to Asp being present in position three instead of Masp (Appendix E.3). Of note was the *m/z* 426 ion (Mdha-Ala-Arg-Asp) in the ESI CID MS/MS spectrum (Figure 3.32B), which demonstrates that both of the isometric fragments (Glu-Mdha-Ala-Arg and Mdha-Ala-Arg-Masp) from MC-RA were present in the *m/z* 440 peak.

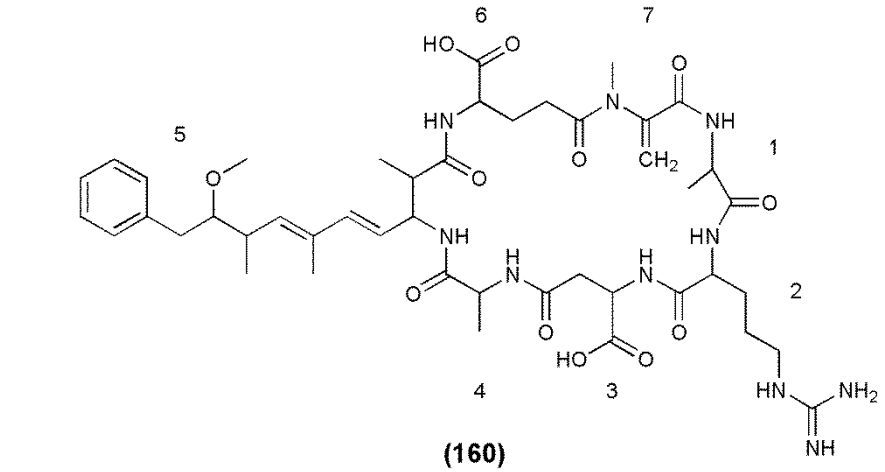

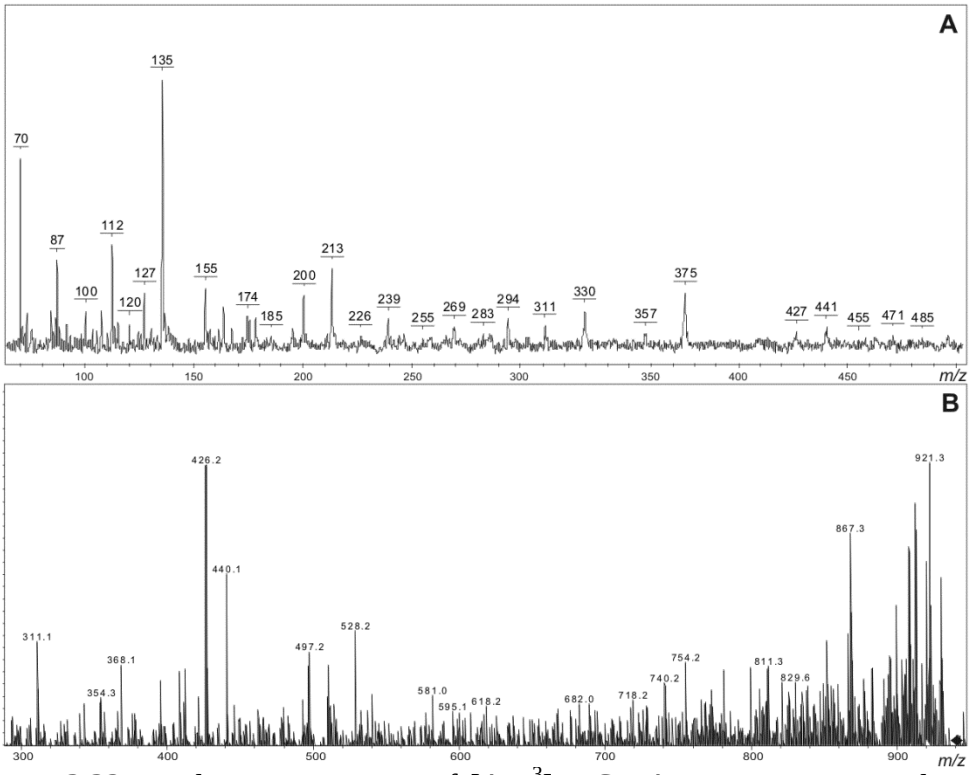

Figure 3.32: Tandem mass spectra of [Asp^3] MC-RA. Fragmentation induced by matrix-assisted laser desorption ionisation post-source decay **(A)** and electrospray ionisation collision-induced dissociation **(B)**.

Structural Characterisation of MC-RAba

The presence and stereochemistry of the amino acids in MC-RAba (**19**) were determined by Advanced Marfey's amino acid analysis. Comparison with standard amino acids facilitated the identification of D-Glu (*m/z* 440; 14.3 min), L-2-aminobutanoic acid (Aba; *m/z* 396; 17.4 min) and D-Ala (*m/z* 382; 18.6 min; Figure 3.33). Comparison with FDLA derivatives of hydrolysed MC-LR (Appendix F.3) led to the identification of D-Masp (*m/z* 440; 15.9 min), *N*-methylamine (*m/z* 324; 19.6 min) and 3(*S*)-Adda (*m/z* 592; 32.9 min). As with MC-RA, the *m/z* 719 derivative representing either L-Arg or L-Orn (27.2 min) was observed.

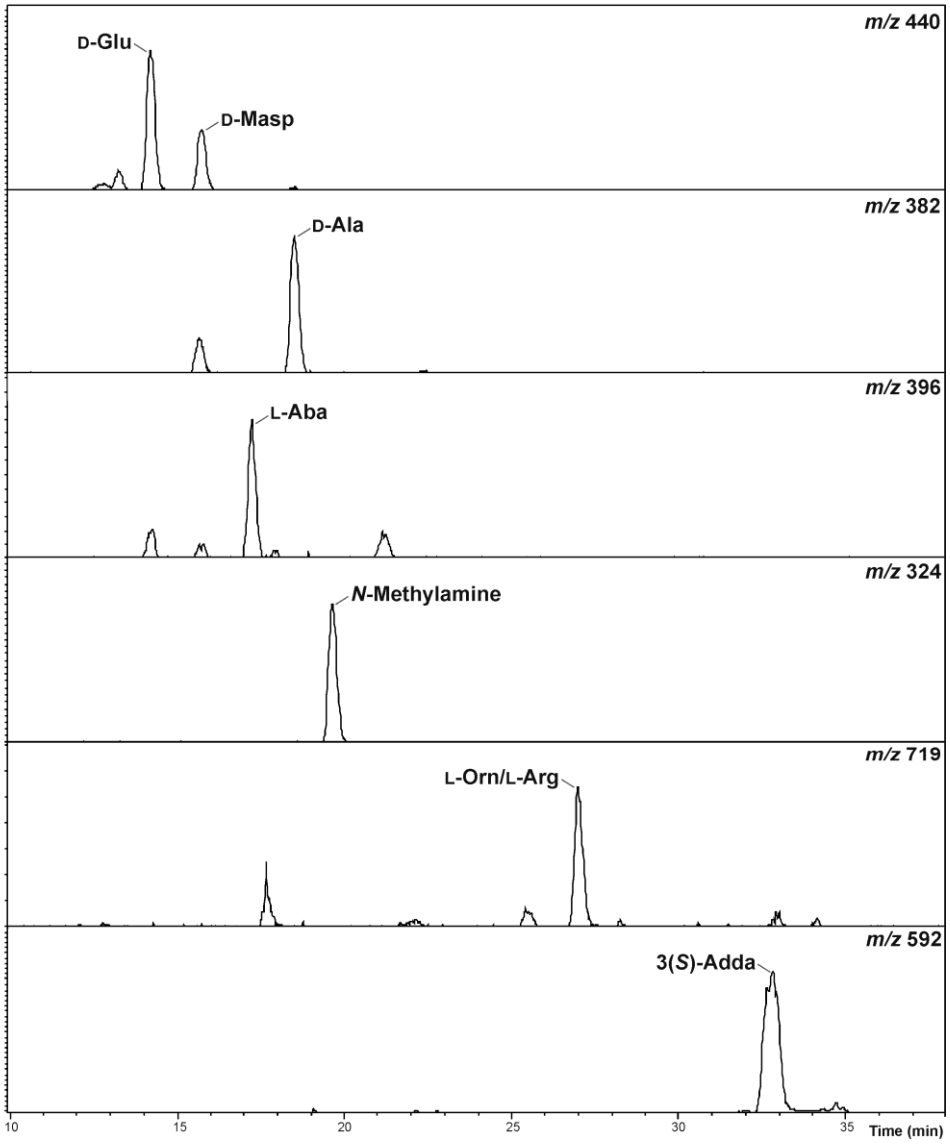

Figure 3.33: Advanced Marfey's amino acid analysis of MC-RAba. Extracted ion chromatograms of hydrolysed MC-RAba derivatised with L-FDLA.

HRMS of **19** yielded a *m/z* of 967.5259, consistent with the protonated ion of a cyclic peptide consisting of the amino acids indicated by the amino acid analysis (Ala, Aba, Glu, Masp, Mdha, Adda) and an Arg residue ($C_{47}H_{71}N_{10}O_{12}$, *m/z* 967.5247, Δ +1.15 ppm).

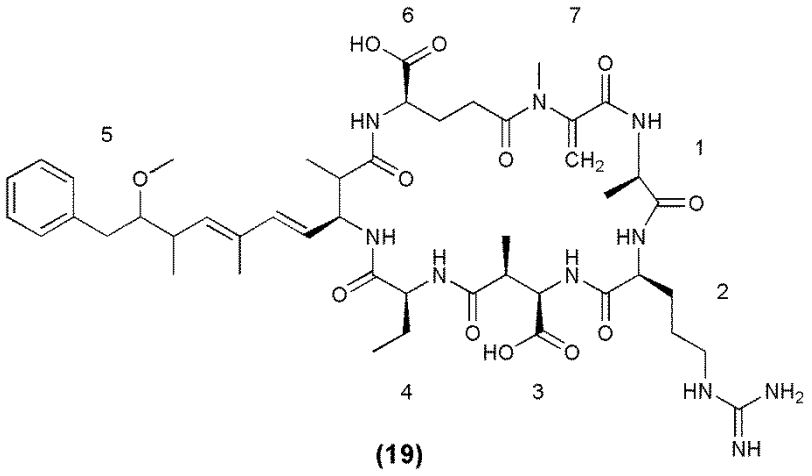

(19)

The MS/MS spectra of **19** (Figure 3.34) were very similar to those of MC-RA, except that the fragments attributed to the position four amino acid contained 14 Da more mass (Appendix E.3). This indicated that the L-Aba detected by amino acid analysis was present in position four instead of L-Ala.

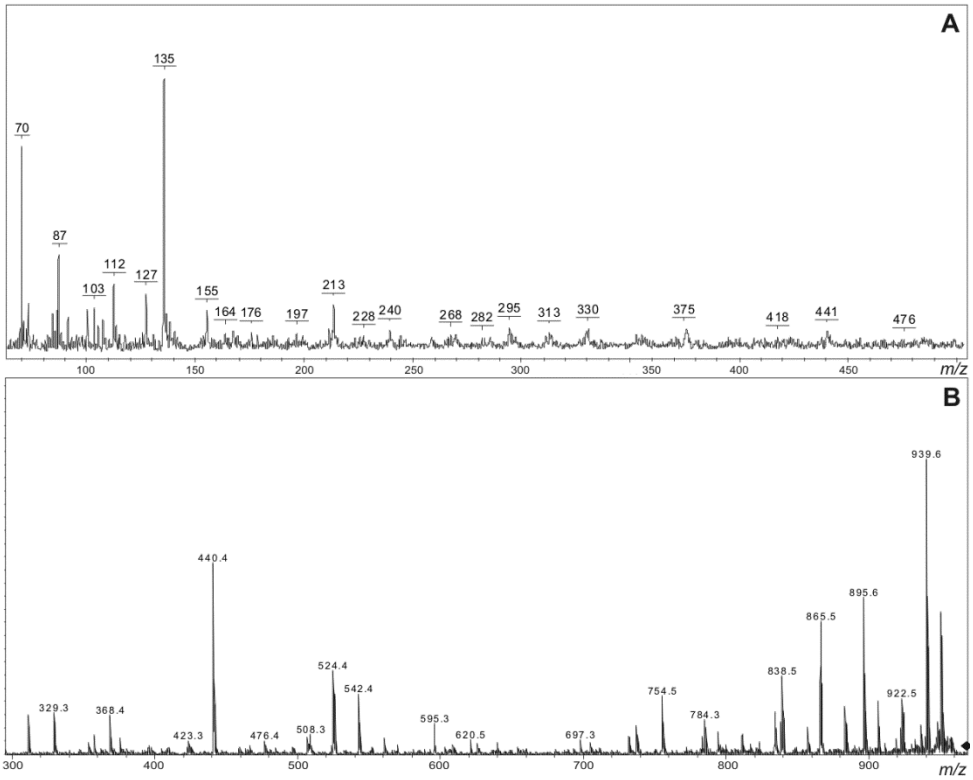

Figure 3.34: Tandem mass spectra of MC-RAba. Fragmentation induced by matrix-assisted laser desorption ionisation post-source decay **(A)** and electrospray ionisation collision-induced dissociation **(B)**.

Structural Characterisation of [Asp^3] MC-RAba

[Asp^3] MC-RAba (**161**) had a similar reversed-phase C_{18} retention time to MC-RAba (Table 3.1) but 14 Da lower mass (952.5 Da). The MS/MS spectrum of **161** (Figure 3.35) indicated that the 14 Da mass loss was due to Asp being present in position three instead of Masp (Appendix E.3). Since this microcystin has the same mass as MC-RA, the two compounds were not resolved by MALDI MS, therefore, only LC-MS/MS was utilised for characterisation of this minor component.

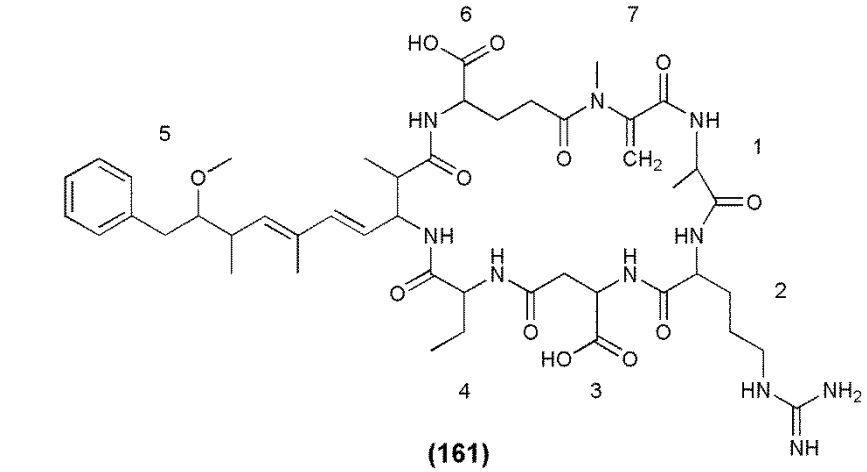

(161)

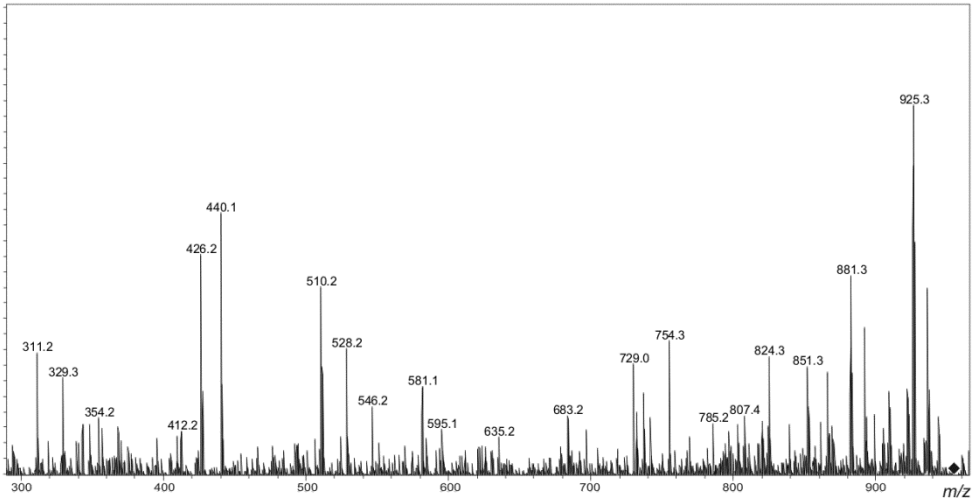

Figure 3.35: Tandem mass spectrum of [Asp^3] MC-RAba. Fragmentation induced by electrospray ionisation collision-induced dissociation.

A combination of amino acid analysis and MS was used to characterise MC-RA (**16**) and MC-RAba (**19**). Amino acid analysis of **16** indicated the presence of D-Ala, L-Ala, D-Glu, D-Masp, *N*-methylamine and (3*S*)-Adda, with either L-Arg or L-Orn. Tandem MS analysis suggested that the *N*-methylamine was due to the breakdown of Mdha and that Arg, not Orn, was present. The

MS/MS also indicated that the amino acids formed a cyclic peptide with the sequence: Ala-Arg-Masp-Ala-Adda-Glu-Mdha. Amino acid analysis of **19** yielded very similar results except that L-Aba was present in position four instead of L-Ala. Using MS/MS, two minor components were determined to be the new microcystins; [Asp^3] MC-RA (**160**) and [Asp^3] MC-RAba (**161**). Whilst only **160** and **161** are new microcystin congeners, the information garnered from the structural characterisation of **16** and **19** was used to characterise the new analogues.

3.2.5 Structural Characterisation of the -XAba Microcystins from CYN06

The -XAba microcystin congeners observed in CYN06 were MC-LAba (**11**), MC-FAba (**166**) and MC-WAba (**167**). MC-LAba has been reported previously,[34,35,249] but MC-FAba and MC-WAba are new variants. MC-FAba and MC-WAba were present at very low levels in CYN06, therefore, no desmethyl analogues were observed and the amount of material obtained was only sufficient to undertake MS/MS and HRMS analyses. Amino acid analysis of MC-RAba confirmed that the Aba utilised by CYN06 was not the isomeric version (2-amino-*iso*-butanoic acid; Aib). As insufficient quantities were present to undertake amino acid analysis on MC-FAba and MC-WAba, it has been assumed that Aba was also present in these microcystins.

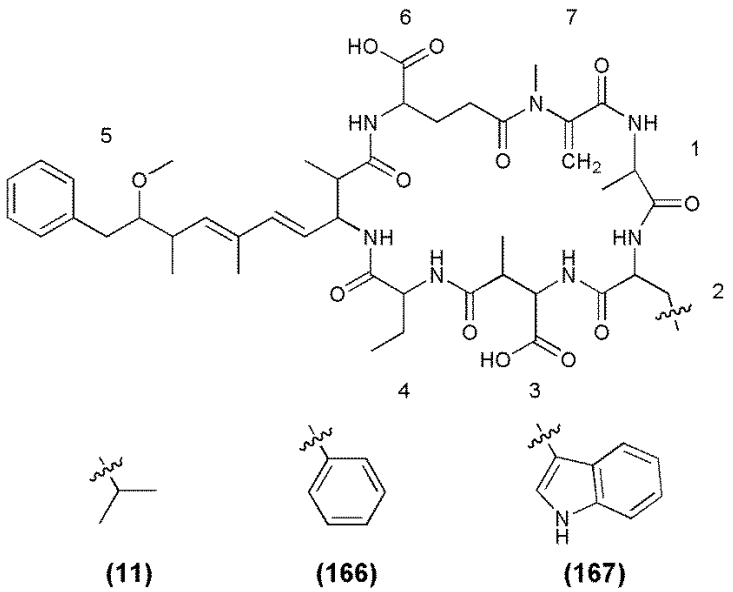

The MS/MS spectra of **166** and **167** (Figure 3.36) indicated that they were microcystins with structures similar to MC-LAba. However, the fragments attributed to the position two amino acid contained either 34 or 73 Da additional

mass (Table 3.7). This was postulated to be due to Phe or Trp being present in position two instead of Leu.

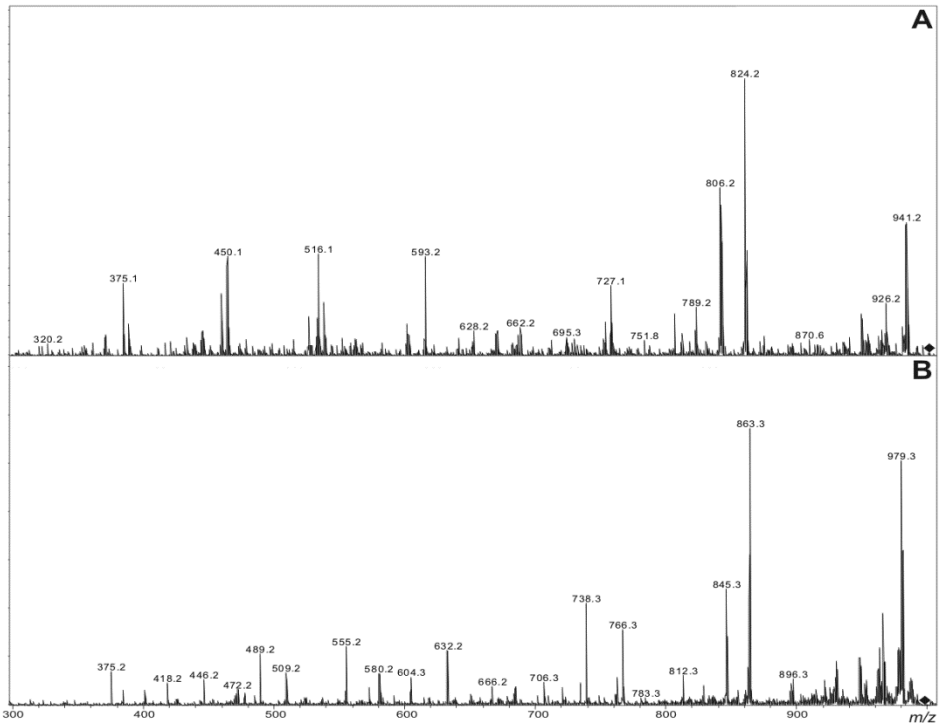

Figure 3.36: Tandem mass spectra of MC-FAba **(A)** and MC-WAba **(B)**. Fragmentation induced by electrospray ionisation collision-induced dissociation.

Table 3.7: Tandem mass spectrometry fragment ions for the -XAba microcystin congeners observed by electrospray ionisation collision-induced dissociation.

Fragment Assignment [a]	**MC-LAba** X = 113 Da	**MC-FAba** X = 147 Da	**MC-WAba** X = 186 Da
M + H	924	958	997
M – H_2O + H	906	940	979
M – Mdha – H_2O + H	823	957	896
M – Adda sidechain + H	790	824	863
M – Adda sidechain – H_2O + H	772	806	845
M – Adda + H	611	645	684
M – Adda – H_2O + H	593	627	666
Adda-Glu-Mdha-Ala-X – NH_3 + H	693	727	766
Adda-Glu-Mdha-Ala – NH_3 + H	580	580	580
Adda-Glu-Mdha – NH_3 + H	509	509	509
Adda'-Glu-Mdha-Ala-X + H	559	593	632
Adda'-Glu-Mdha-Ala + H	446	446	446
Adda'-Glu-Mdha + H	375	375	375
Mdha-Ala-X-Masp-Aba + NH_4	499	533	572
Ala-X-Masp-Aba + NH_4	416	450	489
X-Masp-Aba + NH_4	345	379	418
Mdha-Ala-X-Masp-Aba + H	482	516	555
Ala-X-Masp-Aba + H	399	433	472
X-Masp-Aba + H	328	362	401

[a] X = Position two amino acid; Adda' = Adda minus NH_2 and the sidechain ($C_9H_{11}O$).

The HRMS for MC-FAba and MC-WAba yielded *m/z* of 980.4744 and 1019.4836, consistent with the sodium adduct ions of the structures **166** and **167** ($C_{50}H_{67}N_7O_{12}Na$, *m/z* 980.4740, Δ +0.4 ppm; $C_{52}H_{68}N_8O_{12}Na$, *m/z* 1019.4849, Δ -1.3 ppm).

3.2.6 Structural Characterisation of the -XL Microcystins from CYN06

The -XL microcystin congeners observed in CYN06 were MC-LL (**14**), MC-FL (**168**) and MC-WL (**169**). Whilst MC-LL has been reported previously,[37] MC-FL and MC-WL are new analogues. MC-FL and MC-WL have the same mass as the known microcystins MC-LF and MC-LW,[37,45] however the MS/MS spectra from each indicated that the position two and four amino acids were inverted. Both of these microcystins were present at low levels, therefore only MS/MS characterisation was undertaken on the parent congeners and no desmethyl analogues were observed.

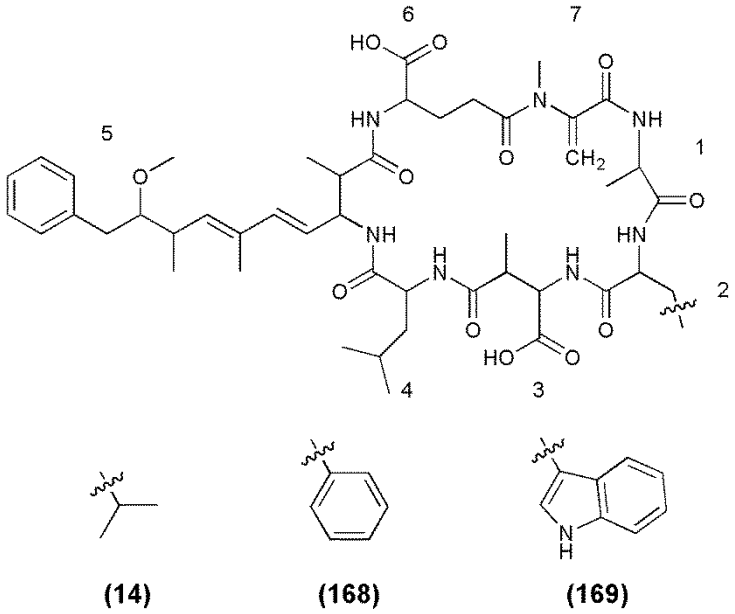

(14) **(168)** **(169)**

The MS/MS spectra of **168** and **169** (Figure 3.37) indicated that they were microcystins with structures similar to MC-LL. However, the fragments attributed to the position two amino acid contained either 34 or 73 Da additional mass (Table 3.8). Again, this was postulated to be due to Phe or Trp being present in position two instead of Leu.

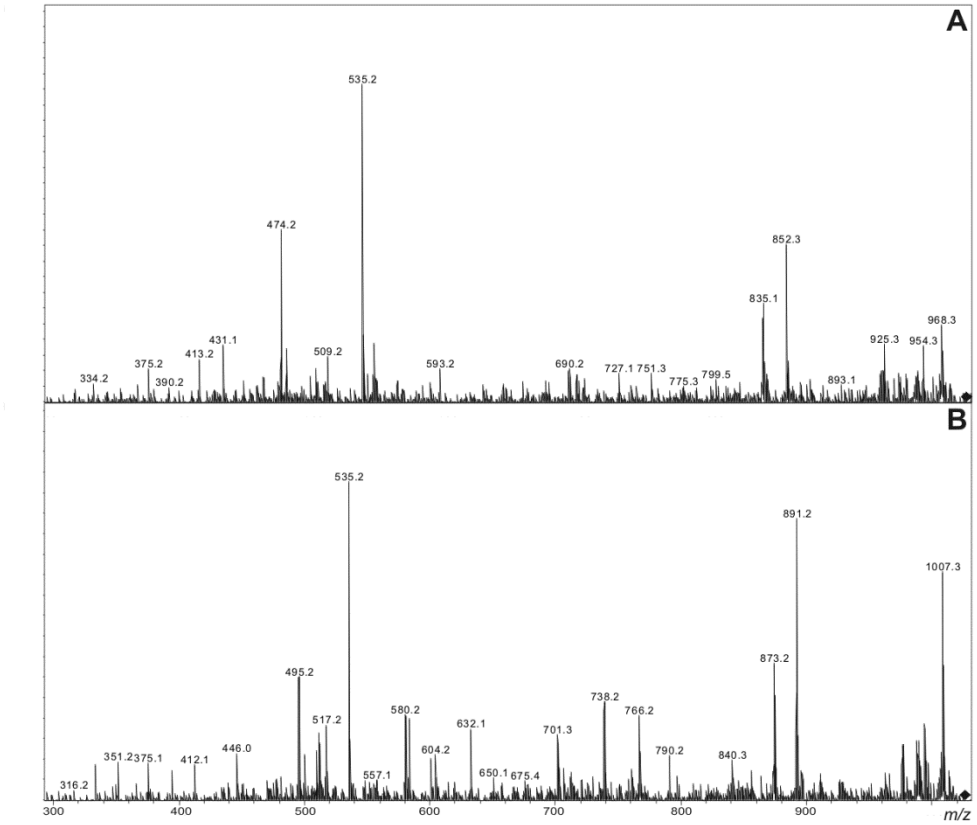

Figure 3.37: Tandem mass spectra of MC-FL **(A)** and MC-WL **(B)**. Fragmentation induced by electrospray ionisation collision-induced dissociation.

Table 3.8: Tandem mass spectrometry fragment ions for the -XL microcystin congeners observed by electrospray ionisation collision-induced dissociation.

Fragment Assignment [a]	MC-LL X = 113 Da	MC-FL X = 147 Da	MC-WL X = 186 Da
M + H	952	986	1025
M – NH_3 + H	935	969	1008
M – H_2O + H	934	968	1007
M – Glu or Masp + H	823	857	896
M – Adda sidechain + H	818	852	891
M – Adda sidechain – H_2O + H	800	834	873
M – Adda + H	639	673	712
M – Adda – H_2O + H	621	655	694
Adda-Glu-Mdha-Ala-X – NH_3 + H	693	727	766
Adda-Glu-Mdha-Ala – NH_3 + H	580	580	580
Adda-Glu-Mdha – NH_3 + H	509	509	509
Glu-Mdha-Ala-X + H	397	431	470
Adda'-Glu-Mdha-Ala-X + H	559	593	632
Adda'-Glu-Mdha-Ala + H	446	446	446
Adda'-Glu-Mdha + H	375	375	375
Unassigned fragment ion	440	474	513
Unassigned fragment ion	535	535	535
Mdha-Ala-X-Masp-Leu + H	509	544	583
Ala-X-Masp-Leu + H	426	461	500
X-Masp-Leu + H	355	390	429

[a] X = Position two amino acid; Adda' = Adda minus NH_2 and the sidechain ($C_9H_{11}O$).

An intense fragment ion that could not be assigned (*m/z* 535) was present in each of the MS/MS spectra from the -XL microcystin congeners (Figure 3.37). As this fragment had the same *m/z* in each of the -XL microcystin congeners, it would be attributed to a common portion of the structure. With another unassigned fragment ion, the mass deviated in each of the microcystins; *m/z* 440 in MC-LL, *m/z* 474 in MC-FL and *m/z* 513 in MC-WL. The mass increments between each of these fragments are the same as the mass increments between Leu, Phe and Trp. These fragments would therefore be attributed to a portion of the structure which contained the position two amino acid.

3.3 DISCUSSION

3.3.1 Microcystin Diversity of CYN06

In this study, 27 different microcystin congeners were detected in cultures of CYN06. This was due to relaxed substrate specificity at positions two, three and four. Five different amino acids were observed to be incorporated into position two of the structure, two amino acids were observed in position three and four amino acids were observed in position four. This equates to a potential 40 microcystins which could be produced by CYN06. This value would increase if the CYN06 microcystin synthase was shown to be able to incorporate more amino acids than reported in the present study.

In order to better understand whether the number of microcystin congeners observed in CYN06 was unique, relevant literature was surveyed to assess the diversity of congeners produced by isolated cyanobacterial strains (Appendix C). In several cases, researchers were not able to identify all the microcystins present and listed these as unknown microcystins.[35,245,252] These unidentified microcystins skew the analysis slightly as it cannot be predicted whether these congeners were similar analogues to those identified or whether they were structurally different. The investigation revealed that the median number of microcystin congeners produced by a cyanobacterial strain was between four and five. When assessing the number of congeners identified, the median was slightly lower (Median = 4.5; Figure 3.38A) than assessments based on the number of congeners observed (Median = 5; Figure 3.38B). The range of the number of microcystin congeners identified in a single cyanobacterial strain spanned from 1 to 16 (Figure 3.38A),

but could be extended to 47 when the unidentified congeners were taken into account (Figure 3.38B).

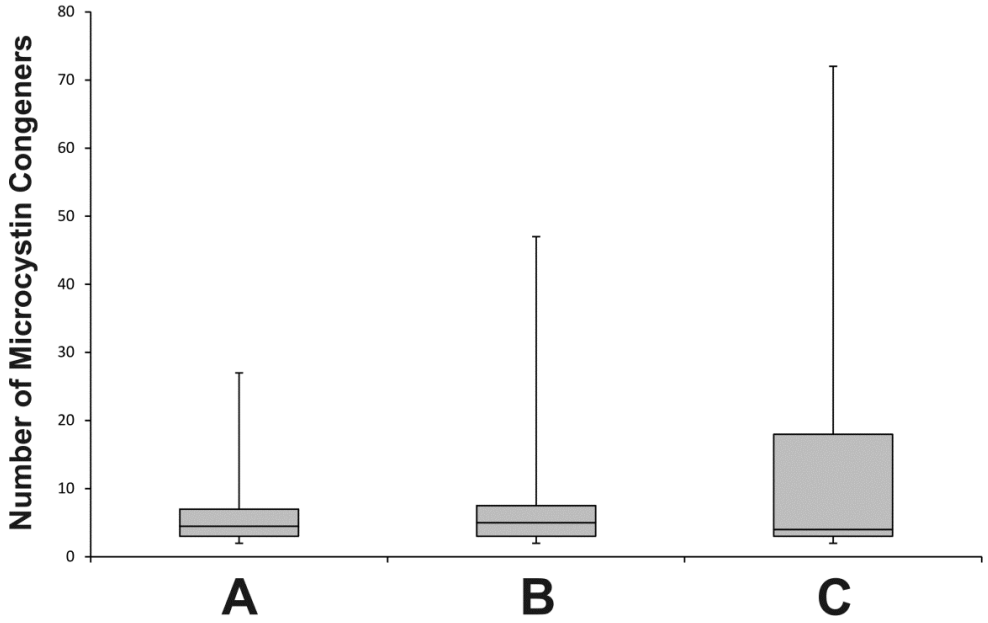

Figure 3.38: Box plots representing the spread in the number of microcystin congeners produced by reported cyanobacterial strains. Plots depict the number of microcystin congeners identified; n = 42 **(A)**, the number of microcystin congeners observed; n = 42 **(B)** and the potential number of congeners which could be produced according to the reported data; n = 33 **(C)**.

When there were no unidentified microcystin congeners present in a cyanobacterial strain, the potential number of congeners which could be produced was calculated. This took account of all of the combinations of the amino acids incorporated into positions two and four, as well as the variable modifications observed. Values ranged from 1 to 72, but there was a slightly lower median of 4 microcystin congeners produced by a cyanobacterial strain (Figure 3.38C). As expected, the range for the potential number of microcystins was higher than that based on the microcystins identified/observed. This was due to some congeners occurring at lower levels and not being detected in the study. The lower median value for the potential number of microcystins compared with the microcystins identified was due to the reduced number of cyanobacterial strains being assessed.

The number of microcystins identified in CYN06 (27 congeners) and the potential number of microcystins which could be produced (40 congeners), positioned CYN06 in the top ten percentile in the distribution of strains assessed. Other

strains in the top ten percentile included *Anabaena* 66A,[245] *Microcystis viridis* NIES102[245] and *Nostoc* 152.[55,56,72,245] These cyanobacterial strains were able to incorporate an array of amino acids into position two and produced variable modifications at other positions in the structure (Appendix C). The strains did not show much variability at the position four amino acid as *Anabaena* 66A and *Microcystis viridis* NIES102 could only incorporate Arg, whilst *Nostoc* 152 was able to incorporate Arg and homoarginine.

In general, the cyanobacterial strains assessed showed a lesser degree of variability in the amino acid incorporated into position four of the structure. The majority of the strains assessed were only able to incorporate one or two amino acids into position four (Appendix C). Interestingly, when strains did exhibit high levels of amino acid variability at position four, they tended to exhibit a high degree of substrate specificity at position two. CYN06 however, showed relaxed substrate specificity at both positions two and four. As a result, CYN06 produced microcystin congeners which contained no arginine residues, a single arginine residue and two arginine residues. Most of the other cyanobacterial strains assessed produced congeners containing one or two arginine residues or congeners that contained one or no arginine residues. None of these strains simultaneously produced microcystin congeners which contained one, two and no arginine residues. As CYN06 produces such a diverse range of microcystin congeners, it provides a useful cyanobacterial strain for culturing experiments to investigate parameters which cause the modulation of microcystin congeners.

3.3.2 Discovery of Ten New Microcystin Congeners

The discovery of ten new microcystins **160**-**169** in CYN06 is a substantial contribution to the 111 microcystins already characterised (Appendix A). The ten new congeners were present in varying quantities and only MC-FA (**163**) and MC-WA (**165**) were purified in sufficient quantities to undertake structural characterisation with NMR spectroscopy. The other new microcystin congeners were characterised using MS/MS and chemical derivatisation.

Six of the new microcystins **163** and **165**-**169** followed the general structure of a microcystin; consisting of Adda, Glu, Mdha, Ala and Masp with variable amino acids in positions two and four.[11] These congeners contained either Phe or Trp in

position two with Ala, Aba or Leu in position four. The remaining four new microcystins **160**-**162** and **164** were [Asp^3] desmethyl analogues of other congeners produced by CYN06. A recently developed thiol derivatisation technique[248] indicated that all of the new microcystin congeners contained Mdha in position seven. This was also indicated during amino acid analysis (for several of the CYN06 microcystins) by the presence of *N*-methylamine.[205] However, the thiol derivatisation (see Section 9.1.5) consumes much less sample and unlike amino acid analysis, it is able to discriminate between Mdha and Mdhb, which both break down to *N*-methylamine upon acid hydrolysis.[250]

Eight of the new congeners **162**-**169** were hydrophobic microcystins containing neutral amino acids in positions two and four. As the structures of these microcystin congeners are relatively conventional, it is surprising that they have not been observed previously. However, this could be due to the lower occurrence of hydrophobic microcystins compared with arginine-containing variants.[12] The presence of Aba-containing microcystins is relatively uncommon, with only four congeners having been reported (Appendix A). Amino acid analysis of MC-RAba indicated that the Aba utilised by CYN06 was the straight chain version in the L-configuration. This was consistent with the only other study of an Aba-containing microcystin, where discrimination was made between Aba and Aib.[36]

Two of the new congeners **160** and **161** contained position two arginine residues in conjunction with a neutral amino acid in position four (MC-RZs). Until recently,[41,66,77] these types of microcystin congeners were rare, with only MC-RA having been reported.[39] An interesting feature of the -RZ microcystin congeners is that whilst the amino acid composition may be identical to an -XR microcystin, the -RZ congeners are retained for longer during reversed-phase C_{18} chromatography (MC-LR = 7.35 min; MC-RL = 8.35 min). This observation has been noted by others,[39,66] and enables a very straightforward means of differentiating between -XR and -RZ microcystin congeners.

The change in retention time of the -RZ microcystins is most likely due to the position five Adda moiety being the major hydrophobic region of a microcystin. As a result, the alkyl chains of the C_{18} column packing are likely to interact

predominantly with this region of the compound. When an Arg residue is present in position four (MC-XRs) next to the Adda moiety, it would also be likely to interact substantially with the alkyl chains of the packing material. When an Arg residue is present in position two (MC-RZs) and is no longer located next to the Adda moiety, the hydrophilic effect of the protonated guanidinium group would not be as pronounced and the microcystin would be retained on the column for longer.

Whilst the isolated quantities of MC-FA and MC-WA were sufficient to conduct toxicology or protein phosphatase inhibition studies, the purity of the samples was not. Further HPLC purification of the samples could yield enough material of sufficient purity to conduct this work; however, there was inadequate time for the additional purification during the present study. However, the Adda-Glu portion of the microcystin structure, which has previously been shown to be important for protein phosphatase inhibition,[33] is not modified in these congeners. Therefore it is likely that the two microcystins would inhibit protein phosphatases and pose a health risk to humans and animals.

3.4 CONCLUSIONS

Assessment of *Microcystis* CYN06 indicated the presence of numerous oligopeptides including aeruginosins, microviridins and microcystins. Further investigation of the microcystin diversity indicated that CYN06 produced at least 27 microcystin congeners, of which, ten had not been reported previously. The structures of MC-FA and MC-WA were determined by NMR spectroscopy whilst the other new variants were characterised by MS/MS. The number of microcystin congeners produced by CYN06 was in the upper ten percentile of the cyanobacterial strains assessed. The relaxed substrate specificity observed in this cyanobacterial strain provides a unique opportunity to investigate the influence of environmental parameters on the abundance of microcystin congeners.

CHAPTER 4

Characterisation of Oxidised Tryptophan Microcystins from *Microcystis* CYN06

4.1 INTRODUCTION

The oxidation of tryptophan (Trp) residues was first reported in 1903[253] and in 1931 kynurenine (Kyn) was identified as a by-product of the biological oxidation of Trp.[254] Since then, the pathway for the enzymatic degradation of Trp has been expanded to include four intermediates which result in either kynurenic acid or quinolinic acid.[255] Whilst the function of this oxidative pathway is to degrade Trp residues, the oxidation of Trp in intact polypeptides is also apparent.[256-259] The major products of this oxidation are oxindolyalanine (Oia), *N*-formylkynurenine (Nfk) and Kyn (Figure 4.1), with Nfk being the most abundant.[256,257]

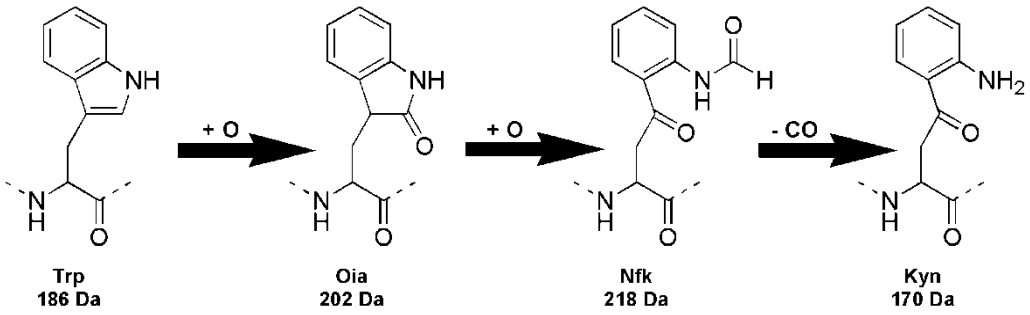

Figure 4.1: Products of the chemical oxidation of tryptophan (Trp).[256] Oia is oxindolyalanine, Nfk is *N*-formylkynurenine and Kyn is kynurenine.

It is still unclear as to whether the oxidation of Trp residues in polypeptides is due to natural levels of reactive oxygen species in the cell,[260] oxidative stress in the cell,[261] post-translational modification of the Trp,[256] or is an artefact of sample handling. It has been shown that the production of Trp oxidation products is intensified by increased levels of reactive oxygen species,[257,262] therefore oxidation of Trp may be an artefact of sample handling, although, this does not disprove the natural intracellular occurrence of oxidised Trp residues.

The oxidation of methionine is also observed in proteins,[261,263,264] and the presence of oxidised methionine-containing microcystins has been reported on two occasions.[38,67] Whilst five Trp-containing microcystins have been reported previously,[38,44,45,49,58] the presence of oxidised Trp residues in microcystins has not. As discussed in Section 3.2.1, CYN06 produces at least six Trp-containing microcystins, four of which are new. Analogues which contained oxidised Trp residues were also present. The characterisation of these microcystins will be presented in this chapter.

4.2 RESULTS

4.2.1 LC-MS Identification of Oxidised Tryptophan Microcystins from *Microcystis* CYN06

LC-MS analysis of a CYN06 extract showed the presence of 27 conventional microcystin congeners (see Table 3.1), as well as nine microcystins which contained oxidised Trp residues in position two (**170**-**178**; Table 4.1). The presence of Kyn, Oia and Nfk was observed in place of Trp, with an arginine (Arg; MC-XRs), alanine (Ala; MC-XAs) and 2-aminobutanoic acid (Aba; MC-XAbas). It is likely that oxidised Trp congeners containing a position four leucine (Leu; MC-XLs) were also present, but were not observed due to low abundance.

Table 4.1: Structure, molecular masses and retention times of the tryptophan- and oxidised tryptophan-containing microcystins found in CYN06.

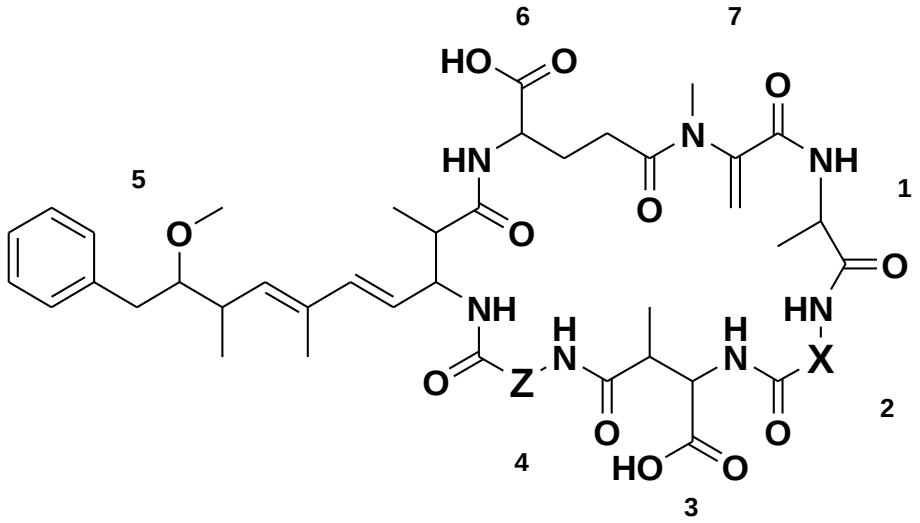

Microcystin		M_r [a] (Da)	RT [b] (min)	X	Z
MC-XRs	MC-WR (**113**)	1067.5	7.60	Trp	Arg
	MC-KynR (**170**)	1071.5	7.45	Kyn	Arg
	MC-OiaR (**171**)	1083.5	7.37	Oia	Arg
	MC-NfkR (**172**)	1099.5	7.32	Nfk	Arg
MC-XAs	MC-WA (**165**)	982.5	9.54	Trp	Ala
	MC-KynA (**173**)	986.5	9.41	Kyn	Ala
	MC-OiaA (**174**)	998.5	9.31	Oia	Ala
	MC-NfkA (**175**)	1014.5	9.07	Nfk	Ala
MC-XAbas	MC-WAba (**167**)	996.5	10.24	Trp	Aba
	MC-KynAba (**176**)	1000.5	9.80	Kyn	Aba
	MC-OiaAba (**177**)	1012.5	9.58	Oia	Aba
	MC-NfkAba (**178**)	1028.5	9.46	Nfk	Aba

[a] Molecular weights are rounded to one decimal place. [b] RT = Retention time on a C_{18} column as per Table 9.3.

4.2.2 Structural Characterisation of MC-NfkA

MC-NfkR (**172**) and MC-NfkA (**175**) were the most abundant of the oxidised Trp microcystins. Whilst MC-NfkR was not able to be separated from MC-LR using the current fractionation procedure, sufficient MC-NfkA was purified in order to conduct structural characterisation by nuclear magnetic resonance (NMR) spectroscopy.

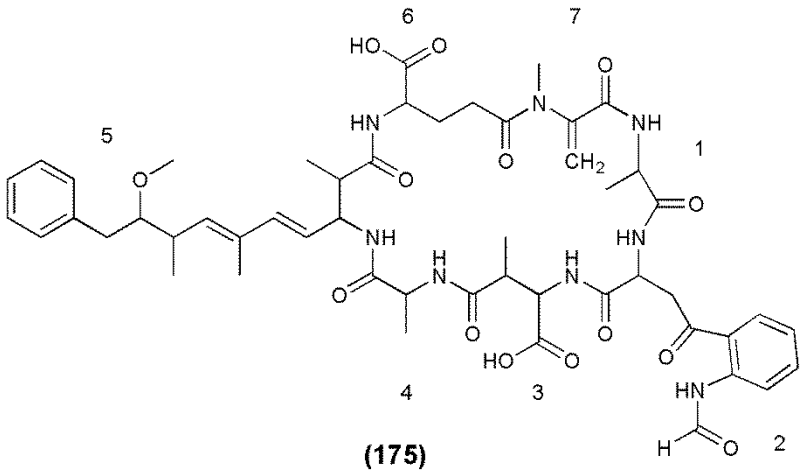

(175)

The electrospray ionisation collision-induced dissociation (ESI CID) tandem mass spectrometry (MS/MS) of **175** (Figure 4.2) indicated that it was a microcystin with a structure similar to MC-WA, but containing a position two amino acid with a mass 32 Da greater than Trp (Nfk, 218 Da; Table 4.2). MC-NfkA also eluted earlier from a reversed-phase C_{18} column than MC-WA (Table 4.1). The presence of an amidoaldehyde like that observed in Nfk would account for this reduced retention time.[257]

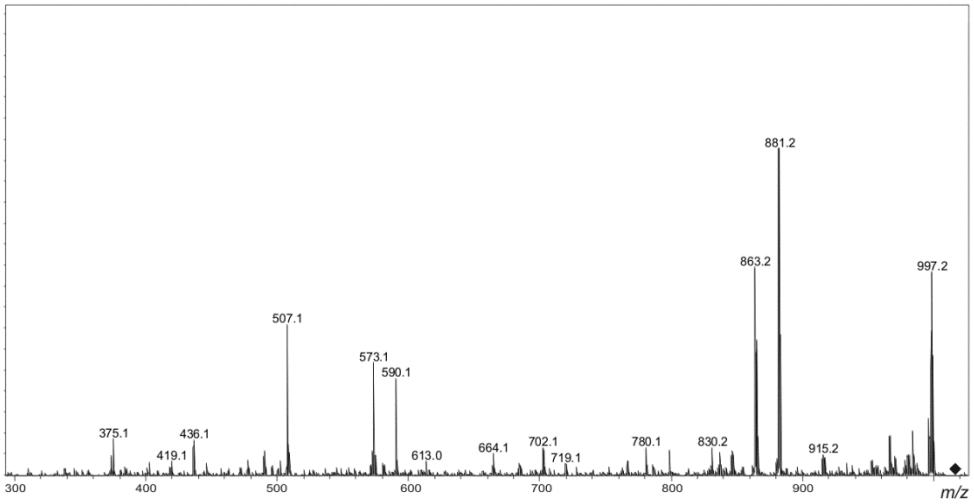

Figure 4.2: Tandem mass spectrum of MC-NfkA. Fragmentation induced by electrospray ionisation collision-induced dissociation.

Table 4.2: Tandem mass spectrometry fragment ions for MC-NfkA observed by electrospray ionisation collision-induced dissociation.

m/z	Fragment Assignment [a]	*m/z*	Fragment Assignment [a]
373	Mdha-Ala-Nfk + H	375	Adda'-Glu-Mdha + H
419	Nfk-Masp-Ala + H	446	Adda'-Glu-Mdha-Ala + H
490	Ala-Nfk-Masp-Ala + H	509	Adda-Glu-Mdha – NH_3 + H
573	Mdha-Ala-Nfk-Masp-Ala + H	580	Adda-Glu-Mdha-Ala – NH_3 + H
664	Adda'-Glu-Mdha-Ala-Nfk + H	684	M – Adda – H_2O + H
702	M – Adda + H	798	Adda-Glu-Mdha-Ala-Nfk – NH_3 + H
863	M – Adda sidechain – H_2O + H	881	M – Adda sidechain + H
914	M – Mdha – H_2O + H	997	M – H_2O + H
1015	M + H		

[a] Fragments containing NH_4^+ adducts were not included; Adda' = Adda minus NH_2 and the sidechain ($C_9H_{11}O$).

The Adda'-Glu-Mdha fragment ion (*m/z* 375) commonly observed in microcystins[265] was extended to include Ala and Nfk (Figure 4.3A). This sequence was supported by the ion series containing Adda minus NH_3 (*m/z* 509, 580, 798; Figure 4.3B). A fragment ion series which began with Nfk-Masp-Ala (*m/z* 419; Figure 4.3B) and extended in the opposite direction to include a second Ala residue gave the complete amino acid sequence of Adda-Glu-Mdha-Ala-Nfk-Masp-Ala. A fragment where Mdha and water were lost from the compound (*m/z* 914; Table 4.2) indicated that Adda and the second Ala residue were joined and that the structure was cyclic.

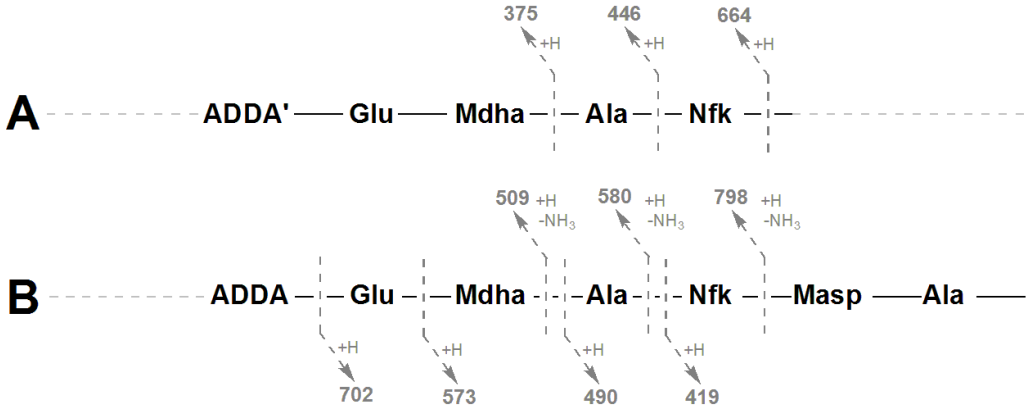

Figure 4.3: Tandem mass spectrometry fragment ions indicating the amino acid sequence in MC-NfkA.

High resolution mass spectrometry (HRMS) of MC-NfkA yielded a *m/z* of 1037.4598, consistent with the sodium adduct ion of the proposed structure **175** ($C_{51}H_{66}N_8O_{14}Na$, *m/z* 1037.4591, Δ −0.75 ppm).

The structure suggested by the MS/MS analysis was investigated further by NMR spectroscopy. Interpretation of COSY, TOCSY, ROESY, HSQC and HMBC spectra allowed for the assignment of the ^{1}H and ^{13}C signals (Table 4.3). These spectra were acquired in a solvent which allowed exchangeable protons to be detected (CD_3OH) and on a 600 MHz instrument. Nuclear magnetic resonance spectra for MC-NfkA are presented in Appendix I.

Table 4.3: Nuclear magnetic resonance spectroscopy assignment of MC-NfkA at 600 MHz in CD_3OH.

AA[a]	^{13}C	^{1}H	Mult.[b] (*J* in Hz)	AA[a]	^{13}C	^{1}H	Mult.[b] (*J* in Hz)
Ala-1				**Adda**-5			
1	175.7	-		1	176.5	-	
2	49.9	4.54	m	2	44.6	3.16	m
3	17.1	1.40	d (7.3)	3	56.7	4.57	m
NH	-	8.22	d (8.5)	4	127.3	5.58	dd (9.3, 15.5)
				5	138.6	6.24	d (15.5)
Nfk-2				6	136.0	-	
1	nd	-		7	136.4	5.41	d (10.0)
2	55.9	4.26	m	8	37.7	2.59	m
3	29.1	2.02 (2H)	m	9	88.4	3.25[c]	m
4	nd	-		10	39.3	2.68	dd (7.4, 14.0)
5	124.9	-				2.82	dd (4.7, 14.0)
6	132.4	8.06	d (7.2)[d]	11	140.3	-	
7	125.5	7.24	dd (7.2, 8.6)[d]	12 & 16	130.1	7.19	d (7.8)
8	134.6	7.49	dd (8.0, 8.6)	13 & 15	128.7	7.24	dd (7.4, 7.8)
9	122.2	8.49	d (8.0)	14	126.9	7.16	t (7.4)
10	139.5	-		17	15.9	1.07	d (6.7)
11	162.5	8.43	s	18	12.9	1.64	s
CHO-NH	-	8.93	br s	19	16.4	1.00	d (6.9)
NH	-	8.32	d (6.8)	20	58.7	3.24	s
				NH	-	8.01	d (9.2)
Masp-3							
1	nd	-		**Glu**-6			
2	58.5	4.36	m	1	nd	-	
3	42.3	3.14	m	2	56.5	4.06	m
4	177.8	-		3	29.7	1.93	m
5	15.8	1.06	d (6.9)			2.22	m
NH	-	8.06	d (8.3)	4	33.5	2.48	m
						2.66	m
Ala-4				5	177.1	-	
1	172.5	-		NH	-	8.39	d (7.2)
2	49.0	4.41	m				
3	17.5	1.26	d (7.3)	**Mdha**-7			
NH	-	8.72	d (9.2)	1	165.9	-	
				2	146.3	-	
				3	113.6	5.27	s
						5.71	s
				N-CH_3	38.2	3.28[c]	s

[a] AA = Amino acid (number indicates the position in the structure); nd = Not detected; br = Broad signal. [b] Mult. = Multiplicity of the proton signal; *J* = Coupling constant. [c] Signals were overlapped so chemical shifts were determined using correlations observed in 2D HSQC spectra. [d] Multiplicity and coupling constants were determined using 1D-selective TOCSY experiments.

Much of the structure of MC-NfkA was the same as those of MC-FA and MC-WA and, as a result, similar chemical shifts and coupling constants were observed for the corresponding parts of the structure (Tables 3.2, 3.4 and 4.3). The differences resulted from use of a solvent which allowed exchangeable protons to be detected, and hence the amine proton signals were observed in the spectrum. These signals overlapped with the aromatic signals from Nfk, however the identity of the signals was easily determined by comparing the proton spectrum acquired in CD_3OD with that acquired in CD_3OH (Figure 4.4). Analysis of the COSY coupling between the amine protons and the adjacent methines allowed each of the amine proton signals to be attributed to one of the amino acids present in MC-NfkA.

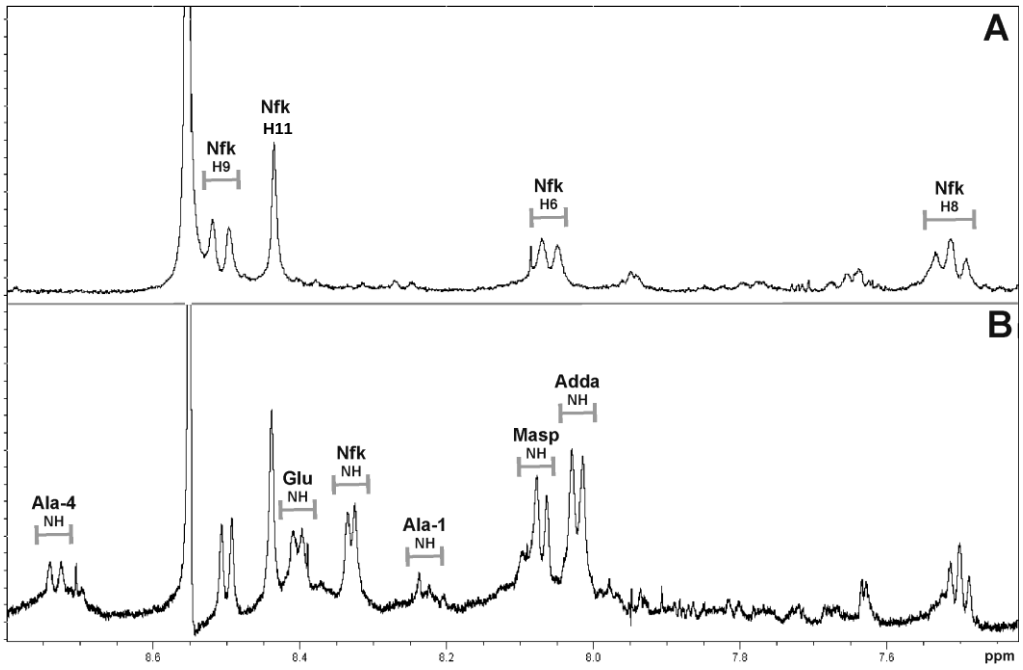

Figure 4.4: Proton nuclear magnetic resonance spectra of the downfield region of MC-NfkA in CD_3OD **(A)** and CD_3OH **(B)**.

The presence of the amide protons caused additional ^1H-^1H coupling, which led to splitting of the adjacent methine proton signals. As a result, the multiplicities of these signals were no longer able to be discerned (Table 4.3). The ROESY correlations observed from the amine protons showed connectivity between several of the amino acids in the microcystin. The ROESY spectrum of MC-NfkA showed an interaction between the Glu amine and the Adda H2 (Figure 4.5), which indicated these two amino acids were adjacent. Several ROESY correlations between the Adda amine and the Ala residue with the more upfield

methyl proton resonance (1.26 ppm), placed this Ala in position four. This reinforced the assertion made with MC-FA and MC-WA, that the Ala with the more upfield methyl proton resonance was in position four (see Section 3.2.2). A correlation between the amine of the position four Ala and the Masp H3 confirmed that Masp was in position three. Another ROESY correlation between one of the Nfk aromatic protons and the Masp amine, reinforced its placement in position two. An HMBC correlation between the *N*-methyl of Mdha and the Glu C5 carbonyl confirmed that these two amino acids were also adjacent.

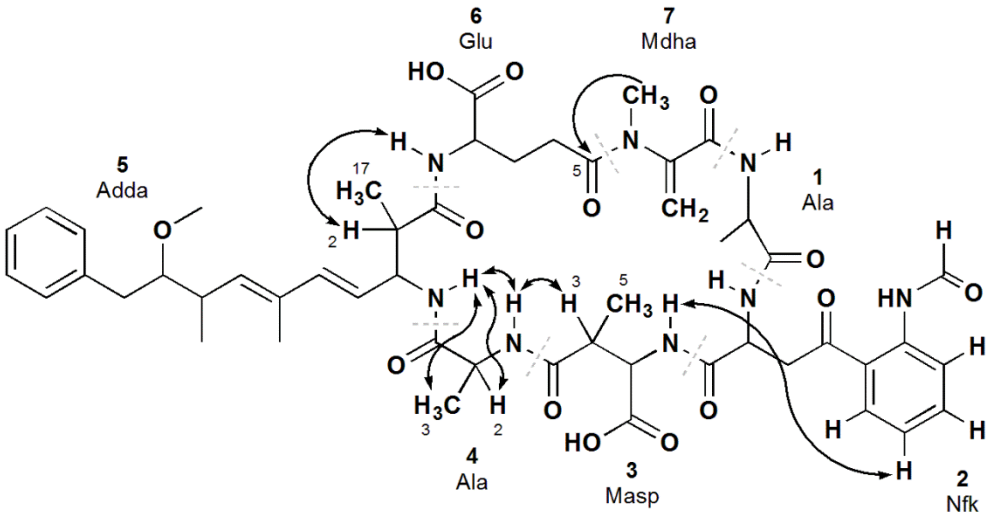

Figure 4.5: Connectivity within MC-NfkA shown by nuclear magnetic resonance spectroscopy correlations. Double-headed arrows are ROESY correlations and the single-headed arrow is an HMBC correlation.

NMR Characterisation of the N-formylkynurenine residue in MC-NfkA

The Nfk residue gave rise to nine proton signals; a sharp singlet at 8.43 ppm, a broad singlet at 8.93 ppm, three doublets at 8.06, 8.49 and 8.32 ppm, two doublets of doublets at 7.24 and 7.49 ppm, and two multiplets at 2.02 and 4.26 ppm (Table 4.3). The HSQC spectrum indicated that the 8.32 and 8.93 ppm signals were not attached to a carbon, which suggested they were amine proton signals. The HSQC spectrum also correlated the 2.02 ppm proton signal to a carbon resonance at 29.1 ppm, which the DEPT-135 designated as the only methylene in the structure (C3). This proton signal showed a COSY coupling to the multiplet at 4.26 ppm (H2; Figure 4.6) which, due to its chemical shift, was adjacent to two electron withdrawing environments. One of these environments was shown to be an amine, as there was a COSY coupling between the 4.26 ppm signal and the

8.32 ppm amine doublet. The other environment was most likely the carbonyl of an intact peptide bond, although an HMBC correlation to this was not observed.

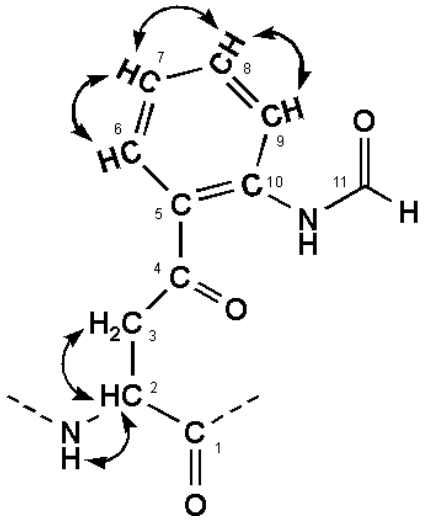

Figure 4.6: COSY correlations for the *N*-formylkynurenine residue in MC-NfkA.

As with the Trp residue in MC-WA, the aromatic signals in MC-Nfk were in an asymmetric environment and produced individual resonances. However, the chemical shifts of the aromatic proton signals in Nfk were more downfield than those observed in Trp (7.24-8.49 ppm as opposed to 7.00-7.67 ppm; Tables 3.5 and 4.3). The 8.49 ppm doublet (H9) in Nfk showed a COSY coupling to the 7.49 ppm signal (H8; Figure 4.7), which was coupled to the signal at 7.24 ppm (H7) which was in turn coupled to the 8.06 ppm doublet (H6). This ^{1}H-^{1}H coupling pattern indicated an intact aromatic ring, however, the more downfield chemical shifts compared to MC-WA, suggested that two electron-withdrawing substituents were located on the two remaining carbons.

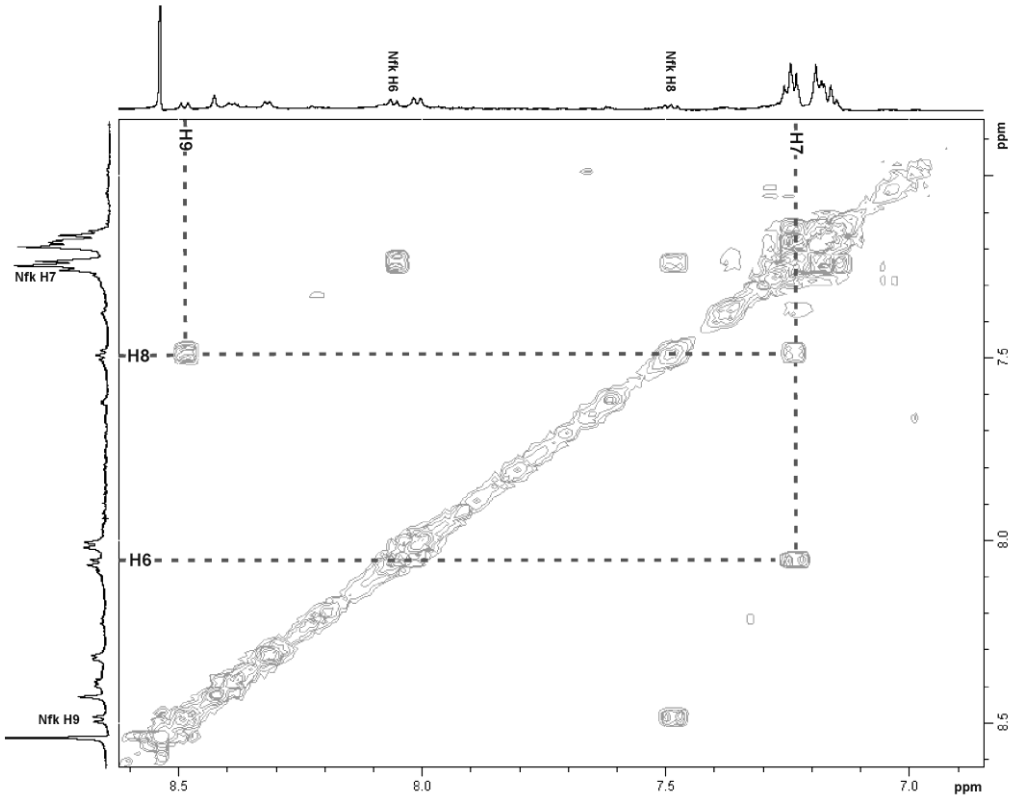

Figure 4.7: COSY spectrum for the *N*-formylkynurenine aromatic protons in MC-NfkA. Lines indicate coupling between proton signals.

A ^{3}J HMBC correlation between the H6 doublet and a quaternary carbon signal at 139.5 ppm indicated that it was the C10 quaternary carbon. Another ^{3}J HMBC correlation between the H9 doublet and a quaternary carbon which resonated at 124.9 ppm indicated that the latter arose from the C5 quaternary carbon (Figure 4.8).

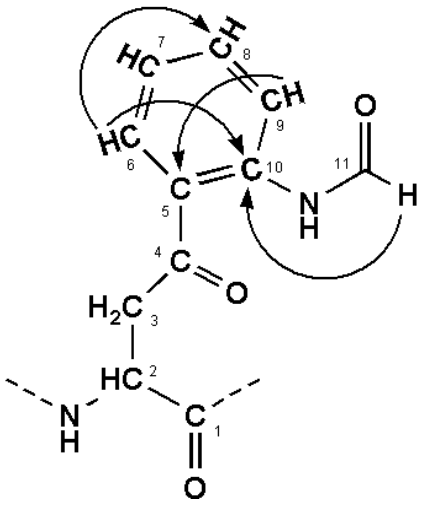

Figure 4.8: HMBC correlations for the *N*-formylkynurenine residue in MC-NfkA.

The chemical shift of the singlet at 8.43 ppm (H11) indicated that the proton was in a very electron-withdrawing environment, but it was not as downfield as would be expected for an aldehyde. In a ROESY experiment this peak showed a proton exchange with a broad peak at 8.93 ppm. The downfield chemical shift and the broad appearance of the 8.93 ppm peak could be due to an amine rapidly exchanging a proton. The presence of an amidoaldehyde would also explain the upfield chemical shift of the H11 signal.[266] The H11 singlet also showed an HMBC correlation to a quaternary carbon (C10). Assuming a ^{3}J coupling; this indicated that the amidoaldehyde was the C10 substituent of the aromatic ring (Figure 4.8). The presence of this electron-withdrawing environment would, to some degree, explain the more downfield chemical shifts observed for the aromatic protons (H6-H9).

N-Formyl moieties can form rotational isomers, which are able to be distinguished by NMR spectroscopy.[267] When in the *trans*-configuration, the amidoaldehyde proton signal (H11) is coupled to the amide proton with a coupling constant of ca. 10 Hz. In the *cis*-configuration, this ^{1}H-^{1}H coupling is not evident.[267] As the H11 signal in MC-NfkA resonated as a singlet, the *N*-formyl moiety was determined to be in the *cis*-configuration.

MS/MS analysis of MC-NfkA indicated that it possessed a structure similar to MC-WA, but with an amino acid which was 32 Da larger in position two. This mass increase correlated well with the presence of Nfk instead of Trp and was supported by a reduced retention time on reversed-phase C_{18}.[257] The NMR data matched that reported for Nfk.[266] Due to restricted amounts of sample, the C1 and C4 carbonyls were not detected, however the mass of the amino acid at position two indicated by the MS/MS analysis, supported the inclusion of these two carbonyls in the structure.

4.2.3 Identification of Two Further -XA Oxidised Tryptophan Congeners

The oxidation of Trp residues yields several major oxidation products (Kyn, Oia and Nfk), as well as other minor components.[257] Whilst MC-NfkA was present in large enough quantities to purify and characterise by NMR spectroscopy, the presence of -XA microcystins containing Kyn (**173**) and Oia (**174**) was also apparent.

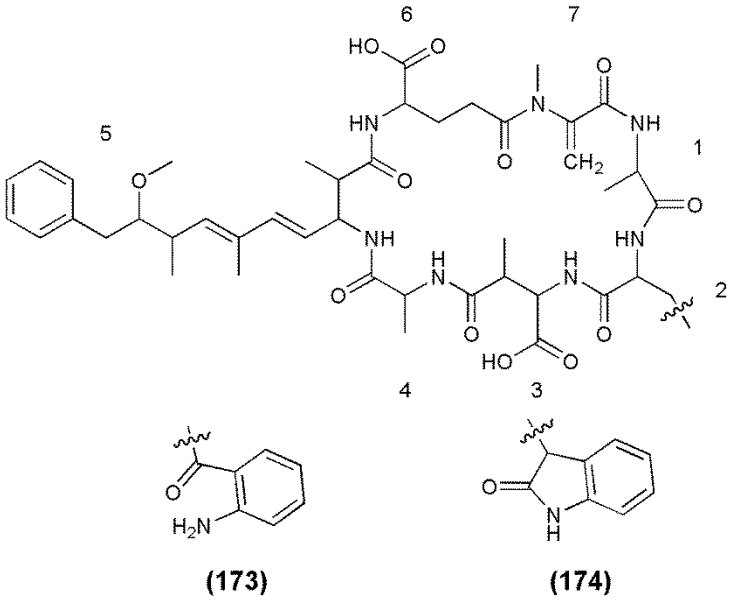

(173) **(174)**

The MS/MS spectra of **173** and **174** (Figure 4.9) indicated that they were microcystins very similar to MC-WA, but containing a position two amino acid with additional mass of 4 or 16 Da, respectively (Table 4.4). These amino acids were postulated to be the Trp oxidation products, Kyn and Oia, due to their mass and the presence of MC-NfkA in CYN06.

The HRMS of MC-KynA and MC-OiaA yielded *m/z* 1009.4670 and 1021.4634, consistent with sodium ions of the proposed structures **173** and **174** ($C_{50}H_{66}N_8O_{13}Na$, *m/z* 1009.4642, Δ +2.82 ppm; $C_{51}H_{66}N_8O_{13}Na$, *m/z* 1021.4642, Δ −0.76 ppm).

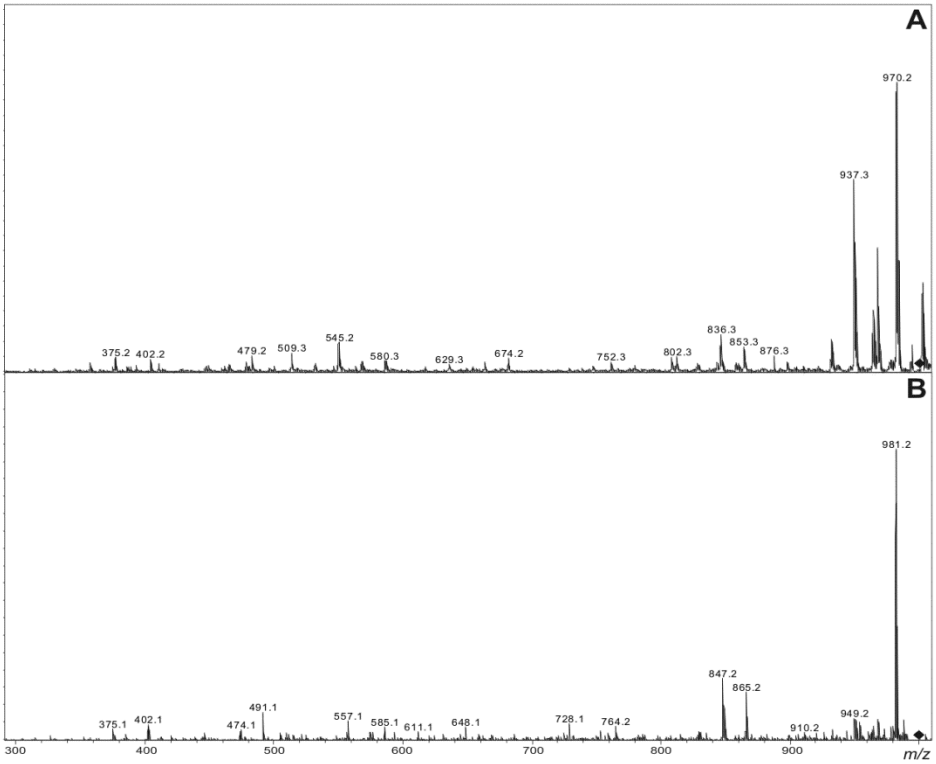

Figure 4.9: Tandem mass spectra of MC-KynA **(A)** and MC-OiaA **(B)**. Fragmentation was induced by electrospray ionisation collision-induced dissociation.

Table 4.4: Tandem mass spectrometry fragment ions for the -XA oxidised tryptophan microcystin congeners observed by electrospray ionisation collision-induced dissociation.

Fragment Assignment [a]	**MC-WA** X = 186 Da	**MC-KynA** X = 190 Da	**MC-OiaA** X = 202 Da
M + H	983	987	999
M – H_2O + H	965	969	981
M – Mdha – H_2O + H	882	886	898
M – Adda sidechain + H	849	853	865
M – Adda sidechain – H_2O + H	831	835	847
M – Adda + H	670	674	
M – Adda – H_2O + H	652	656	668
Adda-Glu-Mdha-Ala-X-Masp – NH_3 + H	895	899	911
Adda-Glu-Mdha-Ala-X – NH_3 + H	766	770	782
Adda-Glu-Mdha-Ala – NH_3 + H	580	580	580
Adda-Glu-Mdha – NH_3 + H	509	509	509
Adda'-Glu-Mdha-Ala-X + H	632	636	648
Adda'-Glu-Mdha-Ala + H	446	446	446
Adda'-Glu-Mdha + H	375	375	375
Mdha-Ala-X-Masp-Ala + H	541	545	557
Ala-X-Masp-Ala + H	458	462	474
X-Masp-Ala + H	387	391	
Mdha-Ala-X + H	341	345	357

[a] Fragments containing NH_4^+ adducts were not included; X = Position two amino acid; Adda' = Adda minus NH_2 and the sidechain ($C_9H_{11}O$).

4.2.4 Identification of Three -XR Oxidised Tryptophan Congeners

Three microcystins in *Microcystis* CYN06 contained Arg at position four with a position two amino acid consistent with Kyn (**170**), Oia (**171**) or Nfk (**172**).

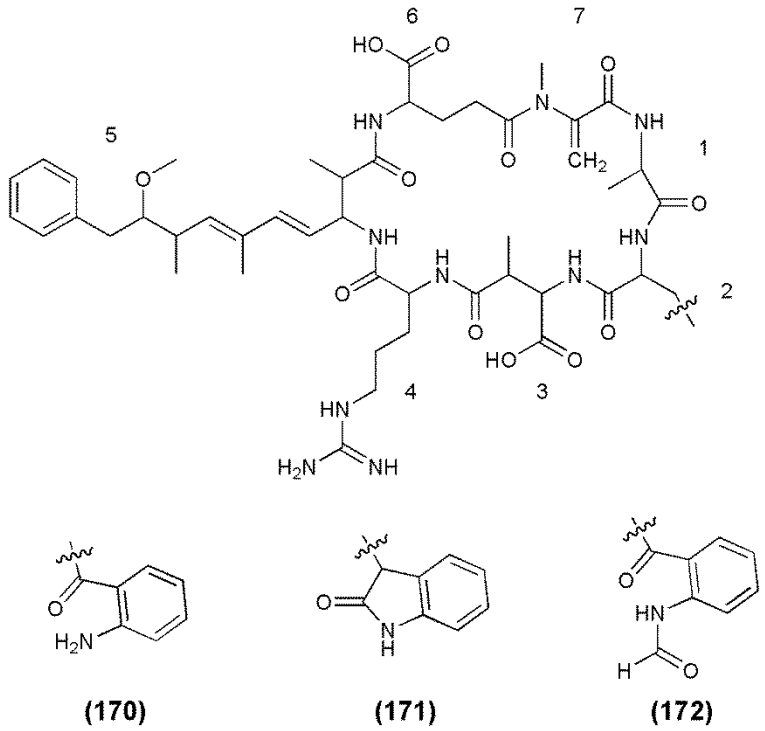

(170) **(171)** **(172)**

As each of these microcystins **170**-**172** contained an Arg residue, they ionised well using matrix-assisted laser desorption/ionisation (MALDI) MS. Therefore, both MALDI post-source decay (PSD) and ESI CID MS/MS were utilised for their characterisation. The MS/MS spectra of **170**-**172** (Figure 4.10) indicated they had structures very similar to MC-WR, but containing an amino acid in position two with additional mass of 4, 16 or 32 Da, respectively (Table 4.5). These amino acids were postulated to be Kyn, Oia and Nfk.

The HRMS of MC-KynR, MC-OiaR and MC-NfkR yielded *m/z* of 1072.5431, 1084.5449 and 1100.5548, consistent with protonated ions of the proposed structures **170**-**172** ($C_{53}H_{73}N_{11}O_{13}$, *m/z* 1072.5431, Δ −2.93 ppm; $C_{54}H_{73}N_{11}O_{13}$, *m/z* 1084.5462, Δ −1.24 ppm; $C_{54}H_{73}N_{11}O_{14}$, *m/z* 1100.5411, Δ +3.42 ppm).

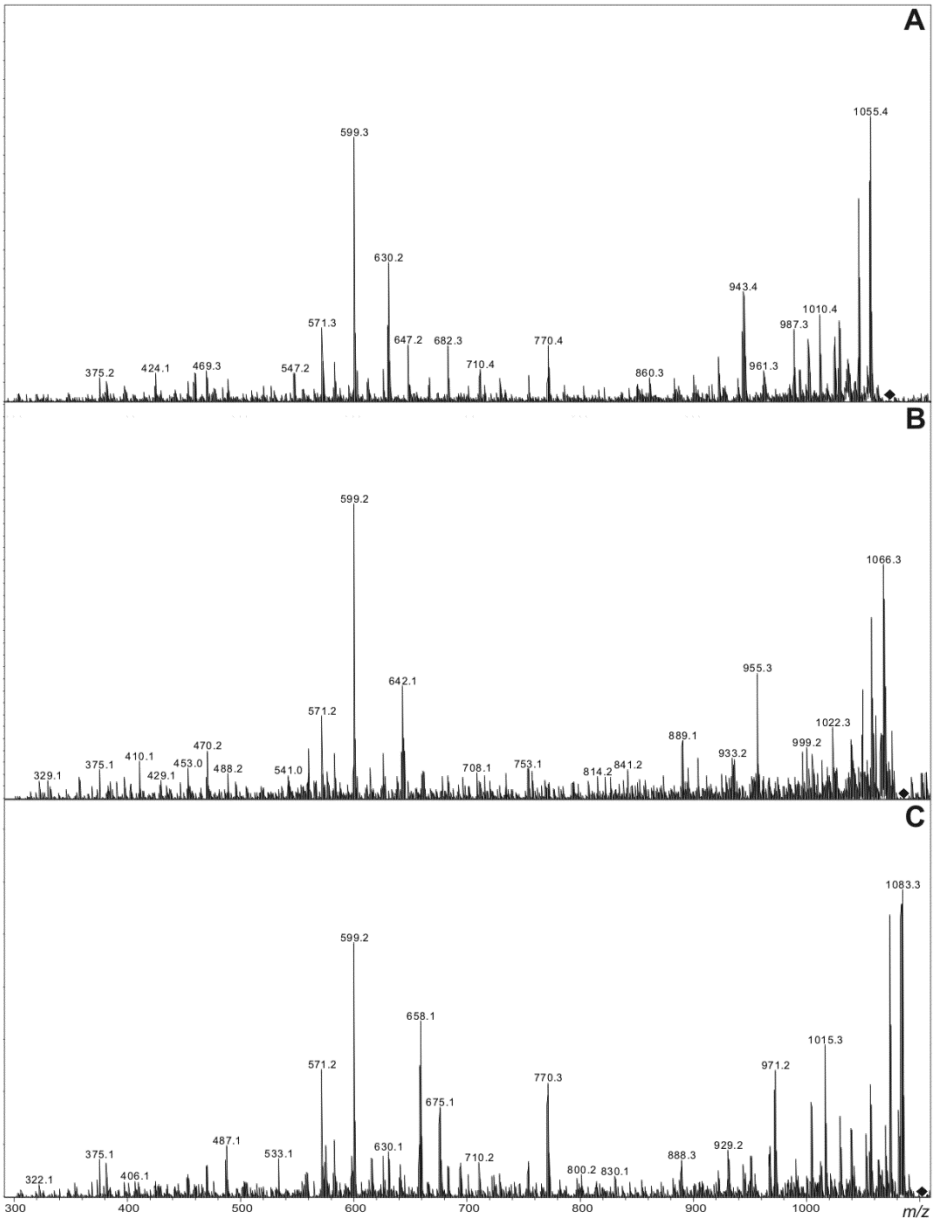

Figure 4.10: Tandem mass spectra of MC-KynR **(A)**, MC-OiaR **(B)** and MC-NfkR **(C)**. Fragmentation was induced by electrospray ionisation collision-induced dissociation.

Table 4.5: Tandem mass spectrometry fragment ions for the -XR oxidised tryptophan microcystin congeners observed by electrospray ionisation collision-induced dissociation and matrix-assisted laser desorption/ionisation post-source decay.

Fragment Assignment [a]	**MC-WR** X = 186 Da	**MC-KynR** X = 190 Da	**MC-OiaR** X = 202 Da	**MC-NfkR** X = 218 Da
M + H	1068	1072	1084	1100
M – H_2O + H	1050	1054	1066	1082
M – Ala + H	997	1001	1013	1029
M – $CH_2NHCN_2H_3$ + H	996	1000	1012	1028
M – Glu or Masp + H	939	943	955	971
M – Adda sidechain + H	934	938	950	966
M – Adda + H	755	759	771	787
Arg-Adda-Glu – NH_3 + H	582	582	582	582
Arg-Adda – NH_3+ H	453	453	453	453
Masp-Arg-Adda – CO + H or Arg-Adda-Glu – CO + H	571	571	571	571
Masp-Arg-Adda-Glu + H	728	728	728	728
Masp-Arg-Adda + H or Arg-Adda-Glu + H	599	599	599	599
Arg-Adda + H	470	470	470	470
Mdha-Ala-X-Masp-Arg + H	626	630	642	658
Ala-X-Masp-Arg + H	543	547	559	575
X-Masp-Arg + H	472	476	488	504
Mdha-Ala-X-Masp + H	470	474	486	502
Mdha-Ala-X + H	341	345	357	373
Mdha-Ala + H	155	155	155	155
Adda'-Glu-Mdha-Ala + H	446	446	446	446
Adda'-Glu-Mdha + H	375	375	375	375
Glu-Mdha + H	213	213	213	213
ADDA' + H	163	163	163	163
ADDA sidechain	135	135	135	135
Arg related ions	70/84/112/174	70/84/112/174	70/84/112/174	70/84/112/174

[a] X = Position two amino acid; Adda' = Adda minus NH_2 and the sidechain ($C_9H_{11}O$); $CH_2NHCN_2H_3$ is a fragment of the Arg sidechain.

4.2.5 Identification of -XAba Oxidised Tryptophan Congeners

Two microcystins in *Microcystis* CYN06 contained Aba at position four and a position two amino acid consistent with Oia (**177**) or Nfk (**178**). A further compound possessing a molecular mass consistent with that of MC-KynAba (**176**) was also observed.

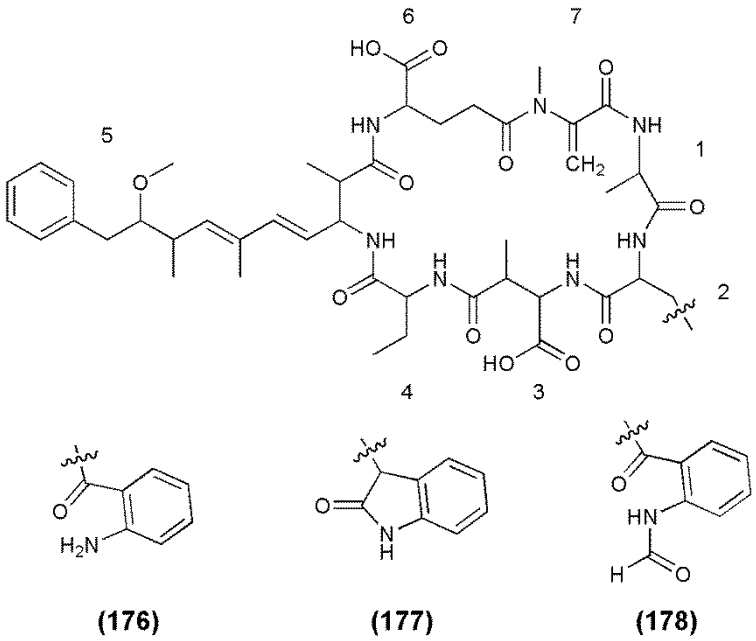

(176) **(177)** **(178)**

The MS/MS spectra of **177** and **178** (Figure 4.11) indicated that they were microcystins very similar to MC-WAba, but contained an amino acid at position two with additional mass of 16 or 32 Da, respectively (Table 4.6). These amino acids were postulated to be Oia and Nfk according to their mass and the presence of MC-NfkA. Because the -XAba microcystins were present in such low quantities, the presence of an $[M+H]^+$ 1001.5 ion was the only indication of MC-KynAba (**176**). This also meant there were not sufficient quantities to undertake purification and HRMS analysis of MC-OiaAba and MC-NfkAba.

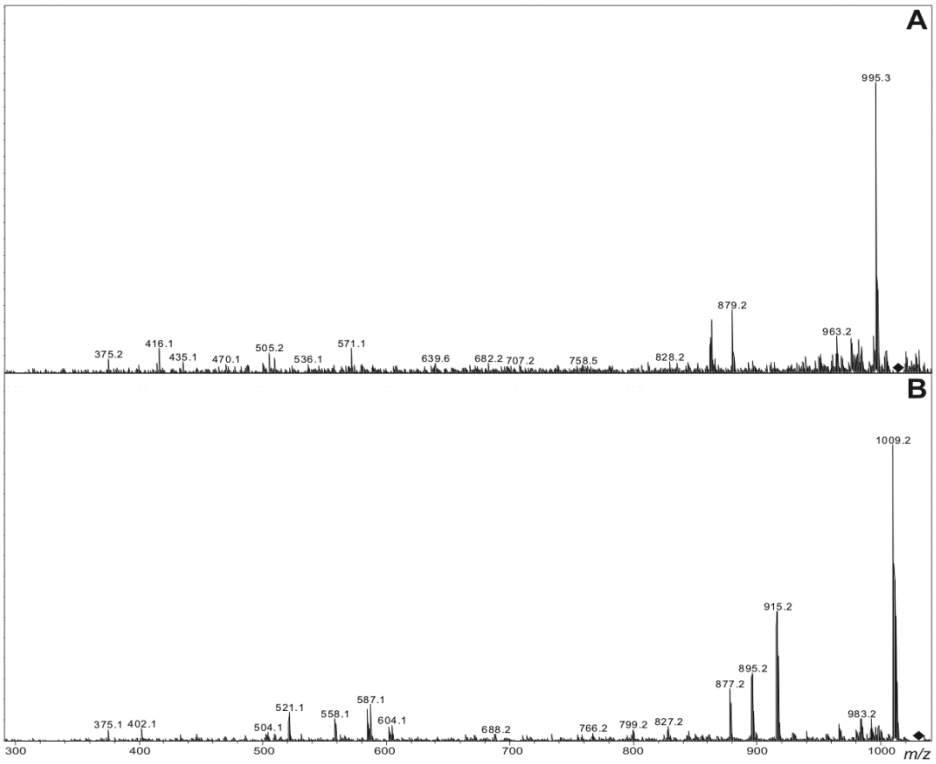

Figure 4.11: Tandem mass spectra of MC-OiaAba **(A)** and MC-NfkAba **(B)**. Fragmentation was induced by electrospray ionisation collision-induced dissociation.

Table 4.6: Tandem mass spectrometry fragment ions for the -XAba oxidised tryptophan microcystin congeners observed by electrospray ionisation collision-induced dissociation.

Fragment Assignment [a]	**MC-WAba** X = 186 Da	**MC-OiaAba** X = 202 Da	**MC-NfkAba** X = 218 Da
M + H	997	1013	1029
M – H_2O + H	979	995	1011
M – Mdha – H_2O + H	896		928
M – Aba – H_2O + H		910	
M – Glu or Masp – H_2O + H	850	866	878
M – Adda sidechain + H	863	879	895
M – Adda sidechain – H_2O + H	845	861	877
M – Adda + H	684	700	716
M – Adda – H_2O + H	666		698
Adda-Glu-Mdha-Ala-X-Masp – NH_3 + H	895	911	
Adda-Glu-Mdha-Ala-X – NH_3 + H	766	782	798
Adda-Glu-Mdha-Ala – NH_3 + H	580	580	580
Adda-Glu-Mdha – NH_3 + H	509	509	509
Adda'-Glu-Mdha-Ala-X + H	632	648	664
Adda'-Glu-Mdha-Ala + H	446	446	446
Adda'-Glu-Mdha + H	375	375	375
Mdha-Ala-X-Masp-Aba + H	555	571	587
Ala-X-Masp-Aba + H	472		504
X-Masp-Aba + H	401	417	433

[a] Fragments containing NH_4^+ adducts were not included; X = Position two amino acid; Adda' = Adda minus NH_2 and the sidechain ($C_9H_{11}O$).

4.2.6 Oxidation of Tryptophan-Containing Microcystins

Several experiments were conducted in order to determine if the oxidised Trp microcystins could be produced via oxidation of existing Trp microcystins. An extract of CYN06 was shielded from light and exposed to atmospheric oxygen while sub-samples were analysed periodically by LC-MS (Figure 4.12A). After 124 h, the level of Trp-containing microcystins (for example, MC-WA) had

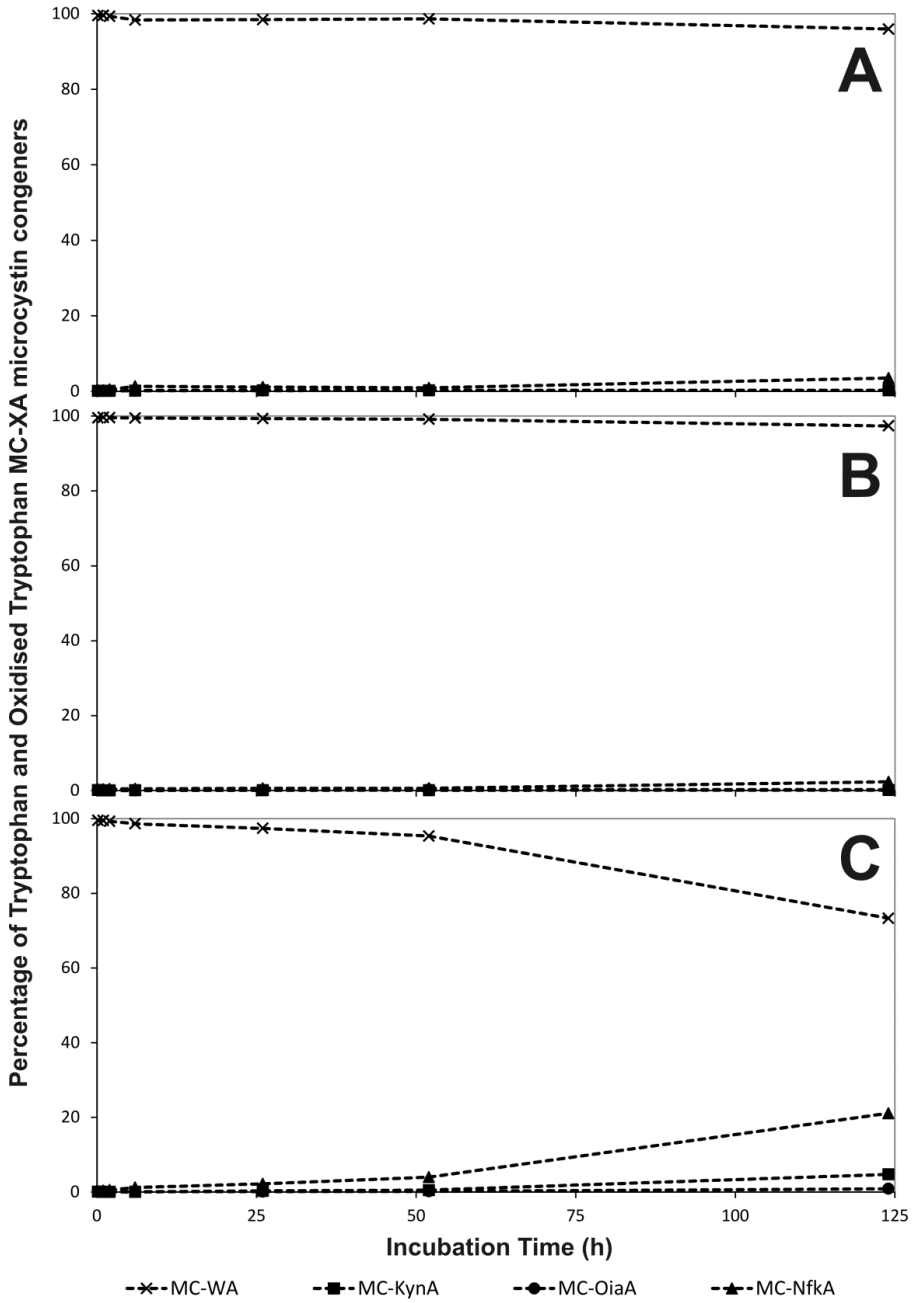

Figure 4.12: Oxidation of a tryptophan-containing microcystin from a CYN06 extract. Graphs depicting the oxidation of MC-WA into MC-KynA, MC-OiaA and MC-NfkA through diffusion with atmospheric oxygen **(A)**, the application of stirring **(B)** and the application of hydrogen peroxide **(C)**.

dropped by ca. 4%. In-turn, the level of the oxidised Trp microcystins (for example, MC-NfkA) had increased. Stirring at ca. 250 rpm did not have any effect on the rate of Trp oxidation. After 124 h of stirring, the levels of Trp- and oxidised Trp-containing microcystin were the same as observed through diffusion alone (Figure 4.12B). Addition of an oxidising agent (hydrogen peroxide) increased the rate of Trp oxidation and after 124 h, the level of oxidised Trp microcystins had increased by ca. 28% (Figure 4.12C).

4.2.6 Presence of Oxidised Tryptophan Microcystins inside CYN06 Cells

A healthy culture of CYN06 was harvested on nylon net, washed with fresh media and extracted in degassed 70% MeOH (v/v). The duration of the concentration and extraction procedure was 50 min and LC-MS analysis of the extract revealed the conventional microcystins produced by CYN06 as well as low levels of Nfk-containing microcystins (Figure 4.13).

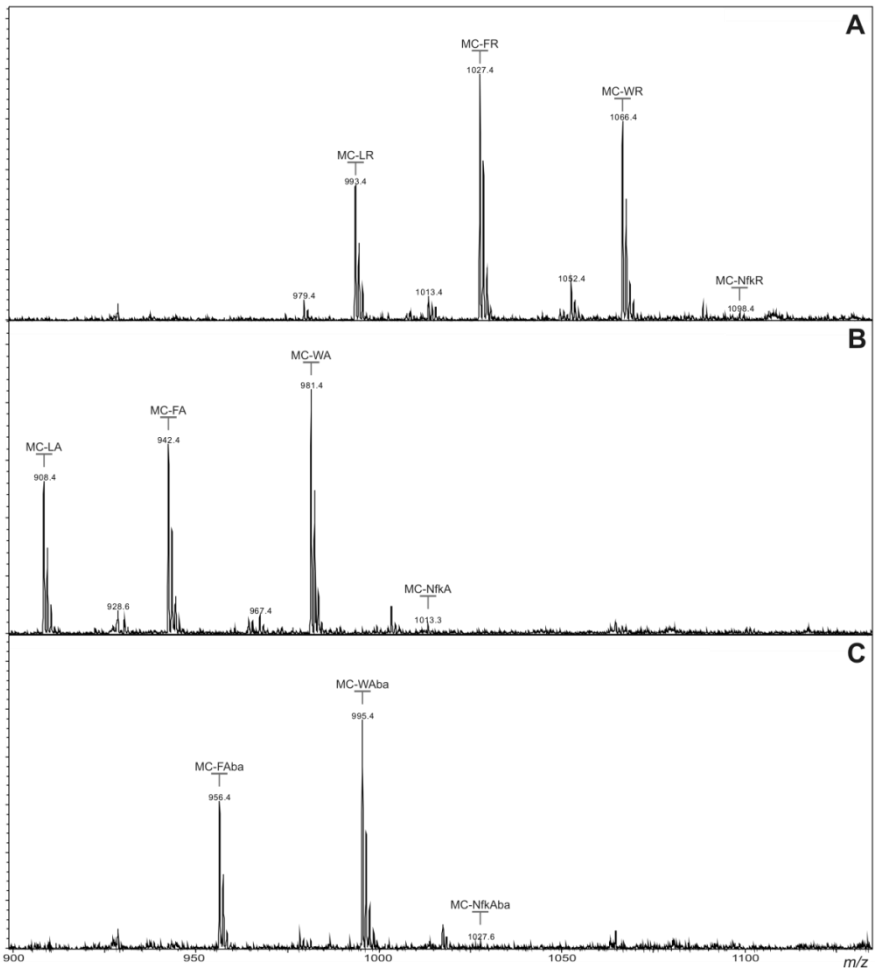

Figure 4.13: Negative ion mass spectra of a mild extraction of CYN06. Spectra focussing on the -XR congeners **(A)**, the -XA congeners **(B)** and the -XAba congeners **(C)**.

4.3 DISCUSSION

Whilst oxidised Trp residues have been noted in polypeptides,[256-259] their presence in microcystins has not. LC-MS analysis of nine unknown microcystins observed in CYN06 indicated the presence of position two amino acids with the mass of known Trp oxidation products (Kyn, Oia and Nfk). A sufficient quantity of one of the microcystins (MC-NfkA) was purified in order to characterise it by NMR spectroscopy. This demonstrated that Nfk was present in position two of the microcystin.

It is likely that some of these microcystin congeners have been encountered previously, as mass-to-charge ratios consistent with MC-OiaR and MC-NfkR were observed in the Lake Wiritoa sample which contained anabaenopeptin 906 (see Section 2.2). A microcystin with *m/z* 1100.6 has also been reported previously which could have been MC-NfkR.[265] In both of these studies, MC-WR was present in the samples, making it likely that oxidised Trp microcystins would also be observed. The findings of this study will allow researchers working with samples of Trp-containing microcystins to assign the previously unidentified oxidised analogues.

The oxidation of Trp-containing microcystins into the oxidised analogues poses a concern for researchers quantifying microcystins in samples which include Trp-containing microcystins. Whilst the rate of oxidation under normal storage conditions is unknown, it is likely that during prolonged storage of a Trp-containing microcystin standard or sample, some of the microcystin will become oxidised. This would result in a lower than expected signal from the sample or standard and cause inaccurate measurements. Further investigation into storage procedures to minimise the oxidation of Trp microcystins will need to be performed.

Whilst the oxidation of Trp-containing microcystins into Kyn-, Oia- and Nfk-containing microcystins was apparent over a long time period (124 h), over a short period of time (2 h), Trp-oxidation was only detected when hydrogen peroxide was present. A mild extraction of *Microcystis* CYN06, where colonies were concentrated on nylon net and washed with fresh medium, revealed the presence of Nfk-containing microcystins. As this extraction was completed in less

than 2 h, the oxidised Trp microcystins observed were most likely present inside the cells. It is not clear how the oxidised Trp-containing microcystins are produced in cyanobacteria. Whilst it is possible that Kyn, Oia and Nfk could be incorporated into the structure, it is more likely that the oxidation occurs post-synthesis. Whether the oxidation was due to natural oxygen levels, reactive oxygen species or is enzymatically driven, remains to be elucidated.

During the purification of **175** it is probable that some MC-WA was oxidised to form MC-NfkA. However, such oxidation artefacts still pose a potential health concern when produced in the environment. As with other microcystin congeners, it is very likely that these microcystins will inhibit protein phosphatases 1 and 2A and pose a health threat to animals. Unfortunately, the material isolated for characterisation was insufficiently pure to proceed with toxicology or protein phosphatase inhibition studies.

4.4 CONCLUSIONS

A combination of MS/MS and NMR spectroscopy was used to investigate the structure of an unknown microcystin (MC-NfkA) and demonstrated that the microcystin contained Nfk; a known oxidation product of Trp. Tandem MS analysis of other microcystins observed in CYN06 indicated the presence of further known oxidation products of Trp (Kyn and Oia). This resulted in the identification of nine new microcystin analogues and is the first report of a microcystin containing an oxidation product of Trp.

CHAPTER 5

Characterisation of New Oligopeptides from an Antarctic Cyanobacterial Sample

5.1 INTRODUCTION

The McMurdo Dry Valleys in Eastern Antarctica form the largest ice-free region on the continent and are characterised by low temperatures, minimal precipitation, strong winds,[268] and high salinity.[269] Despite these harsh conditions, life is still present in this arid environment in the form of microbial communities.[270-272] In the moist areas in and around glacial streams and lakes, cyanobacteria proliferate forming thick benthic mats.[273-275]

Cyanobacteria which produce microcystins have been reported in almost every environment on Earth,[3] including Antarctica.[276-278] In 2008, we showed microcystin-producing cyanobacteria to be particularly prolific in the Dry Valleys, with each sample collected testing positive for at least low levels of microcystins.[279] Previously, only [Asp^3] MC-LR, MC-LR and nodularin had been reported in Antarctic cyanobacteria,[276-278] but our 2008 study also identified [Asp^3, Dha^7] MC-LR, MC-FR and MC-RR (including the [Asp^3] and [Asp^3, Dha^7] congeners of MC-RR).[279]

During the course of this study,[279] a discrepancy between the different methods of determining microcystin content was noted in several samples. Whilst a high level of microcystin was detected using an enzyme-linked immunosorbent assay and protein phosphatase inhibition assay, a low level was detected by liquid chromatography-mass spectrometry (LC-MS). Further investigation demonstrated that these samples contained several new microcystins which were not detected by the LC-MS multiple reaction monitoring method. This chapter details the partial characterisation of these new microcystins, as well as that of six novel linear peptides also present in the samples.

5.2 RESULTS

5.2.1 Assessment of the Oligopeptide Diversity in the Miers Valley Cyanobacterial Mats

Methanol extracts of two samples (MVAG1 and MVMG1) collected from Miers Valley, Antarctica were analysed by matrix-assisted laser desorption/ionisation-time of flight (MALDI-TOF) MS. The positive ion mass spectrum (Figure 5.1) and post source decay experiments indicated the presence of two groups of oligopeptides; several linear peptides with masses between 800 and 844 Da, and eight microcystins between 966 and 1051 Da.

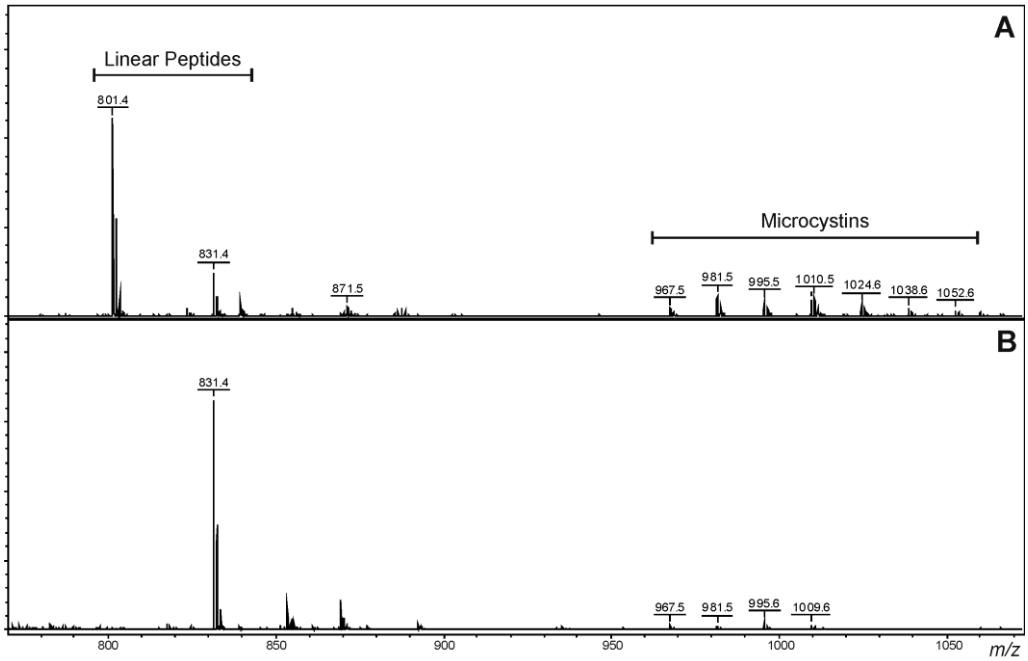

Figure 5.1: Positive ion MALDI mass spectra of the two Miers Valley samples; MVAG1 **(A)** and MVMG1 **(B)**.

5.2.2 Structural Characterisation of Eight New Microcystins

The Miers Valley samples were also analysed by LC-MS, which initially suggested that they contained four MC-LR congeners and four MC-RR congeners. The microcystins eluted from a reversed-phase C_{18} column within an appropriate retention region and possessed protonated ions which matched those of previously described microcystins (Appendix A). However, closer assessment of the retention times showed that most of the congeners eluted earlier than MC-LR/MC-RR or their demethylated analogues (Table 5.1). A combination of amino acid analysis, chemical derivatisation and MS confirmed that the eight microcystins were new and led to the putative structures for **179-186**.

Table 5.1: Structures, molecular masses and retention times of the eight new Antarctic microcystins and two common congeners.

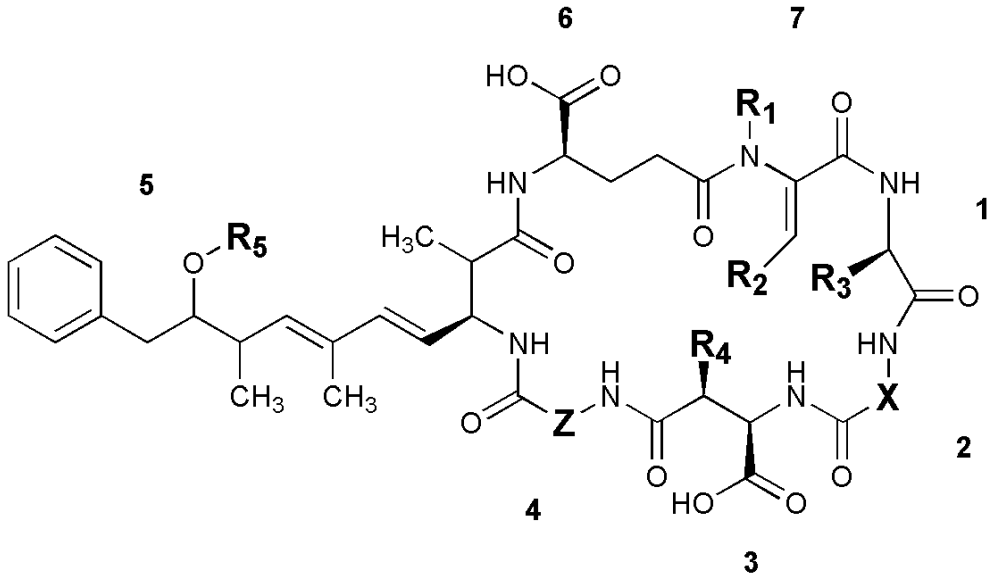

Microcystin	M_r [a] (Da)	RT [b] (min)	X	Z	R_1	R_2	R_3	R_4	R_5
MC-LR (**7**)	994.5	7.40	L-Leu	L-Arg	$-CH_3$	-H	$-CH_3$	$-CH_3$	$-CH_3$
[Gly[1], Asp[3], Dhb[7]] MC-LR (**179**)	966.5	7.27	L-Leu	Arg	-H	$-CH_3$	-H	-H	$-CH_3$
[Gly[1], Asp[3], Dhb[7]] MC-LHar (**180**)	980.5	7.34	L-Leu	Har	-H	$-CH_3$	-H	-H	$-CH_3$
[Gly[1], Asp[3], ADMAdda[5], Dhb[7]] MC-LR (**181**)	994.5	7.29	L-Leu	Arg	-H	$-CH_3$	-H	-H	$-COCH_3$
[Gly[1], Asp[3], ADMAdda[5], Dhb[7]] MC-LHar (**182**)	1008.5	7.36	L-Leu	Har	-H	$-CH_3$	-H	-H	$-COCH_3$
MC-RR (**85**)	1023.6	6.48	L-Arg	L-Arg	$-CH_3$	-H	$-CH_3$	$-CH_3$	$-CH_3$
[Gly[1], Asp[3], Dhb[7]] MC-RR (**183**)	1009.6	6.29	Arg	Arg	-H	$-CH_3$	-H	-H	$-CH_3$
[Gly[1], Asp[3], Dhb[7]] MC-RHar (**184**)	1023.6	6.38	Arg	Har	-H	$-CH_3$	-H	-H	$-CH_3$
[Gly[1], Asp[3], ADMAdda[5], Dhb[7]] MC-RR (**185**)	1037.6	6.33	Arg	Arg	-H	$-CH_3$	-H	-H	$-COCH_3$
[Gly[1], Asp[3], ADMAdda[5], Dhb[7]] MC-RHar (**186**)	1051.6	6.42	Arg	Har	-H	$-CH_3$	-H	-H	$-COCH_3$

[a] Molecular weights are rounded to one decimal place. [a] RT = Retention time on a C_{18} column as per Table 9.3.

On account of the small amount of material, fractionation of the Antarctic microcystins did not proceed beyond separating a mixture of the four -LR congeners and a mixture of the four -RR congeners from the other components in the extract. These two mixtures of four microcystins were individually hydrolysed and subjected to Advanced Marfey's amino acid analysis[204,205] to determine the amino acids present and their stereochemistry.

Derivatisation of amino acids with L-FDLA allowed the separation of both stereoisomers by reversed-phase C_{18} high performance liquid chromatography (HPLC).[204,205] LC-MS analysis of the L-FDLA derivatives of the hydrolysed -LR

Antarctic microcystin congeners, and comparison with standard amino acids, confirmed the presence of D-aspartic acid (Asp; *m/z* 426; 12.9 min; Figure 5.2), D-glutamic acid (Glu; *m/z* 440; 14.3 min), glycine (Gly; *m/z* 368; 15.2 min) and L-leucine (Leu; *m/z* 424; 21.0 min). Comparison with the L-FDLA derivatives of hydrolysed MC-LR (Appendix F.3) indicated the presence of 3(*S*)-Adda (3-amino-9-methoxy-2,6,8-trimethyl-10-phenyldeca-4,6-dienoic acid; *m/z* 592; 32.9 min).[205]

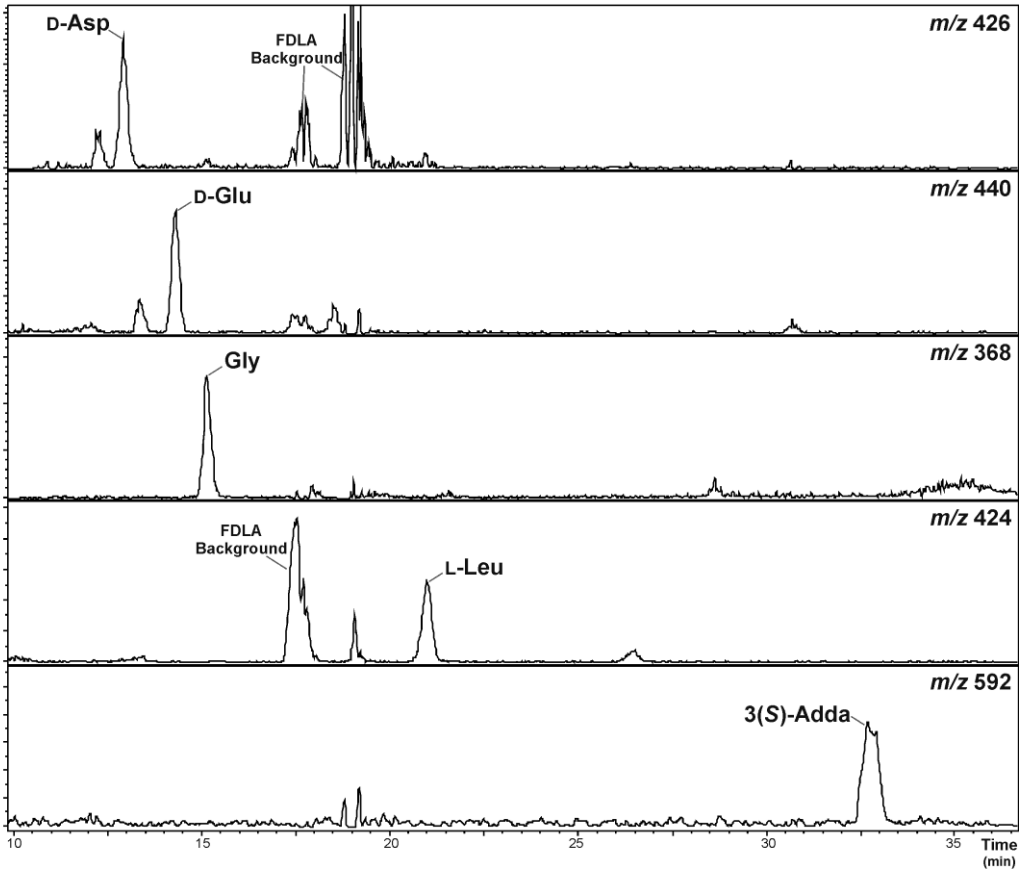

Figure 5.2: Advanced Marfey's amino acid analysis of the -LR Antarctic microcystins. Extracted ion chromatograms for a hydrolysate of the -LR Antarctic microcystins derivatised with L-FDLA.

Liquid chromatography-MS analysis of the L-FDLA derivatives of the hydrolysed -RR Antarctic microcystin congeners revealed similar results. The presence of D-Asp (*m/z* 426; 12.9 min; Figure 5.3), D-Glu (*m/z* 440; 14.3 min), Gly (*m/z* 368; 15.2 min) and 3(*S*)-Adda (*m/z* 592; 32.9 min) was confirmed by comparison with standard amino acids and hydrolysed MC-LR.

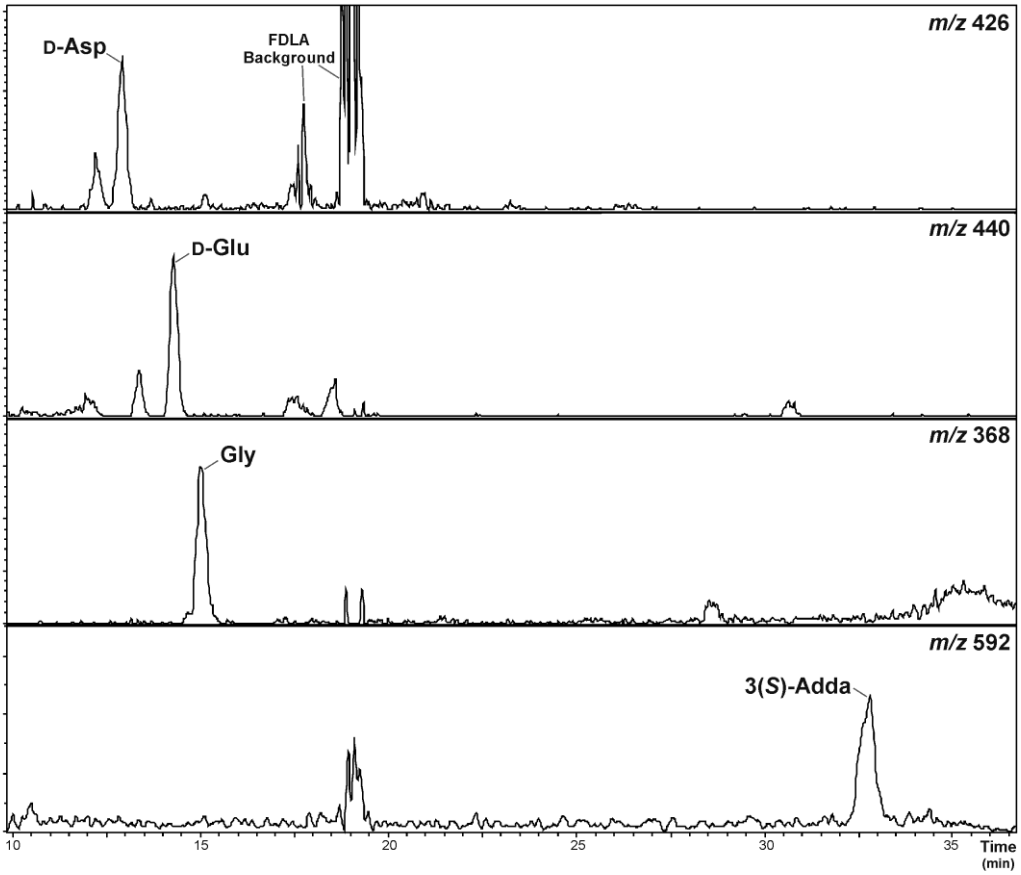

Figure 5.3: Advanced Marfey's amino acid analysis of the -RR Antarctic microcystins. Extracted ion chromatograms for a hydrolysate of the -RR Antarctic microcystins derivatised with L-FDLA.

N-Methylamine (*m/z* 324; 19.6 min) was not observed in the amino acid analysis of the Antarctic microcystin mixtures but is commonly observed during microcystin analysis,[205] as it is the product of the hydrolytic breakdown of *N*-methyldehydroalanine (Mdha). A simple thiol derivatisation was used to verify the absence of Mdha in the Antarctic microcystins. A microcystin containing a terminal alkene, like that found in Mdha, will readily react with β-mercaptoethanol under alkaline conditions.[41] Monitoring of the derivatisation by LC-MS showed that MC-LR, which contains Mdha, reacted quickly with β-mercaptoethanol ($t_{½}$ = 4.8 min; Appendix D.1). A reaction rate approximately twice as fast was observed with a microcystin containing two arginine residues (MC-RR; $t_{½}$ = 2.6 min). The -LR Antarctic microcystins reacted over two orders of magnitude slower than MC-LR ($t_{½}$ = 1089 min; Appendix D.3). A similar difference in reaction rate was observed with the Antarctic -RR congeners when compared to MC-RR ($t_{½}$ = 632 min). The slow reaction rate with β-mercaptoethanol, in combination with the absence of *N*-methylamine in the

amino acid analysis, suggested that the Antarctic microcystins contained a dehydrobutyrine (Dhb).

The electrospray ionisation collision-induced dissociation (ESI CID) tandem MS (MS/MS) spectrum of **179** indicated that the compound contained Adda, as an intense *m/z* 135 fragment ion was present (Figure 5.4).[34,265] The *m/z* 112, 129 and 157 ions indicated that the microcystin contained an Arginine (Arg) residue.[181] The later retention time on reversed-phase C_{18} (7.27 min; Table 5.1) and the absence of a loss of 42 Da (CN_2H_2) in the MS/MS spectrum,[78] suggested that it was not likely that there were two Arg residues present. The mass difference between the fragment ions indicated the position of the remaining amino acids in the compound (Table 5.2).

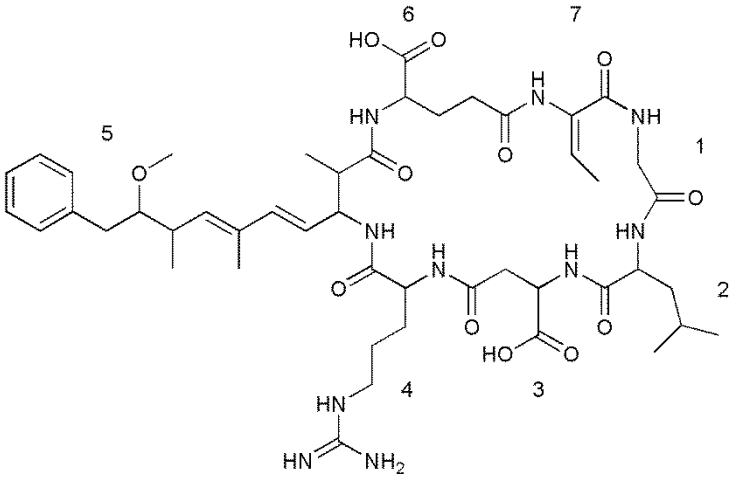

(179)

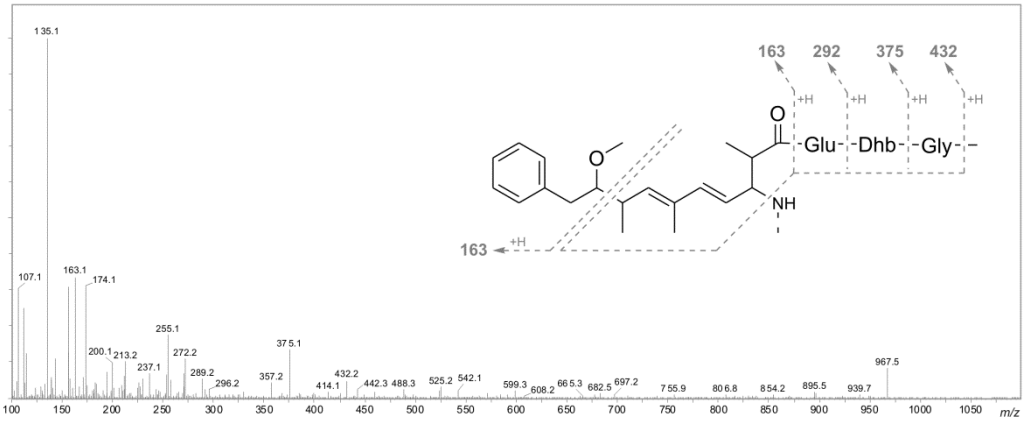

Figure 5.4: Tandem mass spectrum of [Gly[1], Asp[3], Dhb[7]] MC-LR and fragments observed in the Adda-containing Antarctic microcystins. Fragmentation induced by electrospray ionisation collision-induced dissociation.

Table 5.2: Tandem mass spectrometry fragment ions for [Gly[1], Asp[3], Dhb[7]] MC-LR observed by electrospray ionisation collision-induced dissociation.

m/z	**Fragment Assignment** [a]	*m/z*	**Fragment Assignment** [a]
112	Arg fragment	129	Arg immonium
135	Adda sidechain	141	Dhb-Gly + H
157	Arg + H	163	Adda' + H
171	Gly-Leu + H	213	Glu-Dhb + H
254	Dhb-Gly-Leu + H	270	Glu-Dhb-Gly + H
272	Asp-Arg + H	292	Adda'-Glu + H
375	Adda'-Glu-Dhb + H	385	Leu-Asp-Arg + H
432	Adda'-Glu-Dhb-Gly + H	442	Gly-Leu-Asp-Arg + H
525	Dhb-Gly-Leu-Asp-Arg + H	599	Arg-Adda-Glu + H
682	Arg-Adda-Glu-Dhb + H	967	M + H

[a] Fragments containing CO losses and NH_4^+ adducts were not included; Adda' = Adda minus NH_2 and the sidechain fragment ($C_9H_{11}O$).

The fragment ion series beginning with the Adda' fragment (Adda minus NH_2 and $C_9H_{11}O$; *m/z* 163) indicated that **179** contained Glu and Dhb in positions six and seven, respectively (Figure 5.5A). The *m/z* 432 ion extended this ion series to include a Gly in position one, yielding a sequence of Adda-Glu-Dhb-Gly. Another fragment ion series which began with Arg (*m/z* 157), extended to include Asp, Leu, Gly, Dhb and Glu (Figure 5.5B). This gave a sequence of Arg-Asp-Leu-Gly-Dhb-Glu, the end of which overlapped with the previous sequence, resulting in a complete peptide sequence of Adda-Glu-Dhb-Gly-Leu-Asp-Arg. The *m/z* 599 ion (Arg-Adda-Glu) indicated that the Arg was joined to Adda and that the structure was cyclic (Figure 5.5C).

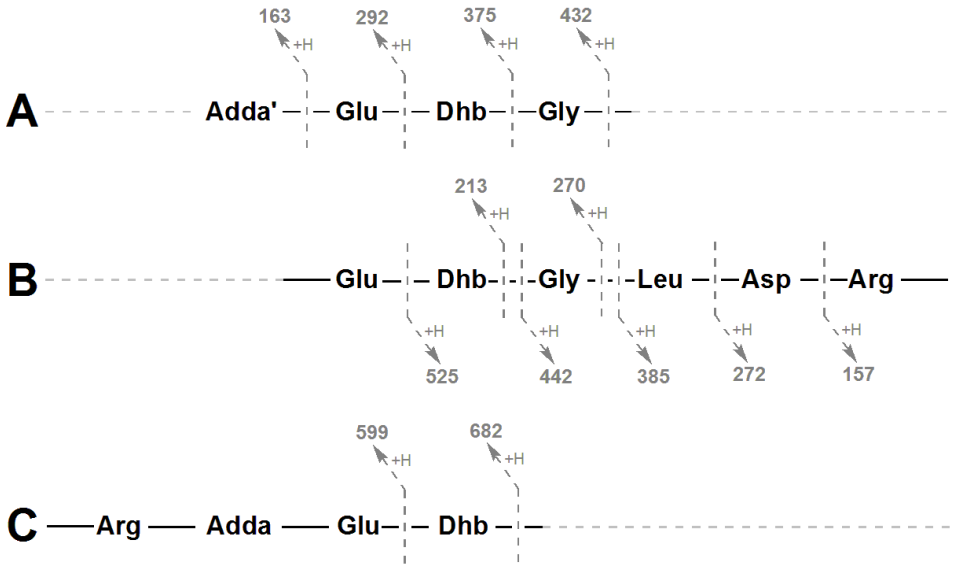

Figure 5.5: Tandem mass spectrometry fragment ions indicating the amino acid sequence in [Gly[1], Asp[3], Dhb[7]] MC-LR.

The MS/MS spectrum for **180** again indicated that it contained Adda, because of the *m/z* 135 fragment ion (Figure 5.6). However, the *m/z* 126, 143 and 171 ions in this spectrum suggested that the microcystin contained a homoarginine (Har) residue. The later retention time on reversed-phase C_{18} (7.34 min; Table 5.1) and the absence of a 42 Da (CN_2H_2) loss in the MS/MS spectrum, suggested there were not two Har residues present. Comparison with the MS/MS spectrum for **179** indicated that much of the structure was the same (Appendix J.1), apart from the position four amino acid which appeared to be Har.

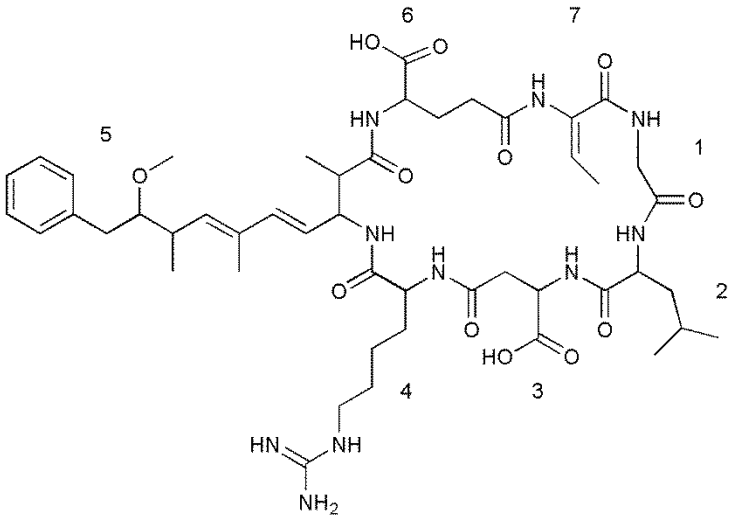

(180)

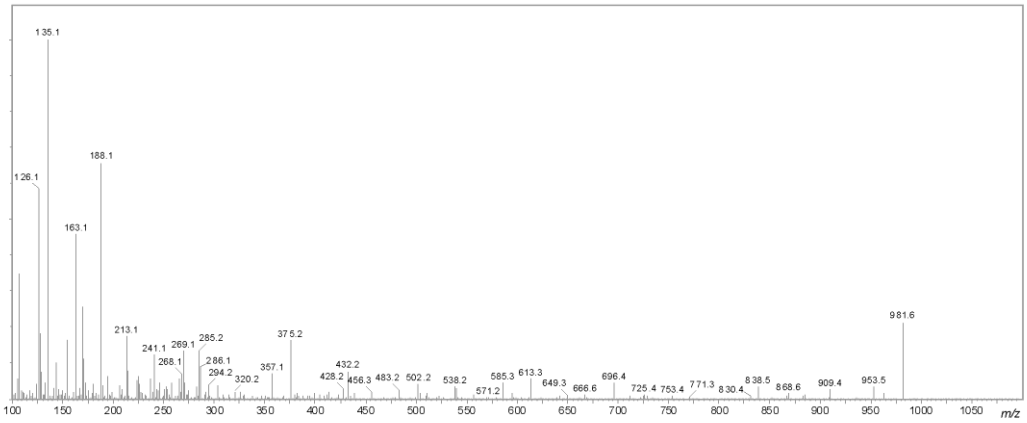

Figure 5.6: Tandem mass spectrum of [Gly[1], Asp[3], Dhb[7]] MC-LHar. Fragmentation induced by electrospray ionisation collision-induced dissociation.

The MS/MS spectrum for **181** (Figure 5.7) did not contain the intense *m/z* 135 fragment ion, which was observed in the previous microcystins. However, a loss of 60 Da (HOAc) was evident, which indicated that **181** contained an *O*-acetyl group. The *m/z* 265 ion suggested that this was due to an *O*-acetyl group on the Adda moiety (ADMAdda; Figure 5.7).[79] As with **179**, it was likely that a single Arg residue was present in this microcystin. Comparison with the MS/MS spectrum for **179** indicated that much of the structure for **181** was the same (Appendix J.1), apart from the inclusion of ADMAdda at position five.

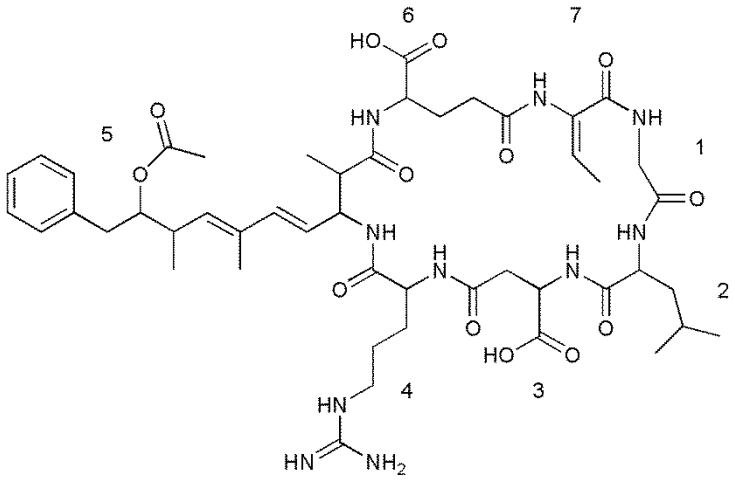

(181)

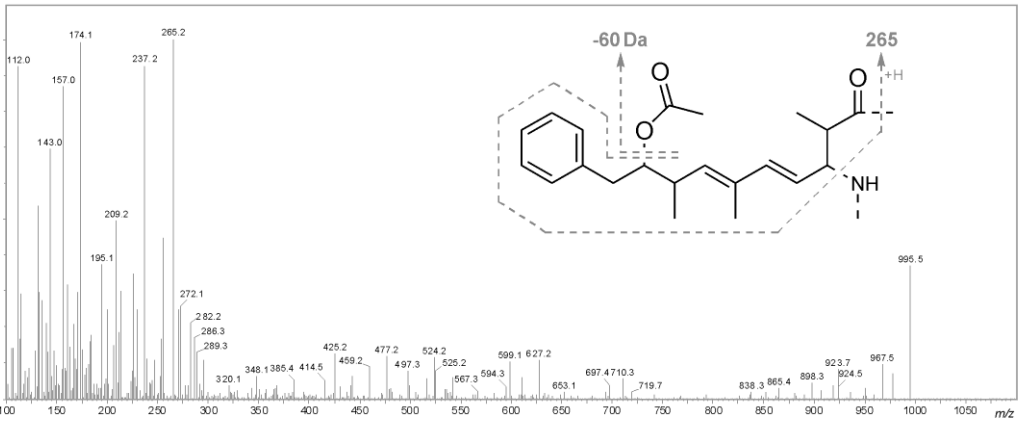

Figure 5.7: Tandem mass spectrum of [Gly[1], Asp[3], ADMAdda[5], Dhb[7]] MC-LR and fragments commonly observed in the ADMAdda-containing microcystins. Fragmentation induced by electrospray ionisation collision-induced dissociation.

The MS/MS spectrum for **182** did not contain an intense *m/z* 135 fragment ion, but the presence of ADMAdda was suggested by the *m/z* 265 fragment and a loss of 60 Da (Figure 5.8). Comparison with the MS/MS spectrum for **181** indicated that much of the structure was the same (Appendix J.1), apart from the position four amino acid which was consistent with a Har.

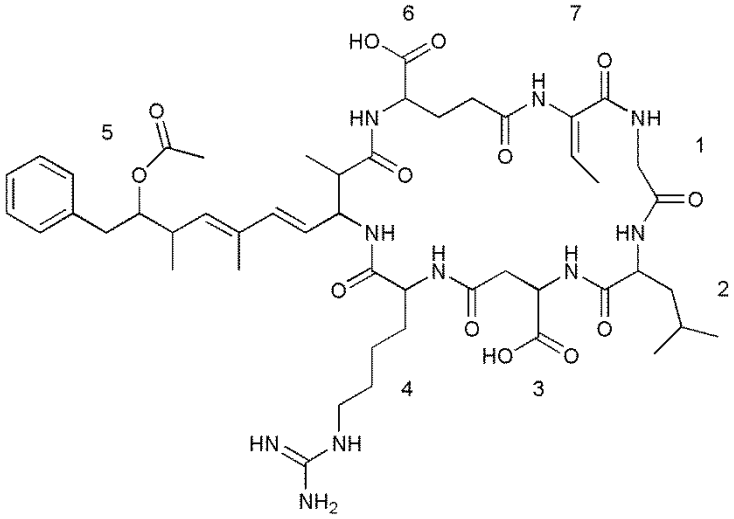

(182)

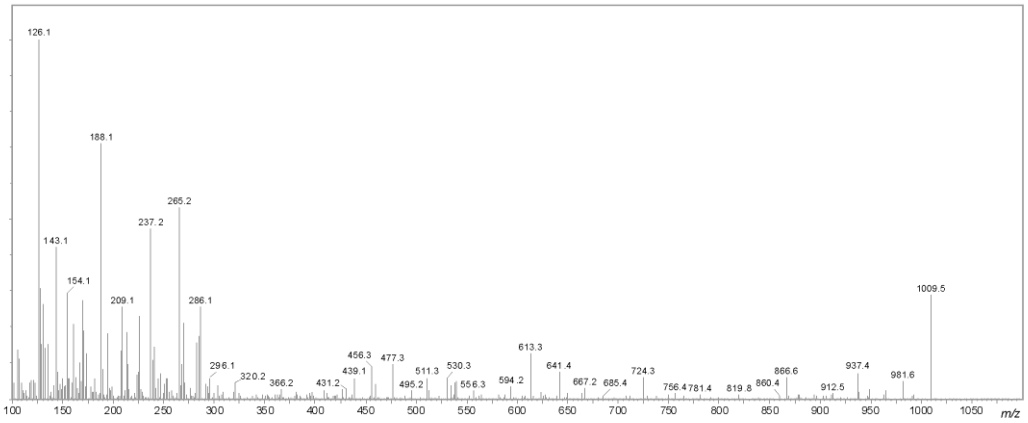

Figure 5.8: Tandem mass spectrum of [Gly[1], Asp[3], ADMAdda[5], Dhb[7]] MC-LHar. Fragmentation induced by electrospray ionisation collision-induced dissociation.

The MS/MS spectrum for **183** contained an intense *m/z* 135 fragment ion, suggesting the presence of Adda (Figure 5.9). The *m/z* 112, 129 and 157 ions in the spectrum indicated that **183** contained an Arg residue. However, the earlier retention time on C_{18} (6.29 min; Table 5.1) and loss of 42 Da (CN_2H_2) in the MS/MS spectrum, suggested that there were two Arg residues present. Comparison with the MS/MS spectrum for **179** indicated that much of the structure was the same (Appendix J.2) except that the Leu at position two had been replaced with Arg.

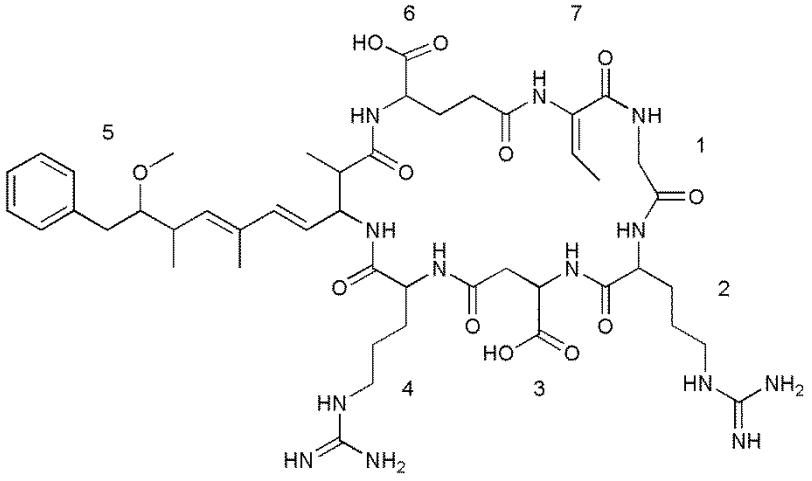

(183)

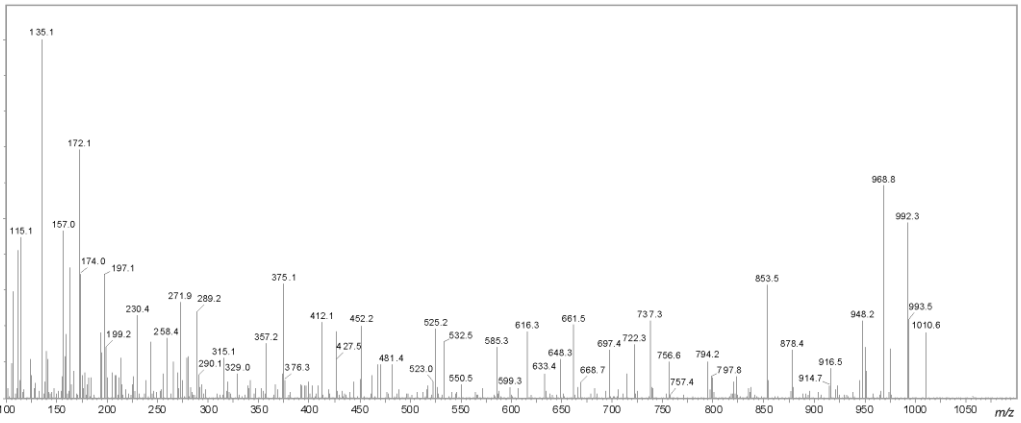

Figure 5.9: Tandem mass spectrum of [Gly[1], Asp[3], Dhb[7]] MC-RR. Fragmentation induced by electrospray ionisation collision-induced dissociation.

The MS/MS spectrum for **184** contained an intense *m/z* 135 fragment ion, suggesting the presence of Adda (Figure 5.10). The *m/z* 112, 129 and 157 ions in the spectrum indicated that **184** contained an Arg residue. However, the *m/z* 126, 143 and 188 ions suggested that there was also a Har present. The presence of both a Har and an Arg residue in the compound was reinforced by the earlier retention time on C_{18} (6.38 min; Table 5.1) and the loss of 42 Da (CN_2H_2) in the MS/MS spectrum. Comparison with the MS/MS spectrum for **183** indicated that much of the structure was the same (Appendix J.2) except that the position four amino acid was Har.

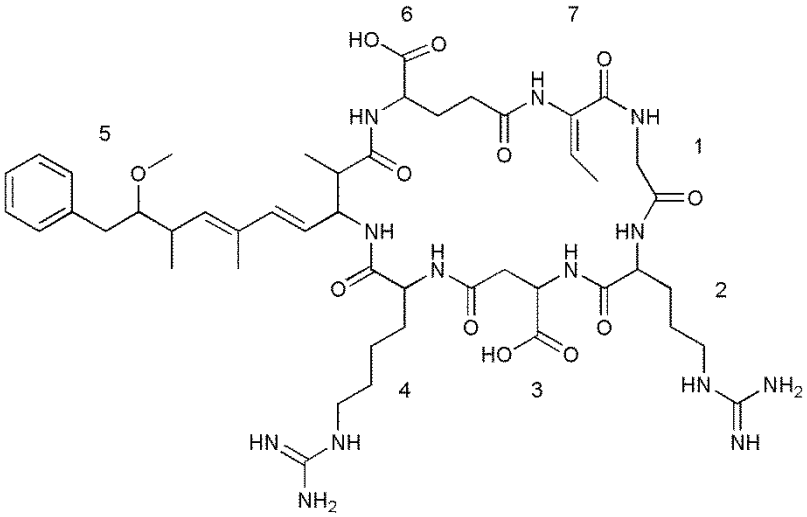

(184)

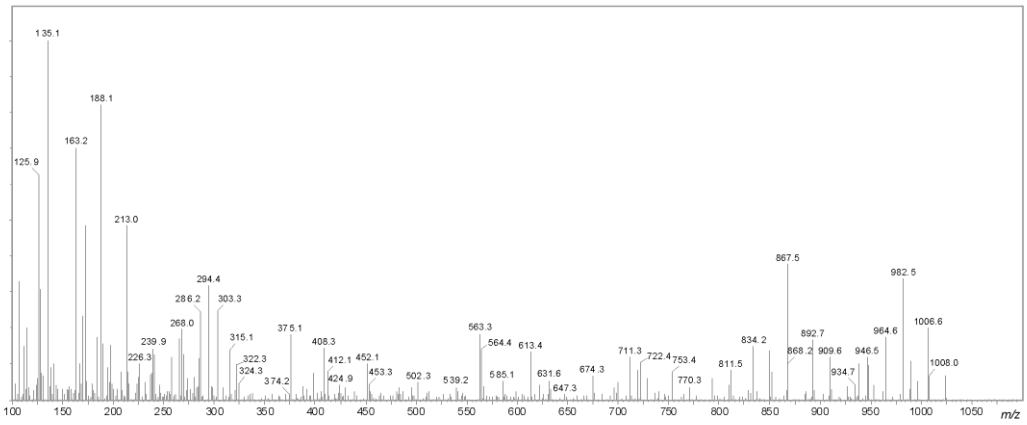

Figure 5.10: Tandem mass spectrum of [Gly[1], Asp[3], Dhb[7]] MC-RHar. Fragmentation induced by electrospray ionisation collision-induced dissociation.

The MS/MS spectrum for **185** did not contain an intense *m/z* 135 fragment ion, but the presence of ADMAdda was suggested by the *m/z* 265 fragment and a loss of 60 Da (Figure 5.11). As with **183**, the inclusion of two Arg residues was indicated by the *m/z* 112, 129 and 157 ions, and the earlier retention time on reversed-phase C_{18} (6.33 min; Table 5.1). Comparison with the MS/MS spectrum for **183** indicated that much of the structure for **185** was the same (Appendix J.2), apart from the inclusion of ADMAdda at position five.

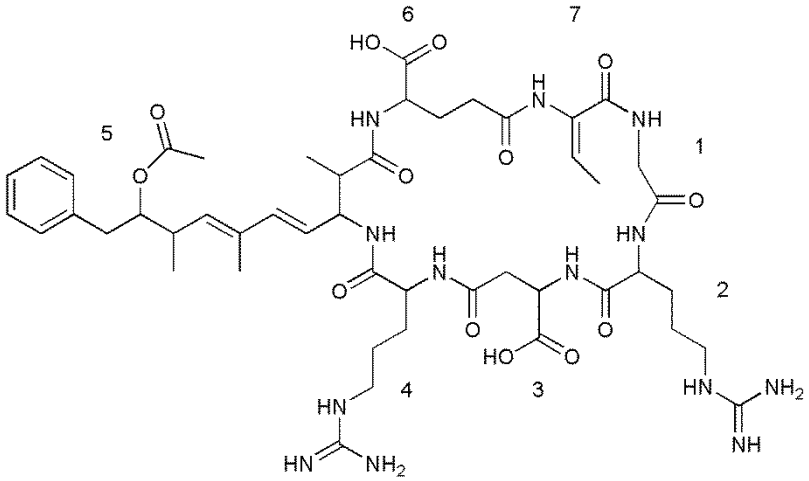

(185)

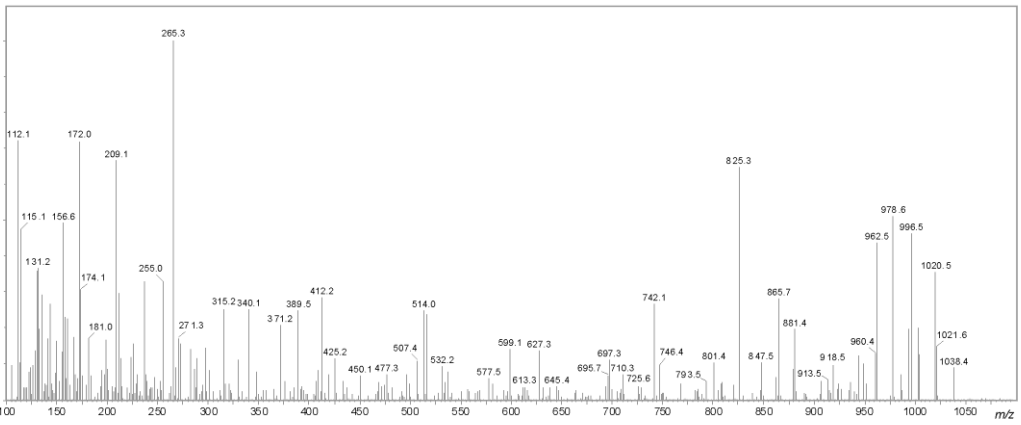

Figure 5.11: Tandem mass spectrum of [Gly[1], Asp[3], ADMAdda[5], Dhb[7]] MC-RR. Fragmentation induced by electrospray ionisation collision-induced dissociation.

The MS/MS spectrum for **186** did not contain an intense *m/z* 135 fragment ion, but the presence of ADMAdda was indicated by the *m/z* 265 fragment and a loss of 60 Da (Figure 5.12). As with **184**, the inclusion of an Arg and Har residue was indicated by low mass fragments in the MS/MS spectrum (*m/z* 112, 129 and 157; *m/z* 126, 143 and 171) and the earlier retention time on reversed-phase C_{18} (6.42 min; Table 5.1). Comparison with the MS/MS spectrum for **185** indicated that much of the structure for **186** was the same (Appendix J.2) except that Har was present at position five.

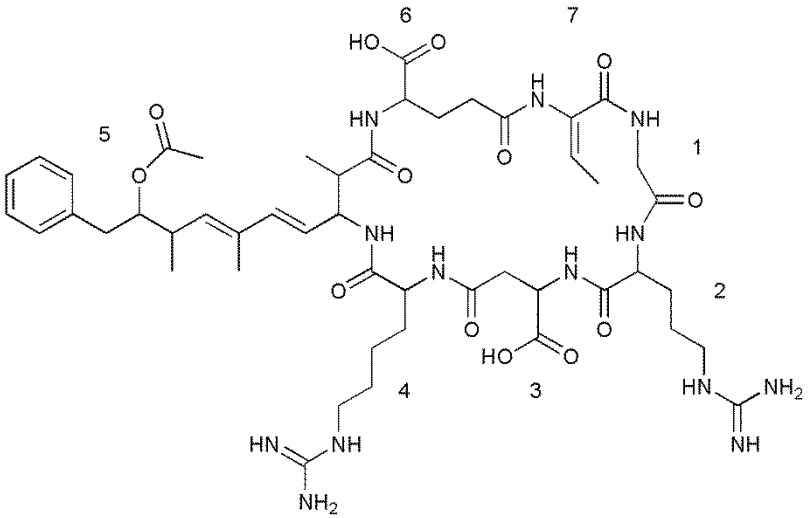

(186)

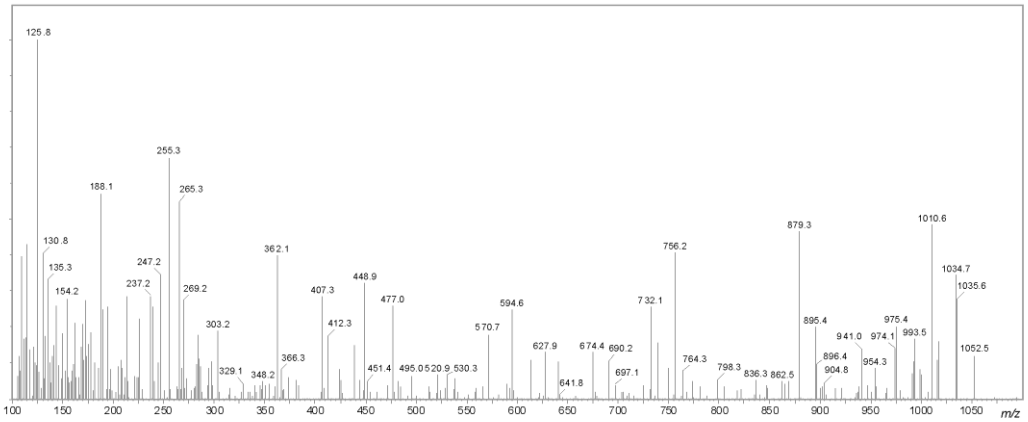

Figure 5.12: Tandem mass spectrum of [Gly[1], Asp[3], ADMAdda[5], Dhb[7]] MC-RHar. Fragmentation induced by electrospray ionisation collision-induced dissociation.

High resolution mass spectrometry (HRMS) analysis was conducted on semi-pure mixtures of the -LR and -RR Antarctic microcystins. Each mixture yielded mass-to-charge ratios consistent with the singly protonated ions of the structures **179**-**186** and mass deviations of less than 4 ppm (Table 5.3). The accurate masses

for **181-182** and **185-186** indicated that the 28 Da mass increase observed in the position five amino acid of these compounds, was more likely due to an additional carbonyl (ADMAdda) than the addition of two methylations to the Adda moiety.

Table 5.3: High resolution mass spectrometry analysis of the Antarctic microcystins.

Microcystin	Measured *m/z*	Molecular Formula	Calculated *m/z*	Error (ppm)
[Gly^1, Asp^3, Dhb^7] MC-LR (**179**)	967.5285	$C_{47}H_{71}N_{10}O_{12}$	967.5247	+ 3.86
[Gly^1, Asp^3, Dhb^7] MC-LHar (**180**)	981.5413	$C_{48}H_{73}N_{10}O_{12}$	967.5404	+ 0.87
[Gly^1, Asp^3, ADMAdda^5, Dhb^7] MC-LR (**181**)	995.5206	$C_{48}H_{71}N_{10}O_{13}$	995.5197	− 0.94
[Gly^1, Asp^3, ADMAdda^5, Dhb^7] MC-LHar (**182**)	1009.5348	$C_{49}H_{73}N_{10}O_{13}$	1009.5353	+ 0.47
[Gly^1, Asp^3, Dhb^7] MC-RR (**183**)	1010.5442	$C_{47}H_{72}N_{13}O_{12}$	1010.5418	− 2.44
[Gly^1, Asp^3, Dhb^7] MC-RHar (**184**)	1024.5569	$C_{48}H_{74}N_{13}O_{12}$	1024.5574	+ 0.53
[Gly^1, Asp^3, ADMAdda^5, Dhb^7] MC-RR (**185**)	1038.5405	$C_{48}H_{72}N_{13}O_{13}$	1038.5367	− 3.82
[Gly^1, Asp^3, ADMAdda^5, Dhb^7] MC-RHar (**186**)	1052.5541	$C_{49}H_{74}N_{13}O_{13}$	1052.5524	− 1.60

Although every effort was made to garner as much structural information as possible on these new microcystins, the amount of material available was limited (< 50 µg of each congener), restricting purification of each individual congener and making nuclear magnetic resonance (NMR) studies unfeasible.

A mixture of the four -LR congeners and a mixture of the four -RR Antarctic microcystin congeners were each subjected to Advanced Marfey's amino acid analysis. This indicated that each microcystin contained Gly, D-Asp and D-Glu. The mixture of -LR congeners was shown to contain L-Leu, whilst this peak was absent in the -RR congeners. Comparison with the L-FDLA derivatives of hydrolysed MC-LR showed that each mixture of microcystins contained the amino acid Adda in the 3(*S*)-configuration.

The *N*-methylamine signal commonly observed in microcystins was not observed in the amino acid analysis. This was further investigated using a thiol derivatisation, which verified that Mdha was not present in the Antarctic microcystins. The slow reaction rate observed, in combination with the MS/MS analysis, indicated that Dhb was very likely present in position seven. This substitution could be confirmed by analysis of the 2-ketobutyric acid produced

from the hydrolytic breakdown of Dhb,[250] however there was only sufficient material to conduct amino acid analysis of the semi-purified microcystins.

The MS/MS analysis indicated the presence of Arg in six of the microcystins and Har in four of the congeners. The amino acid analysis protocol used had poor sensitivity for arginine-like residues and with the small sample size available, these amino acids were not detected. The MS/MS analysis also suggested that four of the microcystins contained ADMAdda. Whilst there was no direct evidence of ADMAdda from the amino acid analysis, it is unclear how this moiety behaves during the acid hydrolysis and subsequent derivatisation. It is highly probable that ADMAdda would lose the *O*-acetyl group in the same manner that the *O*-methyl group of Adda is lost during acid hydrolysis;[54,205] hence the two moieties would form the same product (Figure 5.13).

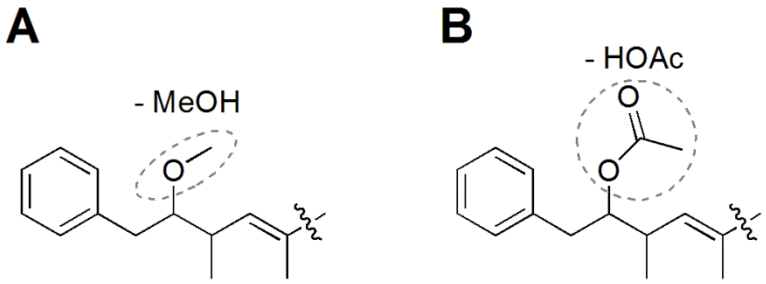

Figure 5.13: Proposed system for the loss of the *O*-methyl group from Adda **(A)** and the *O*-acetyl group from ADMAdda **(B)** during acid hydrolysis.

The MS/MS assignments laid out in Section 5.2.2 and Appendix J were consistent with previous analyses of low-energy, collision-activated spectra from similar microcystin variants.[80,280-282] Whilst the Gly substitution in position one is novel, the fragment ion series observed were similar to those reported for other microcystin congeners containing a position one substitution.[72,111]

In several of the spectra, possible contamination from MC-LR and MC-RR was observed, with *m/z* 155 (Mdha/Dhb-Ala) and *m/z* 135 (Adda sidechain fragment) ions present with the ADMAdda congeners. This is likely due to the high concentration of extract used to achieve these spectra and the ease with which those fragment ions form. However, the contaminant ions were present at much lower intensities than would be expected had the congener contained Adda or Ala.

Furthermore, in each of the spectra containing these ions, the contaminant ion series do not continue further than these few easily formed, low-mass ions.

5.2.3 Structural Characterisation of Six New Linear Peptides

The MALDI MS analysis of the Miers Valley samples showed the presence of five compounds with molecular weights of 800, 814, 816, 830 and 844 Da (Figure 5.1). Additional analysis by LC-MS indicated the presence of a sixth compound which also possessed a mass of 830 Da. Since the two 830 Da peptides have the same mass, they were not resolved by MALDI MS but were distinguished by their retention time on reversed-phase C_{18} (Table 5.4). MS/MS analysis suggested that each peptide contained an unusual 168 Da moiety at the N-terminus with the molecular formula $C_9H_{14}NO_2$, isoleucine (Ile), two aromatic amino acids and a hydroxyphenyllactic acid (Hpla) C-terminus (**187**-**192**). Whilst a methyltyrosine (MeTyr) was consistently observed in position four, the position three amino acid varied between methylphenylalanine (MePhe), MeTyr and methoxy MeTyr (MeTyr(*O*Me)). **187**-**189** possessed an ester-linked Hpla at the carboxyl end, whilst **190**-**192** contained a methoxyphenyllactic acid (Mpla).

Table 5.4: Structures, molecular masses and retention times of the six new Antarctic peptides.

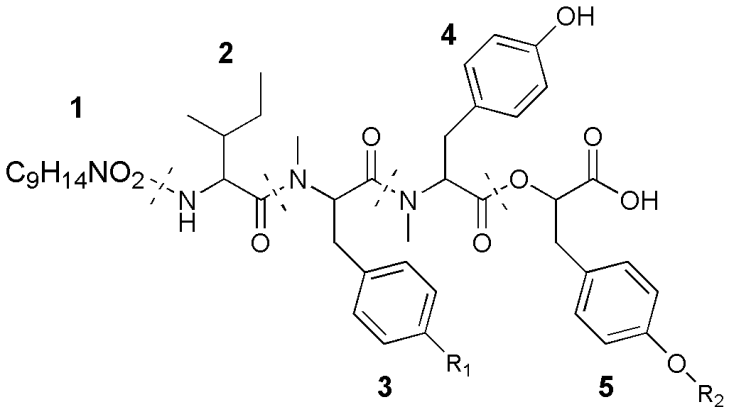

Compound	M_r (Da)	RT[a] (min)	R_1	R_2
Antarctic peptide 800 (**187**)	800.4	5.94	-H	-H
Antarctic peptide 816 (**188**)	816.4	5.45	-OH	-H
Antarctic peptide 830A (**189**)	830.4	5.96	$-OCH_3$	-H
Antarctic peptide 814 (**190**)	814.4	6.72	-H	$-CH_3$
Antarctic peptide 830B (**191**)	830.4	6.36	-OH	$-CH_3$
Antarctic peptide 844 (**192**)	844.4	6.77	$-OCH_3$	$-CH_3$

[a] RT = Retention time on a C_{18} column as per Table 9.3.

The MALDI post-source decay (PSD) MS/MS spectrum of **187** (Figure 5.14) showed a strong fragment ion series beginning with a protonated 168 Da moiety ($C_9H_{14}NO_2$; *m/z* 169) which extended to include Ile, MePhe, MeTyr and a 181 Da C-terminus. The mass of the C-terminus did not match with any generally observed amino acids, but could be Hpla incorporated through the 2-hydroxyl. Other less abundant ions included a fragment ion series beginning at the C-terminus and fragments of the amino acids (Table 5.5).

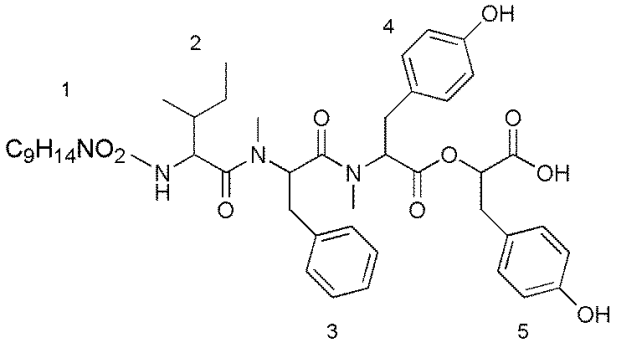

(187)

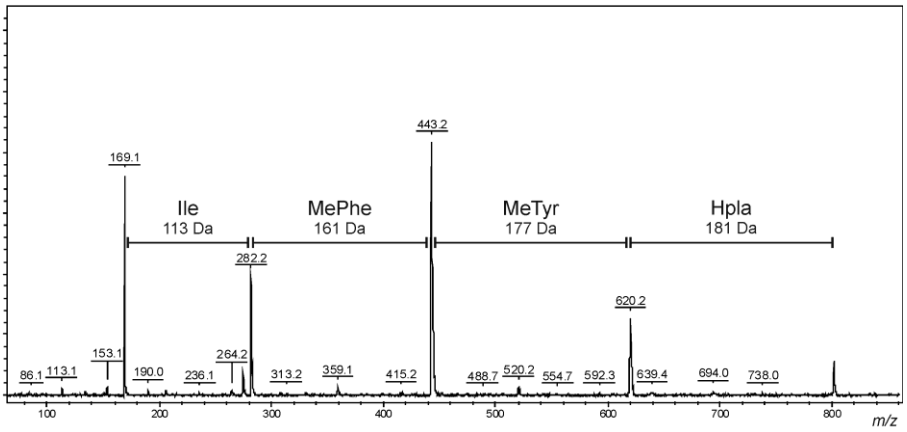

Figure 5.14: Tandem mass spectrum of Antarctic peptide 800. Fragmentation induced by matrix-assisted laser desorption/ionisation post-source decay.

Table 5.5: Tandem mass spectrometry fragment ions for Antarctic peptide 800 observed by matrix-assisted laser desorption/ionisation post-source decay and electrospray ionisation collision-induced dissociation.

m/z	**Fragment Assignment** [a]	*m/z*	**Fragment Assignment** [a]
86	Ile immonium	91	MePhe sidechain
107	MeTyr/Hpla sidechain	113	Fragment of $C_9H_{14}NO_2$
134	MePhe immonium	141	$C_9H_{14}NO_2 - CO + H$
151	$C_9H_{14}NO_2 - H_2O + H$	169	$C_9H_{14}NO_2 + H$
275	Ile-MePhe + H	282	$C_9H_{14}NO_2$-Ile + H
359	Hpla-MeTyr + H	443	$C_9H_{14}NO_2$-Ile-MePhe + H
520	Hpla-MeTyr-MePhe + H	620	$C_9H_{14}NO_2$-Ile-MePhe-MeTyr + H
801	M + H		

[a] $C_9H_{14}NO_2$ is the unidentified 168 Da N-terminus

The MS/MS spectrum of **188** (Figure 5.15) also showed a strong fragment ion series, beginning with the protonated 168 Da moiety (*m/z* 169) and extending to include Ile, a 177 Da residue, MeTyr and an Hpla C-terminus. The 177 Da amino acid contained an additional 16 Da mass to the MePhe observed in **187**. This mass increase could be due to a substitution of the MePhe in position three for MeTyr. This substitution was supported by a reduced retention time on reversed-phase C_{18} (5.45 vs. 5.94 min; Table 5.5), as the additional hydroxyl group would increase the polarity of the compound.

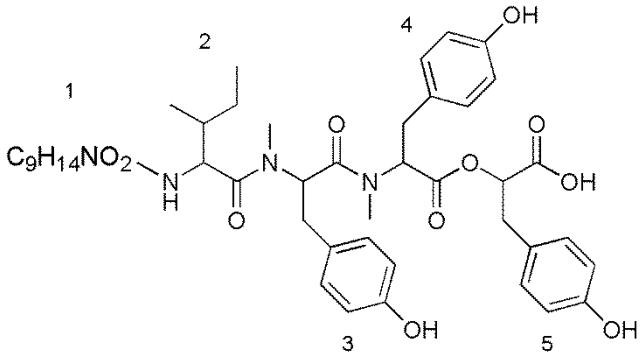

(188)

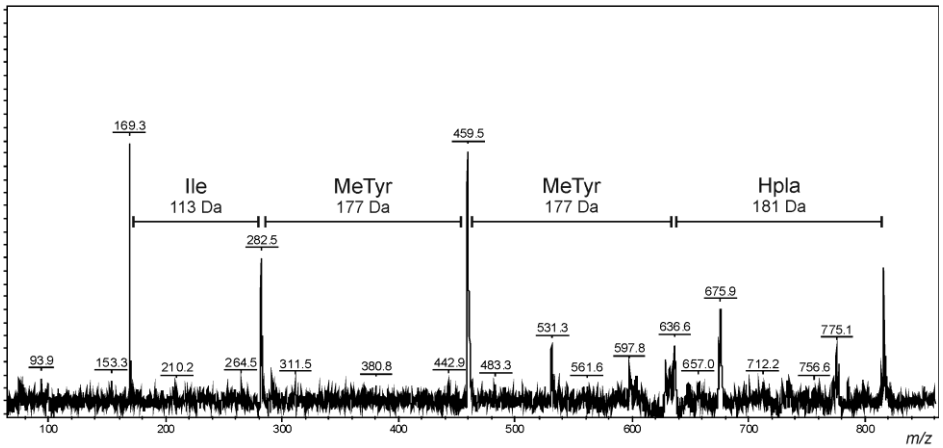

Figure 5.15: Tandem mass spectrum of Antarctic peptide 816. Fragmentation induced by matrix-assisted laser desorption/ionisation post-source decay.

The MS/MS spectrum of **189** (Figure 5.16) showed the same fragment ion series observed in **187** and **188**, but with a 191 Da residue in position three. The 191 Da amino acid contained an additional 14 Da mass to the MeTyr observed in **188**. This mass increase could be due to an additional methylene in the sidechain arm or an *O*-methylation. Since the retention time of peptide 830A was very similar to that of peptide 800 (Table 5.5), the most likely modification would be an

O-methylation of the hydroxyl group of the MeTyr. The *O*-methylation would nullify the hydrophilic effect of the substitution observed in peptide 816.

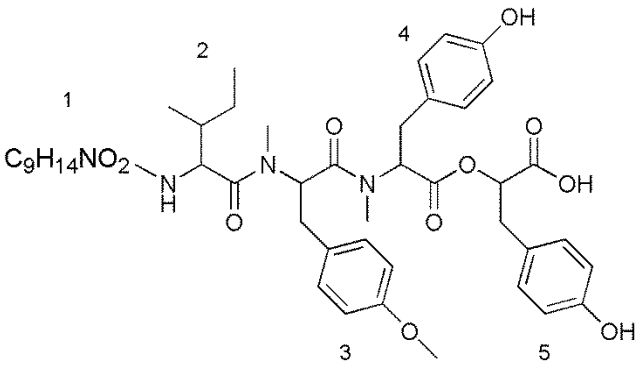

(189)

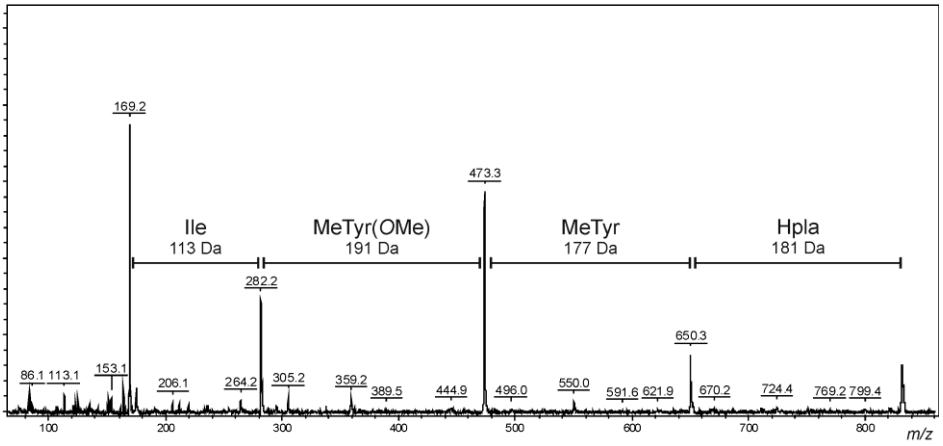

Figure 5.16: Tandem mass spectrum of Antarctic peptide 830A. Fragmentation induced by matrix-assisted laser desorption/ionisation post-source decay.

The MS/MS spectrum of **190** (Figure 5.17) indicated that the compound was very similar to peptide 800. The fragment ion series extending from the protonated 168 Da moiety (*m/z* 169) indicated that peptide 814 had the sequence; $C_9H_{14}NO_2$-Ile-MePhe-MeTyr, except that the C-terminus contained an additional 14 Da mass. This could be due to an additional methylene or an *O*-methylation. The increased retention time on reversed-phase C_{18} (6.72 vs. 5.94 min; Table 5.5) indicated this modification had disrupted a hydrophilic group on the residue. This suggested that the modification was a methylation of one of the hydroxyl groups present.

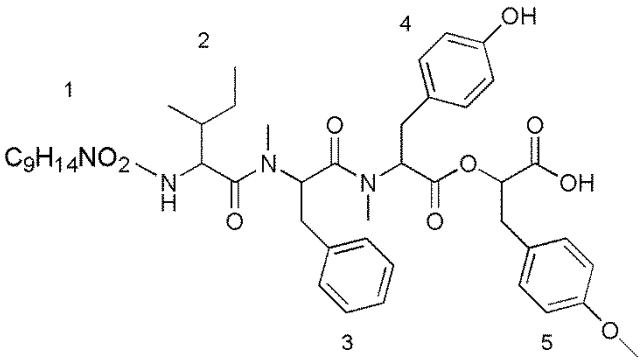

(190)

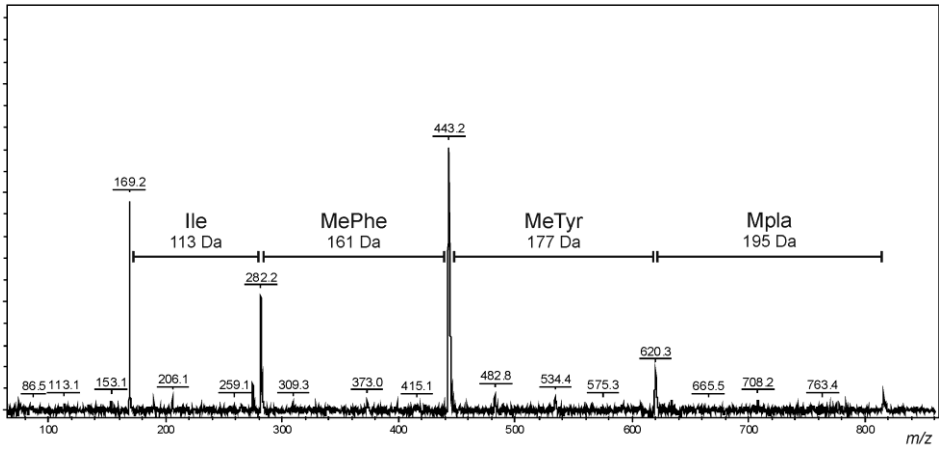

Figure 5.17: Tandem mass spectrum of Antarctic peptide 814. Fragmentation induced by matrix-assisted laser desorption/ionisation post-source decay.

As peptide 830B (**191**) had the same mass as peptide 830A and was present in much lower quantities, the structure of **191** could not be deduced from the MALDI MS/MS, therefore, only the LC-MS/MS data was utilised. Whilst the fragment for the protonated 168 Da moiety (*m/z* 169) was too low to be observed in the LC-MS/MS spectrum presented (Figure 5.18), an MS^3 experiment performed on the $C_9H_{14}NO_2$-Ile fragment ion (*m/z* 282) confirmed that the same lower-mass fragments were present. The fragment ion series which extended from $C_9H_{14}NO_2$-Ile included two MeTyr residues and the Mpla C-terminus present in **190**. As with peptides 800 vs. 816, peptide 830B had a reduced retention time on reversed-phase C_{18} compared to peptide 814 (6.36 vs. 6.72 min; Table 5.5), supporting the presence of an additional hydroxyl group.

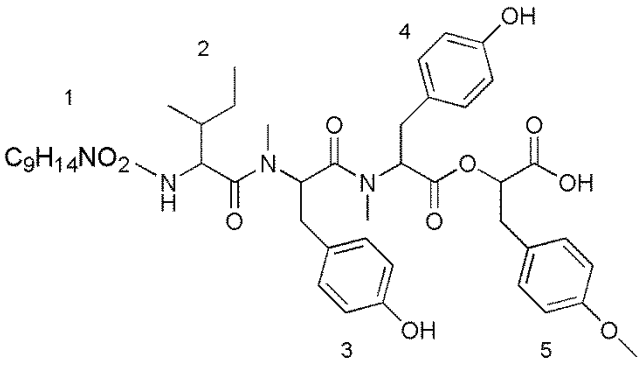

(191)

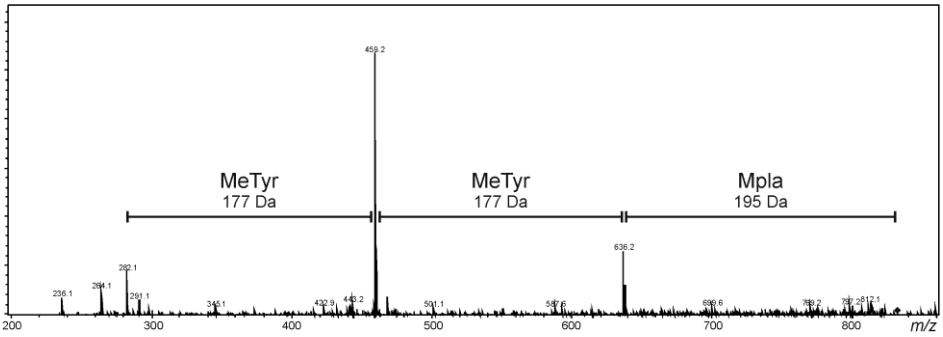

Figure 5.18: Tandem mass spectrum of Antarctic peptide 830B. Fragmentation induced by electrospray ionisation collision-induced dissociation.

The MS/MS spectrum of peptide 844 (**192**; Figure 5.19) showed great similarity to that of peptide 830A, except that the C-terminus possessed 14 Da extra mass. The fragment ion series indicated that **192** had an amino acid sequence of $C_9H_{14}NO_2$-Ile-MeTyr(*O*Me)-MeTyr-Mpla. The later retention time on reversed-phase C_{18} compared to peptide 830A indicated that the position five modification was most likely an *O*-methylation, and the later retention time compared to peptide 830B indicated that the position three modification was also most likely an *O*-methylation.

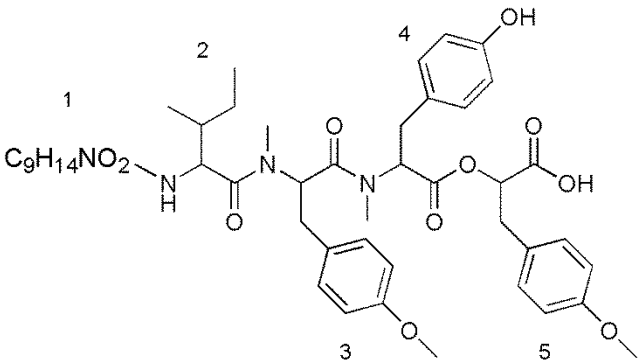

(192)

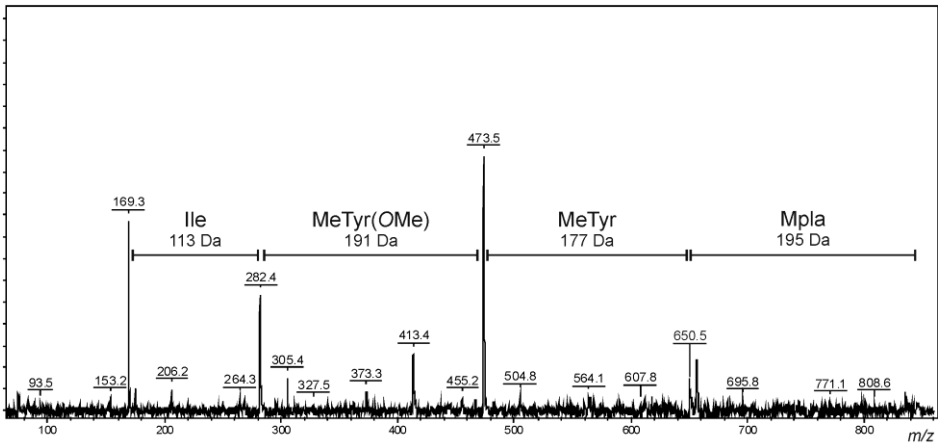

Figure 5.19: Tandem mass spectrum of Antarctic peptide 844. Fragmentation induced by matrix-assisted laser desorption/ionisation post-source decay.

As discussed in Section 2.3, the amino acids Ile and Leu which possess the same mass, in some circumstances, can be distinguished by mass spectrometry.[242,243] This process involves performing MALDI MS/MS on the sample under PSD conditions and under conditions combining PSD and high-energy CID. As CID induces a harsher fragmentation, some of the amino acid sidechain dissociates and the two structural isomers can be distinguished (Figure 5.20). As the resulting sidechain fragment is produced at such low levels, the technique requires an intense parent fragment ion containing the Ile/Leu to be determined.

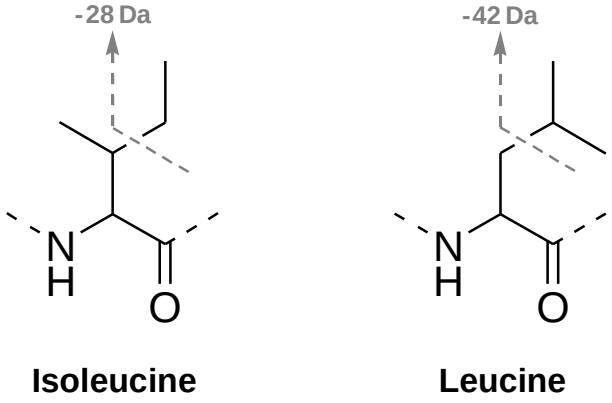

Figure 5.20: Sidechain fragmentation of the amino acids isoleucine and leucine by high-energy collision-induced dissociation.

This analysis was undertaken on the $C_9H_{14}NO_2$-Ile/Leu fragment ion (*m/*z 282) of the two most abundant Antarctic peptides; 800 and 830A. When the PSD spectrum was compared with the PSD-CID spectrum, there was a small ion representing a loss of 28 Da (*m/*z 254) present in the PSD-CID spectrum which was not as prominent in the PSD spectrum (Figure 5.21). No loss of

42 Da (*m/z* 240) was observed in the PSD-CID spectrum, which indicated that the amino acid present in peptides 800 and 830A was likely to be Ile and not Leu. This analysis was not successful when undertaken on the other Antarctic peptides, most likely because they were present in lower quantities. In the putative structures **187-192**, it has been assumed that of the peptides all contain Ile.

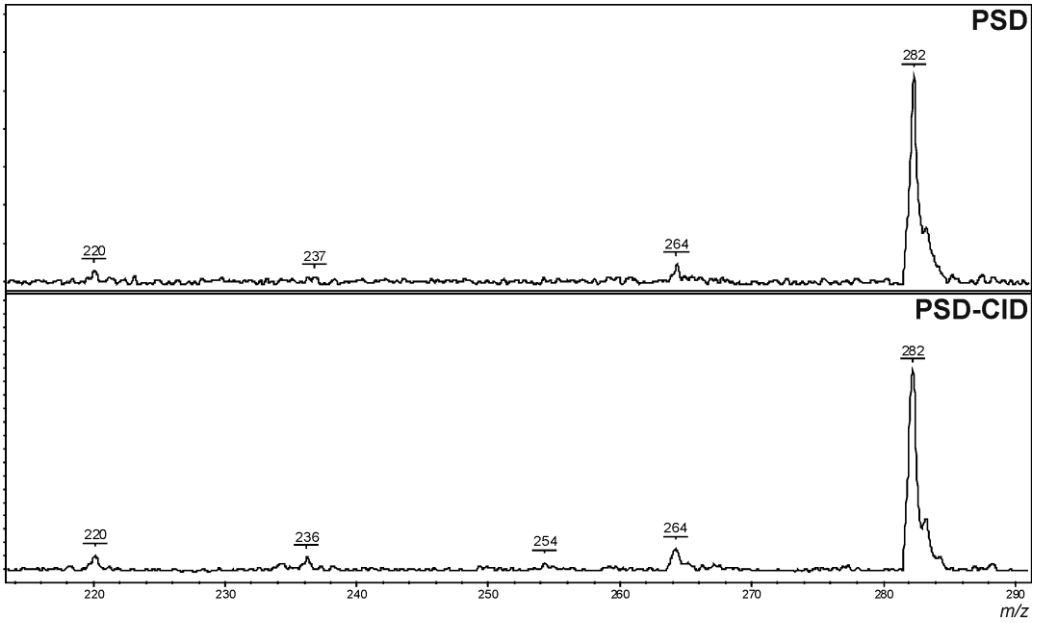

Figure 5.21: Isoleucine/leucine determination performed on Antarctic peptide 830A. Fragmentation induced by MALDI PSD **(A)** and MALDI PSD-CID **(B)**.

The N-terminus of the Antarctic peptides was a 168 Da moiety which showed high ionisation efficiency by MALDI. Under MS^3 conditions by ESI CID, a loss of water and carbon monoxide was evident, as well as a fragment at *m/z* 113. These pieces of evidence suggest that the 168 Da group contains at least one nitrogen atom in order to ionise readily by MALDI.[283] The loss of water suggests that it contains an hydroxyl group[284] and the loss of carbon monoxide, that it is linked to the next amino acid by the carbonyl of a peptide bond[285] or that there is a hydroxyl group present on an aromatic ring.[286]

Having determined the structure of the rest of each peptide, the accurate masses yielded from HRMS were used to generate potential molecular formulae for the remaining moiety. The already allocated molecular formula was set as the minimum value for the carbon, hydrogen, nitrogen and oxygen atoms, and a tolerance of ±5 ppm was utilised. Across the five different accurate masses, ten different molecular formulae were generated (Table 5.6).

Table 5.6: High resolution mass spectrometry analysis for the determination of the N-terminal moiety.

#	Potential Formula	Calculated *m/z*	Frequency	Comments
1	$C_9H_{14}NO_2$	168.1025	5	
2	$C_7H_{12}N_4O$	168.1011	3	Nitrogen Rule
3	$C_6H_{16}O_5$	168.0998	2	No Nitrogen
4	$C_5H_{10}N_7$	168.0998	2	No Oxygen
5	$C_3H_{14}N_5O_3$	168.1097	2	Not Plausible
6	$C_2H_{18}NO_7$	168.1083	3	Not Plausible
7	$CH_{141}N$	168.1064	4	No Oxygen
8	$CH_{12}N_8O_2$	168.1083	3	Not Plausible
9	$CH_{121}N$	168.1064	1	No Oxygen
10	$H_{16}N_4O_6$	168.1070	5	Not Plausible

Most of the potential formulae did not possess one of the structural attributes mentioned previously. Formulae 3, 4, 7 and 9 were ruled out as they did not contain an oxygen or a nitrogen (Table 5.6). Formulae 5, 6, 8 and 10 were also not plausible, as they contained too few carbon atoms. Formula 2 did not contain the correct valency to form the 168 Da substructure as it had four nitrogen atoms and twelve hydrogen atoms. This left only one viable molecular formula (Formula 1; $C_9H_{14}NO_2$) for the N-terminus.

The proportion of H:C/N/O in the resulting molecular formula indicated that the 168 Da moiety contained three double bond equivalents. Assuming one of these was due to a carbonyl, the N-terminus could contain an alkyne, two alkenes, two rings or a combination of an alkene and a ring. Multiple structures can be designed using this formula, which could also account for the mass spectrometric observations (Figure 5.22). Therefore, the structure of the 168 Da N-terminal moiety in the Antarctic peptides remains undetermined.

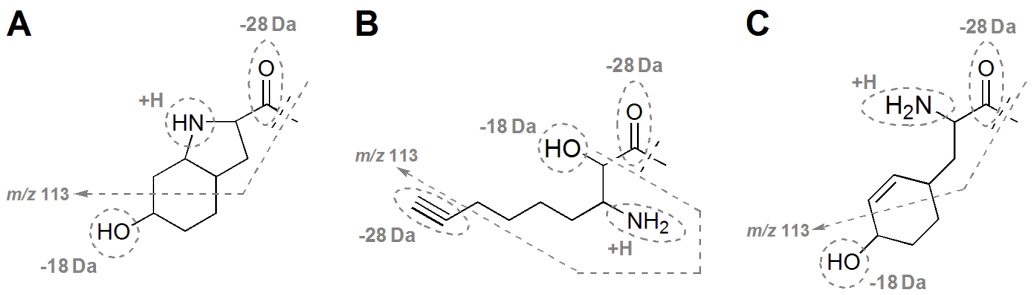

Figure 5.22: Potential structures for the N-terminal moiety of the Antarctic linear peptides. 2-carboxy-6-hydroxyoctahydroindole; Choi **(A)**, 3-amino-2-hydroxy-non-8-ynoic acid; Ahnya **(B)**, tetrahydro-tyrosine; (H_4)Tyr **(C)**.

High resolution MS of the Antarctic peptides yielded mass-to-charge ratios consistent with the singly protonated ions of the structures **187**-**190** and **192** and mass deviations of less than 4.5 ppm (Table 5.7). The accurate mass for peptide 830B was not listed, as this minor component was not separated from the major component, peptide 830A, during the fractionation.

Table 5.7: High resolution mass spectrometry analysis of the Antarctic linear peptides.

Compound	Measured *m/z*	Molecular Formula	Calculated *m/z*	Error (ppm)
Antarctic peptide 800 (**187**)	801.4082	$C_{44}H_{57}N_4O_{10}$	801.4069	−1.54
Antarctic peptide 816 (**188**)	817.4053	$C_{44}H_{57}N_4O_{11}$	817.4018	−4.32
Antarctic peptide 830A (**189**)	831.4183	$C_{45}H_{59}N_4O_{11}$	831.4175	−0.95
Antarctic peptide 814 (**190**)	815.4262	$C_{45}H_{59}N_4O_{10}$	815.4226	−4.36
Antarctic peptide 844 (**192**)	845.4359	$C_{46}H_{61}N_4O_{11}$	845.4331	−3.32

The putative structures of the Antarctic linear peptides (**187**-**192**) were assembled using a combination of MS/MS and HRMS. A strong fragment ion series indicated that each of the peptides contained a 168 Da N-terminus, Ile, two aromatic amino acids and an ester-linked Hpla.

The position two amino acid was provisionally determined as Ile rather than Leu using high-energy MALDI-PSD/CID analysis. Further investigations using a LC-MS ion trap system and increasing collision energies could yield a more conclusive identification of this residue. The position three amino acid varied between MePhe, MeTyr and MeTyr(*O*Me). These assignments were made due to the retention time on reversed-phase C_{18}. However, it was possible that these amino acids, and the position four MeTyr, could be the isometric homo-versions. The assignment of the *N*-methylated amino acids was made due to the structural similarities between these peptides and the microginins (see Section 1.2.5). In the microginins, *N*-methylated amino acids are frequently observed in positions three and four,[14] whilst non-methylated versions are seen less frequently. In half of the peptides, the ester-linked Hpla C-terminus contained an *O*-methylation. This was assigned due to the different retention times observed on reversed-phase C_{18}; however, it was not clear whether this was present on the C1 carboxylic acid or the C7 ring hydroxyl.

The structure of the N-terminus could not be assigned with the current data, but the analysis performed suggested that it possessed the molecular formula $C_9H_{14}NO_2$. Due to the mass spectrometric characteristics it displayed, it was likely to contain a carbonyl, a hydroxyl and an amine. The H:C/N/O ratio indicated that it contained two additional unsaturations besides the carbonyl. As this could represent multiple structures, the moiety was left unassigned.

5.3 DISCUSSION

5.3.1 Discovery of Eight New Glycine-Containing Microcystins

The identification of these new microcystins adds an additional eight congeners to the 111 microcystins already characterised (Appendix A). The eight different congeners all contain Gly in position one, D-Asp in position three, D-Glu in position six and what is highly likely to be Dhb in position seven. Variations of L-Leu/Arg, Arg/Har and Adda/ADMAdda in positions two, four and five, respectively, resulted in eight unique microcystin congeners (**179**-**186**). This work is the first report of glycine-containing microcystins and the first report of ADMAdda-containing microcystins from the Southern Hemisphere.[279]

Each of the new microcystins contained a D-Asp in position three, as has been frequently observed in multiple cyanobacterial genera including; *Anabaena*,[51] *Microcystis*,[34] *Nosotc*,[55] *Oscillatoria*[61] and *Plankothrix*,[50] as well as cyanobacteria from Antarctica.[278] The position seven Dhb has been reported in nine other microcystins (Appendix A), three of which were ADMAdda-containing microcystins.[54] However, the frequency of occurrence of Dhb-containing microcystins is potentially underestimated, as many microcystin congeners have been characterised solely by MS/MS. This does not allow for discrimination between the isometric Mdha and Dhb. The microscale thiol derivatisation[41,248] utilised in this work would be of great benefit to other researchers working with a small sample size, in order to easily confirm the presence of Mdha-containing microcystins.

Substitution of Arg for Har is rare, with only four microcystin congeners containing this amino acid being characterised to date (Appendix A). Two further microcystins have been identified as containing Har, but a full structure was never

elucidated.[280] Thirteen ADMAdda-containing microcystins have been reported (Appendix A), these were produced by *Nostoc* and *Planktothrix* species from across Europe. Although the cyanobacterial strain responsible for production of the new Antarctic microcystins was not isolated and cultured, molecular investigations identified the microcystin-producing cyanobacterium to be of the genus *Nostoc*.[279]

The position one alanine in microcystins is highly conserved and although substitutions for Leu and serine have been reported,[68,72,111] a substitution for Gly has not. Whilst the Gly substitution has not been observed, it is not an unreasonable proposition, as the adenylation domain responsible for incorporating the position one amino acid (McyA2; see Section 1.3.1) shows structural similarity to the saframycin synthetase Gly adenylation domain.[99,287]

The small sample size available prevented purification of the Antarctic microcystins from proceeding beyond the separation of two mixtures containing the -LR and -RR congeners from the other components in the extract, therefore, no bioactivity screening was conducted. Other microcystins containing similar modifications to these new congeners have been shown to inhibit serine/threonine protein phosphatases 1 and 2A (Appendix A), so it is possible that these congeners would also exert the same effect.

The Dry Valleys in Eastern Antarctica are a unique environment. The low temperatures are coupled with minimal precipitation, strong winds, high salinity, high ultraviolet light exposure during summer and extended periods of darkness during winter.[268,269] These harsh conditions lead to simple ecosystems and predator-free environments for the cyanobacteria. There has been a lot of interest in the biological function of microcystins, with many researchers speculating that they may be produced as a defence mechanism against predators. The common occurrence of microcystins in this predator-free environment (as well as other investigations; see Section 1.3.3), suggest that microcystin production is not solely a predator-driven phenomenon.

5.3.2 Discovery of Six New Linear Peptides

The discovery of six new linear peptides from the Antarctic hydroterrestrial mat samples was of significance, as the compounds do not identify directly with any class of known cyanobacterial oligopeptide. Each of the peptides contained a 168 Da N-terminus, Ile, two aromatic amino acids and an ester-linked Hpla. Substitutions of the position three amino acid and methylation of the C-terminus resulted in six unique structures.

The N-terminus of the Antarctic linear peptides did not match any previously observed N-terminal moieties from cyanobacterial oligopeptides. This 168 Da moiety could be the 2-carboxy-6-hydroxyoctahydroindole (Choi) observed in position three of the aeruginosins (see Section 1.2.1), although Choi has never been observed as the N-terminus of a peptide. Other possibilities for the moiety included 3-amino-2-hydroxy-non-8-ynoic acid, similar to the N-terminus of the microginins (see Section 1.2.5). Due to the small sample size available, the structure of the N-terminus could not be determined without more material or more sensitive characterisation techniques.

An ester-linked Hpla has never been observed in aquatic cyanobacterial oligopeptides. Conceivably, this could be mediated by an ester-forming ligase acting upon the carboxylic acid of the position four amino acid and the 2-hydroxyl of Hpla (Figure 5.23). Supporting this theory is the presence of ester-linkages between amino acids in the cyanopeptolins and microviridins (see Section 1.2). The genes encoding the enzymes responsible for these reactions have been

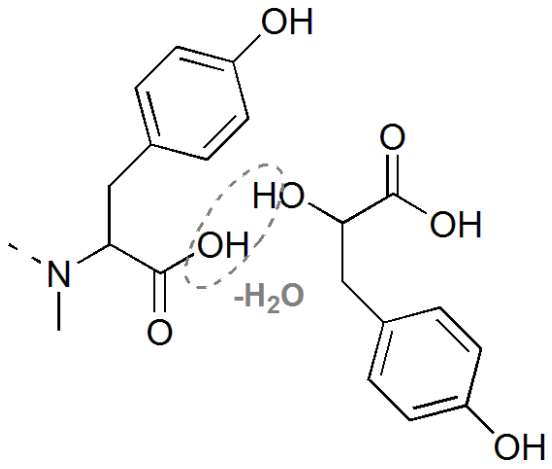

Figure 5.23: Potential pathway for the biosynthesis of the ester-linked hydroxyphenyllactic acid C-terminus.

identified for both oligopeptides.[29,30,288] No investigations of the peptide synthetases and polyketide synthases responsible for the production of the Antarctic peptides were made.

5.4 CONCLUSIONS

A cyanobacterial mat sample from Miers Valley in Antarctica was investigated for the presence of new oligopeptides. The structures of eight new microcystins (**179**-**186**) containing a position one Gly were determined using a combination of amino acid analysis, chemical derivatisation and MS/MS. Amino acid analysis and a β-mercaptoethanol derivatisation indicated that the position seven amino acid was not the Mdha commonly observed in microcystins, but was highly likely to be Dhb. Tandem MS analysis indicated the presence of Har and ADMAdda residues. The combination of these two uncommon modifications, with the rare substitution of the position one amino acid is a significant observation. The addition of eight new microcystin congeners is also a significant increase to the 111 structures presently characterised.

Six new linear peptides (**187**-**192**) were also present in the Antarctic sample, which did not match any of the presently characterised cyanobacterial oligopeptides. The putative structures for the peptides were determined using a combination of MS/MS and HRMS. Each peptide contained a unique ester-linked Hpla C-terminus, two aromatic amino acids, Ile and an N-terminus with the molecular formula $C_9H_{14}NO_2$. Although the structures could not be fully determined using the present sample, the information gathered points towards a novel class of cyanobacterial oligopeptides.

CHAPTER 6

Enhanced Sample Preparation for Quantitation of Microcystins by Matrix-Assisted Laser Desorption/Ionisation-Time of Flight Mass Spectrometry

6.1 INTRODUCTION

On account of the health risk posed by microcystins (MCs), the World Health Organisation has recommended a 'safe level' for drinking waters of 1 µg/L of MC-LR.[152] Microcystin concentrations in environmental water samples are generally analysed by enzyme-linked immunosorbent assay (ELISA), protein phosphatase inhibition assay (PPIA) or high performance liquid chromatography (HPLC).[153]

ELISA and PPIA provide no information on the different microcystin congeners present in a sample, but the PPIA method gives an indication of the toxicity of the sample according to the strength of protein phosphatase inhibition observed.[157] HPLC coupled to a photo-diode array detector gives limited information on the congeners present, based upon their retention time on a C_{18} column and the ultraviolet spectrum of the eluting congener.[167] Liquid chromatography in combination with mass spectrometry (LC-MS) is the most robust of current methods used for microcystin analysis as it gives definitive information on the congeners present according to their retention time on a C_{18} column and their mass-to-charge ratio (*m/z*).[166] The major disadvantage with these methods of quantifying microcystins is the long duration of both sample handling and analytical procedures. Recent advances in small particle and monolithic silica columns have decreased run times significantly from those achieved using conventional HPLC.[173,174] However, run times are still greater than the time it takes to obtain a matrix-assisted laser desorption/ionisation-time of flight (MALDI-TOF) spectrum (< 30 s).

As discussed in Section 1.4, MALDI MS gives comparable information to LC-MS, but analysis times are much shorter. MALDI MS is also well suited to automated high-throughput sample preparation and data acquisition,[177] making it an ideal technology for analysing large numbers of microcystin-containing samples quickly. The technique has frequently been used for qualitative detection of microcystins in cyanobacterial samples,[44,176,178-182] but has only recently been used as a quantitative tool.[184] During quantitative MALDI analyses, an internal standard is commonly added to sample and standard solutions to improve the 'spot-to-spot' and 'shot-to-shot' reproducibility.[188-192]

Howard and Boyer found that of four internal standards tested for microcystin quantitation, nodularin gave the best results.[184] Nodularin is a cyclic pentapeptide very similar to microcystins, but with a mass lower than any known microcystin. It is commercially available, but relatively expensive (> NZ$2,500/mg). Howard and Boyer's work used a simple MALDI sample preparation technique which involved sonication of a mixture of microcystin and internal standard with matrix solution, followed by deposition onto a polished steel target. This technique provided good spot-to-spot reproducibility and sensitivity, but it is not well suited for automated sample preparation or for use in an instrument automatically acquiring data.

Many manufacturers of MALDI mass spectrometers also produce targets modified with hydrophilic/hydrophobic regions to hold sample/matrix solutions in a certain location on the target whilst the solution dries. These targets generally yield a matrix/sample spot which is uniformly distributed at a designated location,[289] an essential prerequisite for automated acquisitions. Such targets are also particularly useful for producing thin-layer preparations, where a layer of matrix crystals is formed on the target followed by sample deposition on top. This technique is amenable to automated sample preparation and generally gives better signal homogeneity than a dried droplet preparation.[290,291]

In order for quantitative MALDI MS to reach its full potential as a high-throughput technique for microcystin analysis, different protocols are required to allow automated sample preparation and data acquisition. In the current study, angiotensin I was utilised as an internal standard in preference to

nodularin since it was a more cost effective option for analysis of large numbers of samples (ca. NZ$50/mg). The objective of this study was to establish a protocol compatible with automated sample preparation and data acquisition, whilst maintaining reproducibility and sensitivity. The performance of different MALDI sample preparation techniques was tested using a traditional polished steel target and a target modified with hydrophilic centres (Bruker Anchorchip).

6.2 RESULTS

6.2.1 Comparison of MALDI Sample Preparations

Seven different MALDI sample preparations were tested for reproducibility and sensitivity. The sonicated dried droplet method was based on Howard and Boyer's research.[184] Traditionally, this sample preparation may have been performed by mixing the two solutions directly on the target with an auto-pipette (a dried droplet preparation). Three thin-layer preparations were also assessed. These were prepared on a Bruker anchorchip, on a polished steel target where the matrix was laid in a line, and also in a spot. Refer to Section 9.6.1 for more detail on on each of these sample preparations.

Visually, the sonicated dried droplet and dried droplet preparations were very similar (Figure 6.1A-D). Those prepared on a polished steel target beaded during crystallisation, resulting in areas rich in matrix/sample and areas within the sample spot where no sample was present (Figure 6.1A & C). This irregular distribution makes these preparations unreliable for automated data acquisition on a mass spectrometer, due to the non-uniform distribution of matrix/sample on the target. The sonicated dried droplet and dried droplet preparations on an anchorchip showed a more uniform distribution of matrix/sample, as the droplet was held in place by the hydrophilic spot as it dried (Figure 6.1B & D). This would mean that matrix/sample would be present anywhere within this sample spot if automated data acquisition were undertaken.

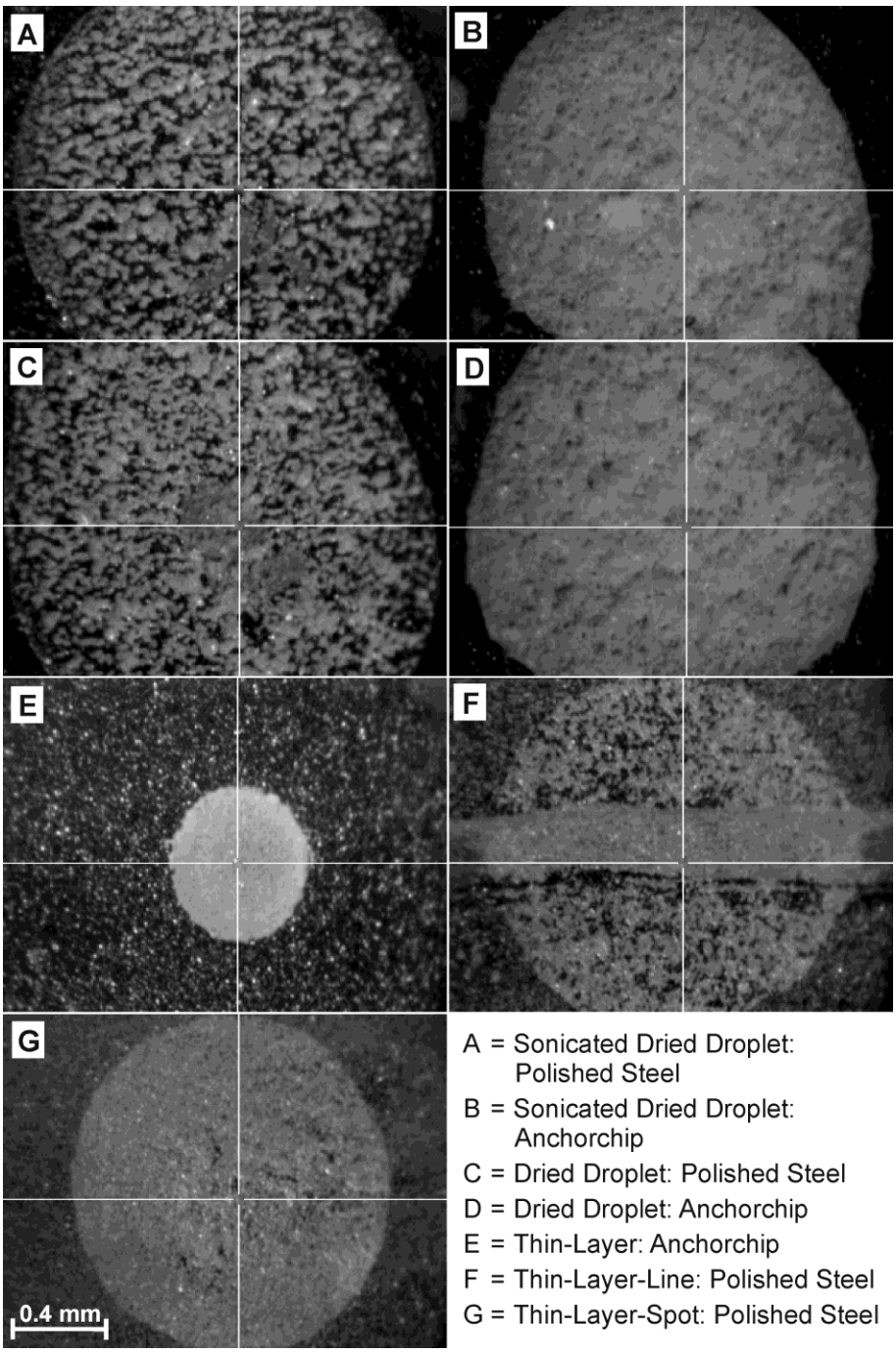

Figure 6.1: Digital images of the sample preparations used in this study. Images acquired using the charged-coupled device camera installed in the mass spectrometer.

The thin-layer preparation performed on an anchorchip was much smaller than the other preparations, as the matrix was restricted to the hydrophilic spot on the anchorchip (ca. 600 µm diameter; Figure 6.1E). The thin-layer-line preparation had small crystals of matrix on the surface of the polished steel target and a lighter circle where the sample had been laid and the matrix recrystallised (Figure 6.1F). The line through the centre was where the auto-pipette tip was dragged down the length of the target during preparation of the thin layer of matrix. The thin-layer-

spot preparation looked similar to the thin-layer-line preparation, in that it had small crystals of matrix on the surface of the target and a lighter circle where the sample was laid, but it lacked the line down the centre (Figure 6.1G). This was because each spot was formed individually from a drop of matrix dissolved in acetone, making the technique suitable for automated sample preparation.

An assessment of the spot-to-spot reproducibility for each of the seven preparations was performed using the peak height ratio (PHR) of 2.5 µM [Dha^7] MC-LR/50 µM angiotensin I. The coefficients of variation (CVs) reported in Table 6.1 are the average of three separate analyses performed using fresh preparations on different days. High levels of reproducibility were not achieved using both the sonicated dried droplet and dried droplet preparations on either the polished steel or anchorchip targets, giving CVs of around 20%. During the analysis of the thin-layer preparation on an anchorchip, it was noted that both microcystin and angiotensin I signals were low in the centre of the sample spot and increased in intensity towards the outside edge. This preparation yielded a CV of 22.5%. The two thin-layer preparations performed on a polished steel target gave good signal reproducibility, returning CVs of 11.9% for the line preparation and 9.5% for the spot preparation. The thicker line of matrix in the thin-layer-line preparation (Figure 6.1F) did not affect the signal compared with the rest of the sample spot.

Table 6.1: Performance of seven MALDI sample preparations.

Sample Preparation	CV [a] (%)	MDL [b] (µM)
Sonicated dried droplet: Polished Steel	18.7	0.100
Sonicated dried droplet: Anchorchip	18.8	0.088
Dried droplet: Polished Steel	18.1	0.086
Dried droplet: Anchorchip	24.8	0.228
Thin-layer: Anchorchip	22.5	0.073
Thin-layer-line: Polished Steel	11.9	0.077
Thin-layer-spot: Polished Steel	9.5	0.087

Values are the average of triplicate analyses conducted over three days using fresh sample preparations. [a] CV = Coefficients of variation; determined using 2.5 µM [Dha^7] MC-LR. [b] MDL = Method detection limit for [Dha^7] MC-LR; as per Section 9.6.3.

The method detection limit (MDL) was used to assess the sensitivity of each preparation (Table 6.1; Refer to Section 9.6.3 for more details on how the MDL was determined). The sonicated dried droplet preparations had detection limits of 0.1 µM [Dha^7] MC-LR on polished steel and 0.088 µM on the anchorchip. The dried droplet preparation performed on polished steel displayed a similar sensitivity, with a detection limit of 0.086 µM, but only 0.228 µM when using the anchorchip. The thin-layer preparation performed on the anchorchip had a detection limit of 0.073 µM, but required a higher laser power than the other preparations, to ionise the microcystin/angiotensin I. The thin-layer preparations on polished steel performed well, with detection limits of 0.077 µM for the line preparation and 0.087 µM for the spot preparation.

The performance of the thin-layer-spot preparation was also assessed using two other microcystin congeners; MC-RR and MC-YR. Both MC-RR and MC-YR yielded good CVs on the thin-layer-spot preparation (6.2% and 6.8%, respectively; Table 6.2). The MDLs were 0.031 µM for MC-RR and 0.056 µM for MC-YR. Both the reproducibility and sensitivity for these two congeners were better than that observed with [Dha^7] MC-LR (CV 9.5%, MDL 0.087 µM).

Table 6.2: Quantitative performance of the thin-layer-spot preparation performed on polished steel using three microcystin congeners.

Microcystin	CV [a] (%)	MDL [b] (µM)	Range [c] (µM)	Regression Equation	R^2
[Dha^7] MC-LR	9.5	0.087	0.279-10	$y = 0.1288x + 0.0153$	0.99
MC-RR	6.2	0.031	0.116-10	$y = 0.0752x + 0.0034$	0.99
MC-YR	6.8	0.056	0.180-10	$y = 0.1705x + 0.0645$	0.98

[a] CV = Coefficients of variation; determined using 2.5 µM microcystin. [b] MDL = Method detection limit for each microcystin. [c] Quantitative ranges begin at the limit of quantitation.

The quantitative performance of these three microcystin congeners was also tested using the thin-layer-spot preparation. Standard curves for each of the individual microcystins were constructed using microcystin concentrations in the range of 0.1-10 µM. Each microcystin congener showed good linearity over this range, with R^2 values between 0.98 and 0.99 (Table 6.2).

6.2.2 Laser Power Attenuation for Quantitative Analyses

Assessment of the microcystin concentration, relative to that of the angiotensin I added to the sample, not only improves reproducibility[188-192] but also allows the laser power to be attenuated to some degree. Use of an internal standard gave a limited range of laser powers where the PHR remained consistent (Figure 6.2). In this instance, the acceptable laser power fell in the range of 20 to 24%, corresponding to an intensity/shot ratio between 25 and 150 angiotensin I intensity/shot. At lower laser powers, the angiotensin I was ionised whilst the microcystin was not, resulting in a lower PHR. At laser powers higher than the optimal level, the angiotensin I signal saturated the detector whilst the microcystin signal continued to increase, resulting in a higher PHR.

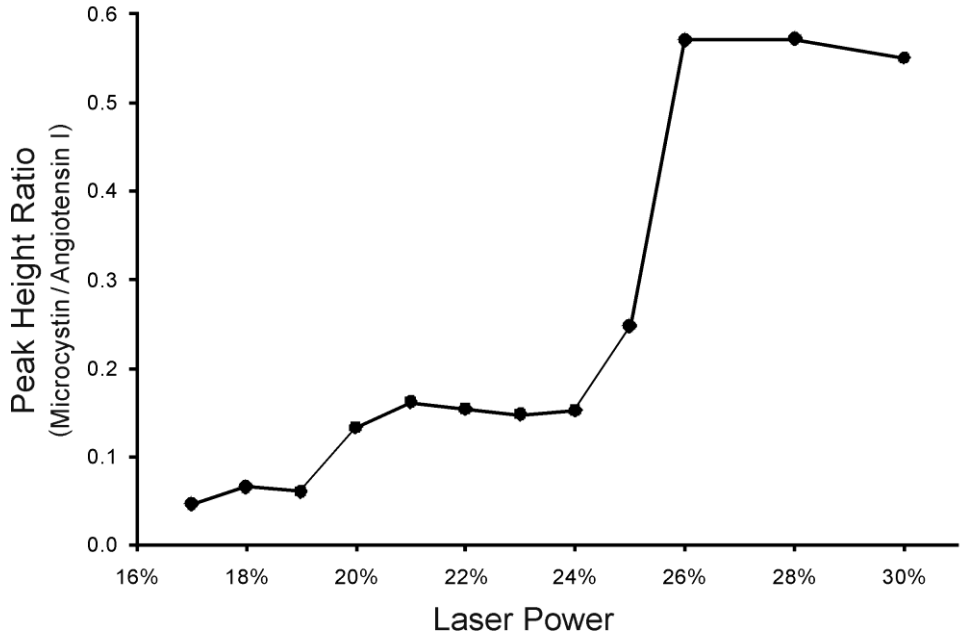

Figure 6.2: The effect of MALDI mass spectrometer laser power on the peak height ratio.

6.3 DISCUSSION

6.3.1 Enhanced Sample Preparation for Quantitative MALDI-TOF Mass Spectrometry Analysis of Microcystins

Seven different MALDI sample preparation protocols were assessed for their effectiveness to quantify microcystins. The desired attributes were reproducibility (assessed using the CV) and sensitivity (assessed using the MDL) whilst using a cost-effective internal standard (angiotensin I), as well as compatibility with automated sample preparation and data acquisition systems.

The reproducibility achieved using the sonicated dried droplet preparations was higher than that reported previously using the same concentration of microcystin (CV 8%).[184] In that instance, nodularin was used as the internal standard instead of the less expensive alternative used in this study (angiotensin I). Whilst the reproducibility could not be matched using the same sample preparation, the thin-layer preparations performed on polished steel did achieve CVs close to those reported using nodularin. The low reproducibility achieved using the thin-layer preparation on the anchorchip target was surprising, but could be due to the hydrophobic/hydrophilic regions present on the target. It was observed that both microcystin and angiotensin I signals were low in the centre of the sample spot and increased in intensity towards the outer edge. This would suggest a higher concentration of these slightly hydrophobic peptides at the edge of the sample spot, as they were repelled from the hydrophilic spot and attracted to the hydrophobic surface of the target.

Excluding the dried droplet preparation performed on the anchorchip, the detection limits achieved were all lower than those reported elsewhere using angiotensin I as an internal standard.[184] This was most likely due to the modern mass spectrometer used in the current study, since the enhanced sensitivity was observed across most of the preparations tested, including the sonicated dried droplet preparation used in the aforementioned study.[184] The detection limits observed were not as low as those achieved by Howard and Boyer using nodularin as an internal standard (MDL of 0.015 μM). In studies where maximum sensitivity is desired and cost per sample is not restrictive, consideration should be given to using nodularin as an internal standard over the less expensive angiotensin I. The poor sensitivity achieved with the dried droplet preparation on the anchorchip was due to a lower PHR ratio than the other preparations, possibly resulting from deeper embedding of the microcystin in the matrix causing a lower microcystin signal within the 25-shot cycle.

Each of the MALDI sample preparations used in this study, except the dried droplet preparation on an anchorchip, achieved reasonable sensitivities (MDLs of 0.073-0.1 μM). However, most of the preparations did not show good reproducibility (CVs of 18.1-24.8%), except for the two thin-layer preparations performed on a traditional polished steel target (CVs of 11.9% and 9.5%). The

thin-layer-spot preparation was the only sample preparation which possessed all of the desired attributes of reproducibility (low CV), sensitivity (low MDL) and compatibility with automated high-throughput systems. Whilst not compatible with automated sample preparation, the thin-layer-line preparation yielded reproducibility and sensitivity rivalling the thin-layer-spot preparation, and it was less cumbersome to prepare manually. This sample preparation technique could be adopted when automated target-laying systems are not available.

The quantitative performance achieved using the thin-layer-spot preparation was equal to that observed previously,[184] with each microcystin congener showing R^2 values of at least 0.98. The present study also demonstrated that the linear range of quantitation can be extended up to 10 µM; the previous study had a linear range up to 5 µM.[184] As noted by Howard and Boyer, the MALDI ionisation efficiency of different microcystin congeners varied,[184] and hence, the regression equations observed in this study have different gradients. This demonstrates the necessity to construct a standard curve for each microcystin congener present in a sample, as opposed to using an MC-LR equivalent as is commonly used with other microcystin quantitation techniques. Howard and Boyer also recommended that a fresh standard curve be run with each set of samples analysed, as the slopes can vary from day to day.[184]

On account of the potential for quantitative MALDI analysis to be used in studies with large sample numbers, a cost effective internal standard (angiotensin I) was utilised to provide a low cost per sample. We have shown that with modern instrumentation and different sample preparation techniques, reproducibility and sensitivity could be improved whilst using angiotensin I. Whilst the MDL for [Dha^7] MC-LR could not be reduced to the levels obtained with the internal standard nodularin, those of MC-RR and MC-YR were very close to, or better than, those previously observed with the more expensive internal standard.[184]

6.3.2 Laser Power Attenuation during Quantitative MALDI-TOF Mass Spectrometry Analyses

When operating without an internal standard, modulation of the laser power alters the analyte signal intensity, and hence affects the measurement of microcystin concentration. This would necessitate the use of a single laser power for an entire sample set or some sort of compensatory adjustment. Assessment of a microcystin/angiotensin I mixture over a range of laser powers indicated that there was a region where the PHR was consistent. The plateau in PHR means that the laser power can be attenuated to some degree when a sample gives a higher or lower response than the other samples present. Caution must be taken, however, to ensure the intensity/shot ratio stays within acceptable levels.

6.3.3 Application of Quantitative MALDI-TOF Mass Spectrometry Analysis of Microcystins

Although the detection limits achieved in the present study were within the range expected for quantitative MALDI analyses (ca. 100 nM), they were not near those required to detect microcystins directly from water samples used for regulatory requirements (1 nM; World Health Organisation advisory level).[152] To achieve this level of sensitivity would necessitate concentrating the sample, a lengthy additional step in the sample handling protocol, which would negate the advantage of the rapid sample handling procedure possible with MALDI MS. Therefore, using this technique on water samples, while possible, would be cumbersome.

However, if whole cells were being investigated, the concentration of the extracted microcystin could be controlled to some degree by reducing the extraction volume. This would allow analysis on, for example, surface cyanobacterial scum or benthic mat samples to determine the microcystin content present in the cyanobacterial biomass. A particularly promising application of quantitative MALDI MS is the quantification of the intracellular microcystin content of samples taken during culture experiments. Such samples are particularly amenable to analysis by this technique as there are usually large numbers of them and the microcystin congeners produced by the cyanobacterial species would likely be known. Thus the correct microcystin calibration standards could be on hand and the sample preparation could remain quick and simple.

6.4 CONCLUSIONS

Most of the sample preparations tested during this study showed reasonable sensitivity, but poor reproducibility, apart from the two thin-layer preparations performed on polished steel. Both of these thin-layer preparations achieved low MDLs, low CVs, and the thin-layer-spot protocol was also compatible with high-throughput automated sample preparation. Assessment of the thin-layer-spot preparation using two other microcystin congeners also showed good sensitivity and reproducibility. Assessment of the quantitative performance yielded R^2 values of at least 0.98 and a linear range which extended up to 10 µM. Furthermore, these results were achieved using a less expensive internal standard than was utilised in the previous work.[184]

CHAPTER 7

A Preliminary Investigation into the Modulation of Microcystin Congener Abundance in Response to Nitrogen Supply

7.1 INTRODUCTION

Over the past 30 years, many studies have been conducted investigating the influence of environmental parameters on microcystin production (see Section 1.3.3).[292] Most of these studies have focussed on the net production of microcystins and not on the levels of individual congeners. However, several studies have reported modulation of microcystin congener abundance under different environmental conditions. These studies examined responses to light intensity,[148,151] temperature,[135,149] growth phase[146] and amino acid availability.[150] Previous investigations into the effect of nitrogen concentration on the abundance of microcystin congeners have observed no modulation over the time-course of the experiments.[146,150,151] It was suggested that the lack of response could be due to the presence of phycocyanin pigments, which are utilised in times of nitrogen shortage, resulting in internal nitrogen stores not being fully depleted during the experimental period.

Microcystins are produced by a hybrid polyketide synthase (PKS)/non-ribosomal peptide synthetase (NRPS) called microcystin synthase (see Section 1.3.1).[99-101] The occurrence of different microcystin congeners is due to differences in the coding of the microcystin synthase genes of different cyanobacterial strains which can affect the substrate specificity of the adenylation domains responsible for incorporating amino acids into the structure (see Section 1.3.2).[110] When one of the adenylation domains has relaxed substrate specificity, a single strain of cyanobacteria can produce more than one microcystin congener.[110]

A cyanobacterial strain will generally produce around four microcystin congeners, in most cases; MC-LR, MC-RR and desmethyl analogues of each congener

(Appendix C). *Microcystis* CYN06, which was isolated from Lake Hakanoa (Huntly, New Zealand),[246], produces at least 27 microcystin congeners, however, this cyanobacterial strain could potentially produce 40 different congeners (see Section 3.3.1). In CYN06 this is due to relaxed substrate specificity at McyB1, McyB2 and McyC. As a result, five amino acids are incorporated at position two, four amino acids are incorporated at position four, and position three desmethyl analogues are also observed (see Section 3.2.1). Whilst cyanobacterial strains which produce at least 47 microcystin congeners have been reported,[245] CYN06 is unique as it has been shown to display relaxed substrate specificity at position four as well as at position two (see Section 3.3.1). As a result, CYN06 produces microcystin congeners which contain no arginine residues (MC-XAs and MC-XLs), a single arginine residue (MC-XRs and MC-RZs) and two arginine residues (MC-RRs).

As discussed in Section 1.3.2, structural variation of the microcystins can have a marked effect on the potency of the toxin. The most common microcystin; MC-LR, has a toxicity of 50 µg/kg,[115] whilst another common congener; MC-RR, is an order of magnitude less toxic (500-600 µg/kg).[120] Therefore, a change in microcystin congener levels in a cyanobacterial strain which produces multiple variants may lead to an increase or decrease in toxicity. The differing toxicities of microcystin congeners make it essential to acquire more knowledge about the environmental variables which regulate microcystin congener abundance.

Previous investigations into the effect of nitrogen concentration on microcystin congener abundance have utilised cyanobacterial strains which only produced arginine-containing microcystin congeners.[146,150,151] Use of a strain which also produces microcystins containing no arginine residues might allow new insights into the regulation of arginine incorporation in microcystins. In this study, the effect of nitrogen concentration on microcystin congener abundance was investigated by monitoring a batch culture of *Microcystis* CYN06 for 40 days until cells were nitrogen deplete. It is hypothesised that as the cells become starved of nitrogen, the abundance of the arginine-containing microcystins will decrease.

7.2 RESULTS

Six batch cultures of *Microcystis* CYN06 were grown in 1 L Schott bottles for 40 days (see Section 9.7.1 for more information). After this time, the cultures had changed colour from green to yellow (Figure 7.1), suggesting that the nitrogen stored in the phycocyanin pigments had been drawn upon.[293,294]

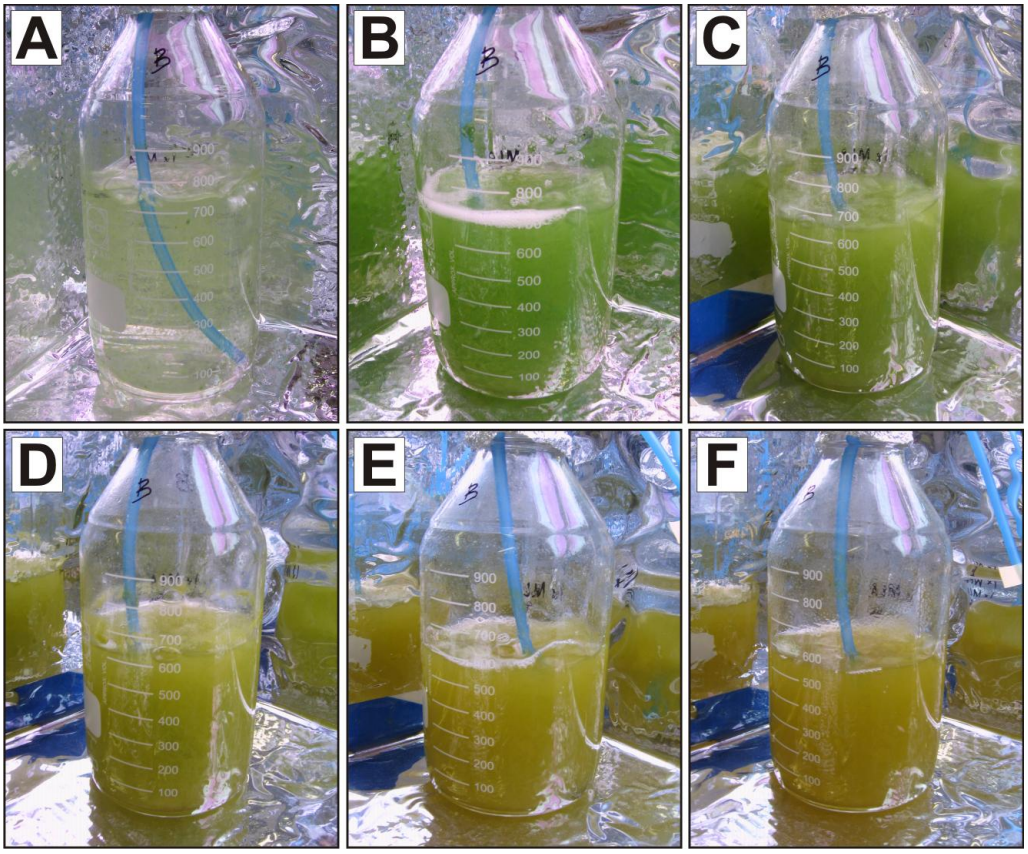

Figure 7.1: Images from a batch culture of *Microcystis* CYN06. Images recorded in a 1 L Schott bottle on day 8 **(A)**, 15 **(B)**, 22 **(C)**, 29 **(D)**, 36 **(E)** and 40 **(F)**.

During the time course of the experiment, each batch culture was sampled once a week for dissolved nutrient concentrations, cell concentrations and microcystin content. Cell density of *Microcystis* CYN06 increased steadily to 3.9×10^6 cells/mL over 40 days (Figure 7.2A). Concentrations of nitrate in the media decreased from 1.8 mM to below the detection limit of the flow injection analysis (FIA) method used (< 0.005 mM). The concentration of dissolved reactive phosphorus remained relatively constant and never decreased below 0.03 mM. Ammonium and nitrite were not detectable throughout the course of the experiment (≤ 0.005 mM). The total microcystin content increased from 2.5 to 4.2 femtomoles/cell on day 8 and then decreased steadily to 0.6 femtomoles/cell

by day 40 (Figure 7.2B). The microcystin content for each congener followed the same general pattern (Figure 7.2C).

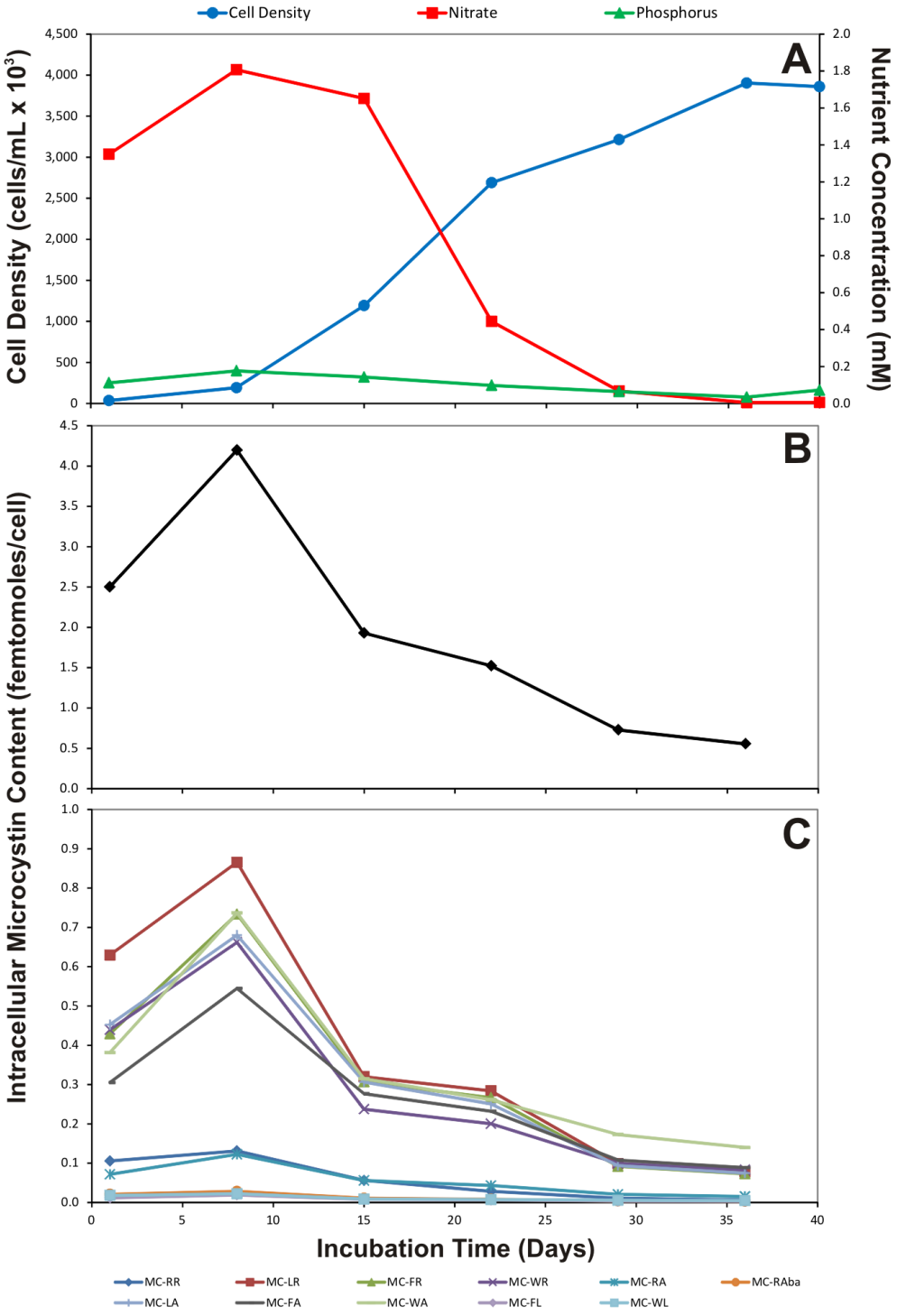

Figure 7.2: The effect of nitrogen depletion on microcystin content during a 40-day batch culture of *Microcystis* CYN06. Graphs depicting the cells, nitrate and dissolved reactive phosphorus concentrations **(A)**, total microcystin concentration **(B)** and microcystin concentration of eleven individual congeners **(C)**.

Linear regression of the relationship between $\log_{10}$ microcystin content and duration of incubation (days 8-36) revealed a strong correlation for each microcystin congener ($R^2 \geq 0.87$; Table 7.1), but with different slopes. The reduction in microcystin content of the congener containing two arginine residues (MC-RR) was more rapid than that of the congeners containing a single arginine residue (MC-XRs and MC-RZs), which in turn was more rapid than the congeners containing no arginine residues (MC-XAs and MC-XLs). In each case, the slope of decay for the tryptophan-containing congeners was less steep than the leucine- and phenylalanine-containing congeners (Table 7.1).

Table 7.1: Linear regression of $\log_{10}$ microcystin content verses incubation time for days 8-36.

Microcystin		Regression Equation	R^2	Average Gradient [a]
MC-RRs	MC-RR	$y = -0.048x + 2.47$	0.99	−0.048 (A)
MC-XRs	MC-LR	$y = -0.038x + 3.10$	0.95	−0.036 (B)
	MC-FR	$y = -0.037x + 2.95$	0.96	
	MC-WR	$y = -0.032x + 2.96$	0.93	
MC-RZs	MC-RA	$y = -0.032x + 2.26$	0.97	−0.033 (B)
	MC-RAba	$y = -0.034x + 1.62$	0.96	
MC-XAs	MC-LA	$y = -0.036x + 3.06$	0.96	−0.030 (B,C)
	MC-FA	$y = -0.029x + 2.91$	0.97	
	MC-WA	$y = -0.026x + 2.96$	0.92	
MC-XLs	MC-FL	$y = -0.029x + 1.41$	0.94	−0.026 (C)
	MC-WL	$y = -0.023x + 1.39$	0.87	

[a] The letters in brackets indicate three groups that the gradients of the grouped congeners were divided into by a Student's t-test ($p < 0.05$).

The congener gradients were separated into three groups using a Student's t-test (see Section 9.7.5 for more information). The gradient for MC-RR was significantly steeper than those of the other congeners ($p \leq 0.001$). The gradients of the -XR, -RZ and -XA congeners were not significantly different from each other ($p > 0.1$). The third group encompassed the gradients of the -XA and -XL congeners, as they were not significantly different from each other ($p > 0.05$). However, the gradients of the lines representing the -XL congeners were significantly different from those of the -XR and -RZ congeners ($p \leq 0.05$).

The result of these differing rates of decay was a change in the relative abundance of the microcystin congeners produced by *Microcystis* CYN06. As the microcystin content of the arginine-containing congeners decreased more quickly, the relative abundance of these microcystins decreased with time (Figure 7.3). As the microcystin content of the congeners containing no arginine residues decreased less quickly, the relative abundance of these congeners increased. This trend coincided with a decrease in the concentration of nitrate (Figure 7.2A). Graphs of the relative abundance for each individual microcystin congener are presented in Appendix K.1.

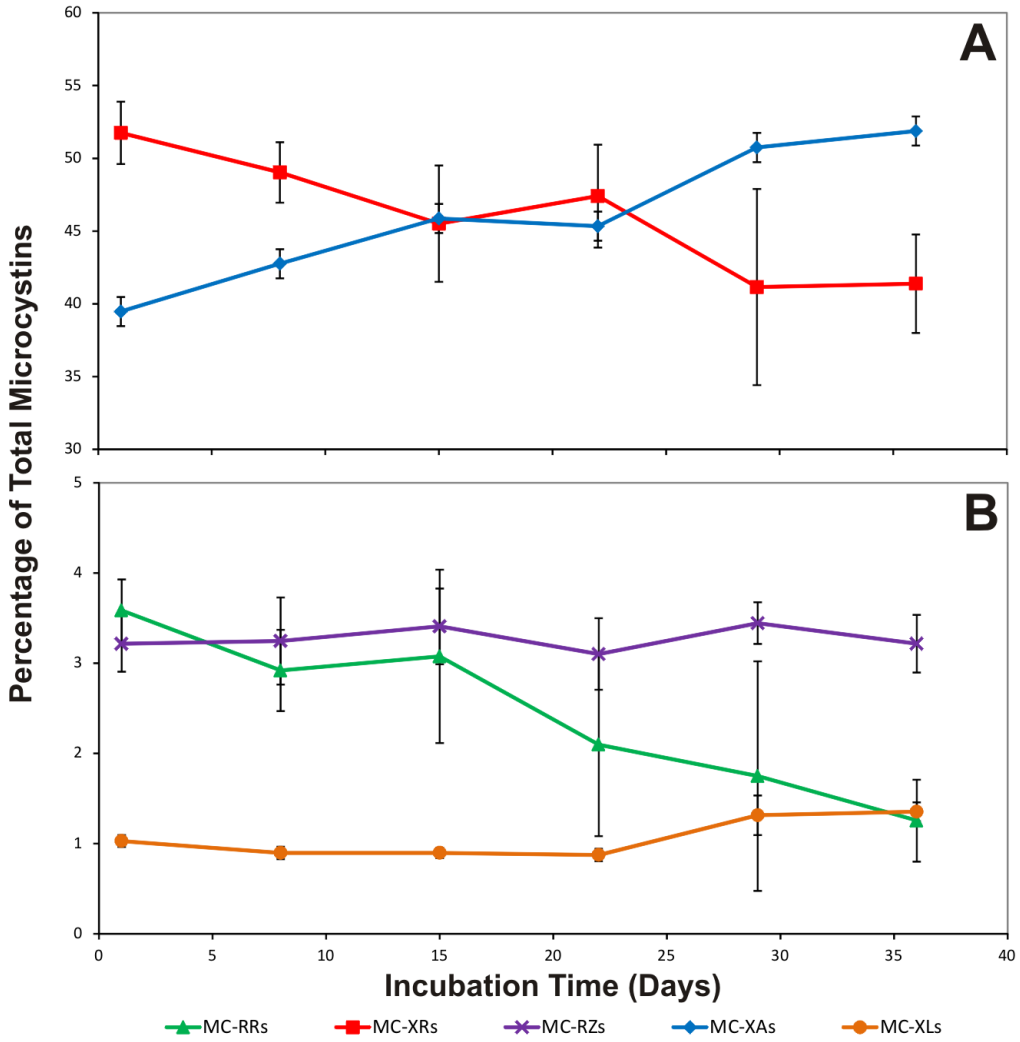

Figure 7.3: Microcystin congener abundance during a 40-day batch culture of *Microcystis* CYN06. Graphs depicting the grouped relative abundance of the -XR and -XA microcystin congeners **(A)** and the grouped relative abundance of the -RR, -RZ and -XL microcystin congeners **(B)**. Error bars indicate ±1 standard deviation; $n = 6$.

Over the 40-day incubation period, the abundance of MC-RR steadily decreased to less than one half of its initial value (from 3.6% to 1.5%; Figure 7.3B). Likewise, the -XR congeners (MC-LR, MC-FR and MC-WR) decreased in abundance from 51% to 41% (Figure 7.3A). In contrast, the -XA congeners (MC-LA, MC-FA and MC-WA) increased in abundance from 40% to 52%. The -XL congeners (MC-FL and MC-WL) showed a very slight increase in abundance from 1% to 1.4% (Figure 7.3B). The -RZ congeners (MC-RA and MC-RAba) did not change significantly ($p > 0.05$) during the 40-day incubation period.

Apart from the -RZ congeners, a statistically significant change in relative abundance was observed for each of the groups of microcystins between day 1 and day 36 (Figure 7.4). The -XA and -XR congeners displayed a significant change in abundance within 7 days (Day 8; $p \leq 0.05$). A significant decrease in MC-RR abundance was evident by day 22 ($p \leq 0.01$), whilst the -XL congeners did not show a significant increase in abundance until day 29 ($p > 0.05$). Correlation matrices for each group of congeners are presented in Appendix K.2.

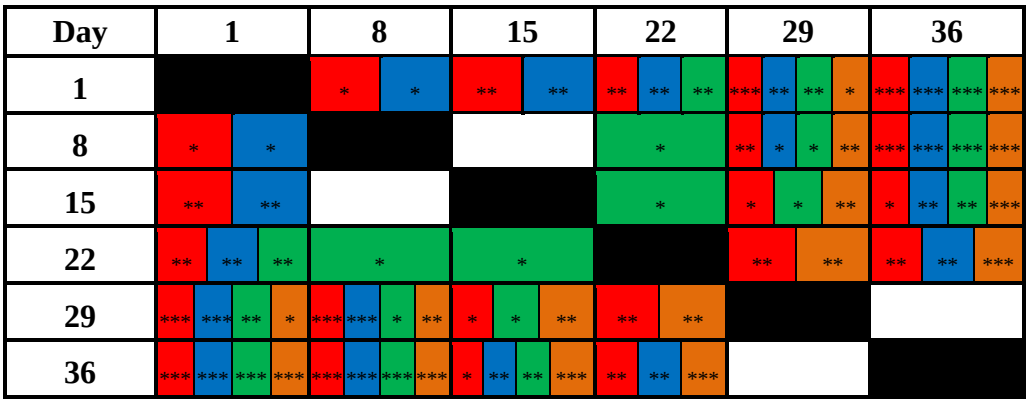

Figure 7.4: Correlation matrix indicating the statistically significant differences in the relative abundance of the grouped microcystin congeners. No shading indicates that there was no significant difference in microcystin abundance between those two sampling points ($p > 0.05$). Coloured shading indicates that a significant difference in microcystin abundance was observed between those two sampling points. The colour of the shading indicates the microcystin congeners where the significant difference was observed; Green = MC-RR, Red = MC-XRs, Blue = MC-XAs and Orange = MC-XLs. No significant differences were observed for the MC-RZs ($p > 0.05$). The level of significance observed is indicated by the number of asterisks; * $p \leq 0.05$, ** $p \leq 0.01$, *** $p \leq 0.001$.

Scatter-plots for $\log_{10}$ microcystin content against nitrate concentration (days 8-36; Figure 7.5A) revealed a linear relationship between the two parameters. However, for the low nitrate concentrations there was spread in the microcystin content which lowered the observed correlation coefficients. When $\log_{10}$ microcystin content of the time-points with nitrate concentrations less than

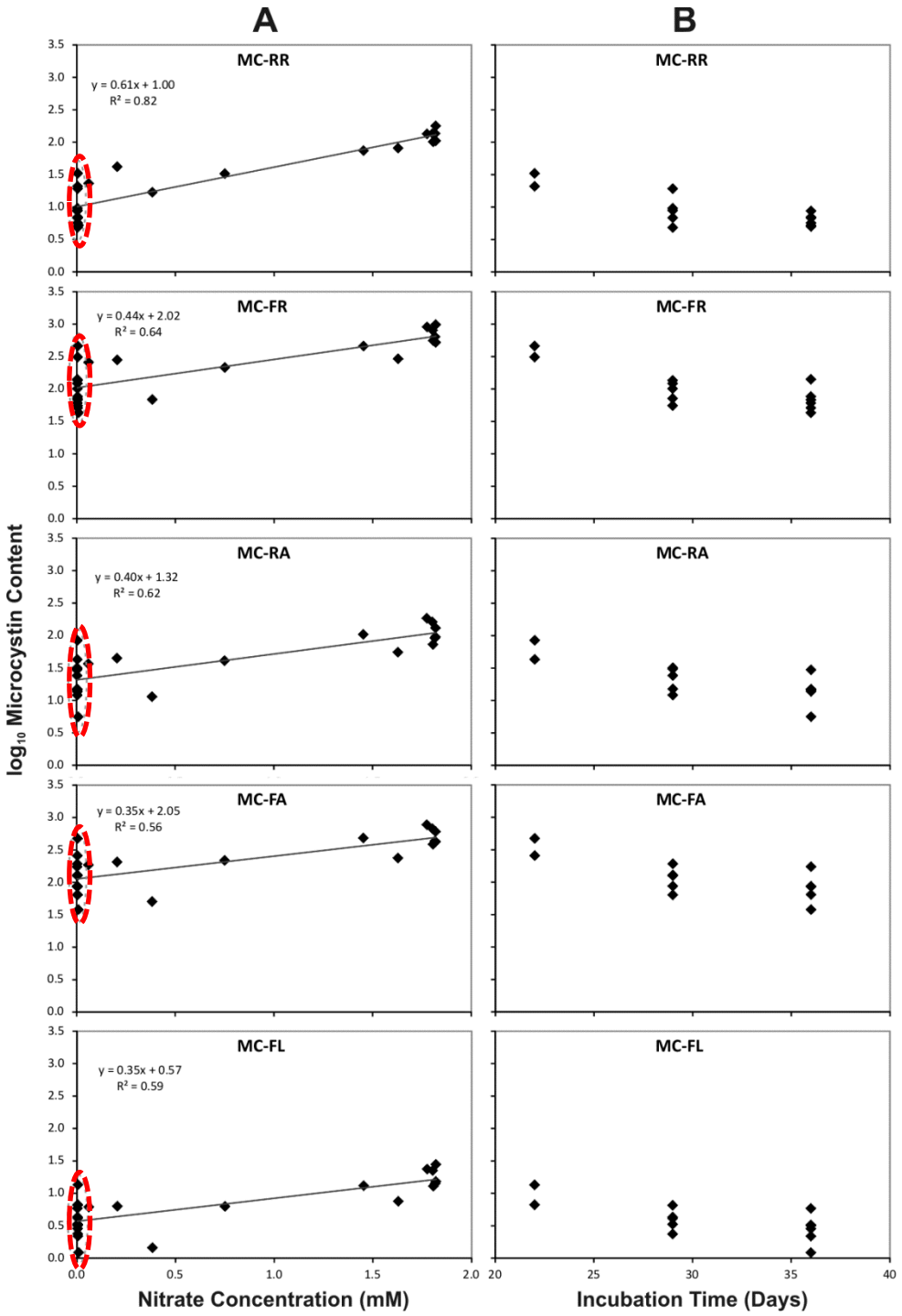

Figure 7.5: Scatter-plots depicting the relationship between $\log_{10}$ microcystin content and nitrate concentration **(A)**. The dashed circles in (A) indicate the time-points with low nitrate concentrations and these values were plotted against incubation time **(B)**.

0.005 mM was plotted against the incubation time, modulation of the microcystin content of the cells was still observed (Figure 7.5B). These changes may have been due to the utilisation of internal cell quotas of nitrogen, as nitrate concentrations in the media were negligible by this time. An attempt at modelling the internal nitrogen content was made, but due to a lack of data for the total nitrogen content, this has thus far proven unsuccessful. Scatter-plots for each individual congener can be found in Appendix K.3 and K.4.

Comparison of the gradients produced from linear regression of the relationship between $\log_{10}$ microcystin content and nitrate concentration revealed different slopes related to the number of arginine residues present in the microcystin (Table 7.2). The gradient for the nitrate dependence of MC-RR was steeper than that of the congeners containing a single arginine residue (MC-XRs and MC-RZs), which had a steeper gradient than the -XA and -XL congeners. Again, the slopes for the tryptophan-containing microcystin congeners were less than those of the leucine- and phenylalanine-containing counterparts.

Table 7.2: Linear regression of $\log_{10}$ microcystin content verses nitrate concentration for days 8-36.

Microcystin		Regression Equation	R^2	Average Gradient [a]
MC-RRs	MC-RR	$y = 0.610x + 1.00$	0.82	0.610 (A)
MC-XRs	MC-LR	$y = 0.455x + 2.05$	0.66	0.433 (B)
	MC-FR	$y = 0.436x + 2.02$	0.64	
	MC-WR	$y = 0.407x + 2.02$	0.70	
MC-RZs	MC-RA	$y = 0.398x + 1.32$	0.62	0.415 (B)
	MC-RAba	$y = 0.431x + 0.61$	0.72	
MC-XAs	MC-LA	$y = 0.434x + 2.00$	0.59	0.370 (B,C)
	MC-FA	$y = 0.350x + 2.05$	0.56	
	MC-WA	$y = 0.326x + 2.21$	0.58	
MC-XLs	MC-FL	$y = 0.355x + 0.57$	0.59	0.325 (C)
	MC-WL	$y = 0.295x + 0.73$	0.55	

[a] The letters in brackets indicate three groups that the gradients of the grouped congeners were divided into by a Student's t-test ($p < 0.05$).

Student's t-test was used to divide the congener gradients for nitrate dependence into three significantly different groups. The slope from MC-RR was again significantly higher than those of the other congeners ($p \leq 0.001$). The second

group consisted of the gradients from the -XR, -RZ and -XA congeners, which were not significantly different from each other ($p > 0.05$). The final group encompassed the gradients of the -XA and -XL congeners, as they were not significantly different from each other ($p > 0.05$). However, the gradients of the -XL congeners were significantly different from those of the -XR and -RZ congeners ($p \leq 0.05$).

Following the 40-day incubation of six replicate CYN06 batch cultures where nitrate was progressively depleted, triplicate cultures were supplemented with 1.5 mM nitrate and 0.1 mM phosphate, then monitored for a further 16 days. Triplicate control cultures received 0.1 mM phosphate but did not receive any nitrate. Two days post-supplementation, the cultures which had received 1.5 mM nitrate had regained their green colour whereas the cultures which did not receive nitrate remained a yellow colour. However, there was a large degree of variability between the individual cultures during this portion of the experiment and as a result, no significant changes in congener abundance were observed. The variability in congener abundance may have been related to differences in the level of nitrogen depletion between the replicates, which caused the individual cultures to react to the supplementary nitrogen at different rates.

7.3 DISCUSSION

Previous research has shown that microcystin production is regulated in response to environmental factors that influence cell growth.[129,144,292] Factors which yield increased cell growth, such as increased nutrient concentrations, result in increased microcystin concentrations. During the present experiment the total microcystin content of *Microcystis* CYN06 increased within the first seven days, before steadily decreasing. This response coincided with changes in the nitrate concentration of the medium, which was in accordance with previous research investigating microcystin production in relation to nitrogen supply.[134,136]

Microcystins are synthesised by a hybrid PKS/NRPS which incorporates amino acids into a cyclic peptide (see Section 1.3.1).[99-101] The amino acid arginine is nitrogen-rich compared to other amino acids; arginine contains four nitrogen atoms, tryptophan contains two nitrogen atoms, whilst phenylalanine, leucine,

alanine and 2-aminobutanoic acid contain only one nitrogen atom. During this experiment, the abundance of arginine-containing microcystins decreased as nitrate was depleted. This response might be expected as nitrogen-rich amino acids would be less abundant when cells become starved for nitrogen.

Linear regression of $\log_{10}$ microcystin content and nitrate (Table 7.2) revealed slopes which differed based on the number of arginine residues present in the microcystin. However, the correlation coefficients were reduced by a spread in microcystin contents at low nitrate concentrations. This bias was most likely due to the cells utilising internal nitrogen stores,[295] as cell replication still occurred despite no nitrate being detected in the filtered media, and the microcystin content continued to decrease in the pattern observed over the previous fourteen days.

The abundance of the microcystin congeners which contained a single arginine residue at position two (MC-RZs) did not change significantly throughout the nitrogen depletion period. During this same period, the abundance of MC-RR and the -XR congeners did show a significant decrease in abundance. As these congeners both contain a position four arginine, this observation suggests that there could be an element of selectivity in regards to which arginine in the structure is modulated.

Three studies have investigated the effects of nitrogen concentration on the abundance of microcystin congeners.[146,150,151] One of these studies used a chemostat culture set-up where media with 6 mM nitrate was provided to one set of cultures and media with 0.2 mM nitrate was provided to another set, however, no modulation in congener abundance was observed during the experiment.[150] As the cultures were continuously supplied with nitrogen, albeit at a lower level, it is unlikely that the cells were strongly depleted of nitrogen. The second study used a similar set-up but with different concentrations of nitrate, which yielded similar results.[151] The third study used a batch culture set-up with a starting nitrate concentration of 0.016 mM and observed no change in congener abundance.[146] As this study was conducted over a 36 hour period, it is unlikely that any modulation would be observed over such a short period. Furthermore, each of these experiments[146,150,151] utilised cyanobacterial strains which produced only -RR and -XR microcystin congeners. If selectivity between the position two and four

arginine occurred during these studies, then no modulation in congener abundance would be observed in a cyanobacterial strain that produces microcystins which only contain arginine at position four.

Whether the change in microcystin congener abundance observed during this experiment would cause a change in toxicity is hard to gauge as there is no toxicity data available for three of the major microcystin congeners present in *Microcystis* CYN06 (MC-LA, MC-FA and MC-WA). However, the seven-fold reduction in microcystin content observed with lower nitrate concentrations would have a definite effect on the toxicity of the strain.

Whilst the results from this study indicate nitrogen supply may play a role in regulating the abundance of arginine-containing microcystin congeners, a nitrogen supplementation experiment did not yield statistically significant results (data not shown). This was likely due to variability in level of depletion of nitrogen between the culture replicates. As a result, the microcystin congener abundance varied and the cultures reacted to the supplementary nitrogen at different rates. Future work in this area is required to confirm the causative factor of the changes in microcystin congener abundance observed.

7.4 CONCLUSIONS

Modulation of the abundance of microcystin congeners in response to nitrogen supply was investigated during a 40-day batch culture of *Microcystis* CYN06. A decrease in the abundance of the arginine-containing microcystin congeners coincided with a decrease in the concentration of nitrate. Linear regression of $\log_{10}$ microcystin content and nitrate revealed slopes which were dependent upon the number of arginine residues present in the microcystin congener. The abundance of the congeners which contained a single arginine at the position two did not change significantly throughout the experiment. However, the abundance of the congeners containing a position four arginine did vary, which suggests an element of selectivity to which arginine in the microcystin is modulated. This study is the first to correlate changes in microcystin congener abundance with nitrogen supply.

CHAPTER 8

Future Directions

During this study, several new microcystin congeners were purified in sufficient quantities to conduct toxicology examinations (MC-FA, MC-WA and MC-NfkA). However, the purity of the samples was not adequate to proceed and there was insufficient time to undertake further purification. The other new microcystins characterised were not present in sufficient quantities to undertake toxicology studies. Fractionation of more material could yield sufficient amounts of compound to determine the toxicity of these microcystins. Toxicity data for these congeners would be of great benefit to the microcystin research community and allow further interpretation of the results of the culturing experiment conducted in Chapter 7.

It was not possible to fully characterise the structures of the Antarctic microcystins and linear peptides with the small sample size available. Continued monitoring of the region where the original sample was collected could yield a larger sample or a cyanobacterial specimen which could be cultured. This would enable further purification of the microcystins and nuclear magnetic resonance spectroscopy could be used to confirm the presence of homoarginine, dehydrobutyrine and ADMAdda. Amino acid analysis could also be conducted to determine the stereochemistry of the arginine and homoarginine residues. With the Antarctic peptides, it would allow characterisation of the 168 Da N-terminus and confirmation of other amino acids, including deduction of their stereochemistry.

During this study, it was noted that tryptophan residues in microcystins could become oxidised. Further investigations into the rate of oxidation under different storage conditions would be very beneficial, as this has the potential to impact research where tryptophan-containing microcystins are being quantified.

The sample preparations designed for use during quantitative analysis of microcystins by matrix-assisted laser desorption/ionisation-time of flight mass spectrometry were tested using a simple mixture of microcystin standards. Further assessment of this sample preparation technique could be undertaken using complex cyanobacterial extracts and a standardised method for quantifying a sample could be developed.

The culturing experiment performed using CYN06 suggested that nitrogen supply was the main factor responsible for the modulation of microcystin congener abundance. An experiment to determine if nitrogen supply was the causative factor did not yield statistically significant results, as the replicate cultures reacted to supplementary nitrogen at different rates. Supplementing the cultures before complete nitrogen starvation might yield a more consistent result. Collecting additional samples to assess the quantity of intracellular nitrogen throughout the culturing experiment might also allow the relationship between microcystin content and nitrogen concentration to be more accurately modelled. Performing experiments utilising a chemostat culturing setup would allow the nitrogen concentration to be manipulated more easily. If modulation of microcystin congener abundance was also observed using a chemostat setup, it would demonstrate that previous research on the effect of nitrogen concentration on microcystin congener abundance[146,150,151] was due to the use of a cyanobacterial strain which only produced microcystins that contained a position four arginine. Toxicology data for MC-LA, MC-FA and/or MC-WA would allow for an estimation of the toxicity of CYN06 at different nitrate concentrations.

CHAPTER 9

Experimental

9.1 GENERAL EXPERIMENTAL

9.1.1 Materials

Deionised water (> 18 MΩ·cm resistivity) purified on an E-pure still (Barnstead) was used for all solutions. Ethanol (EtOH), methanol (MeOH) and dichloromethane (DCM) were drum-grade solvents which were distilled prior to use, unless otherwise stated. Unless stated, all other chemicals were analytical grade (Table 9.1).

Table 9.1: Chemicals used and their suppliers

Chemical	Source
Trifluoroacetic acid (TFA)	Acros Organics
[Dha^7] MC-LR standard	AgResearch Ruakura
Acetone; Anhydrous magnesium sulphate; Ammonia (28%; NH_3); Ammonium dihydrogen phosphate; Boric acid; Calcium chloride dehydrate; Copper (II) sulphate pentahydrate; Formic acid (88%; FA); HPLC-grade methanol; Hydrochloric acid (HCl); Hydrogen peroxide (30%); Magnessium sulphate heptahydrate; Manganese (II) chloride tetrahydrate; 2-Propanol (IPA); Potassium carbonate; Sodium bicarbonate; Sodium hydroxide	Ajax Chemicals
D-Leucinamide; L-Leucinamide	Bachem
L-Alanine (Ala); 2-Aminoisobutanoic acid (Aib); Ammonium chloride; L-Aspartic acid (Asp); 1,5-Difluoro-2,4-dinitrobenzene (FFDNB); L-Glutamic acid (Glu); Glycine (Gly); Iodine; Iron (III) chloride hexahysrate; L-Ornithine (Orn); Potassium iodide; Sodium nitrate	BDH Chemicals
α-Cyano-4-hydroxycinnamic acid (CHCA); Peptide calibration standard	Bruker Daltonics
2-Aminobutanoic acid (Aba); L-Arginine (Arg); L-Isoleucine (Ile); L-Leucine (Leu); L-Lysine (Lys); L-Phenylalanine (Phe)	Calbiochem
MC-LR standard; MC-RR standard; MC-YR standard	DHI Lab Products
Glacial acetic acid	Fisher Scientific
HPLC-grade acetonitrile (ACN)	Honeywell International
Cobalt (II) chloride hexahydrate; Sodium nitrite	Hopkins and Williams

Dipotassium phosphate; Sodium formate; Sodium molybdate dihydrate;	May and Baker
Ammonium acetate; Selenous acid	Riedel-de Haën
HPLC-grade ethanol; Sodium ethylenediaminetetraacetic acid (EDTA); Zinc sulphate heptahydrate	Scharlau
Angiotensin I; β-Mercaptoethanol; Biotin; Methanol-d_3 (CD_3OH); Methanol-d_4 (CD_3OD); Thiamine·HCl; Vitamin B_{12}	Sigma-Aldrich

9.1.2 Common Solutions

The compositions of the solutions commonly used during this study are listed in Table 9.2.

Table 9.2: Commonly used solutions.

Solution	Composition
10% Formic acid	11.4 mL of 88% formic acid (10%; v/v) - Make up to 100 mL with H_2O and filter (0.45 µm)
LC-MS Solvent A	10 mL of 10% formic acid (0.1%; v/v) 20 mL of HPLC-grade acetonitrile (2%; v/v) - Make up to 1 L with H_2O
LC-MS Solvent B	10 mL of 10% formic acid (0.1%; v/v) 10 mL of H_2O (2%; v/v) - Make up to 1 L with HPLC-grade acetonitrile
L-FDLA	10 mg L-FDLA (1%; w/v) - Dissolve in 1 mL acetone
DL-FDLA	10 mg of L-FDLA (1%; w/v) 10 mg of D-FDLA (1%; w/v) - Dissolve in 1 mL of acetone
MALDI matrix solution	500 µL of MeOH (50%; v/v) 250 µL of acetonitrile (25%; v/v) 250 µL of 0.1% (v/v) TFA (0.025%; v/v) - Discard after one week
MALDI wash solution	100 µL of 1% (v/v) TFA (0.1%; v/v) 900 µL of 11.1 mM $NH_4H_2PO_4$ (10 mM) - Store at 4 °C and discard after one month
Ammonium acetate stock	7.71 g of ammonium acetate (200 mM) - Make up to 500 mL with H_2O and filter (0.45 µm)
Ammonium acetate solution	50 mL of ammonium acetate stock (10 mM) - Make up to 1 L with H_2O
MLA^{296} vitamin stock	10 mg of thiamine·HCL (332 µM) 50 µL of 409 µM biotin (205 nM) 50 µL of 73 µM vitamin B_{12} (37 nM) - Make up to 100 mL with H_2O and store at 4 °C

MLA[296] micronutrient stock	4.36 g of $Na_2EDTA \cdot 2H_2O$ (11.7 mM) - Add 800 mL H_2O and stir over a low heat to dissolve 1.58 g of $FeCl_3 \cdot 6H_2O$ (5.8 mM) 0.60 g of $NaHCO_3$ (3.5 mM) 0.36 g of $MnCl_2 \cdot 4H_2O$ (1.8 mM) 10 mL of 4 mM $CuSO_4 \cdot 5H_2O$ (40 µM) 10 mL of 7.7 mM $ZnSO_4 \cdot 7H_2O$ (77 µM) 10 mL of 4.2 mM $CoCl_2 \cdot 6H_2O$ (42 µM) 10 mL of 2.5 mM $Na_2MoO_4 \cdot 2H_2O$ (25 µM) - Make up to 1 L with H_2O and store at 4 °C
40× MLA[296] stock	10 mL of 200 mM $MgSO_4 \cdot 7H_2O$ (8 mM) 20 mL of 1 M $NaNO_3$ (80 mM) 50 mL of 40 mM K_2HPO_4 (8 mM) 10 mL of 40 mM H_3BO_3 (1.6 mM) 10 mL of 10 µM H_2SeO_3 (400 nM) 10 mL of vitamin stock 10 mL of micronutrient stock - Make up to 250 mL with H_2O, filter sterilise (0.2 µm) and store at 4 °C
MLA[296] sodium bicarbonate stock	4.23 g of $NaHCO_3$ (200 mM) - Make up to 250 mL with H_2O, autoclave and store at 4 °C
MLA[296] calcium chloride stock	0.29 g of $CaCl_2 \cdot 2H_2O$ (200 mM) - Make up to 100 mL with H_2O, autoclave and store at 4 °C
MLA[296] culturing medium	25 mL of 40× MLA Stock 10 mL of sodium bicarbonate stock (2 mM) 1 mL of calcium chloride stock (200 µM) - Make up to 1 L with autoclaved H_2O and store at 4 °C
Lugol's solution	10 g of potassium iodide (602 mM) - Dissolve in 70 mL H_2O 5 g of iodine (394 mM) 10 mL of acetic acid (10%; v/v) - Make up to 100 mL with H_2O and store in the dark

9.1.3 Commonly Used Laboratory Techniques

Freeze-Drying

Lyophilisation of samples was conducted using a FreeZone6 freeze-drier (Labconco).

Centrifugation

Centrifugation was undertaken on one of three centrifuges; a Labnet Z150A centrifuge (samples greater than 1.5 mL), an Eppendorf MiniSpin Plus centrifuge (samples less than 1.5 mL) or an Eppendorf 5810 centrifuge (when temperature control was required).

Sonication

Samples and solvents were sonicated at ambient temperature in an ultrasonic bath (Aquawave, Barnstead International).

Microscopy

Microscopy was conducted using an inverted microscope (Olympus CK40).

Nutrient Analysis

Dissolved nutrient concentrations were determined by flow injection analysis (Lachat Quickchem FIA+ 8000; Zellweger Analytics). Stored nutrient samples were thawed and allowed to come to room temperature. The concentration of the total oxidised nitrogen species (NO_x) was determined by passing the sample through a copperised cadmium column to reduce nitrate to nitrite. This was performed using Lachat QuickChem Method 10-107-04-1-A (MDL = 5 µM). Nitrite concentrations were determined using Lachat QuickChem Method 10-107-05-1-A (MDL = 5 µM). As nitrite levels were below the detection limit, nitrate concentrations were determined directly from the NO_x measurements. Lachat QuickChem Method 10-107-06-2-L was used to determine ammonia concentrations (MDL = 5 µM). Dissolved reactive phosphorus concentrations were determined using Lachat QuickChem Method 10-115-01-1-A (MDL = 0.6 µM).

The concentration of each nutrient was determined by comparing the response from a sample with a standard curve constructed using KH_2PO_4, NH_4Cl and KNO_3 or $NaNO_2$ at known concentrations (0.16-32 µM for phosphorous and 7-140 µM for the nitrogen-containing standards). Quality control checks were conducted every fifteen samples using a mid range calibration standard.

9.1.4 Commonly Used Fractionation Techniques

All fractions were collected in conical flasks and concentrated under vacuum using a rotary evaporator (Büchi). Fractions were then transferred to a glass vial and dried at 35 °C under a stream of nitrogen. As microcystins are a harmful substance, precautions for personal protection were taken. Cultures were labelled as hazardous, gloves and safety galsses were worn and a facemask was used when floculant material was being handled.

Reversed-Phase C_{18} Chromatography

Reversed-phase column chromatography was conducted using C_{18} material (YMC-gel ODS-A, YMC). Samples were prepared for chromatography by dissolution in one part MeOH, which was diluted with six parts H_2O and lyophilised in a glass vial. The resulting solid was scraped into a powder with a stainless steel spatula before being loaded onto the top of the column. The sample vial was rinsed with DCM (0.5 mL) then MeOH (0.5 mL), and eluted using a stepped gradient under the pressure of nitrogen gas.

Size Exclusion Chromatography

Size exclusion column chromatography was conducted using LH-20 material (Sephadex LH-20, Pharmacia Fine Chemicals). The samples were dissolved in minimal MeOH, applied to the top of the column and eluted with MeOH.

Gradient High Performance Liquid Chromatography

Gradient high performance liquid chromatography (HPLC) was performed using two HPLC pumps (Waters 515) controlled by Empower Pro (Waters). Eluting compounds were detected by a photo-diode array detector (PDA; 200-400 nm; Waters 2996). Samples were dissolved in HPLC-grade MeOH (1.2 mL) and syringe filtered (0.2 µm). Repeated injections (100 µL) were fractionated on a C_{18} HPLC column (Luna C_{18}, 150 × 4.6 mm, 5-µ; Phenomenex) using the H_2O→ACN gradient (1 mL/min) specified in each section.

Isocratic High Performance Liquid Chromatography

Isocratic HPLC was performed using two HPLC pumps (Waters 515) set to deliver different volumes of solvent. Eluting compounds were detected by a PDA detector (200-400 nm; Waters 2996). Samples were dissolved in HPLC-grade MeOH (1.25 mL) and syringe filtered (0.2 µm). Repeated injections (100 µL) were fractionated on a C_{18} HPLC column (Econosil C_{18}, 250 × 10 mm, 10-µ; Alltech) using a mixture of ACN and 10 mM ammonium acetate (5 mL/min).

Solid-Phase C_{18} Cleanup

Solid-phase cleanup was performed using a glass Pasteur pipette lightly plugged with cotton wool and filled with C_{18} material (200 mg; YMC-gel ODS-A; YMC). The solid-phase cleanup column was primed with MeOH (2 × 0.6 mL) then

equilibrated with 15% MeOH (3 × 0.6 mL; v/v). Lyophilised samples were resuspended in MeOH (0.3 mL) and diluted with H_2O (1.8 mL). The sample was loaded onto the solid-phase cleanup column and allowed to flow through. The column was washed with 15% MeOH (5 × 0.6 mL; v/v) before the microcystin was eluted using 80% MeOH (3 × 0.6 mL; v/v).

9.1.5 Commonly Used Characterisation Techniques

Matrix-Assisted Laser Desorption/Ionisation-Time of Flight Mass Spectrometry

Samples were analysed using an AutoFlex II matrix-assisted laser desorption/ionisation-time of flight (MALDI-TOF) mass spectrometer (Bruker Daltonics) operated with FlexControl (Bruker Daltonics). Samples were prepared for MALDI-TOF analysis as described in each section. Mass calibration was performed using a peptide calibration standard which was prepared in the same manner as the samples. Spectra were acquired over various *m/z* ranges, with an acceleration voltage of 19 kV and a reflector voltage of 20 kV. Pulsed ion extraction of 60 ns was used to build up the concentration of ions in the ion source and ions below 500 *m/z* were suppressed to avoid detector saturation from matrix ions. Mono-isotopic peaks were manually annotated using FlexAnalysis (Bruker Daltonics).

Tandem mass spectrometry (MS/MS) data was acquired using the same instrument. Fragmentation was induced by post-source decay (PSD) or a combination of PSD and collision-induced dissociation (CID). Because of the "LIFT" capabilities of this particular MALDI-TOF mass spectrometer, the resulting fragment ions could be resolved in a single spectrum. The spectra were annotated in FlexAnalysis, where each spectrum was smoothed (Savitzky Golay algorithm) and the baseline subtracted (Median algorithm), before the mono-isotopic peaks were automatically selected (SNAP algorithm).

Liquid Chromatography-Mass Spectrometry

Samples were separated using an HPLC system (UltiMate 3000; Dionex) which was directly coupled to an electrospray ionisation (ESI)-ion trap mass spectrometer (AmaZon X; Bruker Daltonics). HyStar (Bruker Daltonics) was used to control the duel systems. Samples (20 µL) were separated on a C_{18} column (Ascentis Express C_{18}, 100 × 2.1 mm, 2.7-µ; Supleco Analytical) using the

$H_2O \rightarrow$ACN gradient outlined in Table 9.3 (200 µL/min; 40 °C). The *m/z* of the eluting compounds was assessed using a capillary voltage of 3.5 kV for negative ions and 4.5 kV for positive ions and a nebuliser pressure of 1.5 bar. Desolvation was accomplished with a nitrogen flow of 8 L/min at 225 °C.

Table 9.3: HPLC gradient for general LC-MS analysis. [a]

Time (min)	%A (98:2 H_2O/ACN + 0.1% Formic Acid)	%B (2:98 H_2O/ACN + 0.1% Formic Acid)
0	90	10
1	90	10
13	0	100
15	0	100
16	90	10
20	90	10

[a] Flow rate = 200 µL/min; Column temperature = 40 °C.

Tandem mass spectra were gathered using the protonated ion of a compound and CID to induce fragmentation of the parent ion (collision amplitude of 1.0). In some cases MS^3 spectra were acquired; where the parent ion was fragmented, one of the resulting fragment ions was isolated then fragmented, and the *m/z* of those fragment ions were recorded.

Chromatograms and spectra were annotated in DataAnalysis (Bruker Daltonics), where each chromatogram was smoothed (Gauss algorithm; 0.2 s; 1 cycle). Mass spectra were smoothed (Gauss algorithm; 0.2 *m/z*; 1 cycle) and the peaks were automatically selected (Apex algorithm).

High Resolution Mass Spectrometry

Semi-pure and purified compounds were analysed using an ESI-TOF mass spectrometer (MicrOTOF; Bruker Daltonics) operated with MicrOTOF Control (Bruker Daltonics). Samples were resuspended at a concentration of ≤ 0.1 mg/mL in HPLC-grade MeOH + 0.1% formic acid (v/v) and introduced into the mass spectrometer using a syringe pump (3 µL/min). Positive ions were assessed, using a capillary voltage of 4.5 kV and a nebuliser pressure of 0.5 bar. Desolvation was accomplished with a nitrogen flow of 4 L/min at 180 °C. The instrument was

calibrated before each sample was analysed using a solution of sodium formate (2 mM), the cluster ions of which spanned the mass range assessed.

Spectra were annotated in DataAnalysis, where each spectrum was smoothed (Gauss algorithm; 0.2 *m/z*; 1 cycle) and the peaks were automatically selected (Sum Peak algorithm). Molecular formulae were generated using the accurate mass obtained and the Generate Molecular Formula tool.

Amino Acid Analysis

Semi-pure and purified microcystins were subjected to amino acid analysis according to the Advanced Marfey's method.[202-205] 1-Fluoro-2,4-dinitrophenyl-5-leucine (FDLA) was synthesised according to the method of Marfey,[201] but using leucinamide instead of alaninamide. Both the D- and L- forms of the reagent were synthesised from the respective stereoisomers of leucinamide. The resulting product was characterised by visual appearance, melting point and ESI MS (yellow crystals; m.p.: 168-170 °C; *m/z* 315 $[M+H]^+$, 337 $[M+Na]^+$, 353 $[M+K]^+$, 270 $[M-NO_2+2H]^+$).[202]

Samples were dried at 35 °C under a stream of nitrogen in a glass reaction vial, resuspended in 6 N HCl (0.5 mL) and incubated at 110 °C for 16 h. The HCl was removed at 35 °C under a stream of nitrogen. Hydrolysates were resuspended in H_2O (105 µL) and aliquoted into two microcentrifuge tubes (50 µL each), to which 1 M $NaHCO_3$ (20 µL) and 1% L- or DL-FDLA (100 µL; w/v) were added. The tubes were vortexed and incubated at 40 °C for 1 h, before being quenched with 1 N HCl (20 µL). The derivatised hydrolysates were diluted with HPLC-grade MeOH (810 µL), centrifuged (14,000 rcf, 5 min) and the supernatant (950 µL) transferred to a septum-capped LC vial.

The resulting derivatives were analysed by LC-MS using the instrumentation described above. The derivatised sample (20 µL) was separated on a C_{18} column (Econosil C_{18}, 250 × 3.2 mm, 5-µ; Alltech) using the $H_2O \rightarrow$ACN gradient outlined in Table 9.4 (600 µL/min; 40 °C). Eluting derivatives were detected by ultraviolet (UV) absorption (250-500 nm) and ESI MS (*m/z* 300-1,100). Negative ions were assessed using a capillary voltage of 3.5 kV and a nebuliser pressure of

1.5 bar. Desolvation was accomplished with a nitrogen flow of 10 L/min at 220 °C.

Table 9.4: HPLC gradient for Advanced Marfey's amino acid analysis. [a]

Time (min)	%A (98:2 H_2O/ACN + 0.1% Formic Acid)	%B (2:98 H_2O/ACN + 0.1% Formic Acid)
0	75	25
1	75	25
31	35	65
33	0	100
35	0	100
38	75	25
45	75	25

[a] Flow rate = 600 µL/min; Column temperature = 40 °C.

The resulting chromatograms and spectra were annotated in DataAnalysis, where extracted ion chromatograms were generated and smoothed (Gauss algorithm; 0.643 s; 2 cycles).

β-mercaptoethanol Derivatisation

Standards, extracts and semi-pure mixtures of microcystins (1,420 µL) were mixed with 200 mM $NaHCO_3$ (pH 9.7; 360 µL) in a septum-capped vial and left to equilibrate to 30 °C.[41] Following an LC-MS injection (as described previously) β-mercaptoethanol (20 µL) was added and the tube inverted to mix. The reaction was maintained at 30 °C in the sample tray of the LC-MS and injections were performed periodically over an 8 h period when Mdha/Dha was suspected to be present and over a 90 h period when Dhb was suspected to be present.

400 MHz Nuclear Magnetic Resonance Spectroscopy

Nuclear magnetic resonance (NMR) spectra for **163** and **165** were recorded on a Bruker AVIII-400 NMR spectrometer. Chemical shifts were determined at 300 K and are reported relative to the solvent signal (CD_3OD; ^1H 3.31 ppm, ^{13}C 49.15 ppm). Standard pulse sequences were used for HSQC, HMBC, COSY, TOCSY and ROESY experiments. TOCSY experiments were conducted with mixing times optimised for the detection of short, medium and long range

couplings. HMBC spectra were acquired using parameter sets optimised for $^{2\text{-}3}J_{^{1}H\text{-}^{13}C}$ correlations.

600 MHz Nuclear Magnetic Resonance Spectroscopy

Nuclear magnetic resonance spectra for **175** were recorded by Dr. Chris Miles (Norwegian Veterinary Institute, Oslo, Norway) on a Bruker AVII-600 NMR spectrometer equipped with a TCI cryoprobe and Z-gradient coils. Chemical shifts were determined at 298 K and are reported relative to the solvent signal (CD_3OH; ^{1}H 3.31 ppm, ^{13}C 49.0 ppm). Spectra (^{1}H, HSQC, COSY, TOCSY, and ROESY) were obtained with continuous wave presaturation and/or excitation sculpturing of either or both of the residual O*H*/H_2O and C*H*D_2OH signals. TOCSY experiments were conducted with mixing times optimised for the detection of short, medium and long range couplings. HMBC spectra were acquired using parameter sets optimised for $^{2}J_{^{1}H\text{-}^{13}C}$ correlations.

Ultraviolet Absorption Spectrophotometry

The UV absorption of the purified microcystins was determined using an UV-visible spectrophotometer (Cary 100 Scan; Varian). Microcystins dissolved in HPLC-grade MeOH were assessed over a wavelength range of 200-800 nm.

Optical Rotation

Optical rotation of the purified microcystins was determined using a polarimeter (AUTOPOL IV; Rudolph Research Analytical). Microcystins were dissolved in HPLC-grade MeOH at concentrations of ≤ 0.6 mg/mL.

9.2 WORK DESCRIBED IN CHAPTER TWO

9.2.1 Sample Preparation

An environmental bloom sample containing several *Microcystis* species was collected from Lake Wiritoa (Manawatu, New Zealand; Voucher LW20403 is stored in the University of Waikato Chemistry Department). The sample was extracted in MeOH (100 µL) overnight. Extract (0.5 µL) was mixed 1:1 with a saturated solution of α-cyano-4-hydroxycinnamic acid (CHCA) dissolved in MALDI matrix solution (2:1:1 MeOH/ACN/0.1% TFA), directly on a 600 µm anchorchip (Bruker Daltonics). The dried spot was washed by pipetting MALDI

wash solution (5 µL; 0.1% TFA in 10 mM $NH_4H_2PO_4$) onto the spot for 5 s, then withdrawing the liquid.

9.2.2 MALDI-TOF Mass Spectrometry

The sample was analysed as described in Section 9.1.5. Positive ion MS spectra were acquired over a 600-2,000 *m/z* range by summing 500 shots. MS/MS data was acquired using the same sample preparation. Fragmentation was induced by PSD for structural characterisation and by a combination of PSD and CID for leucine/isoleucine determination.

9.3 WORK DESCRIBED IN CHAPTER THREE

9.3.1 Culturing of CYN06

The *Microcystis* species CYN06 (Micro-algae culture collection, Cawthron Institute, Nelson, New Zealand) was grown in 20 × 20 L plastic carboys, each containing 16 L of MLA[296] media. Cultures were grown at 18 °C under a 12:12 h light/dark cycle with a photon-flux of 100 $\mu Ein \cdot m^{-2} \cdot s^{-1}$. After 40 days, the cultures were harvested using plankton net (11 µm mesh diameter). The concentrated cell material was lyophilised and stored at −20 °C until extracted.

9.3.2 Extraction of CYN06 Material

Freeze-dried CYN06 (76.9 g) was extracted in 70% EtOH (5 × 800 mL; v/v). This involved; homogenisation of the cells in a Waring blender followed by vacuum filtration (#1 filter paper). The remaining cell pellet was then re-homogenised and filtered four more times. The resulting extract was gravity filtered, concentrated under vacuum, and dried at 35 °C under a stream of nitrogen to yield 5.6 g. In addition, the cell pellet which remained after the initial extraction was re-extracted in 100% MeOH (5 × 250 mL), in the same manner as the initial extraction. This yielded 0.45 g of extract. A voucher of the lyophilised material is retained in the University of Waikato Chemistry Department, Hamilton, New Zealand (24.5 mg; JP2-033-05).

9.3.3 Assessment of the Fraction Composition

The composition of the CYN06 fractions was assessed by LC-MS using the instrumentation and protocols outlined in Section 9.1.5. Fractions were

resuspended in HPLC-grade MeOH (500 µL), an aliquot (5 µL) was syringe filtered (0.2 µm) into a septum-capped LC vial. The filter and syringe were then washed with 50% HPLC-grade MeOH (995 µL; v/v). Negative ions were assessed over a 100-2,000 *m/z* range and the resulting ion-chromatograms were integrated using QuantAnalysis (Bruker Daltonics).

9.3.4 Isolation of the -XA Microcystins

The two CYN06 extracts (5.6 and 0.45 g) were individually separated on a reversed-phase C_{18} column (50 g), where the extract components were eluted with a steep stepped gradient from H_2O→MeOH→DCM. The fractions between 7:3 and 1:1 H_2O/MeOH contained the -XA microcystins.

The fractions which contained the -XA microcystins (331.8 mg) were combined and loaded onto a reversed-phase C_{18} column (20 g) which had been equilibrated with H_2O + 0.1% formic acid (FA; v/v). The sample components were eluted with increasing concentrations of H_2O + FA→MeOH + FA→MeOH→DCM. The fractions at 3:7 H_2O/MeOH + 0.1% FA (v/v) contained the -XA microcystins.

The fractions which contained the -XA microcystins (127.5 mg) were combined and dried. The sample was resuspended in MeOH, K_2CO_3 (40 mg) was added and the sample was left for 1 min. The solution was then transferred to a new vial and prepared for C_{18} chromatography. The sample was loaded onto a reversed-phase C_{18} column (20 g) and the sample components eluted with more refined increments of H_2O→MeOH. The fractions at 3:1 H_2O/MeOH contained the -XA microcystins.

The fractions which contained the -XA microcystins (34.2 mg) were combined, loaded onto a LH-20 column (35 g) and eluted with MeOH. MC-LA eluted after 90 mL of MeOH had passed through the column, MC-FA and several oxidised tryptophan congeners after 100 mL, and MC-WA after 110 mL. This yielded three mixtures with varying proportions of the different microcystins.

The three mixtures (4.9 mg, 6.7 mg and 10.2 mg) were individually prepared for and fractionated by isocratic HPLC using 27:73 ACN/10 mM ammonium acetate. The dried samples were lyophilised before the residual ammonium acetate was

removed by solid-phase cleanup. This yielded a mixture of MC-LA and the oxidised -XA tryptophan congeners (6 min), MC-FA (9 min), MC-WA (10 min) and a mixture of MC-FAba, MC-WAba with other contaminants (14-20 min).

MC-FA (**163**): White amorphous solid (2.3 mg, 2.99×10^{-3} %); $[\alpha]^{20}_{D}$ −173° (*c* 0.06 g/100 mL, MeOH); UV (MeOH) λ_{max} (log ε) 207 (4.20), 238 (4.13) nm; ^{1}H NMR data at 400 MHz, ^{13}C NMR data at 101 MHz (CD_3OD) see Table 3.3; HRESIMS *m/z* 966.4550 (calculated for $C_{49}H_{65}N_7O_{12}Na$, 966.4583, Δ −3.41 ppm).

MC-WA (**165**): White amorphous solid (0.8 mg, 1.04×10^{-3} %); $[\alpha]^{20}_{D}$ −40° (*c* 0.04 g/100 mL, MeOH); UV (MeOH) λ_{max} (log ε) 207 (4.19), 224 (4.25), 238 (4.13) nm; ^{1}H NMR data at 400 MHz, ^{13}C NMR data at 101 MHz (CD_3OD) see Table 3.5; HRESIMS *m/z* 1005.4650 (calculated for $C_{51}H_{66}N_8O_{12}Na$, 1005.4692, Δ −4.25 ppm).

9.3.5 Isolation of the -RZ Microcystins

The two CYN06 extracts (5.6 and 0.45 g) were individually separated on a reversed-phase C_{18} column (50 g), where the extract components were eluted with increasing concentrations of H_2O→MeOH→DCM. The fractions between 7:3 and 1:1 H_2O/MeOH contained the -RZ microcystins.

The fractions which contained the -RZ microcystins (130 mg) were combined and loaded onto a reversed-phase C_{18} column (20 g) which had been equilibrated with H_2O + 0.1% FA (v/v). The sample components were eluted with increasing concentrations of H_2O + FA→MeOH + FA→MeOH→DCM. The fractions at 7:13 H_2O/MeOH + 0.1% FA (v/v) contained the -RZ microcystins.

The fractions which contained the -RZ microcystins (36.2 mg) were combined, loaded onto a LH-20 column (35 g) and eluted with MeOH. The -RZ microcystins eluted after 95 mL of MeOH had passed through the column.

The sample (12.5 mg) was fractionated by isocratic HPLC using 13:37 ACN/10 mM ammonium acetate. The dried samples were lyophilised before the residual ammonium acetate was removed by solid-phase cleanup. This yielded MC-RA (12 min) and MC-RAba (20 min).

MC-RA (**16**): White amorphous solid (0.2 mg, 2.60×10^{-4} %); $[\alpha]^{20}_{D}$ −100° (*c* 0.02 g/100 mL, MeOH); UV (MeOH) λ_{max} (log ε) 205 (4.26), 238 (4.26) nm; HRESIMS *m/z* 953.5122 (calculated for $C_{46}H_{69}N_{10}O_{12}$, 953.5091, Δ +3.28 ppm).

MC-RAba (**19**): White amorphous solid (0.1 mg, 1.30×10^{-4} %); $[\alpha]^{20}_{D}$ −60° (*c* 0.013 g/100 mL, MeOH); UV (MeOH) λ_{max} (log ε) 207 (4.29), 238 (4.18) nm; HRESIMS *m/z* 967.5259 (calculated for $C_{47}H_{71}N_{10}O_{12}$, 967.5247, Δ +1.15 ppm).

9.3.6 LC-MS/MS Analysis of the CYN06 Microcystins

Analysis of the CYN06 microcystins by LC-MS/MS was undertaken with semi-pure fractions using the instrumentation and protocols outlined in Section 9.1.5.

9.3.7 MALDI-TOF MS/MS Analysis of the CYN06 Microcystins

Tandem MS spectra for the arginine-containing microcystins were obtained using semi-pure fractions and MALDI PSD. The sample was resuspended in MeOH (0.6 mL) and an aliquot (0.5 µL) was mixed 1:1 with a saturated solution of CHCA in MALDI matrix solution (2:1:1 MeOH/ACN/0.1% TFA), directly on a 600 µm anchorchip. The dried spot was washed by pipetting MALDI wash solution (5 µL; 0.1% TFA in 10 mM $NH_4H_2PO_4$) onto the spot for 5 s, then withdrawing the liquid. The sample was analysed using the instrumentation and protocols described in Section 9.1.5.

9.3.8 High Resolution Mass Spectrometry of the CYN06 Microcystins

Accurate masses for the CYN06 microcystins were determined with semi-pure fractions using the instrumentation and protocols described in Section 9.1.5.

9.3.9 Amino Acid Analysis of the CYN06 Microcystins

The identity and stereochemistry of the amino acids in several of the CYN06 microcystins were determined using the protocols described in Section 9.1.5 and purified samples of MC-FA, MC-WA, MC-RA and MC-RAba (100 µg each).

9.4 WORK DESCRIBED IN CHAPTER FOUR

The isolation of the oxidised tryptophan-containing microcystins from CYN06 utilised the same extract described in Section 9.3.2. The composition of the fractions was assessed by LC-MS as described in Section 9.3.3.

9.4.1 Isolation of the -XA Oxidised Tryptophan Congeners

Isolation of the -XA oxidised tryptophan congeners continued from the desalted 6 min isocratic HPLC fraction containing MC-LA and the oxidised tryptophan congeners (Section 9.3.4). The fraction (1.9 mg) was loaded onto a LH-20 column (35 g) and eluted with MeOH. MC-LA eluted after 90 mL of MeOH had passed through the column, MC-NfkA eluted after 100 mL, MC-OiaA after 105 mL, and MC-KynA after 110 mL. This yielded fractions with varying proportions of the different microcystins.

The fractions which contained a high proportion of MC-NfkA (1.5 mg) were combined and re-fractionated on a LH-20 column (35 g) three more times. This yielded a fraction which contained the MC-NfkA and MC-OiaA, but with low levels of MC-LA.

The fraction (0.6 mg) was fractionated by isocratic HPLC using 27:73 ACN/10 mM ammonium acetate. The residual ammonium acetate in the dried fractions was removed by solid-phase cleanup. This yielded MC-NfkA (5.8 min) and MC-OiaA (6.3-7.3 min).

MC-NfkA (**175**): White amorphous solid (0.4 mg, 5.20×10^{-4} %); ^{1}H NMR data at 600 MHz, ^{13}C NMR data at 151 MHz (CD_3OH) see Table 4.3; HRESIMS *m/z* 1037.4598 (calculated for $C_{51}H_{66}N_8O_{14}Na$, 1037.4591, Δ −0.75 ppm). UV data and optical rotation measurements for this compound remain to be determined.

9.4.2 Isolation of the -XR Oxidised Tryptophan Congeners

The two CYN06 extracts (5.6 and 0.45 g) were individually separated on a reversed-phase C_{18} column (50 g), where the extract components were eluted with increasing concentrations of $H_2O\rightarrow$MeOH$\rightarrow$DCM. The fractions between 7:3 and 1:1 H_2O/MeOH contained the -XR oxidised tryptophan microcystins.

The fractions which contained the -XR oxidised tryptophan microcystins (331.8 mg) were combined and loaded onto a reversed-phase C_{18} column (20 g) which had been equilibrated with H_2O + 0.1% FA (v/v). The sample components were eluted with increasing concentrations of H_2O + FA→MeOH + FA→MeOH →DCM. The fractions at 2:3 H_2O/MeOH + 0.1% FA (v/v) contained the -XR oxidised tryptophan microcystins.

The fractions which contained the -XR oxidised tryptophan microcystins (81.7 mg) were combined and dried. The sample was resuspended in MeOH, K_2CO_3 (40 mg) was added and the sample was left for 1 min. The solution was then transferred to a new vial and prepared for C_{18} chromatography. The sample was loaded onto a reversed-phase C_{18} column (20 g) and the sample components eluted with more refined increments of H_2O→MeOH. The fractions at 7:3 H_2O/MeOH contained the -XR oxidised tryptophan microcystins.

The fractions which contained the -XR oxidised tryptophan microcystins (9.8 mg) were combined, loaded onto a LH-20 column (35 g) and eluted with MeOH. The -XR oxidised tryptophan microcystins eluted with MC-LR after 95 mL of MeOH had passed through the column.

The sample (0.6 mg) was fractionated by isocratic HPLC using 1:3 ACN/10 mM ammonium acetate. Following lyophilisation, residual ammonium acetate was removed by solid-phase cleanup. This yielded MC-OiaR (7.2 min), a mixture of MC-LR and MC-NfkR (9 min), and MC-KynR (11.6 min).

9.4.3 LC-MS/MS Analysis of the Oxidised Tryptophan Microcystins

Analysis of the oxidised tryptophan microcystins by LC-MS/MS was undertaken with semi-pure fractions using the instrumentation and protocols outlined in Section 9.1.5.

9.4.4 MALDI-TOF MS/MS Analysis of the Oxidised Tryptophan Microcystins

Tandem MS spectra for the arginine-containing oxidised tryptophan microcystins were also obtained as described in Section 9.3.7 using semi-pure fractions.

9.4.5 High Resolution Mass Spectrometry of the Oxidised Tryptophan Microcystins

Accurate masses for the oxidised tryptophan microcystins were determined as described in Section 9.1.5 using semi-pure fractions.

9.4.7 Oxidation of Tryptophan-Containing Microcystins

A healthy culture of *Microcystis* CYN06 (150 mL) grown at 20 °C 12:12 h light/dark with no perturbation was harvested on nylon net (100 µm mesh). The concentrated cells were washed with MLA^{296} (3 × 50 mL; at ambient temperature) then sonicated (35 W, 30 min) in 70 % MeOH (25 mL; v/v; previously degassed by sonication). The resulting extract was filtered through nylon net (100 µm mesh) to remove large cellular debris. An aliquot (0.5 mL) was transferred to a microcentrifuge tube, diluted with H_2O (0.5 mL) and centrifuged (14,000 rcf, 5 min). The supernatant (0.9 mL) was transferred to a septum-capped LC vial and analysed by LC-MS according to the protocol laid out in Section 9.1.5. This process was completed in 50 min.

Three aliquots of the remaining CYN06 extract (7 mL each) were transferred to Falcon tubes and centrifuged (2,850 rcf, 10 min). The supernatant (5 mL) was transferred to a beaker, two of the aliquots were diluted with H_2O (5 mL each; degassed by sonication) or 10% hydrogen peroxide (5 mL; degassed by sonication). An aliquot (1 mL) was transferred to a microcentrifuge tube and centrifuged (14,000 rcf, 5 min). The supernatant (0.9 mL) was transferred to a septum-capped LC vial and analysed by LC-MS according to the protocol laid out in Section 9.1.5. As this process took ca. 10 min to complete, no zero time-point was recorded. Each of the extracts were shielded from light using tin foil, lightly covered and left at ambient temperature. One of the aliquots diluted with H_2O was stirred (250 rpm) whilst the other had no further treatment. The extract diluted with hydrogen peroxide was not stirred. Samples (1 mL) were removed at 1, 2, 6, 26, 52 and 124 h, prepared for and analysed by LC-MS as described above.

9.5 WORK DESCRIBED IN CHAPTER FIVE

9.5.1 Sample Collection

In December 2006, two hydro-terrestrial cyanobacterial mat samples were collected from Miers Valley in the McMurdo Dry Valleys, Antarctica. These samples were obtained from the moist areas in front of Adams Glacier (MVAG1; 78°6'36"S, 163°54'20"E; Figure 9.1) and Miers Glacier (MVMG1; 78°5'42"S, 163°55'38"E). Microbial mat material was collected with a stainless steel spatula (swabbed with EtOH between samples) and placed in sterile 50 mL Falcon tubes. Whilst in the field, samples were stored in the dark and below 0 °C, and at −80 °C in the laboratory until analysed. Vouchers of MVAG1 and MVMG1 are retained at the Cawthron Institute (Nelson, New Zealand).

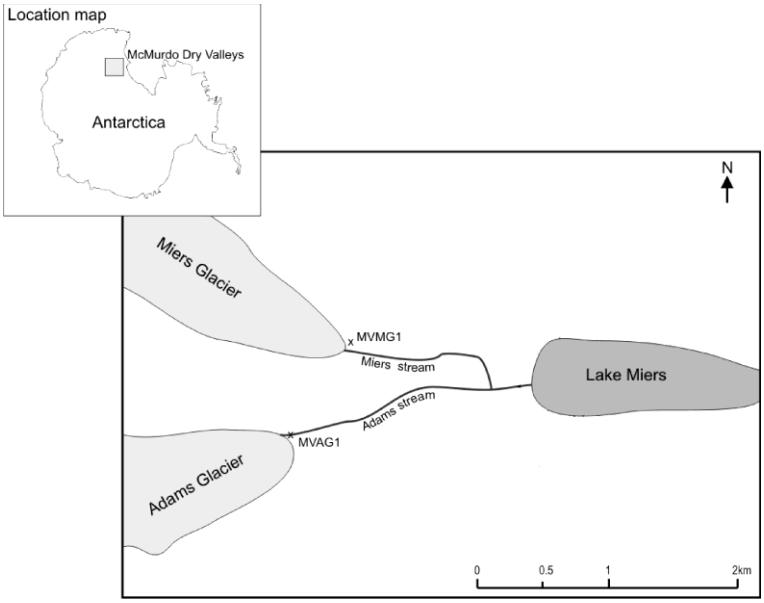

Figure 9.1: Location of the McMurdo Dry Valleys and sampling locations within Miers Valley.

9.5.2 Initial Mass Spectrometric Characterisation

The frozen samples were lyophilised and the freeze-dried material stored at −18 °C. Freeze-dried material (0.2 g) was placed in 50 mL Falcon tubes with 70% MeOH (15 mL; v/v) and sonicated for 60 min, vortexed and centrifuged (20,000 rcf, 10 min, 4 °C). After removing the supernatant, the extraction was repeated and the combined supernatants were dried at 35 °C under a flow of nitrogen. The dried extract was resuspended in 20% MeOH (2 mL; v/v) and filtered (0.45 µm).

The extract (0.5 µL) was mixed 1:1 with a saturated solution of CHCA in MALDI matrix solution (2:1:1 MeOH/ACN/0.1% TFA), directly on a 600 µm Anchorchip. The dried spot was washed by pipetting MALDI wash solution (5 µL; 0.1% TFA in 10 mM $NH_4H_2PO_4$) onto the spot for 5 s, then withdrawing the liquid. The sample was analysed as described in Section 9.1.5. Positive ion mass spectra were acquired over a 600-2,000 *m/z* range by accumulating 500 shots.

The Antarctic microcystins were analysed by LC-MS/MS at the Cawthron Institute (Nelson, New Zealand). The extract (10 µL) was separated by HPLC (Alliance 2695; Waters) using a C_{18} column (Luna C_{18}, 150 × 2 mm, 5-µ; Phenomenex) and the $H_2O \rightarrow$ACN gradient outlined in Table 9.5 (200 µL/min; 30 °C). At the end of the gradient the column was washed with 1:39 MeOH/IPA and re-equilibrated in the starting solvent. A Quattro Ultima TSQ triple-quadrupole mass spectrometer (Waters-Micromass) was operated using ESI in positive ion mode. Tandem mass spectra for the protonated ions were gathered for each microcystin using a collision energy of 52 eV.

Table 9.5: HPLC gradient for LC-MS/MS of the Antarctic microcystins. [a]

Time (min)	**%A (1:9 H_2O/ACN)**	**%B (9:1 H_2O/ACN)**	**%C (200 mM Formic Acid + 33 mM NH_3)**
0	77	18	5
7	35	60	5
9	0	95	5
18	0	95	5

[a] Flow rate = 200 µL/min; Column temperature = 30 °C.

The Antarctic linear peptides were analysed by LC-MS/MS at the University of Waikato. The extract was analysed using the instrumentation and protocols outlined in Section 9.1.5.

9.5.3 Extraction of the Antarctic Cyanobacterial Material

After all other analyses were completed on the MVAG1 and MVMG1 samples,[279] the remaining material was fractionated in order to undertake HRMS and amino acid analysis. MVAG1 (21 g) and MVMG1 (1 g) were extracted in 70% MeOH (5 × 300 mL; v/v). This involved disrupting the cells by sonication (35 W,

30 min), followed by vacuum filtration (#1 filter paper). The remaining cell material was then re-extracted and filtered four more times. The resulting extract was gravity filtered, concentrated under vacuum and dried at 35 °C under a flow of nitrogen to yield 51.2 mg of extract.

9.5.4 Assessment of the Fraction Composition

The composition of the Antarctic oligopeptide fractions was assessed by MALDI-TOF MS using a double dried-droplet sample preparation technique. Fractions were resuspended in MeOH (0.6 mL), loaded onto a 600 µm anchorchip (0.5 µL) and allowed to dry. The dried sample was resuspended, directly on the target, by pipetting up and down with a saturated solution of CHCA in MALDI matrix solution (0.5 µL; 2:1:1 MeOH/ACN/0.1% TFA). The resulting mixture was left on the target to dry at ambient temperature. The sample/matrix spot was washed by pipetting MALDI wash solution (5 µL; 0.1% TFA in 10 mM $NH_4H_2PO_4$) onto the spot for 5 s, then withdrawing the liquid. Samples were analysed using the instrumentation and protocols described in Section 9.1.5.

9.5.5 Isolation of the Antarctic Microcystins

The Antarctic mat extract (51.2 mg) was loaded onto a reversed-phase C_{18} column (20 g) and extract components eluted with increasing concentrations of H_2O→MeOH→DCM. The fractions between 3:7 and 1:9 H_2O/MeOH contained the Antarctic microcystins.

The fractions which contained the microcystins (4.1 mg) were combined and loaded onto a reversed-phase C_{18} column (20 g) and the extract components eluted with more refined increments of H_2O→MeOH. The -LR microcystin congeners eluted from the column with 1:1 H_2O/MeOH and the -RR congeners eluted from the column with 4:6 H_2O/MeOH.

The fractions containing the -RR congeners (1.2 mg) were combined and subjected to gradient HPLC using the H_2O→ACN gradient outlined in Table 9.6 (1 mL/min, ambient temperature). The -RR congeners eluted as a single peak at 17 min.

Table 9.6: HPLC gradient for fractionation of the -RR Antarctic microcystins.[a]

Time (min)	%A (H_2O + 0.05% TFA)	%B (ACN + 0.05% TFA)
0	90	10
4	90	10
20	45	55
22	0	100
24	0	100
26	90	10
30	90	10

[a] Flow rate = 1 mL/min; At ambient temperature.

The fractions containing the -LR congeners (2 mg) were combined and subjected to gradient HPLC using the H_2O→ACN gradient outlined in Table 9.7 (1 mL/min, ambient temperature). The -LR congeners eluted as a single peak at 16 min.

Table 9.7: HPLC gradient for fractionation of the -LR Antarctic microcystins.[a]

Time (min)	%A (H_2O + 0.05% TFA)	%B (ACN + 0.05% TFA)
0	90	10
4	90	10
7	70	30
20	40	60
22	0	100
24	0	100
26	90	10
30	90	10

[a] Flow rate = 1 mL/min; At ambient temperature.

9.5.6 Isolation of the Antarctic Linear Peptides

The Antarctic mat extract (51.2 mg) was loaded onto a reversed-phase C_{18} column (20 g) and extract components eluted with increasing concentrations of H_2O→MeOH→DCM. The fractions between 7:3 and 1:9 H_2O/MeOH contained the Antarctic linear peptides.

The fractions which contained the linear peptides (13.1 mg) were combined, loaded onto a LH-20 column (35 g) and eluted with MeOH. The linear peptides eluted after 80 mL of MeOH had passed through the column.

The fractions containing the linear peptides (7.3 mg) were combined and subjected to gradient HPLC using the $H_2O \rightarrow ACN$ gradient outlined in Table 9.8 (1 mL/min, ambient temperature). Peptide 816 eluted at 20.5 min, Peptides 800 and 830A eluted at 21.5 min, and Peptides 814, 830B and 844 eluted between 23-24 min.

Table 9.8: HPLC gradient for fractionation of the Antarctic linear peptides.[a]

Time (min)	**%A** (H_2O + 0.05% TFA)	**%B** (ACN + 0.05% TFA)
0	90	10
5	90	10
8	75	25
19	60	40
21	0	100
23	0	100
25	90	10
30	90	10

[a] Flow rate = 1 mL/min; At ambient temperature.

9.5.7 High Resolution Mass Spectrometry of the Antarctic Oligopeptides

Accurate masses for the Antarctic oligopeptides were determined with semi-pure fractions using the instrumentation and protocols described in Section 9.1.5.

9.5.8 Amino Acid Analysis of the Antarctic Microcystins

The identity and stereochemistry of the amino acids in the Antarctic microcystins were determined using the protocols described in Section 9.1.5 and a semi-pure mixture of the -LR and the -RR microcystin congeners (200 µg each).

9.6 WORK DESCRIBED IN CHAPTER SIX

9.6.1 Sample Preparation

Seven different sample preparations were utilised during this study. All preparations used CHCA as a matrix and either a 384-spot polished steel MALDI target (Bruker Daltonics) or a 600 µm anchorchip. Angiotensin I was utilised as an internal standard to enhance reproducibility and zinc sulfate heptahydrate was added to eliminate sodium and potassium adducts.[297] Microcystin (MC) standards ([Dha^7] MC-LR, MC-YR or MC-RR) were dissolved in 40% MeOH (v/v) and on

the day of the analyses were mixed 9:1 with 500 µM angiotensin I/50 mM Zn^{2+} (IS), to yield final concentrations of 50 µM and 5 mM, respectively. Coefficients of variation (CVs) were measured using 2.5 µM microcystin. Method detection limits (MDLs) were determined using 40% MeOH (v/v) as a blank and 0.1 µM microcystin. CVs and MDLs were conducted on three separate days; the average of these three results is reported.

The sonicated dried droplet preparation[184] used a saturated solution of CHCA in EtOH/ACN/H_2O (15:9:1), mixed 1:1 with the MC/IS solution and sonicated (35 W, 5 min). This MC/IS/CHCA solution (1 µL) was deposited onto either a polished steel or an anchorchip target, and allowed to dry at ambient temperature. The dried droplet preparation used CHCA saturated in EtOH/ACN/H_2O (15:9:1; 0.5 µL) mixed with the MC/IS solution (0.5 µL) directly on a polished steel or an anchorchip target. These preparations were allowed to dry at ambient temperature.

The three thin-layer preparations were produced using a saturated solution of CHCA in acetone. The anchorchip thin-layer preparation was prepared by dragging a drop of matrix solution (5 µL) over the hydrophilic spots on the target using an auto-pipette tip and allowing the acetone to evaporate. MC/IS solution (0.5 µL) was then applied on top of the matrix crystals and allowed to dry at ambient temperature.

The polished steel thin-layer-line preparation was made by dragging an auto-pipette tip containing matrix solution (5 µL) along the length of the target and allowing the acetone to evaporate. MC/IS solution (0.5 µL) was then applied to the centre of this line of matrix crystals and allowed to dry at ambient temperature. The polished steel thin-layer-spot preparation was prepared by depositing a drop of matrix solution (0.2 µL) onto the centre of each sample spot and allowing the acetone to evaporate. MC/IS solution (0.5 µL) was then applied to the centre of the spot of matrix crystals and allowed to dry at ambient temperature. Prior to each use, the polished steel target was cleaned with a free-rinsing detergent, washed with water, sonicated in 50% MeOH (v/v), rinsed with water and dried with acetone.

All seven sample preparation techniques were assessed for CV and MDL using only [Dha^7] MC-LR. The thin-layer-spot preparation performed on polished steel was also assessed for CV and MDL using MC-RR and MC-YR.

Standard curves for [Dha^7] MC-LR, MC-RR and MC-YR were constructed individually using 0.1-10 µM solutions diluted in 40% MeOH (v/v). These solutions were mixed 9:1 with IS to yield a final concentration of 50 µM angiotensin I and 5 mM Zn^{2+}. This MC/IS solution (0.5 µL) was applied in quadruplicate to a thin-layer-spot preparation performed on polished steel and allowed to dry at ambient temperature. Each standard curve was constructed using the average of these four analyses.

The laser power attenuation and varied volume experiments were both conducted using a 2.5 µM [Dha^7] MC-LR solution which was mixed 9:1 with IS on the day of the analyses. The laser attenuation experiment used 0.5 µL of MC/IS solution on a thin-layer-spot preparation performed on polished steel.

9.6.2 MALDI-TOF Mass Spectrometry

Analyses were performed on the instrumentation described in Section 9.1.5. Spectra were obtained in positive ion reflectron mode with matrix suppression set at 400 Da and pulsed ion extraction of 90 ns. Spectra were accumulated from ten separate 25-shot acquisitions at different locations on each sample spot (250 shots total). Values expressed in this study were based on the $[M+H]^+$ monoisotopic peak and did not include any adduct peaks. Only the peak height was utilised in accordance with the findings of previous studies.[297,298] The peak height ratio (PHR) was found by dividing the microcystin signal by that of the internal standard.

9.6.3 Statistical Treatments

The MDL was determined by analysing seven replicates of the blank (x_0) and a sample (x_s) near the estimated detection limit (0.1 µM).[184] The following equation was then used:

$$\text{MDL} = \frac{(3.14 \times s - b)}{m}$$

where *s* is the standard deviation of the x_s replicates, *b* and *m* are the intercept and the slope of a regression in the region of x_0 to x_s, and 3.14 is the one-tailed t-test value at the 99% confidence level. The limit of quantitation (LOQ) was calculated using a multiplier of 10 instead of 3.14.

9.7 WORK DESCRIBED IN CHAPTER SEVEN

9.7.1 Culture and Sampling Conditions

Six autoclaved 1 L Schott bottles containing MLA medium[296] (800 mL) were inoculated with *Microcystis* CYN06 (4 mL at 8×10^6 cells/mL). Cultures were grown at 20 °C with a photon-flux of 54 $\mu Ein\cdot m^{-2}\cdot s^{-1}$ (12:12 h light/dark) whilst being continuously aerated with sterile filtered air (300 mL/min).

Each culture was grown for 36 days and sampled once a week, 2 h after the light phase had begun. The pH was measured using litmus paper. A sample for nutrient analysis (15 mL) was filtered (0.45 µm) and stored at −20 °C. A sample for cell enumeration (1 to 5 mL) was preserved immediately with Lugol's solution (20 µL) and stored in the dark. A sample for microcystin analysis (5 mL) was taken and concentrated as follows. The sample was pressurised in a blocked syringe to break gas vesicles in the cells and allow them to be pelleted by centrifugation (2,850 rcf, 15 min). The supernatent was removed and the pellet transferred to a microcentrifuge tube and centrifuged (14,000 rcf, 5 min). The remaining supernatant was removed before the sample was lyophilised and stored at −20 °C until extracted for microcystin analysis.

On day 40, the cultures were sampled for nutrient analysis and supplemented with additional nutrients. At this point, 550 mL of culture remained. Additional phosphorous (0.1 mM; 137.5 µL of 400 mM K_2HPO_4) was added to each culture. Additional nitrate (≈ 2 mM; 275 µL of 2 M $NaNO_3$) was added to three randomly selected cultures, however, the subsequent nutrient analysis showed this to only be 1.5 mM of additional nitrate. Water (275 µL) was added to the remaining three cultures (negative control). Samples for nutrient analysis, cell enumeration and microcystin analysis were acquired immediately following the manipulation. For the following 16 days, samples for cell enumeration and microcystin analysis

were taken every second day and a sample for nutrient analysis was taken every fourth day.

9.7.2 LC-MS/MS Quantitation of Microcystins in CYN06

The lyophilised cells were sonicated (35 W, 30 min) in HPLC-grade MeOH (0.3-0.7 mL) and clarified by centrifugation (14,000 rcf, 5 min). The supernatant (180 µL) was then diluted 1:9 in 50% HPLC-grade MeOH (1,620 µL; v/v) directly in a septum-capped LC vial.

The microcystin concentration of the resulting extracts was determined by LC-MS/MS using the instrumentation described in Section 9.1.5. The extract (20 µL) was separated on a C_{18} column (Ascentis Express C_{18}, 100 × 2.1 mm, 2.7-µ; Supleco Analytical) using the $H_2O \rightarrow ACN$ gradient outlined in Table 9.9 (200 µL/min, 40 °C).

Table 9.9: HPLC gradient for microcystin quantitation by LC-MS/MS. [a]

Time (min)	%A (98:2 H_2O/ACN + 0.1% Formic Acid)	%B (2:98 H_2O/ACN + 0.1% Formic Acid)
0	80	20
1	80	20
2	70	30
12	40	60
13	0	100
15	0	100
16	80	20
20	80	20

[a] Flow rate = 200 µL/min; Column temperature = 40 °C.

Microcystins were detected by negative ion ESI MS, using a capillary voltage of 3.5 kV and a nebuliser pressure of 3.0 bar. Desolvation was accomplished with a nitrogen flow of 8 L/min at 250 °C. The parent ions were fragmented by CID using helium as the collision gas and a collision amplitude of 0.85.

Microcystis CYN06 produces at least 27 different microcystin congeners, however many of these are produced at very low levels. Only those microcystins produced at moderate to high levels (MC-RR, MC-YR, [Asp^3] MC-LR, MC-LR,

MC-FR, MC-WR, MC-RA, MC-RAba, MC-LA, MC-FA, MC-WA, MC-FL and MC-WL) were assessed in the current study.

A multiple reaction monitoring (MRM) method was used to determine the abundance of each of the microcystin congeners. The $[M-H]^-$ ion was collected, fragmented by CID and the resulting $[M-H_2O-H]^-$ ion was used to determine the quantity of microcystin present in the sample. To increase the scan rate, the MRM method was split into eight segments corresponding to the retention time of the microcystin congener being monitored and a maximum of two ions were assessed at any given time. The ions acquired in each segment of the MRM method are listed in Table 9.10.

Table 9.10: Multiple reaction monitoring method for microcystin quantification by LC-MS/MS.

Time (min)	Microcystin	$[M-H]^-$	$[M-H_2O-H]^-$
0.00-5.50	MC-RR	1036.5	1018.5
5.50-6.00	MC-YR	1022.5	1004.5
6.00-6.45	[Asp^3] MC-LR	979.5	961.5
	MC-LR	993.5	975.5
6.45-7.00	MC-FR	1027.5	1009.5
	MC-WR	1068.5	1048.5
7.00-9.50	MC-RA	951.5	933.5
	MC-RAba	965.5	947.5
9.50-10.25	MC-LA	908.5	890.5
	MC-FA	942.5	924.5
10.25-12.00	MC-FA	942.5	924.5
	MC-WA	981.5	963.5
12.00-20.00	MC-FL	984.5	966.5
	MC-WL	1023.5	1005.5

The concentration of microcystin present was determined by comparing the abundance of the $[M-H_2O-H]^-$ ion with a standard curve constructed using a mixture of three microcystin standards (MC-LR, 0.5-1,000 nM; MC-RR and MC-YR, 0.25-500 nM). For those microcystin congeners not present in the standard, the concentration was calculated in comparison with the MC-LR standard curve. Quality control checks were conducted every eighteen injections using calibration standards (1 or 10 nM).

9.7.3 Cell Enumeration

Microcystis colonies were disrupted using a Potter-Elvehjem mortar and pestle. Cell concentrations were determined using a Whipple grid and an Utermöhl settling chamber.[299]

9.7.4 Dissolved Nutrient Analysis

Samples of filtered medium were analysed for dissolved nutrient concentrations (nitrite, total oxidised nitrogen species, ammonia and dissolved reactive phosphorus). Assessment of the samples collected on days 1, 36 and 56 indicated that ammonia concentrations were below the detection limit, therefore the other samples were not analysed for ammonia concentration.

9.7.5 Statistical Treatments

All statistical analyses were performed using Minitab 15, where p-values ≤ 0.05 were considered significant.

Data Transformation

Two variables were assessed during the experiment (intracellular microcystin content and microcystin congener abundance). Intracellular microcystin content was determined by dividing the microcystin concentration (MC/mL) by the cell concentration (cells/mL). Microcystin congener abundance was expressed as the percentage of the concentration of an individual microcystin congener compared to the total microcystin concentration. At times, the grouped microcystin congener abundance was utilised, which was the sum of the abundance for each individual congener present in the group.

Regression Analysis

Relationships between the intracellular microcystin content and incubation time or between intracellular microcystin content and nitrate concentration were determined using linear regression analysis. Linear regression of the data for each culture replicate was used to produce gradients which were compared for statistically significant differences.

Analysis of Variance

One-way analysis of variance (ANOVA) was used to determine if there were significant differences within a dataset. When a significant difference was detected, multiple Student's t-tests were used to determine where the significant difference lay.

Student's t-test

Multiple two-sample Student's t-tests were used to determine *p*-values for the differences observed between the gradients produced from linear regression and for each grouped microcystin congener abundance over time. These *p*-values were collated in correlation matrices (Appendix K.2, K.5 and K.6) and used to determine where significant differences between the two parameters were located.

Appendix A: Structures, molecular masses and bioactivity data for the known microcystins.

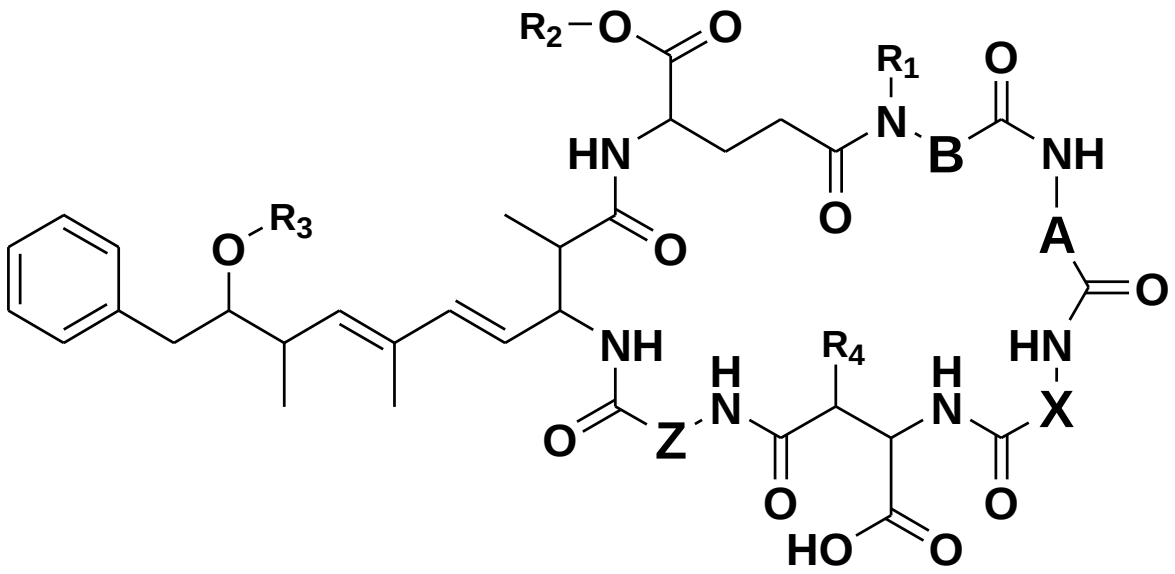

Microcystin	M_r [a] (Da)	X	Z	A	B	R_1	R_2	R_3	R_4	PPIA [b] (IC_{50}; nM)	Toxicity [c] (LD_{50}; µg/kg)	Ref. [d]
[Asp^3] MC-LA (**8**)	895.5	Leu	Ala	Ala	Dha	CH_3	H	CH_3	H			34
MC-LA (**9**)	909.5	Leu	Ala	Ala	Dha	CH_3	H	CH_3	CH_3			32
[Asp^3, Glu(OMe)^6] MC-LAba (**10**)	923.5	Leu	Aba	Ala	Dha	CH_3	CH_3	CH_3	H			35
MC-LAba (**11**)	923.5	Leu	Aba	Ala	Dha	CH_3	H	CH_3	CH_3			36,249
[Asp^3] MC-FA (**162**)	929.5	Phe	Ala	Ala	Dha	CH_3	H	CH_3	H			This Study
MC-LV (**12**)	937.5	Leu	Val	Ala	Dha	CH_3	H	CH_3	CH_3			37
[Asp^3] MC-LL (**13**)	937.5	Leu	Leu	Ala	Dha	CH_3	H	CH_3	H			34

[Asp^3] MC-RA (160)	938.5	Arg	Ala	Ala	Dha	CH_3	H	CH_3	H		This Study
MC-FA (163)	943.5	Phe	Ala	Ala	Dha	CH_3	H	CH_3	CH_3		This Study
MC-LL (**14**)	951.5	Leu	Leu	Ala	Dha	CH_3	H	CH_3	CH_3		37
MC-AR (**15**)	952.5	Ala	Arg	Ala	Dha	CH_3	H	CH_3	CH_3	250	38
MC-RA (**16**)	952.5	Arg	Ala	Ala	Dha	CH_3	H	CH_3	CH_3		39
[Asp^3] MC-RAba (161)	952.5	Arg	Aba	Ala	Dha	CH_3	H	CH_3	H		This Study
MC-FAba (166)	957.5	Phe	Aba	Ala	Dha	CH_3	H	CH_3	CH_3		This Study
MC-YA (**17**)	959.5	Tyr	Ala	Ala	Dha	CH_3	H	CH_3	CH_3		31
MC-AHar (**18**)	966.5	Ala	Har	Ala	Dha	CH_3	H	CH_3	CH_3		40
MC-RAba (**19**)	966.5	Arg	Aba	Ala	Dha	CH_3	H	CH_3	CH_3		41
[Gly^1, Asp^3, Dhb^7] MC-LR (179)	966.5	Leu	Arg	Gly	Dha	CH_3	H	CH_3	H		This Study
[Asp^3, Dha^7] MC-LR (**20**)	966.5	Leu	Arg	Ala	Dha	H	H	CH_3	H		42
[Asp^3] MC-WA (164)	968.5	Trp	Ala	Ala	Dha	CH_3	H	CH_3	H		This Study
[Asp^3, Dha^7] MC-EE(OMe) (**21**)	969.4	Glu	Glu(OMe)	Ala	Dha	H	H	CH_3	H		43
MC-LM (**22**)	969.5	Leu	Met	Ala	Dha	CH_3	H	CH_3	CH_3		37
[Asp^3] MC-LF (**23**)	971.5	Leu	Phe	Ala	Dha	CH_3	H	CH_3	H		44
MC-VF (**24**)	971.5	Val	Phe	Ala	Dha	CH_3	H	CH_3	CH_3		45
[Asp^3, Dha^7] MC-LY (**25**)	973.5	Leu	Tyr	Ala	Dha	H	H	CH_3	H		41
MC-YAba (**26**)	974.5	Tyr	Aba	Ala	Dha	CH_3	H	CH_3	CH_3		41
MC-VR (**27**)	980.5	Val	Arg	Ala	Dha	CH_3	H	CH_3	CH_3		46
MC-RV (**28**)	980.5	Arg	Val	Ala	Dha	CH_3	H	CH_3	CH_3		41

Microcystin	M_r [a] (Da)	X	Z	A	B	R_1	R_2	R_3	R_4	PPIA [b] (IC_{50}; nM)	Toxicity [c] (LD_{50}; µg/kg)	Ref. [d]
MC-RApa (**29**)	980.5	Arg	Apa	Ala	Dha	CH_3	H	CH_3	CH_3			41
[Gly[1], Asp[3], Dhb[7]] MC-LHar (**180**)	980.5	Leu	Har	Gly	Dha	CH_3	H	CH_3	H			This Study
[Asp[3]] MC-LR (**30**)	980.5	Leu	Arg	Ala	Dha	CH_3	H	CH_3	H		160-300	47,74
[Asp[3], Dhb[7]] MC-LR (**31**)	980.5	Leu	Arg	Ala	Dhb	H	H	CH_3	H		70	48,61
[DMAdda[5]] MC-LR (**32**)	980.5	Leu	Arg	Ala	Dha	CH_3	H	H	CH_3	1.5	90-100	38,82
[Dha[7]] MC-LR (**33**)	980.5	Leu	Arg	Ala	Dha	H	H	CH_3	CH_3	5	250	38,42,82
MC-AW (**34**)	982.5	Ala	Trp	Ala	Dha	CH_3	H	CH_3	CH_3			49
MC-WA (**165**)	982.5	Trp	Ala	Ala	Dha	CH_3	H	CH_3	CH_3			This Study
[Dha[7]] MC-EE(OMe) (**35**)	983.4	Glu	Glu(OMe)	Ala	Dha	H	H	CH_3	CH_3			43
[Asp[3], Dha[7]] MC-E(OMe)E(OMe) (**36**)	983.4	Glu(OMe)	Glu(OMe)	Ala	Dha	H	H	CH_3	H			43
MC-LF (**37**)	985.5	Leu	Phe	Ala	Dha	CH_3	H	CH_3	CH_3			37
MC-FL (**168**)	985.5	Phe	Leu	Ala	Dha	CH_3	H	CH_3	CH_3			This Study
[Asp[3]] MC-LY (**38**)	987.5	Leu	Tyr	Ala	Dha	CH_3	H	CH_3	H			41
[Gly[1], Asp[3], ADMAdda[5], Dhb[7]] MC-LR (**181**)	994.5	Leu	Arg	Gly	Dha	CH_3	H	$COCH_3$	H			This Study
[Asp[3], Dhb[7]] MC-HilR (**39**)	994.5	Hil	Arg	Ala	Dhb	H	H	CH_3	H			50
[Asp[3], Glu(OMe)[6]] MC-LR (**40**)	994.5	Leu	Arg	Ala	Dha	CH_3	CH_3	CH_3	H			51
MC-LR (**7**)	994.5	Leu	Arg	Ala	Dha	CH_3	H	CH_3	CH_3	0.3	50	31,82,115
MC-RL (**41**)	994.5	Arg	Leu	Ala	Dha	CH_3	H	CH_3	CH_3			41
[(6*Z*)Adda[5]] MC-LR (**42**)	994.5	Leu	Arg	Ala	Dha	CH_3	H	CH_3	CH_3		> 1,200	52,82,121

MC-WAba (167)	996.5	Trp	Aba	Ala	Dha	CH_3	H	CH_3	CH_3			This Study
[Dha^7] MC-E(OMe)E(OMe) (**43**)	997.5	Glu(OMe)	Glu(OMe)	Ala	Dha	H	H	CH_3	CH_3			43
[Ser^7] MC-LR (**44**)	998.5	Leu	Arg	Ala	Ser	H	H	CH_3	CH_3			53
[Asp^3] MC-HilY (**45**)	1001.5	Hil	Tyr	Ala	Dha	CH_3	H	CH_3	H			41
[Asp^3, Ser^7] MC-E(OMe)E(OMe) (**46**)	1001.5	Glu(OMe)	Glu(OMe)	Ala	Ser	H	H	CH_3	H			43
[Ser^7] MC-EE(OMe) (**47**)	1001.5	Glu	Glu(OMe)	Ala	Ser	H	H	CH_3	CH_3			43
MC-LY (**48**)	1001.5	Leu	Tyr	Ala	Dha	CH_3	H	CH_3	CH_3			45
MC-YL (**49**)	1001.5	Tyr	Leu	Ala	Dha	CH_3	H	CH_3	CH_3			35
[Asp^3, $MeSer^7$] MC-LY (**50**)	1005.5	Leu	Tyr	Ala	Ser	CH_3	H	CH_3	H			41
[Gly^1, Asp^3, ADMAdda^5, Dhb^7] MC-LHar (182)	1008.5	Leu	Har	Gly	Dha	CH_3	H	$COCH_3$	H			This Study
[Asp^3, ADMAdda^5, Dhb^7] MC-LR (**51**)	1008.5	Leu	Arg	Ala	Dhb	H	H	$COCH_3$	H			54
[Asp^3, ADMAdda^5] MC-LR (**52**)	1008.5	Leu	Arg	Ala	Dha	CH_3	H	$COCH_3$	H	≈ 1	160	55,56,80
[$Glu(OMe)^6$] MC-LR (**53**)	1008.5	Leu	Arg	Ala	Dha	CH_3	CH_3	CH_3	CH_3	> 100	> 1,000	33,51,82
[$Mdhb^7$] MC-LR (**54**)	1008.5	Leu	Arg	Ala	Dhb	CH_3	H	CH_3	CH_3			56
MC-HilR (**55**)	1008.5	Hil	Arg	Ala	Dha	CH_3	H	CH_3	CH_3		100	57
[Gly^1, Asp^3, Dhb^7] MC-RR (183)	1009.5	Arg	Arg	Gly	Dha	CH_3	H	CH_3	H			This Study
[Asp^3, Dha^7] MC-RR (**56**)	1009.5	Arg	Arg	Ala	Dha	H	H	CH_3	H			47
[Asp^3] MC-LW (**57**)	1010.5	Leu	Trp	Ala	Dha	CH_3	H	CH_3	H			44
[$MeSer^7$] MC-LR (**58**)	1012.6	Leu	Arg	Ala	Ser	CH_3	H	CH_3	CH_3		150	38,57
[Asp^3] MC-FR (**59**)	1014.5	Phe	Arg	Ala	Dha	CH_3	H	CH_3	H			58
[Dha^7] MC-FR (**60**)	1014.5	Phe	Arg	Ala	Dha	H	H	CH_3	CH_3			59

Microcystin	M_r [a] (Da)	X	Z	A	B	R_1	R_2	R_3	R_4	PPIA [b] (IC_{50}; nM)	Toxicity [c] (LD_{50}; µg/kg)	Ref. [d]
[Asp^3] MC-RF (**61**)	1014.5	Arg	Phe	Ala	Dha	CH_3	H	CH_3	H			41
[Ser^7] MC-E(OMe)E(OMe) (**62**)	1015.5	Glu(OMe)	Glu(OMe)	Ala	Ser	H	H	CH_3	CH_3			43
[Asp^3, Dha^7] MC-RY (**63**)	1016.5	Arg	Tyr	Ala	Dha	H	H	CH_3	H			41
MC-YM (**64**)	1019.5	Tyr	Met	Ala	Dha	CH_3	H	CH_3	CH_3			35
[Asp^3, ADMAdda^5] MC-LHar (**65**)	1022.5	Leu	Har	Ala	Dha	CH_3	H	$COCH_3$	H			56,72
[ADMAdda^5] MC-LR (**66**)	1022.5	Leu	Arg	Ala	Dha	CH_3	H	$COCH_3$	CH_3		≈ 60	55,56
[Gly^1, Asp^3, Dhb^7] MC-RHar (**184**)	1023.6	Arg	Har	Gly	Dha	CH_3	H	CH_3	H			This Study
[Asp^3] MC-RR (**67**)	1023.6	Arg	Arg	Ala	Dha	CH_3	H	CH_3	H		250	60
[Asp^3, Dhb^7] MC-RR (**68**)	1023.6	Arg	Arg	Ala	Dhb	H	H	CH_3	H		250	61
[Dha^7] MC-RR (**69**)	1023.6	Arg	Arg	Ala	Dha	H	H	CH_3	CH_3		180	62
MC-LW (**70**)	1024.5	Leu	Trp	Ala	Dha	CH_3	H	CH_3	CH_3			45
MC-WL (**169**)	1024.5	Trp	Leu	Ala	Dha	CH_3	H	CH_3	CH_3			This Study
MC-M(O)R (**71**)	1028.5	Met(O)	Arg	Ala	Dha	CH_3	H	CH_3	CH_3		700-800	38
MC-FR (**72**)	1028.5	Phe	Arg	Ala	Dha	CH_3	H	CH_3	CH_3		250	38
MC-RF (**73**)	1028.5	Arg	Phe	Ala	Dha	CH_3	H	CH_3	CH_3			41
[Dha^7] MC-HphR (**74**)	1028.5	Hph	Arg	Ala	Dha	H	H	CH_3	CH_3			63
[Asp^3] MC-YR (**75**)	1030.5	Tyr	Arg	Ala	Dha	CH_3	H	CH_3	H			64
[Dha^7] MC-YR (**76**)	1030.5	Tyr	Arg	Ala	Dha	H	H	CH_3	CH_3			65
[Asp^3, Dha^7] MC-HtyR (**77**)	1030.5	Hty	Arg	Ala	Dha	H	H	CH_3	H			63

[Asp^3] MC-RY (**78**)	1030.5	Arg	Tyr	Ala	Dha	CH_3	H	CH_3	H			66
[Dha^7] MC-RY (**79**)	1030.5	Arg	Tyr	Ala	Dha	H	H	CH_3	CH_3			41
MC-LY(OMe) (**80**)	1031.5	Leu	Tyr(OMe)	Ala	Dha	CH_3	H	CH_3	CH_3			41
MC-YM(O) (**81**)	1035.5	Tyr	Met(O)	Ala	Dha	CH_3	H	CH_3	CH_3		56	67
[Leu^1] MC-LR (**82**)	1036.6	Leu	Arg	Leu	Dha	CH_3	H	CH_3	CH_3	0.3-4.43	100	68,111
[ADMAdda^5] MC-HilR (**83**)	1036.6	Hil	Arg	Ala	Dha	CH_3	H	$COCH_3$	CH_3			69
[ADMAdda^5] MC-LHar (**84**)	1036.6	Leu	Har	Ala	Dha	CH_3	H	$COCH_3$	CH_3		≈ 60	55,56
MC-RR (**85**)	1037.6	Arg	Arg	Ala	Dha	CH_3	H	CH_3	CH_3		500-600	70,119,120
[Gly^1, Asp^3, ADMAdda^5, Dhb^7] MC-RR (**185**)	1037.5	Arg	Arg	Gly	Dha	CH_3	H	$COCH_3$	H			This Study
[Asp^3] MC-YY (**86**)	1053.5	Tyr	Tyr	Ala	Dha	CH_3	H	CH_3	H			41
[Asp^3, Glu(OMe)^6] MC-RR (**87**)	1037.6	Arg	Arg	Ala	Dha	CH_3	CH_3	CH_3	H			71
[(6*Z*)Adda^5] MC-RR (**88**)	1037.6	Arg	Arg	Ala	Dha	CH_3	H	CH_3	CH_3		> 1,200	52,121
[Ser^1, ADMAdda^5] MC-LR (**89**)	1038.5	Leu	Arg	Ser	Dha	CH_3	H	$COCH_3$	CH_3			72
[ADMAdda^5, MeSer^7] MC-LR (**90**)	1040.6	Leu	Arg	Ala	Ser	CH_3	H	$COCH_3$	CH_3			72
[Asp^3, MeSer^7] MC-RR (**91**)	1041.6	Arg	Arg	Ala	Ser	CH_3	H	CH_3	H			73
[Ser^7] MC-RR (**92**)	1041.6	Arg	Arg	Ala	Ser	H	H	CH_3	CH_3			53
[Asp^3, Dhb^7] MC-HtyR (**93**)	1044.5	Hty	Arg	Ala	Dhb	H	H	CH_3	H		70	48,61
[Dha^7] MC-HtyR (**94**)	1044.5	Hty	Arg	Ala	Dha	H	H	CH_3	CH_3			63
[Asp^3] MC-HtyR (**95**)	1044.5	Hty	Arg	Ala	Dha	CH_3	H	CH_3	H		160-300	74
MC-YR (**96**)	1044.5	Tyr	Arg	Ala	Dha	CH_3	H	CH_3	CH_3		68	31,120
MC-RY (**97**)	1044.5	Arg	Tyr	Ala	Dha	CH_3	H	CH_3	CH_3			66

Microcystin	M_r [a] (Da)	X	Z	A	B	R_1	R_2	R_3	R_4	PPIA [b] (IC_{50}; nM)	Toxicity [c] (LD_{50}; µg/kg)	Ref. [d]
[Asp^3, MeSer^7] MC-RY (**98**)	1048.5	Arg	Tyr	Ala	Ser	CH_3	H	CH_3	H			41
[Ser^7] MC-YR (**99**)	1048.5	Tyr	Arg	Ala	Ser	H	H	CH_3	CH_3			75
MC-(H_4)YR (**100**)	1048.6	(H_4)Tyr	Arg	Ala	Dha	CH_3	H	CH_3	CH_3			57
[Gly^1, Asp^3, ADMAdda^5, Dhb^7] MC-RHar (**186**)	1051.5	Arg	Har	Gly	Dha	CH_3	H	$COCH_3$	H			This Study
[Asp^3, Dhb^7] MC-HtyY (**101**)	1051.5	Hty	Tyr	Ala	Dhb	H	H	CH_3	H			76
[Asp^3, ADMAdda^5, Dhb^7] MC-RR (**102**)	1051.5	Arg	Arg	Ala	Dhb	H	H	$COCH_3$	H		200	54
[Glu(OC_3H_6OH)^6] MC-LR (**103**)	1052.6	Leu	Arg	Ala	Dha	CH_3	C_3H_6OH	CH_3	CH_3		> 1,000	38,57
[Asp^3] MC-WR (**104**)	1053.5	Trp	Arg	Ala	Dha	CH_3	H	CH_3	H			58
MC-HtyR (**105**)	1058.5	Hty	Arg	Ala	Dha	CH_3	H	CH_3	CH_3		80-100	74
[Ser^7] MC-HtyR (**106**)	1062.5	Hty	Arg	Ala	Ser	H	H	CH_3	CH_3			63
[MeSer^7] MC-YR (**107**)	1062.5	Tyr	Arg	Ala	Ser	CH_3	H	CH_3	CH_3			77
[MeSer^7] MC-RY (**108**)	1062.5	Arg	Tyr	Ala	Ser	CH_3	H	CH_3	CH_3			41
MC-HarHar (**109**)	1065.6	Har	Har	Ala	Dha	CH_3	H	CH_3	CH_3			78
[Asp^3, Dhb^7] MC-HtyHty (**110**)	1065.5	Hty	Hty	Ala	Dhb	H	H	CH_3	H			76
[ADMAdda^5] MC-RR (**111**)	1065.6	Arg	Arg	Ala	Dha	CH_3	H	$COCH_3$	CH_3			79
MC-WR (**112**)	1067.5	Trp	Arg	Ala	Dha	CH_3	H	CH_3	CH_3		150-200	38
[Asp^3, ADMAdda^5] MC-HtyR (**113**)	1072.5	Hty	Arg	Ala	Dha	CH_3	H	$COCH_3$	H	≈ 1.29		80
[Asp^3, ADMAdda^5, Dhb^7] MC-HtyR (**114**)	1072.5	Hty	Arg	Ala	Dhb	H	H	$COCH_3$	H		100	54
MC-RY(OMe) (**115**)	1074.5	Arg	Tyr(OMe)	Ala	Dha	CH_3	H	CH_3	CH_3			41

[ADMAdda^{5}] MC-(H_4)YR (**116**)	1076.6	(H_4)Tyr	Arg	Ala	Dha	CH_3	H	$COCH_3$	CH_3		69
[MeLan^{7}] MC-LR (**117**)	1115.6	Leu	Arg	Ala	Lan	CH_3	H	CH_3	CH_3	1000	57

Also reported was a linear form of a microcystin: seco[Asp^{3}] MC-RR (**119**).[71] [a] Molecular weights are rounded to one decimal place. [b] PPIA = Protein phosphatase inhibition assay. [c] Performed using the mouse bioassay.[153] [d] Ref = Reference(s).

Appendix B: Studies on microcystin (MC) concentration in response to environmental factors. [a]

Parameter	Organism	Analysis Method [b]	Change in MC Concentration/Toxicity	Information Yielded	References
Temperature (°C)					
10-28	*Anabaena* species Continuous cultures	HPLC	3-10	Lowest at 10 °C; Highest at 25 °C	130
10, 25, 34	*Microcystis aeruginosa* Batch cultures	Mouse bioassay	5	Lowest toxicity at 10 °C; Highest at 25 °C	131
15-35	*Microcystis aeruginosa* Batch cultures	Mouse bioassay HPLC	4	Highest toxicity at 20 °C; Different levels of microcystin congeners at different temperatures	132,133
18, 25, 35	*Microcystis aeruginosa* Batch cultures	Mouse bioassay	1.4	Lowest toxicity at 32 °C; Highest at 18 °C	134
20, 28	*Microcystis aeruginosa*, Semi-continuous cultures	HPLC	NC	Different levels of microcystin congeners at different temperatures	135
15-30	*Oscillatoria agardhii* Batch cultures	HPLC	7	Strain dependent; Lowest at 30 °C	136
Light (µEin·m^{-2}·s^{-1})					
2-100; continuous	*Anabaena* species Batch cultures	HPLC	3	Highest at 25 µEin·m^{-2}·s^{-1}	137
7, 19, 42; continuous	*Anabaena* species Continuous cultures	HPLC	2.5-15	Lowest at 10 µEin·m^{-2}·s^{-1}; Highest at 25 µEin·m^{-2}·s^{-1}	130

5-50; continuous	*Microcystis aeruginosa* Batch cultures	Mouse bioassay	2.4	Highest toxicity at 20 $\mu Ein \cdot m^{-2} \cdot s^{-1}$	131
20-75; continuous	*Microcystis aeruginosa* Continuous cultures	HPLC	2.5	Highest at 40 $\mu Ein \cdot m^{-2} \cdot s^{-1}$	138
21-205; continuous	*Microcystis aeruginosa* Batch cultures	Mouse bioassay	1.2	Lowest toxicity at 21 $\mu Ein \cdot m^{-2} \cdot s^{-1}$; Highest at 142 $\mu Ein \cdot m^{-2} \cdot s^{-1}$	132
7.5, 30, 75; continuous	*Microcystis aeruginosa* Batch cultures	Mouse bioassay	3.8	Lowest toxicity at 7.5 $\mu Ein \cdot m^{-2} \cdot s^{-1}$; Highest at 30 $\mu Ein \cdot m^{-2} \cdot s^{-1}$	134
12-95; continuous	*Oscillatoria agardhii* Batch cultures	HPLC	2.5	Highest at 12-44 $\mu Ein \cdot m^{-2} \cdot s^{-1}$	136
6-112; 12 h/12 h	*Planktothrix agardhii* Batch cultures	HPLC ELISA	10	Lowest at 6 $\mu Ein \cdot m^{-2} \cdot s^{-1}$; Highest at 60 $\mu Ein \cdot m^{-2} \cdot s^{-1}$; Different levels of microcystin congeners at different photon irradiations	148
Phosphorous (mg/L)					
0.05-5.5	*Anabaena* species Batch cultures	HPLC	5	Lowest at 0.05 mg/L; Highest at 5.5 mg/L	137
BG-11 medium; with and without phosphorous	*Microcystis aeruginosa* Batch cultures	Mouse bioassay	1.7	Higher toxicity with the medium without phosphorous	131
0.0025, 0.025	*Microcystis aeruginosa* Continuous cultures	HPLC	2.3	Higher at 0.025 mg/L	139

Parameter	Organism	Analysis Method [b]	Change in MC Concentration/Toxicity	Information Yielded	References
Phosphorous (mg/L) continued					
MA medium; diluted 1/10 and 1/20	*Microcystis aeruginosa* Batch cultures	Mouse bioassay	<1	Highest toxicity with the undiluted medium	134
0.1-5.5	*Oscillatoria agardhii* Batch cultures	HPLC	1.7-2.5	Lowest at 0.1 mg/L	136
Nitrogen (mg/L)					
BG-11 medium; with and without nitrogen	*Microcystis aeruginosa* Batch cultures	Mouse bioassay	5	Higher toxicity with the medium containing nitrogen	131
0.05-1.0	*Microcystis aeruginosa* Continuous cultures	HPLC	3	Higher with high nitrogen	139
MA medium; diluted 1/10 and 1/20	*Microcystis aeruginosa* Batch cultures	Mouse bioassay	2.5	Highest toxicity with the undiluted medium	134
Z8 medium; plus 4.3 mg/L of NH_4NO_3	*Microcystis aeruginosa* Semi-continuous cultures	HPLC	0.5	Lower with added NH_4NO_3	135
0.42-0.84	*Oscillatoria agardhii* Batch cultures	HPLC	5	Lowest with low nitrogen; Higher with high nitrogen	136
Micronutrients					
Al, Cd, Cr, Cu, Fe, Mn, Ni, Sn, Zn; at various concentrations	*Microcystis aeruginosa* Batch cultures	HPLC	1.7	Higher with lower Fe concentrations; Zn required for toxin production	140

0.1-3.4 µg/L of Fe	*Microcystis aeruginosa* Continuous cultures	HPLC	1.5	Higher with higher Fe concentrations	139
0.03-1.2 µg/L of Fe	*Microcystis aeruginosa* Continuous cultures	HPLC	0-3	Higher with lower Fe concentrations	141
56, 560 µg/L of Fe	*Microcystis aeruginosa* Semi-continuous cultures	HPLC	2	Higher with higher Fe concentrations	135
Carbon Dioxide					
BG-11 medium; with and without CO_2	*Microcystis aeruginosa* Batch cultures	Mouse bioassay	6	Higher toxicity with the medium containing CO_2	131
pH					
1-14	*Microcystis aeruginosa* Batch cultures	Mouse bioassay	1.8	Toxicity highest at low and high pH	300
Cell Density (cells/mL)					
500,000-7,000,000	*Microcystis* assemblage Lake mesocosms	ELISA	13.8	After cell density reached a threshold; Microcystin content increased with higher cell density	301

[a] Adapted from Table 3.8 of Reference 12. [b] HPLC = High pressure liquid chromatography; ELISA = Enzyme-linked immunosorbent assay.

Appendix C: Microcystin (MC) congeners produced by reported cyanobacterial strains.[a]

Cyanobacterial Strain	Microcystins Identified	Number of MCs[b]	Position Two[c]	Position Four[d]	Other Modifications	Potential MCs[e]	Ref.[f]
Anabaena 18B6	[Dha^7] MC-RR; [Asp^3, Dha^7] MC-RR; Unidentified MCs × 2	4	Arg	Arg	Pos. 3 × 2 Pos. 7 × 1	-	245
Anabaena 60	MC-LR; [Asp^3] MC-LR; MC-RR; [Asp^3] MC-RR	4	Leu Arg	Arg	Pos. 3 × 2	4	302
Anabaena 66	[Dha^7] MC-HphR; [Dha^7] MC-HtyR; [Ser^7] MC-HtyR; [Asp^3, Dha^7] MC-HtyR	4	Hph Hty	Arg	Pos. 3 × 2 Pos. 7 × 2	8	63, 302
Anabaena 66A	[Dha^7] MC-LR; [Ser^7] MC-LR; [Asp^3, Ser^7] MC-LR; [Asp^3, Dha^7] MC-LR; [Dha^7] MC-FR; [Asp^3, Dha^7] MC-FR; [Dha^7] MC-HphR; [Asp^3, Dha^7] MC-HphR; MC-HtyR; [Dha^7] MC-HtyR; [Ser^7] MC-HtyR; [Asp^3, Dha^7] MC-HtyR; [Asp^3, Ser^7] MC-HtyR; Unidentified MCs × 20	33	Leu Phe Hph Hty	Arg	Pos. 3 × 2 Pos. 7 × 3	-	245
Anabaena 90	MC-LR; [Asp^3] MC-LR; [DMAdda^5] MC-LR; [Dha^7] MC-LR; [MeSer^7] MC-LR; [Asp^3, MeSer^7] MC-LR; MC-HilR; [Asp^3] MC-HilR; MC-RR; [Asp^3] MC-RR; [Dha^7] MC-RR	11	Leu Hil Arg	Arg	Pos. 3 × 2 Pos. 5 × 2 Pos. 7 × 3	36	112,130, 245,302
Anabaena 141	MC-LR; [Asp^3] MC-LR; MC-RR; [Asp^3] MC-RR	4	Leu Arg	Arg	Pos. 3 × 2	4	302
Anabaena 186	[Dha^7] MC-E(OMe)E(OMe); [Ser^7] MC-E(OMe)E(OMe); [Asp^3, Dha^7] MC-E(OMe)E(OMe); [Asp^3, Ser^7] MC-E(OMe)E(OMe); [Dha^7] MC-EE(OMe); [Ser^7] MC-EE(OMe); [Asp^3, Dha^7] MC-EE(OMe)	7	Glu Glu(OMe)	Glu(OMe)	Pos. 3 × 2 Pos. 7 × 2	8	43

Anabaena 202 A1	[Dha^7] MC-LR; [Asp^3, Dha^7] MC-LR; [Ser^7] MC-LR; [Asp^3, Ser^7] MC-HilR; [Dha^7] MC-RR; [Asp^3, Dha^7] MC-RR; [Ser^7] MC-RR	7	Leu Hil Arg	Arg	Pos. 3 × 2 Pos. 7 × 2	12	53, 302
Anabaena 202 A2	[Dha^7] MC-LR; [Asp^3, Dha^7] MC-LR; [Ser^7] MC-LR; [Dha^7] MC-RR; [Asp^3, Dha^7] MC-RR; [Ser^7] MC-RR	6	Leu Arg	Arg	Pos. 3 × 2 Pos. 7 × 2	8	53,112, 302
Anabaena flos-aquae CYA83/1	MC-LR; [Asp^3] MC-LR; MC-RR; [Asp^3] MC-RR; [Glu(OMe)^6] MC-LR; [Asp^3, Glu(OMe)^6] MC-LR	6	Leu Arg	Arg	Pos. 3 × 2 Pos. 6 × 2	8	51
Anabaena flos-aquae NRC 525-17	MC-LR; [Asp^3] MC-LR; MC-HtyR; [Asp^3] MC-HtyR	4	Leu Hty	Arg	Pos. 3 × 2	4	74
Fischerella CENA161	MC-LR	1	Leu	Arg		1	93
Hapalosiphon hibernicus BZ-3-1	MC-VA; [Asp^3] MC-VA; MC-LA; [Asp^3] MC-LA; [Dha^7] MC-LA; [Asp^3, DMAdda^5] MC-LA; MC-LV; MC-LL; MC-RA; [Asp^3] MC-RA	10	Val Leu Arg	Ala Val Leu	Pos. 3 × 2 Pos. 5 × 2 Pos. 7 × 2	72	245
***Microcystis* CYN06**	MC-LA; [Asp^3] MC-LA; MC-FA; [Asp^3] MC-FA; MC-YA; MC-WA; [Asp^3] MC-WA; MC-RA; [Asp^3] MC-RA; MC-RAba; [Asp^3] MC-RAba; MC-RL; MC-LAba; MC-FAba; MC-WAba; MC-LL; MC-FL; MC-WL; MC-LR; [Asp^3] MC-LR; MC-FR; [Asp^3] MC-FR; MC-YR; MC-WR; [Asp^3] MC-WR; MC-RR; [Asp^3] MC-RR	27	Leu Phe Tyr Trp Arg	Ala Aba Leu Arg	Pos. 3 × 2	40	This Study
Microcystis HUB 5-2-4	MC-LR; dmMC-LR; MC-RR; dmMC-RR; MC-YR	5	Leu Tyr Arg	Arg	DM × 2	6	180
Microcystis MB-K	MC-LR; dmMC-LR; MC-YR; dmMC-YR	4	Leu Tyr	Arg	DM × 2	4	220

Cyanobacterial Strain	Microcystins Identified	Number of MCs [b]	Position Two [c]	Position Four [d]	Other Modifications	Potential MCs [e]	Ref. [f]
Microcystis MG-K	MC-RR; dmMC-RR; MC-WR	3	Arg Trp	Arg	DM × 2	4	220
Microcystis PCC7806	MC-LR; [Asp^3] MC-LR; [Dha^7] MC-LR; [MeSer^7] MC-LR; [Asp^3, Dha^7] MC-LR; [Asp^3, MeSer^7] MC-LR; Unidentified MCs × 5	11	Leu	Arg	Pos. 3 × 2 Pos. 7 × 3	-	127, 245
Microcystis PCC7813	MC-LR; [Asp^3] MC-LR	2	Leu	Arg	Pos. 3 × 2	2	180
Microcystis aeruginosa	MC-LR	1	Leu	Arg		1	303
Microcystis aeruginosa B2666	MC-LA; [Asp^3] MC-LA; MC-LAba; [Asp^3] MC-LAba; MC-LL; MC-LF; MC-LR; [MeSer^7] MC-LR	8	Leu	Ala Aba Leu Phe Arg	Pos. 3 × 2 Pos. 7 × 2	20	34
Microcystis aeruginosa CALU972	[Dha^7] MC-LR; [Asp^3, Dha^7] MC-LR; [Dha^7] MC-RR; [Asp^3, Dha^7] MC-RR; [Dha^7] MC-YR	5	Leu Tyr Arg	Arg	Pos. 3 × 2 Pos. 7 × 1	6	65
Microcystis aeruginosa K-139	[Dha^7] MC-LR; [Asp^3, Dha^7] MC-LR	2	Leu	Arg	Pos. 3 × 2 Pos. 7 × 1	2	112
Microcystis aeruginosa MK10.10	MC-VR; MC-LR; MC-HilR	3	Val Leu Hil	Arg		3	46

Microcystis aeruginosa NIES90	MC-LR; MC-YR; MC-RR	3	Leu Tyr Arg	Arg		3	182
Microcystis aeruginosa PCC7820	MC-LR; dmMC-LR; [Glu(OMe)^{6}] MC-LR; MC-LF; dmMC-LF; MC-LW; dmMC-LW; MC-LL; MC-LM; MC-LY	10	Leu	Arg Phe Leu Met Trp Tyr	DM × 2 Pos. 6 × 2	24	44
Microcystis aeruginosa TN-2	MC-LR; MC-FR; [Asp^{3}] MC-FR; MC-WR; [Asp^{3}] MC-WR; MC-RR; MC-RA	7	Leu Phe Trp Arg	Arg Ala	Pos. 3 × 2	16	58
Microcystis aeruginosa UAM1303	MC-LR; [Asp^{3}] MC-LR; [MeSer^{7}] MC-LR; MC-HilR; MC LY; MC-LF; MC-LW	7	Leu Hil	Arg Tyr Phe Trp	Pos. 3 × 2 Pos. 7 × 2	32	35
Microcystis aeruginosa UTEX2666	MC-LA; [Asp^{3}] MC-LA; MC-LAba; [Asp^{3}, Glu(OMe)^{6}] MC-LAba; MC-LR; [Asp^{3}] MC-LR; didmMC-LR	7	Leu	Ala Aba Arg	Pos. 3 × 2 Pos. 6 × 2	24	35
Microcystis aeruginosa UTEX2670	MC-YA; MC-YL; MC-YM; MC-YM(O); Unidentified MC	5	Tyr	Ala Leu Met Met(O)		-	35

Cyanobacterial Strain	Microcystins Identified	Number of MCs [b]	Position Two [c]	Position Four [d]	Other Modifications	Potential MCs [e]	Ref. [f]
Microcystis aeruginosa UV-006	MC-LA; MC-LAba; MC-LV; MC-LL; MC-LR; [Asp^3] MC-LR; Unidentified MCs × 2	8	Leu	Ala Aba Val Leu Arg	Pos. 3 × 2	≥ 10	252
Microcystis novacekii UAM250	MC-LR; MC-YR; MC-RR	3	Leu Tyr Arg	Arg		3	304
Microcystis viridis NIES102	[Asp^3] MC-LR; [Dha^7] MC-LR; [Ser^1, Asp^3, Dha^7] MC-LR; MC-HilR; MC-FR; MC-YR; [Asp^3] MC-YR; MC-HtyR; MC-WR; [Asp^3] MC WR; MC-RR; [Asp^3] MC-RR; Unidentified MCs × 35	47	Leu Hil Phe Tyr Hty Trp Arg	Arg	Pos. 1 × 2 Pos. 3 × 2 Pos. 7 × 2	-	245
Nostoc 152	[Asp^3, ADMAdda^5] MC-VR; [DMAdda^5] MC-LR; [ADMAdda^5] MC-LR; [Mdhb^7] MC-LR; [Ser^1, ADMAdda^5] MC-LR; [Ser^1, Asp^3, ADMAdda^5] MC LR; [Asp^3, DMAdda^5] MC-LR; [ADMAdda^5, MeSer^7] MC-LR; [ADMAdda^5, Dha^7] MC-LR; [Asp^3, ADMAdda^5, Dha^7] MC-LR; [ADMAdda^5] MC-LHar; [DMAdda^5] MC-LHar; [Asp^3, ADMAdda^5] MC-LHar; [ADMAdda^5] MC-HilR; [ADMAdda^5] MC-HilHar; [Asp^3, ADMAdda^5] MC-HilR; Unidentified MCs × 9	25	Val Leu Hil	Arg Har	Pos. 1 × 2 Pos. 3 × 2 Pos. 5 × 3 Pos. 7 × 3	≥ 216	55,56, 72,245

Nostoc IO-102-I	[ADMAdda^5] MC-LR; [DMAdda^5] MC-LR; [Asp^3, ADMAdda^5] MC LR; [DMAdda^5] MC-HilR; [ADMAdda^5] MC-YR; Unidentified MCs × 15	20	Leu Hil Tyr	Arg	Pos. 3 × 2 Pos. 5 × 2	-	245, 280
Nostoc species	[Asp^3, ADMAdda^5, Dhb^7] MC-LR; [Asp^3, ADMAdda^5, Dhb^7] MC HtyR; [Asp^3, ADMAdda^5, Dhb^7] MC-RR	3	Leu Hty Arg	Arg	Pos. 3 × 1 Pos. 5 × 1 Pos. 7 × 1	3	54
Planktothrix Max06	[Asp^3, DMAdda^5] MC-HtyR; [Asp^3] MC-YR; [Asp^3, MeSer^7] MC-HtyR; [Asp^3, MeSer^7] MC-LR; [Asp^3] MC-HtyR; [Asp^3] MC-LR; [Asp^3, Dha^7] MC-LR; [Asp^3] MC-HilR; [Asp^3, Glu(OMe)^6] MC-HtyR; [Asp^3] MC-HphR; [Asp^3, Glu(OMe)^6] MC-LR	11	Leu Hil Tyr Hty Hph	Arg	Pos. 3 × 1 Pos. 5 × 2 Pos. 6 × 2 Pos. 7 × 3	60	305
Planktothrix agardhii	[Asp^3] MC-LR; [Asp^3] MC-RR	2	Leu Arg	Arg	Pos. 3 × 1	2	148
Planktothrix agardhii 213	[Asp^3] MC-LR; [Asp^3, Dha^7] MC-LR; [Asp^3] MC-RR	3	Leu Arg	Arg	Pos. 3 × 1 Pos. 7 × 2	4	245
Planktothrix agardhii NIVA 126/8	[Asp^3] MC-LR; [Asp^3] MC-RR; Unidentified MC	3	Leu Arg	Arg	Pos. 3 × 1	-	245
Planktothrix agardhii PH-123	[Asp^3] MC-LR; [Asp^3, ADMAdda^5] MC-LR; [Asp^3] MC-HtyR; [Asp^3, ADMAdda^5] MC-HtyR	4	Leu Hty	Arg	Pos. 3 × 1 Pos. 5 × 2	4	80
Planktothrix rubescens No80	[Asp^3, Dhb^7] MC-HtyY; [Asp^3, Dhb^7] MC-HtyHty	2	Hty	Tyr Hty	Pos. 3 × 1 Pos. 7 × 1	2	76

[a] An assessment of the microcystin diversity of 42 microcystin-producing strains reported in scientific journals. [b] Number of microcystins observed, including unidentified microcystins which the researchers noted during the studies. [c] Amino acids incorporated into position two of the microcystins reported to be produced by the cyanobacterial strain. [d] Amino acids incorporated into position four of the microcystins reported to be produced by the cyanobacterial strain. [e] Potential number of microcystins which could be produced by the cyanobacterial strain according to the information collected; In some cases this is omitted as the presence of unidentified microcystins makes this value difficult to estimate. [f] Ref = Reference(s).

Appendix D

Appendix D.1: β-Mercaptoethanol derivatisation of standard microcystins.

MC-LR (**7**) Half-life = 4.8 min

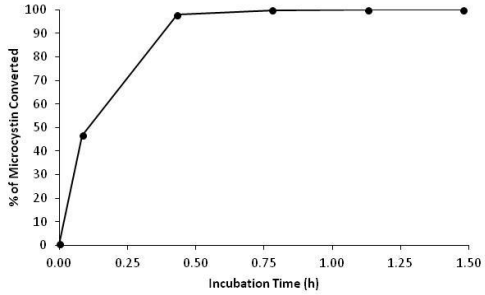

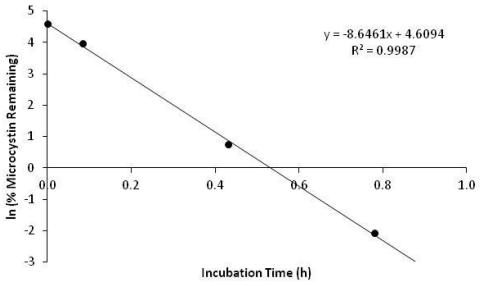

[Dha^{7}] MC-LR (**33**) Half-life = 5.4 min

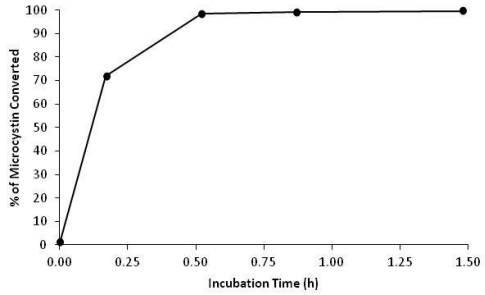

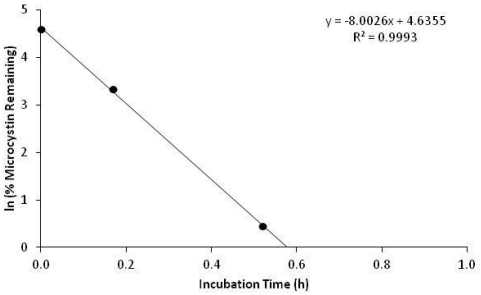

MC-YR (**96**) Half-life = 3.8 min

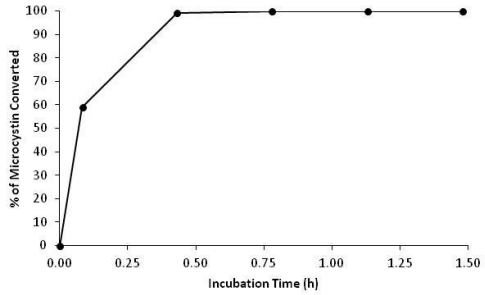

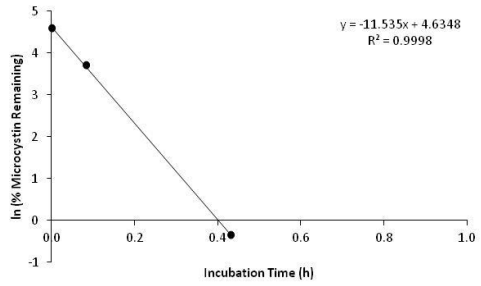

MC-RR (**85**) Half-life = 2.6 min

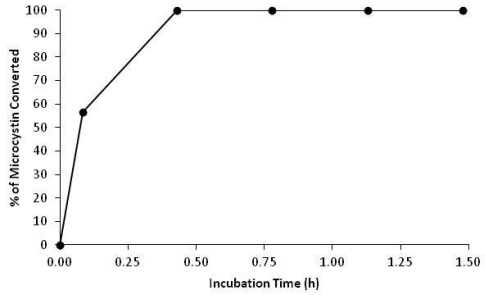

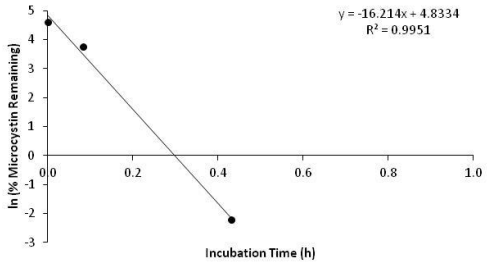

Appendix D.2: β-Mercaptoethanol derivatisation of the CYN06 microcystins.

[Asp^3] MC-RR (67) Half-life = 2.6 min

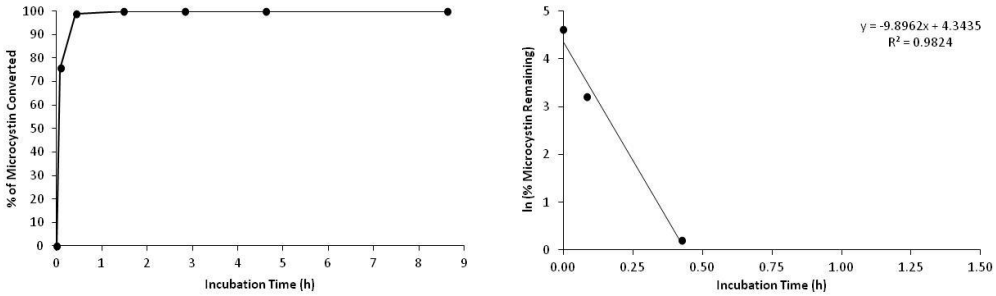

MC-RR (85) Half-life = 3.2 min

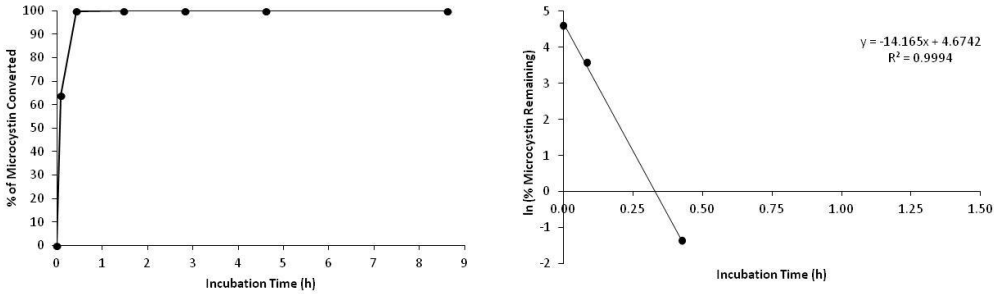

MC-YR (96) Half-life = 6.8 min

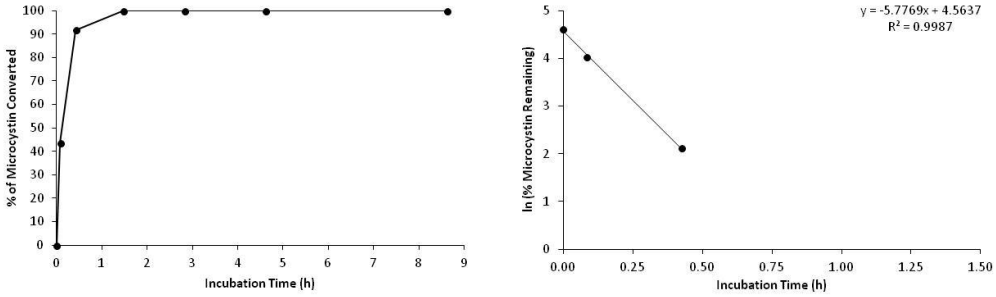

[Asp^3] MC-LR (30) Half-life = 3.5 min

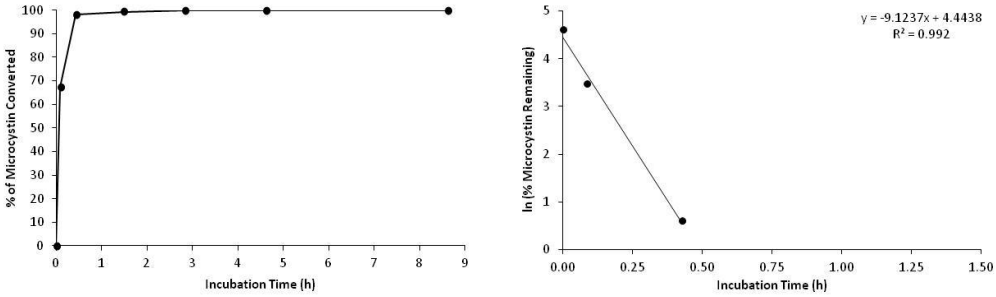

Appendix D

MC-LR (**7**) Half-life = 5.2 min

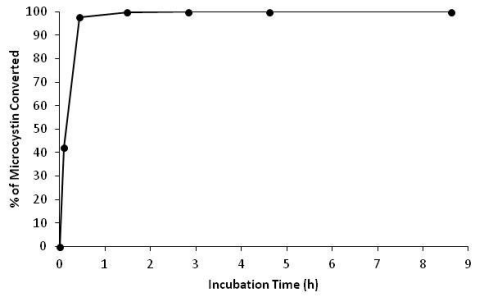

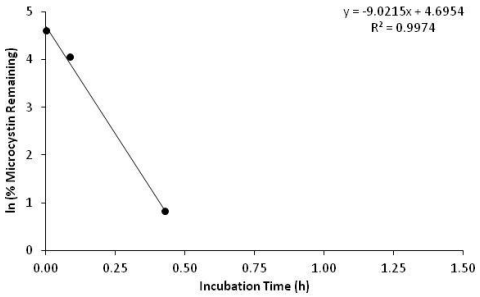

[Asp^3] MC-FR (**59**) Half-life = 5.0 min

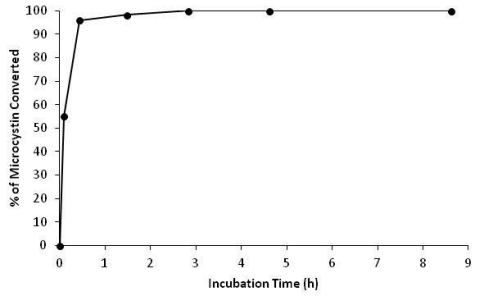

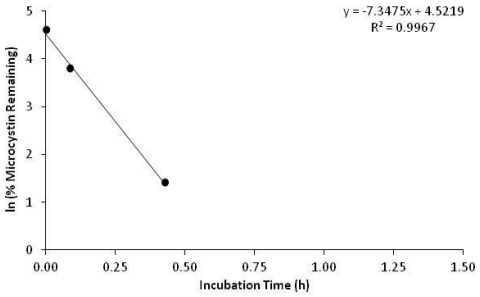

MC-FR (**72**) Half-life = 4.5 min

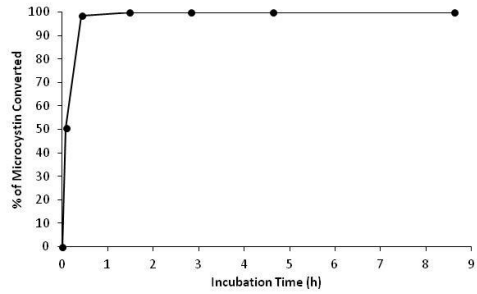

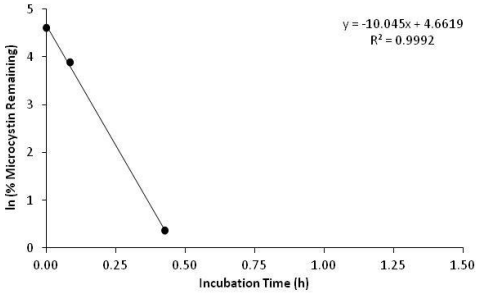

[Asp^3] MC-WR (**104**) Half-life = 3.4 min

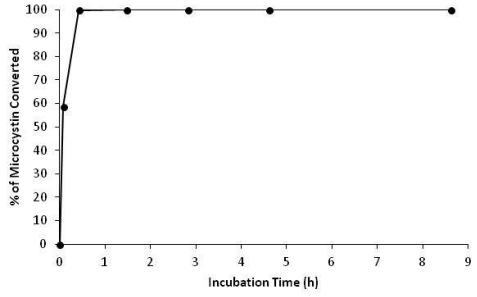

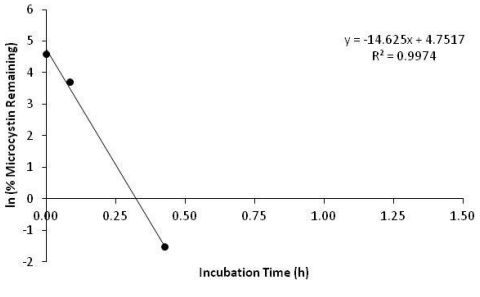

MC-WR (**112**) Half-life = 4.1 min

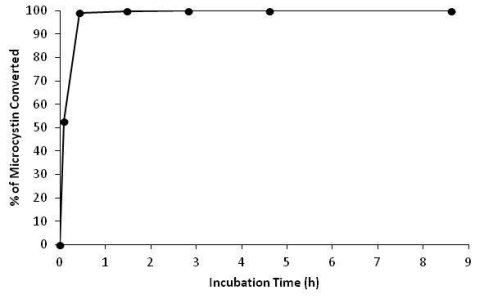

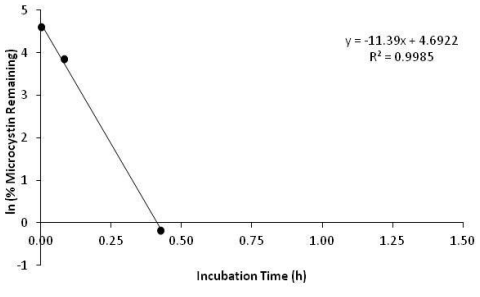

[Asp^3] MC-RA (160) Half-life = 3.5 min

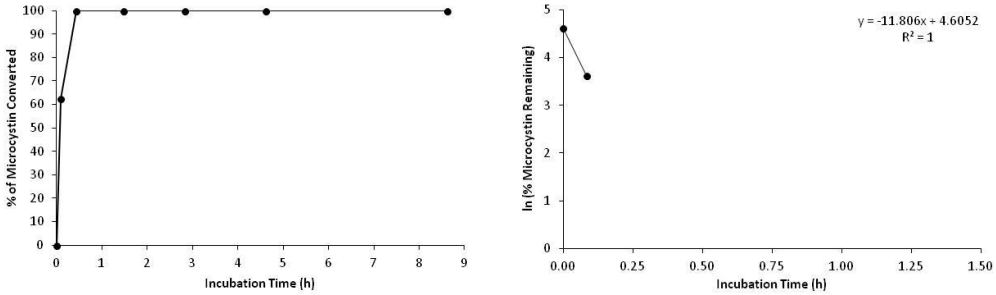

MC-RA (16) Half-life = 5.1 min

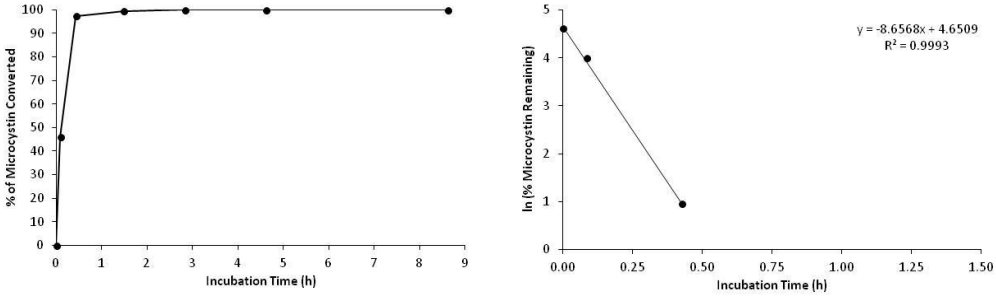

[Asp^3] MC-RAba (161) Half-life = 1.5 min

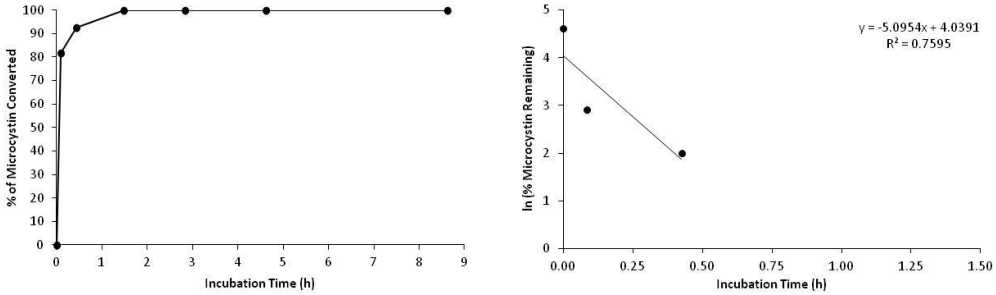

MC-RAba (19) Half-life = 6.0 min

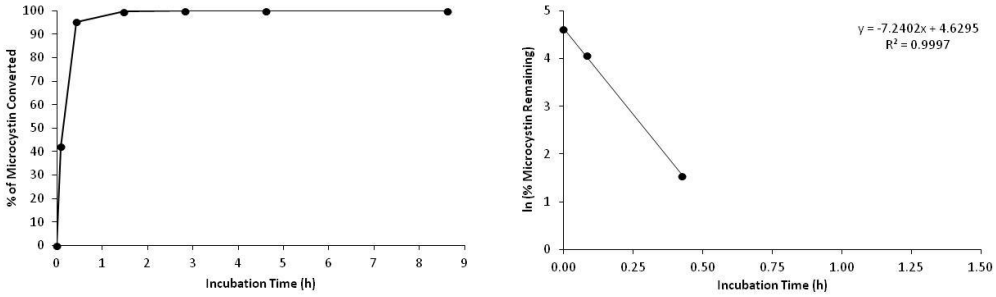

MC-RL (41) Half-life = 3.6 min

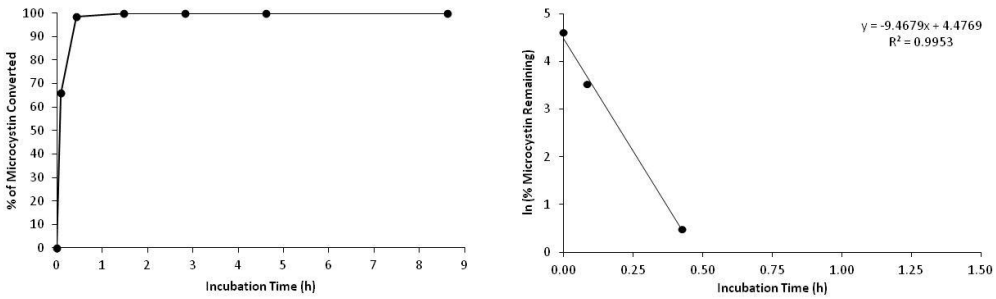

Appendix D

MC-YA (17) Half-life = 6.5 min

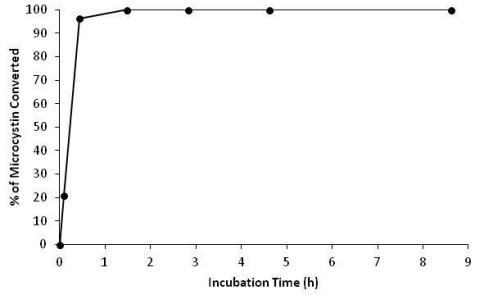

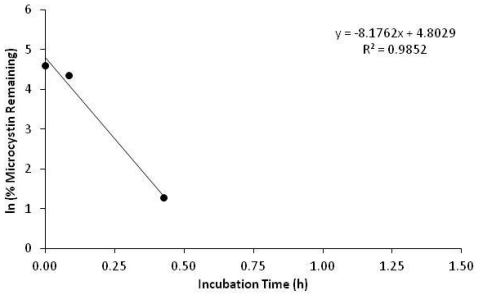

[Asp^3] MC-LA (8) Half-life = 5.8 min

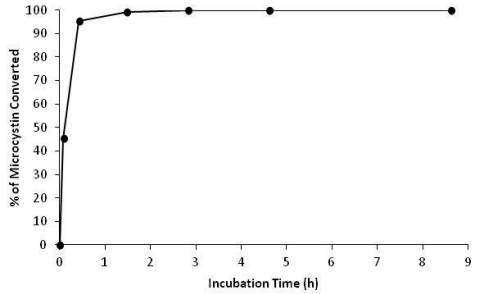

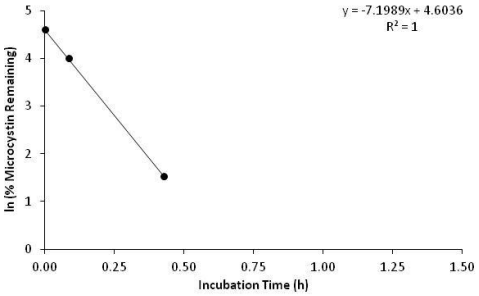

MC-LA (9) Half-life = 4.0 min

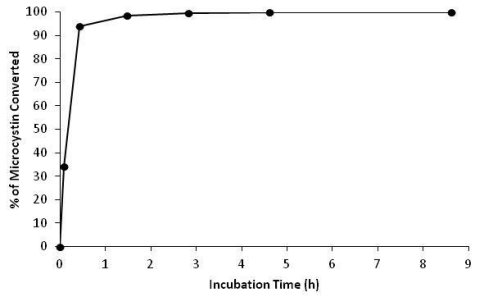

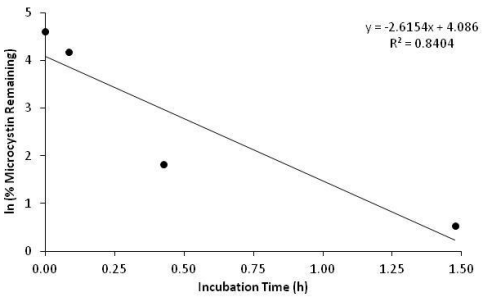

[Asp^3] MC-FA (162) Half-life = 6.2 min

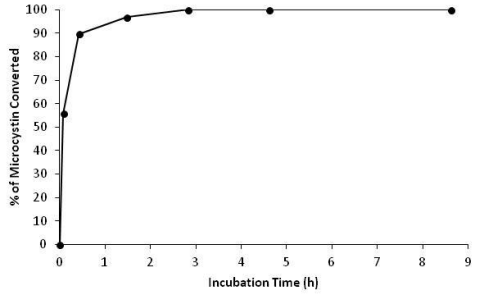

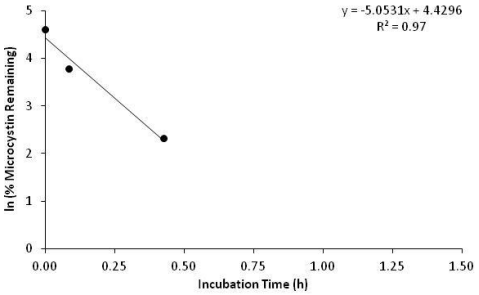

MC-FA (163) Half-life = 5.6 min

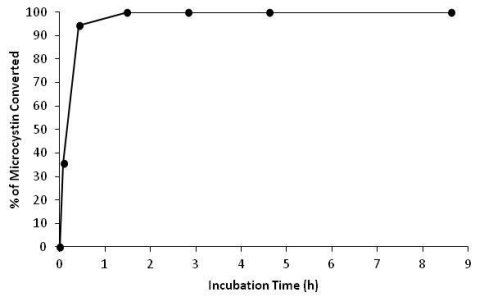

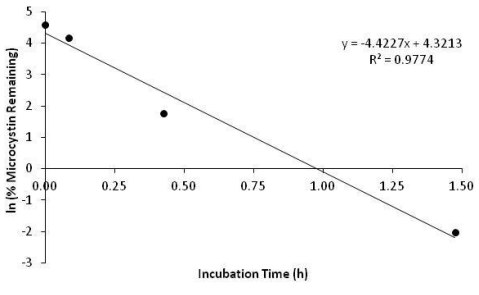

[Asp^3] MC-WA (164) Half-life = 6.9 min

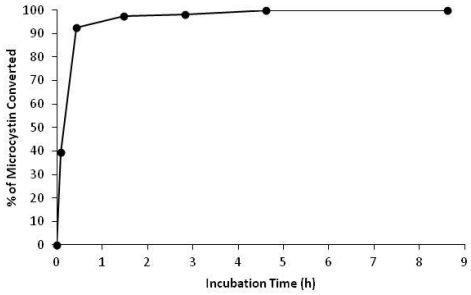

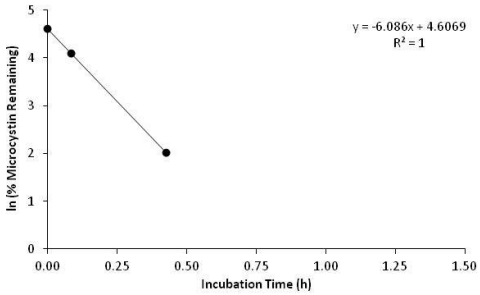

MC-WA (165) Half-life = 5.5 min

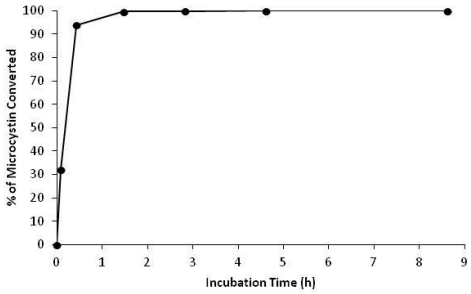

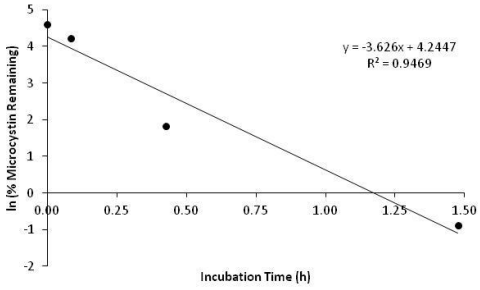

MC-LAba (11) Half-life = 7.4 min

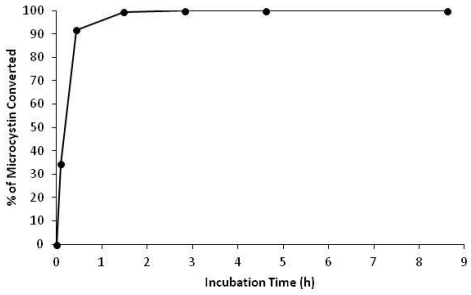

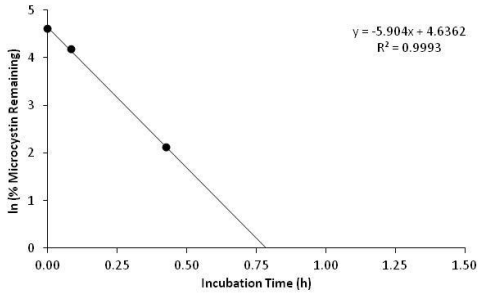

MC-FAba (166) Half-life = 3.9 min

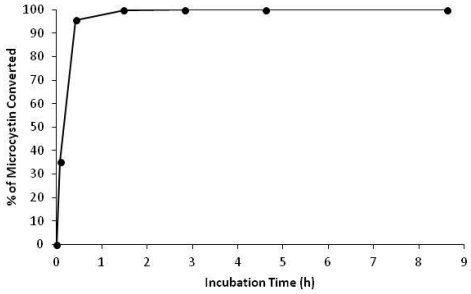

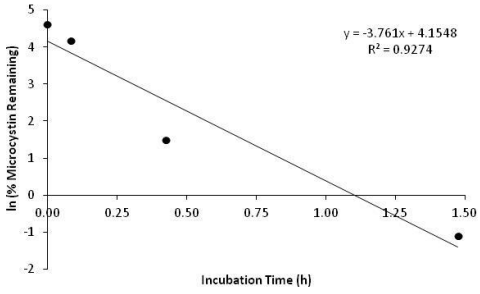

MC-WAba (167) Half-life = 2.2 min

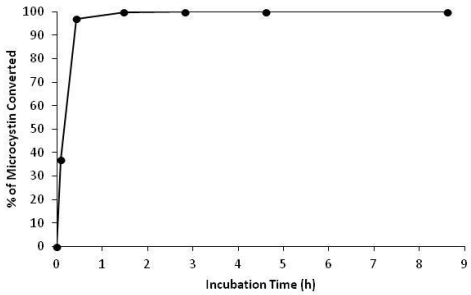

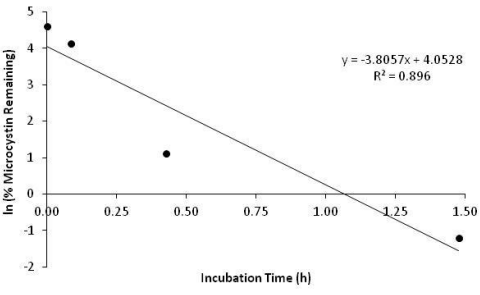

Appendix D

MC-LL (**14**) Half-life = 18.4 min

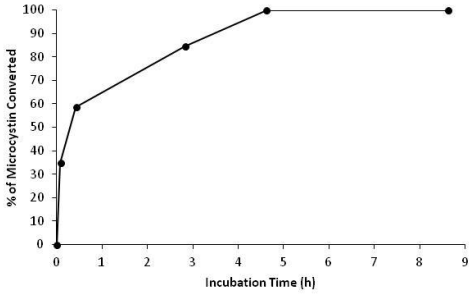

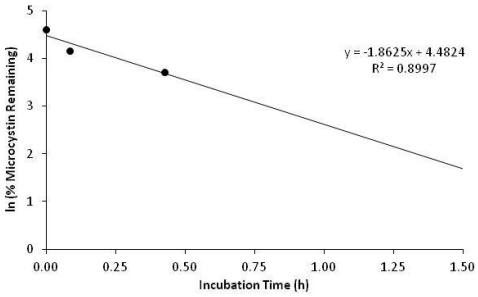

MC-FL (**168**) Half-life = 8.4 min

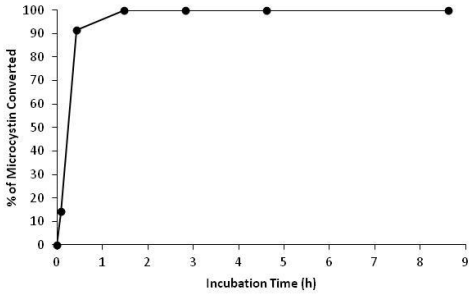

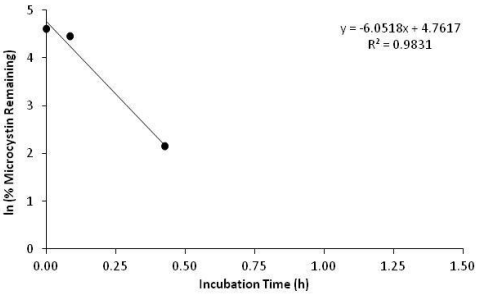

MC-WL (**169**) Half-life = 8.2 min

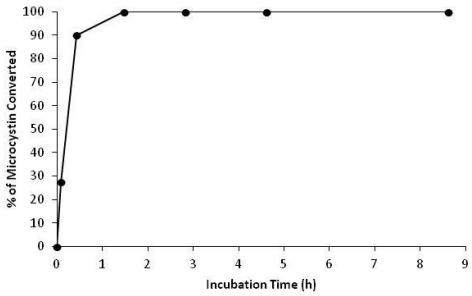

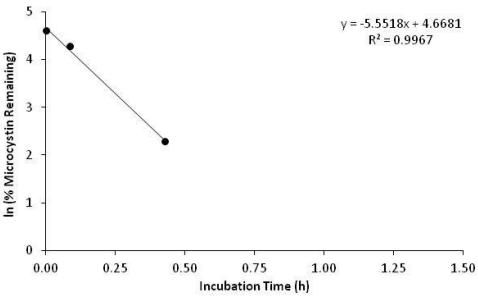

Appendix D.3: β-Mercaptoethanol derivatisation of the Antarctic microcystins.

Antarctic -LR congeners Half-life = 1089.3 min

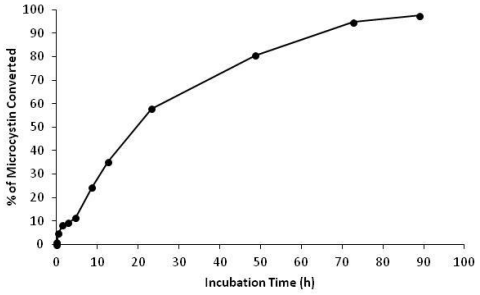

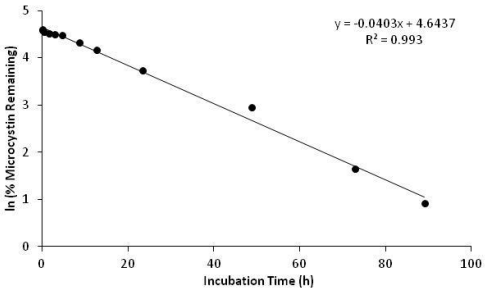

Antarctic -RR congeners Half-life = 632.3 min

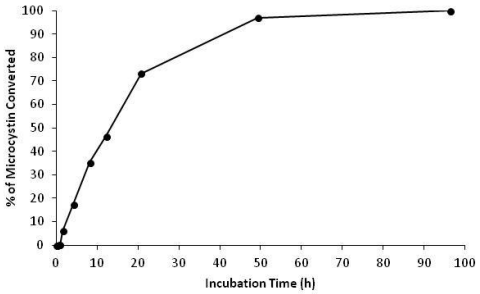

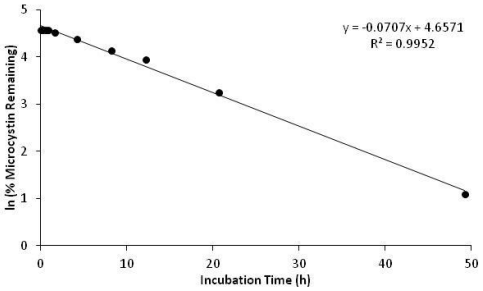

Appendix E.1: Tandem mass spectrometry fragment assignments for the CYN06 -RR microcystin congeners observed by ESI CID.

Fragment Assignment [a]	MC-RR		[Asp^3] MC-RR	
	$[M+2H]^{2+}$	$[M+H]^{+}$	$[M+2H]^{2+}$	$[M+H]^{+}$
M	519.8	1038.6	512.8	1024.6
M – H_2O	510.7	1020.4[b]	503.7	1006.4[b]
M – Mdha – H_2O	469.2	937.4[b]	462.2	923.4[b]
M – Adda sidechain	452.8	904.4	445.7	890.3
M – Adda sidechain – H_2O	443.7	886.4	436.6	872.3
M – Adda	363.2	725.3	356.1	711.3
M – Adda – H_2O	354.2	707.3	347.1	693.3
Arg-Adda-Glu – NH_3		582.2		582.2
Arg-Adda – NH_3+ H		453.2		453.2
Arg-Adda-Glu – CO		571.3		571.2
(Me)Asp-Arg-Adda-Glu		728.3		714.2
(Me)Asp-Arg-Adda		599.3		585.2
Arg-Adda-Glu		599.3		599.2
Mdha-Ala-Arg-(Me)Asp-Arg	298.2	596.3	291.2	582.2
Mdha-Ala-Arg-(Me)Asp		440.2		426.1
Mdha-Ala-Arg		311.2		311.1
Mdha-Ala		155.1		155.0
Adda'-Glu-Mdha		375.2		375.1
Adda'		163.1		163.0
(Me)Asp-Arg		286.2		272.1
Arg		157.1		157.1

[a] Adda' = Adda minus NH_2 and the sidechain ($C_9H_{11}O$). [b] $[M+H]^{+}$ ion was deconvoluted from the $[M+2H]^{2+}$ ion.

Appendix E.2: Tandem mass spectrometry fragment assignments for the CYN06 -XR microcystin congeners observed by MALDI PSD and ESI CID.

Fragment Assignment [a]	**MC-LR** X = 113 Da	**[Asp^3] MC-LR** X = 113 Da	**MC-FR** X = 147 Da	**[Asp^3] MC-FR** X = 147 Da	**MC-YR** X = 163 Da	**MC-WR** X = 186 Da	**[Asp^3] MC-WR** X = 186 Da
M + H	995	981	1029	1015	1045	1068	1054
M – Ala + H	924	910	958	944	974	997	
M – $CH_2NHCN_2H_3$ + H	923	909	957	943	973	996	
M – (Me)Asp + H	866	866	900	900	916	939	939
M – Glu + H	866	852	900	886	916	939	925
M – Adda sidechain + H	861	847	895	881	911	934	920
(Me)Asp-Arg-Adda-Glu + H	728	714	728	714	728	728	714
(Me)Asp-Arg-Adda + H	599	585	599	585	599	599	585
Arg-Adda-Glu + H	599	599	599	599	599	599	599
Arg-Adda + H	470	470	470	470	470	470	470
Mdha-Ala-X-(Me)Asp-Arg + NH_4	570	556	604	590	620	643	629
Ala-X-(Me)Asp-Arg + NH_4	487	473	521	507	537	560	546
Mdha-Ala-X-(Me)Asp-Arg + H	553	539	587	573	603	626	612
Ala-X-(Me)Asp-Arg + H	470	456	504	490	520	543	529
X-(Me)Asp-Arg + H	399		433	419	449		
Mdha-Ala-X-(Me)Asp + H	397	383	431		447	470	456
Mdha-Ala-X + H	268	268	302	302	318	341	341
Mdha-Ala + H	155	155	155	155	155	155	155
Adda'-Glu-Mdha-Ala + H	446	446	446	446	446	446	446
Adda'-Glu-Mdha + H	375	375	375	375	375	375	375
Adda' + H	163	163	163	163	163	163	163
Glu-Mdha + H	213	213	213	213	213	213	213
Adda sidechain	135	135	135	135	135	135	135
Arg related ions	70/84/112/174	70/84/112/174	70/84/112/174	70/84/112/174	70/84/112/174	70/84/112/174	70/84/112/174
X immonium	86	86	120	120	136	159	159

[a] X = Position two amino acid; Adda' = Adda minus NH_2 and the sidechain ($C_9H_{11}O$); $CH_2NHCN_2H_3$ is a fragment of the Arg sidechain; Fragment ions containing NH_3 and CO losses have been omitted.

Appendix E.3: Tandem mass spectrometry fragment assignments for the CYN06 -RZ microcystin congeners observed by MALDI PSD and ESI CID.

Fragment Assignment [a]	**MC-RA** Z = 71 Da	**[Asp^3] MC-RA** Z = 71 Da	**MC-RAba** Z = 85 Da	**[Asp^3] MC-RAba** Z = 85 Da	**MC-RL** Z = 113 Da
M + H	953	939	967	953	995
M – H_2O + H	935	921	949	935	977
M – COOH + H	908	894	922	908	950
M – Z + H	882	868	882	868	882
M – $CH_2NHCN_2H_3$ + H	881	867	895	881	923
M – Glu + H	824	810	838	824	866
M – (Me)Asp + H	824	824	838	838	866
M – Adda sidechain + H	819	787	833	819	861
Mdha-Ala-Arg-(Me)Asp-Z + NH_4	528	514	542	528	570
Mdha-Ala-Arg-(Me)Asp-Z – H_2O + NH_4	510	496	524	510	552
Mdha-Ala-Arg-(Me)Asp-Z + H	511	497	525	511	553
Mdha-Ala-Arg-(Me)Asp – $CH_2NHCN_2H_3$ + H	368	354	368	354	368
Mdha-Ala-Arg-(Me)Asp + H	440	426	440	426	440
Mdha-Ala-Arg + H	311	311	311	311	311
Mdha-Ala + H	155	155	155		
Arg-(Me)Asp-Z + H	357	343		357	
Glu-Mdha-Ala-Arg – COOH + H	395	395	395	395	395
Glu-Mdha-Ala-Arg – $CH_2NHCN_2H_3$ + H	368	368	368	368	368
Glu-Mdha-Ala-Arg + H	440	440	440	440	440
Glu-Mdha + H	213		213		
Adda'-Glu-Mdha + H	375	375	375	375	375
Adda' + H	163	163	163		

[a] Z = Position four amino acid; Adda' = Adda minus NH_2 and the sidechain ($C_9H_{11}O$); $CH_2NHCN_2H_3$ is a fragment of the Arg sidechain.

Appendix E.4: Tandem mass spectrometry fragment assignments for the CYN06 -XA microcystin congeners observed by ESI CID.

Fragment Assignment [a]	**MC-LA** X = 113 Da	**[Asp^3] MC-LA** X = 113 Da	**MC-FA** X = 147 Da	**[Asp^3] MC-FA** X = 147 Da	**MC-YA** X = 163 Da	**MC-WA** X = 186 Da	**[Asp^3] MC-WA** X = 186 Da
M + H	910	896	944	930	960	983	969
M – H_2O + H	892	878	926	912	942	965	951
M – Mdha – H_2O + H	809	795	843	829		882	868
M – Adda sidechain + H	776	762	810	796	826	849	835
M – Adda sidechain – H_2O + H	758	744	792	778	808	831	817
M – Adda + H	597	583	631	617	647	670	656
M – Adda – H_2O + H	579	565	613	599	629	652	
Adda-Glu-Mdha-Ala-X-(Me)Asp – NH_3 + H	822	808	856	842	872	895	881
Adda-Glu-Mdha-Ala-X – NH_3 + H	693	693	727	727	743	766	766
Adda-Glu-Mdha-Ala – NH_3 + H	580	580	580	580	580	580	580
Adda-Glu-Mdha – NH_3 + H	509	509	509	509	509	509	509
Adda'-Glu-Mdha-Ala-X + H	559	559	593	593	609	632	632
Adda'-Glu-Mdha-Ala + H	446	446	446	446	446	446	446
Adda'-Glu-Mdha + H	375	375	375	375	375	375	375
Mdha-Ala-X-(Me)Asp-Ala + NH_4	485	471	519	505	535	558	
Ala-X-(Me)Asp-Ala + NH_4	402	388	436	422	452	475	461
X-(Me)Asp-Ala + NH_4	331	317	365	351	381	404	390
Mdha-Ala-X-(Me)Asp-Ala + H	468	454	502	334	518	541	527
Ala-X-(Me)Asp-Ala + H	385	371	419	405	435	458	444
X-(Me)Asp-Ala + H	314	300	348	488	364	387	373

[a] X = Position two amino acid; Adda' = Adda minus NH_2 and the sidechain ($C_9H_{11}O$).

Appendix E.5: Tandem mass spectrometry fragment assignments for the CYN06 -XAba microcystin congeners observed by ESI CID.

Fragment Assignment [a]	**MC-LAba** X = 113 Da	**MC-FAba** X = 147 Da	**MC-WAba** X = 186 Da
M + H	924	958	997
M – H_2O + H	906	940	979
M – Mdha – H_2O + H	823		896
M – Glu or Masp – H_2O + H	777		
M – Adda sidechain + H	790	824	863
M – Adda sidechain – H_2O + H	772	806	845
M – Adda + H	611	645	684
M – Adda – H_2O + H	593	627	666
Adda-Glu-Mdha-Ala-X-Masp – NH_3 + H			895
Adda-Glu-Mdha-Ala-X – NH_3 + H	693	727	766
Adda-Glu-Mdha-Ala – NH_3 + H	580	580	580
Adda-Glu-Mdha – NH_3 + H	509	509	509
Adda'-Glu-Mdha-Ala-X + H	559	593	632
Adda'-Glu-Mdha-Ala + H	446	446	446
Adda'-Glu-Mdha + H	375	375	375
Mdha-Ala-X-Masp-Aba + NH_4	499	533	572
Ala-X-Masp-Aba + NH_4	416	450	489
X-Masp-Aba + NH_4	345	379	418
Mdha-Ala-X-Masp-Aba + H	482	516	555
Ala-X-Masp-Aba + H	399	433	472
X-Masp-Aba + H	328	362	401

[a] X = Position two amino acid; Adda' = Adda minus NH_2 and the sidechain ($C_9H_{11}O$).

Appendix E.6: Tandem mass spectrometry fragment assignments for the CYN06 -XL microcystin congeners observed by ESI CID.

Fragment Assignment [a]	**MC-LL** X = 113 Da	**MC-FL** X = 147 Da	**MC-WL** X = 186 Da
M + H	952	986	1025
M – NH_3 + H	935	969	1008
M – H_2O + H	934	968	1007
M – Glu or Masp + H	823		896
M – Adda sidechain + H	818	852	891
M – Adda sidechain – H_2O + H	800	834	873
M – Adda + H	639	673	712
M – Adda – H_2O + H	621	655	694
Adda-Glu-Mdha-Ala-X – NH_3 + H	693	727	766
Adda-Glu-Mdha-Ala – NH_3 + H	580	580	580
Adda-Glu-Mdha – NH_3 + H	509	509	509
Glu-Mdha-Ala-X + H	397	431	470
Adda'-Glu-Mdha-Ala-X + H	559	593	632
Adda'-Glu-Mdha-Ala + H	446	446	446
Adda'-Glu-Mdha + H	375	375	375
Mdha-Ala-X-Masp-Leu + NH_4		561	600
Ala-X-Masp-Leu + NH_4		478	517
X-Masp-Leu + NH_4		407	446
Unknown fragment ion	440	474	513
Unknown fragment ion	535	535	535
Mdha-Ala-X-Masp-Leu + H	509	544	583
Ala-X-Masp-Leu + H	426	461	500
X-Masp-Leu + H	355	390	429

[a] X = Position two amino acid; Adda' = Adda minus NH_2 and the sidechain ($C_9H_{11}O$).

Appendix F.1: Advanced Marfey's amino acid analysis of standard amino acids derivatised with L-FDLA **(A)** and DL-FDLA **(B)**.

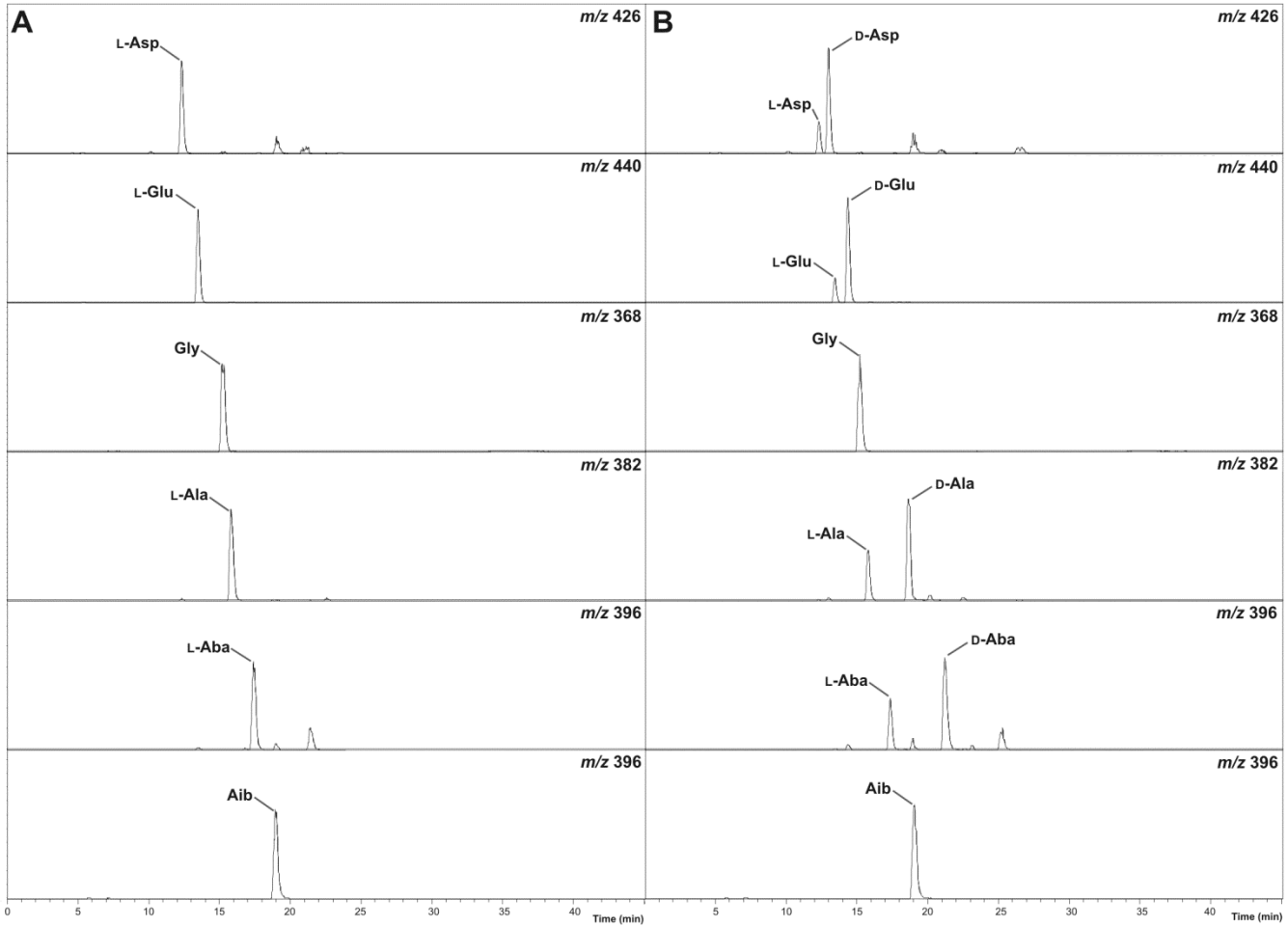

Appendix F.1 continued: Advanced Marfey's amino acid analysis of standard amino acids derivatised with L-FDLA **(A)** and DL-FDLA **(B)**.

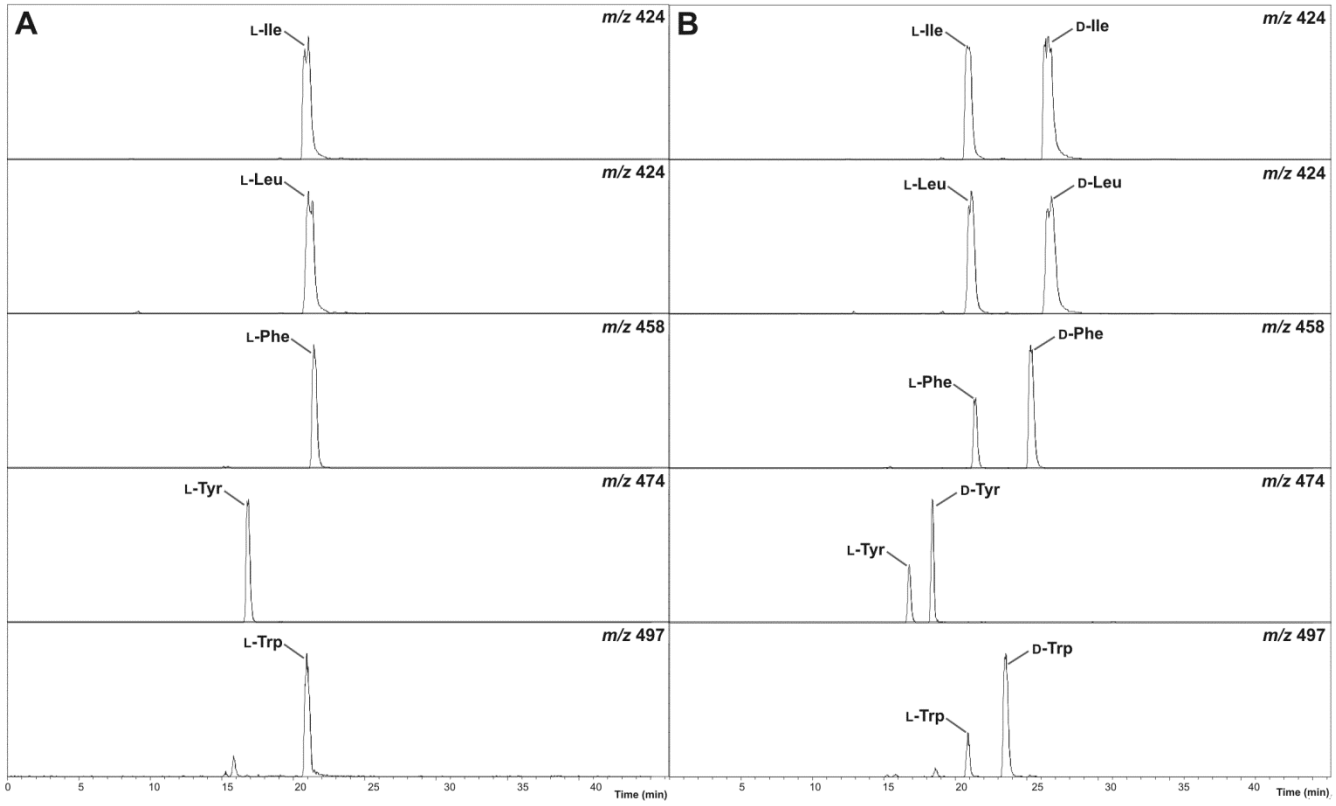

Appendix F.2: Advanced Marfey's amino acid analysis of standard ornithine and arginine derivatised with L-FDLA **(A)**, D-FDLA **(B)** and DL-FDLA **(C)**.

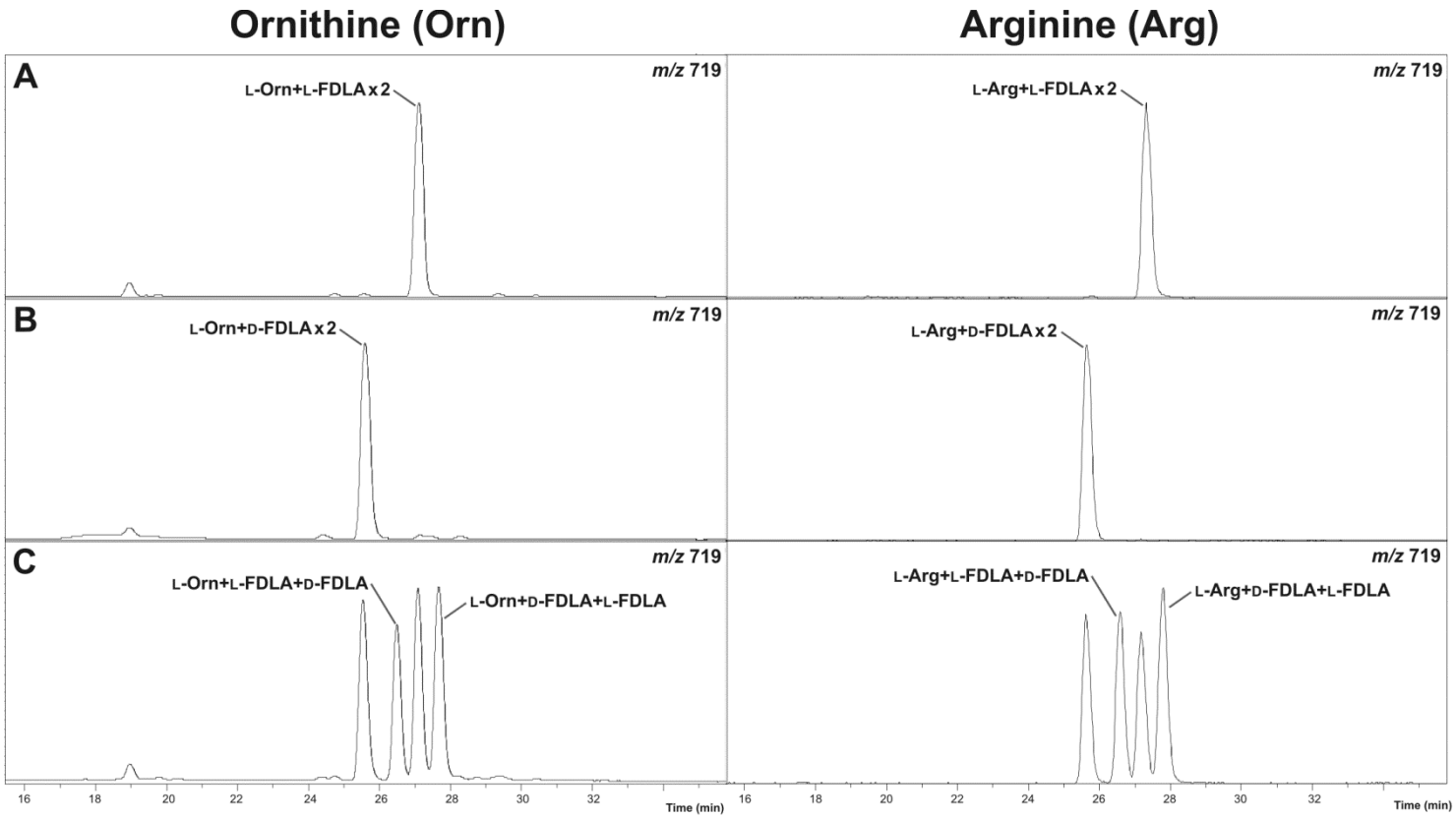

Appendix F.3: Advanced Marfey's amino acid analysis of hydrolysed MC-LR (**7**) derivatised with L-FDLA **(A)** and DL-FDLA **(B)**.

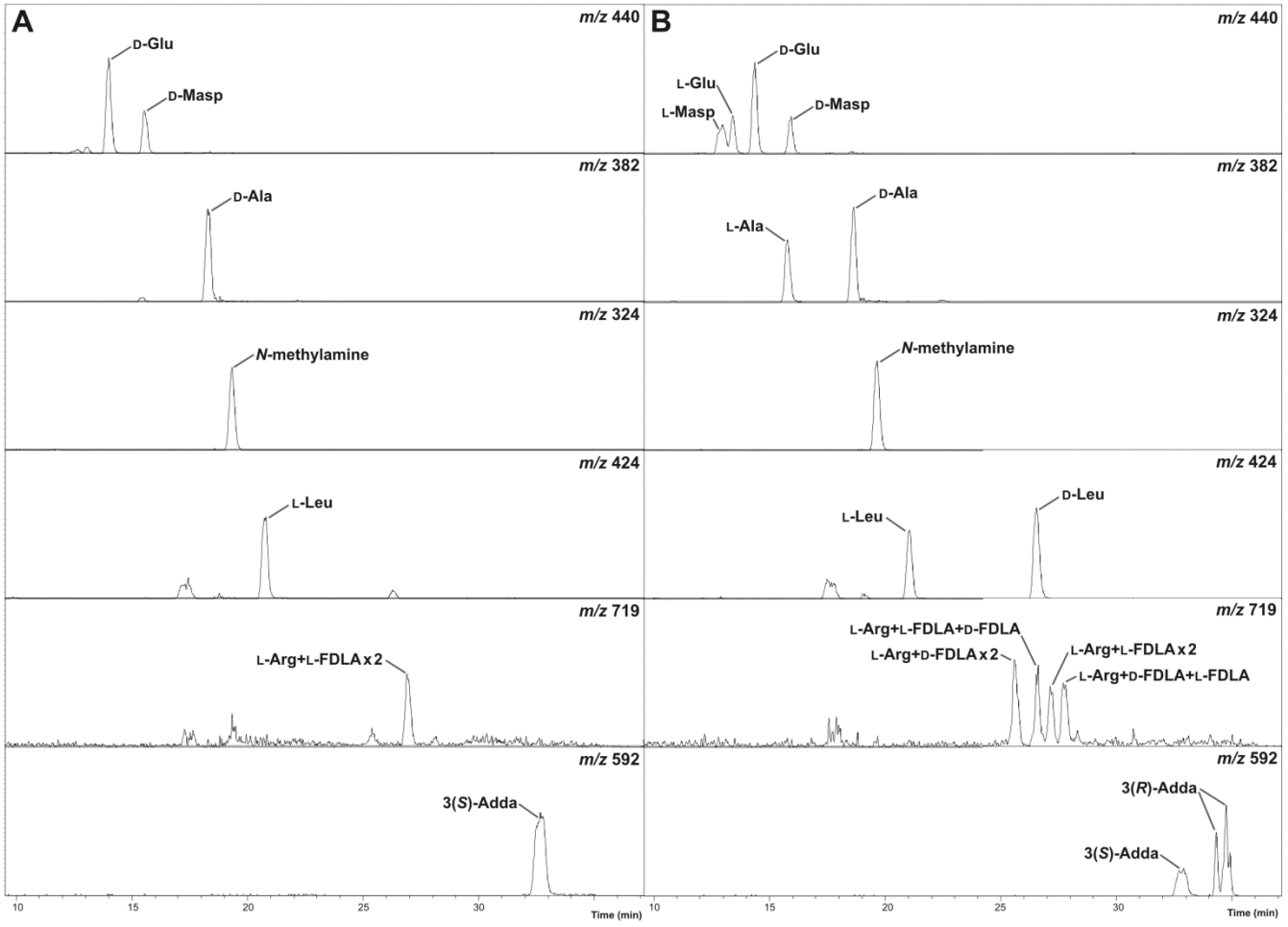

Appendix F.4: Advanced Marfey's amino acid analysis of hydrolysed MC-FA (**163**) derivatised with L-FDLA **(A)** and DL-FDLA **(B)**.

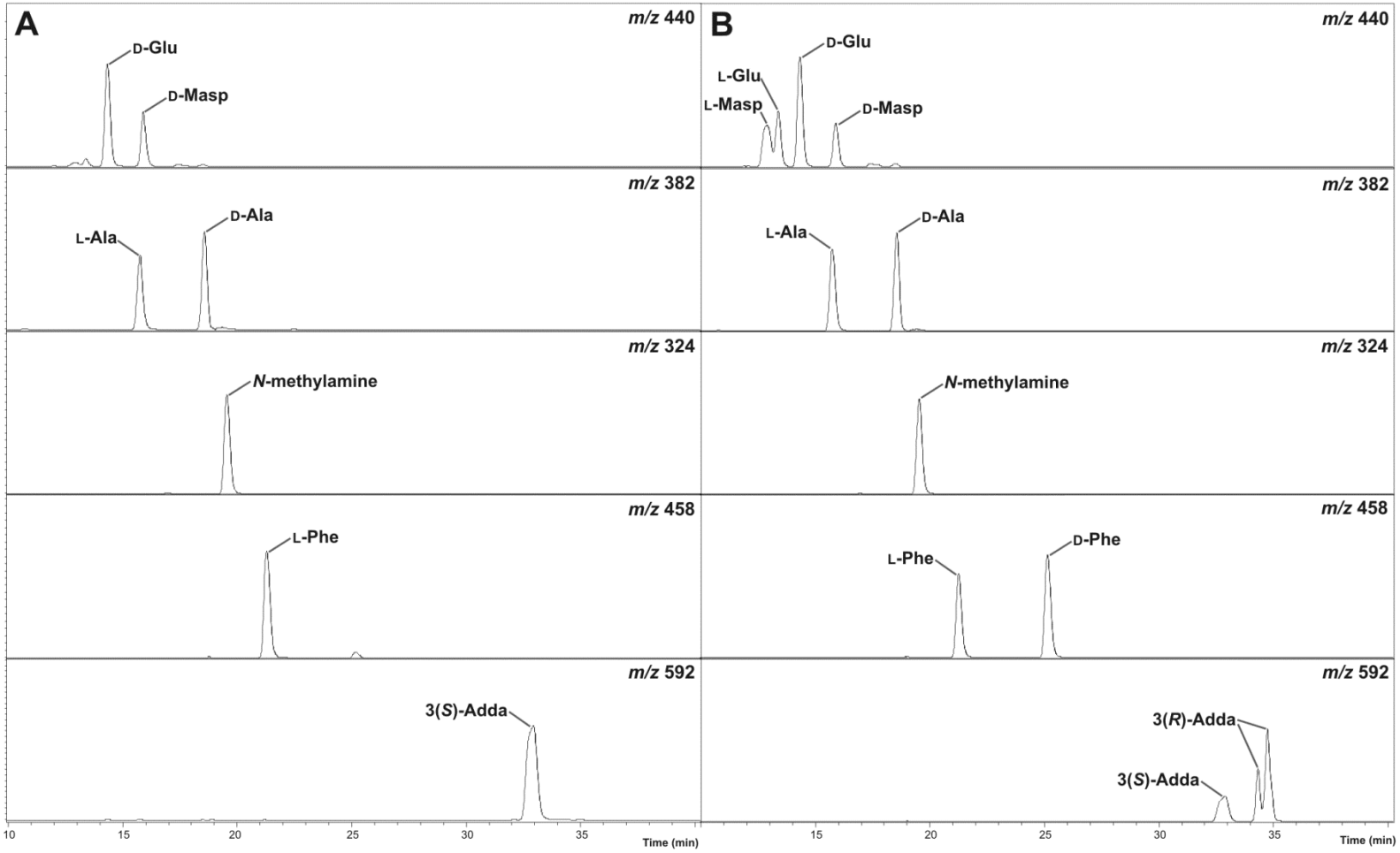

Appendix F.5: Advanced Marfey's amino acid analysis of hydrolysed MC-WA (**165**) derivatised with L-FDLA **(A)** and DL-FDLA **(B)**.

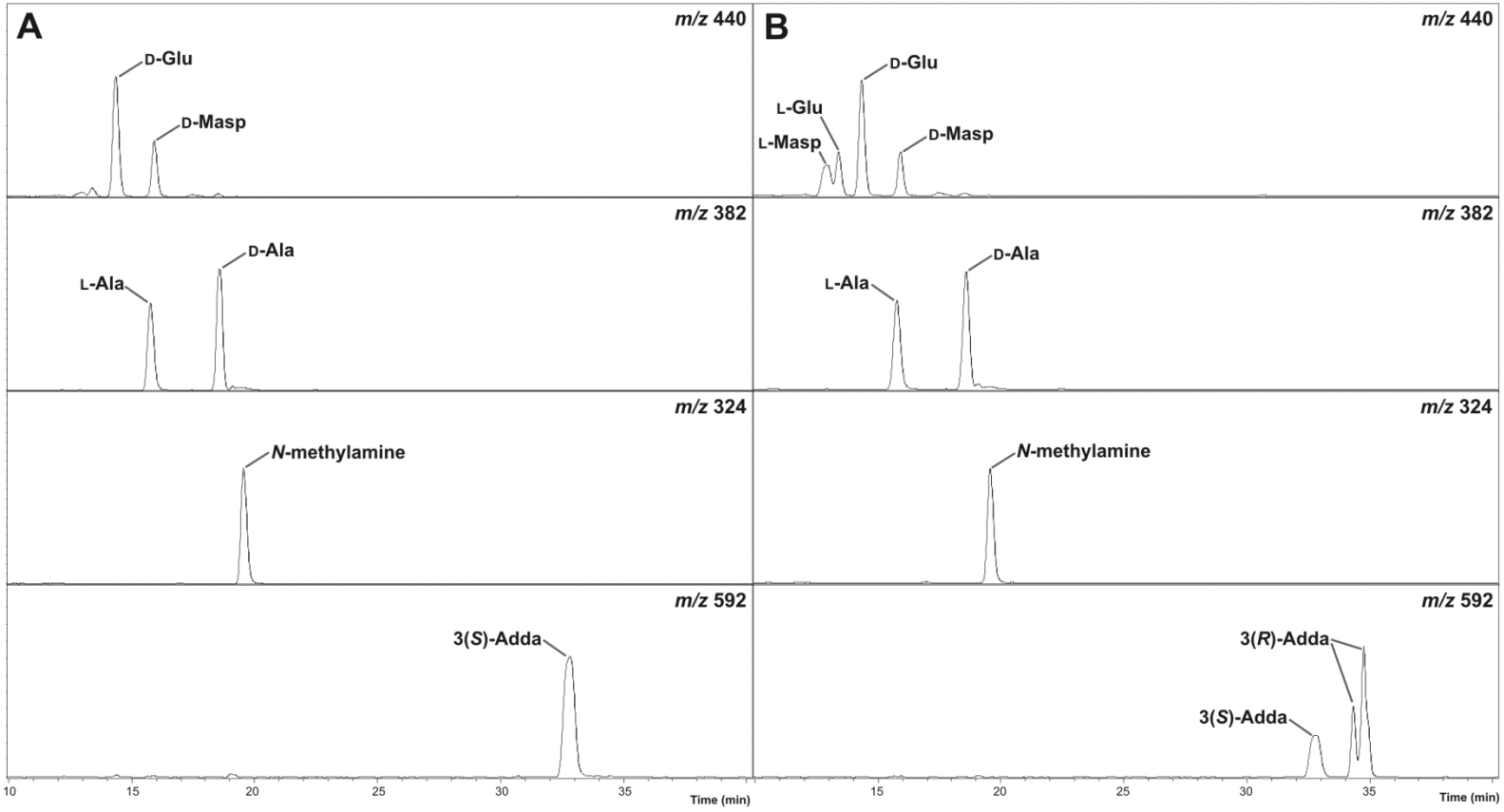

Appendix F.6: Advanced Marfey's amino acid analysis of hydrolysed MC-RA (**16**) derivatised with L-FDLA **(A)** and DL-FDLA **(B)**.

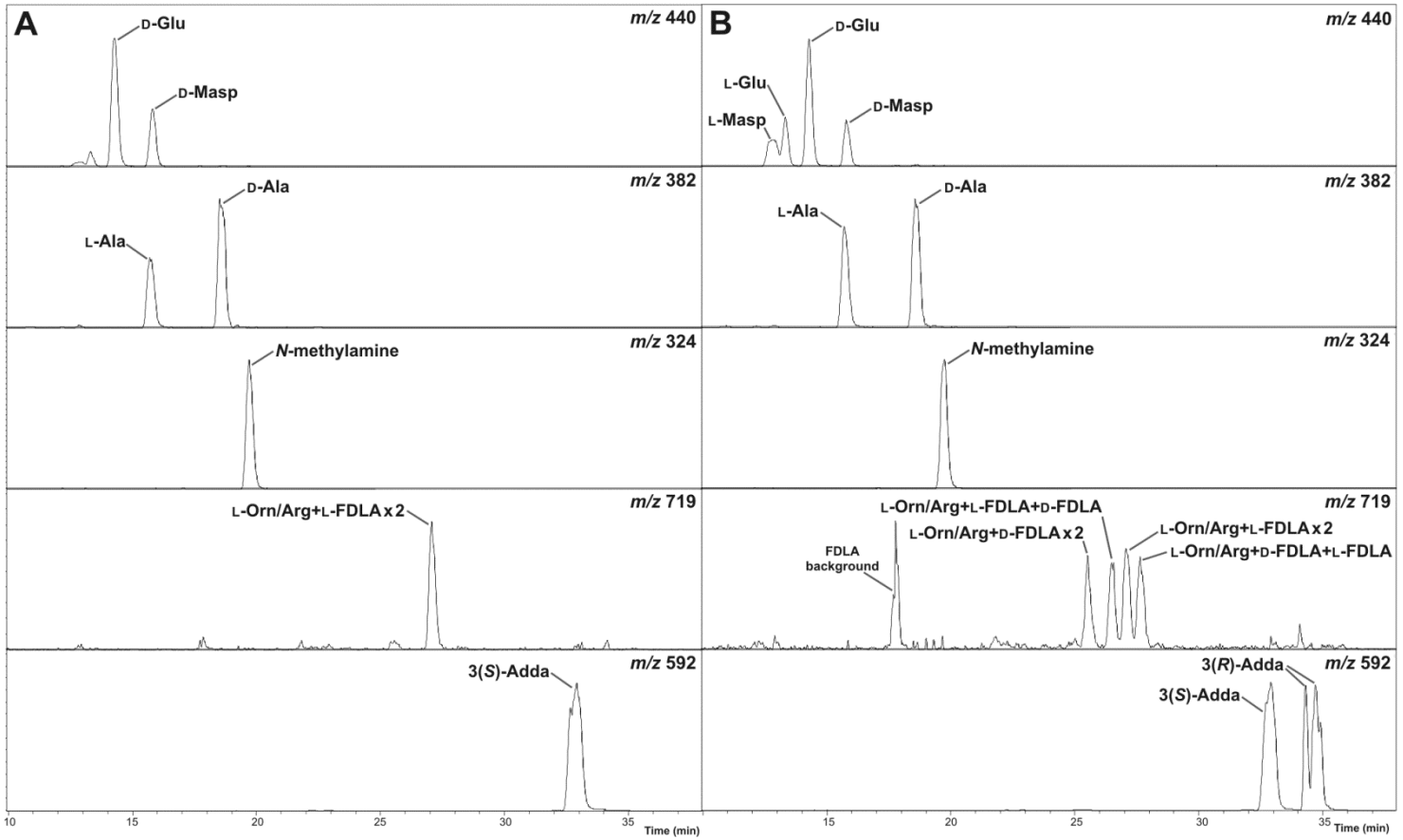

Appendix F.7: Advanced Marfey's amino acid analysis of hydrolysed MC-RAba (**19**) derivatised with L-FDLA **(A)** and DL-FDLA **(B)**.

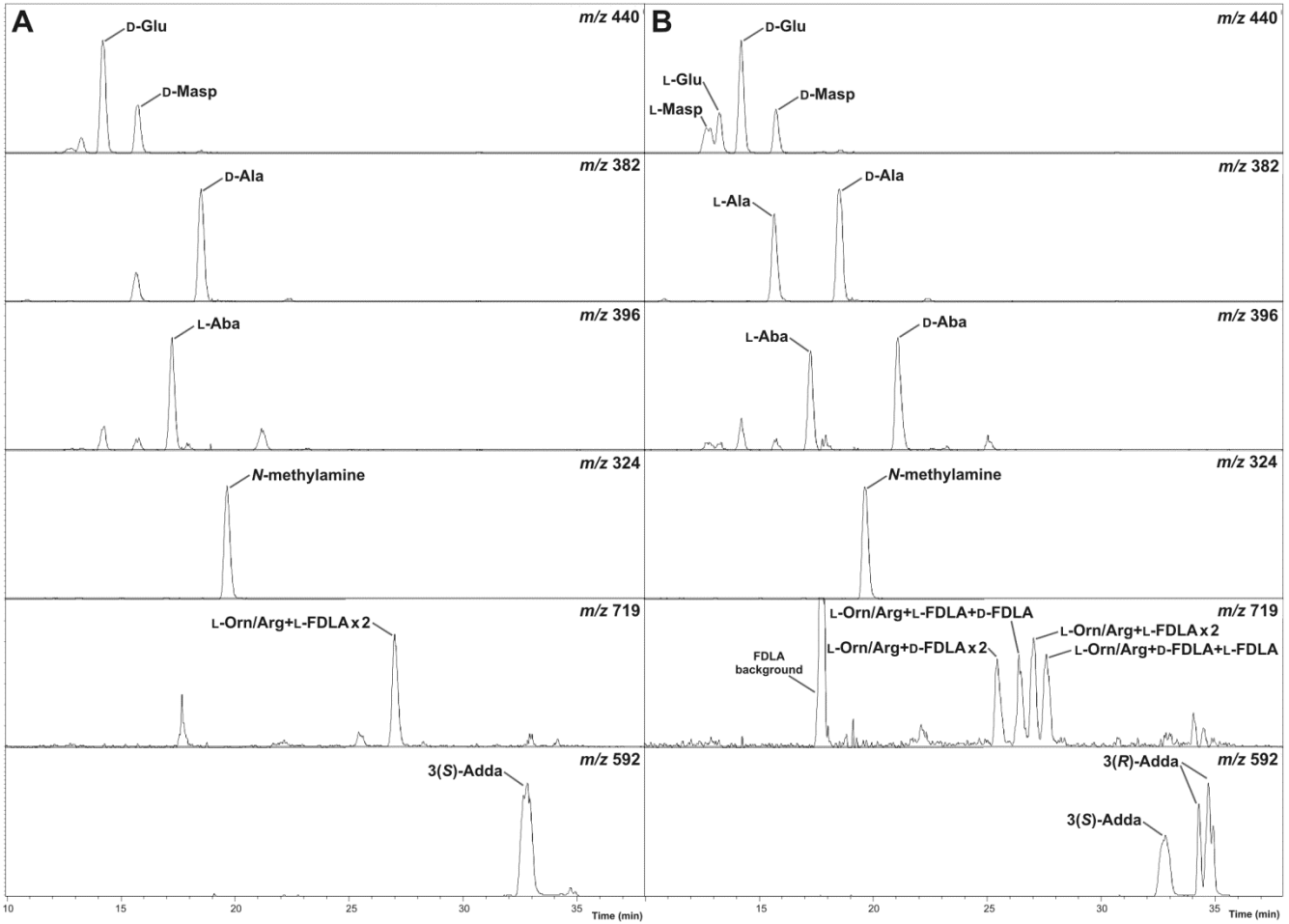

Appendix F.8: Advanced Marfey's amino acid analysis of a hydrolysate of the Antarctic -LR microcystin congeners derivatised with L-FDLA **(A)** and DL-FDLA **(B)**.

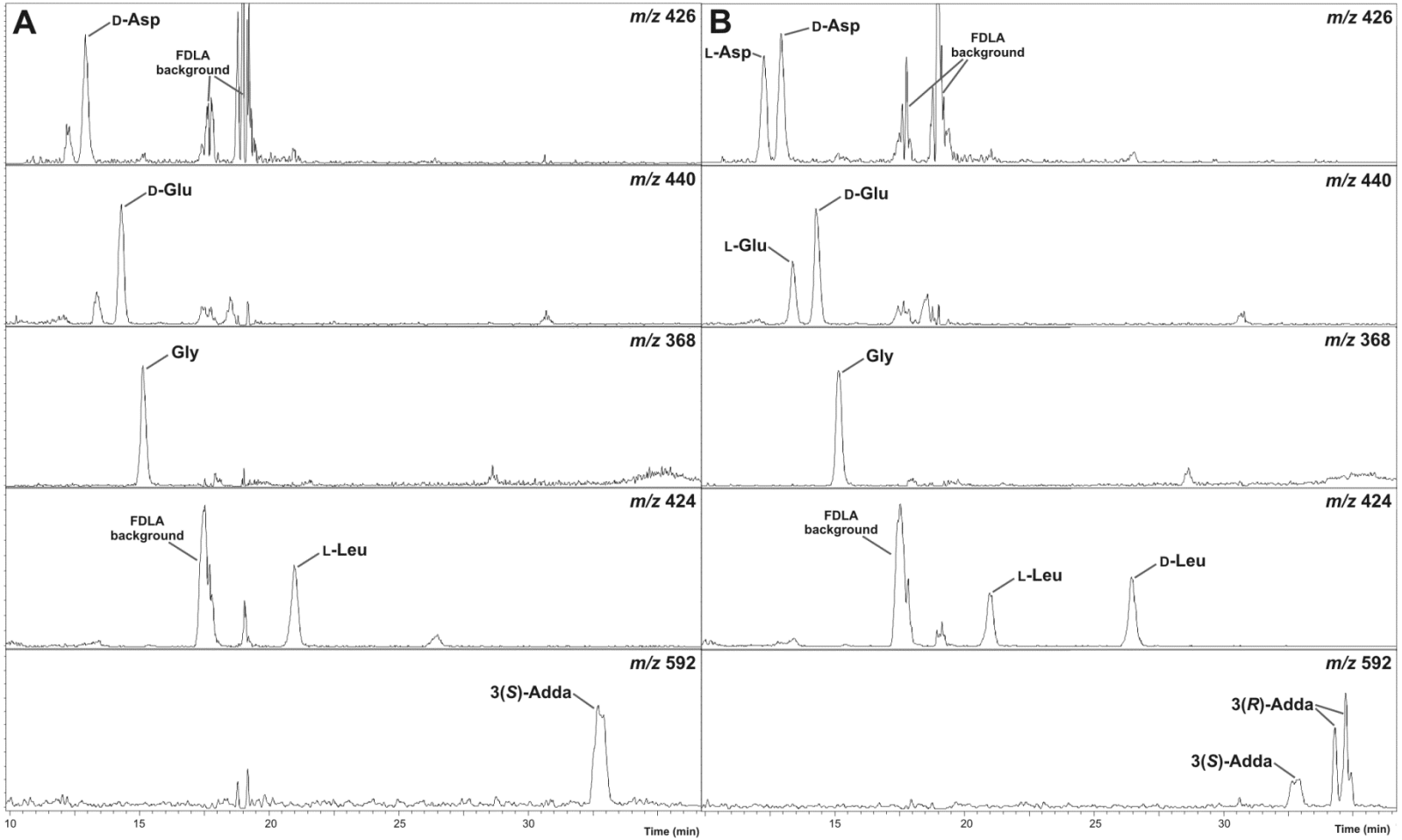

Appendix F.9: Advanced Marfey's amino acid analysis of a hydrolysate of the Antarctic -RR microcystin congeners derivatised with L-FDLA **(A)** and DL-FDLA **(B)**.

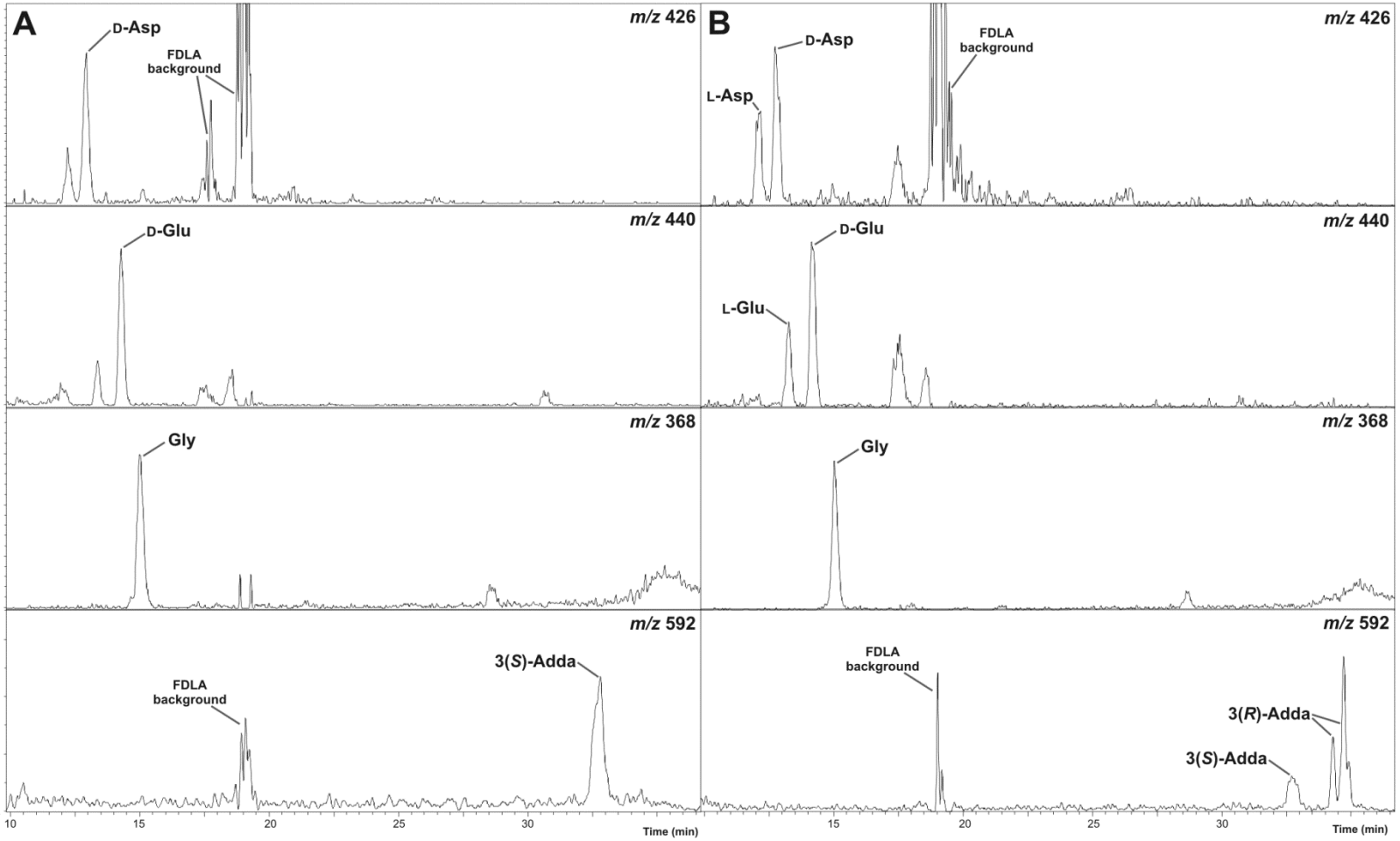

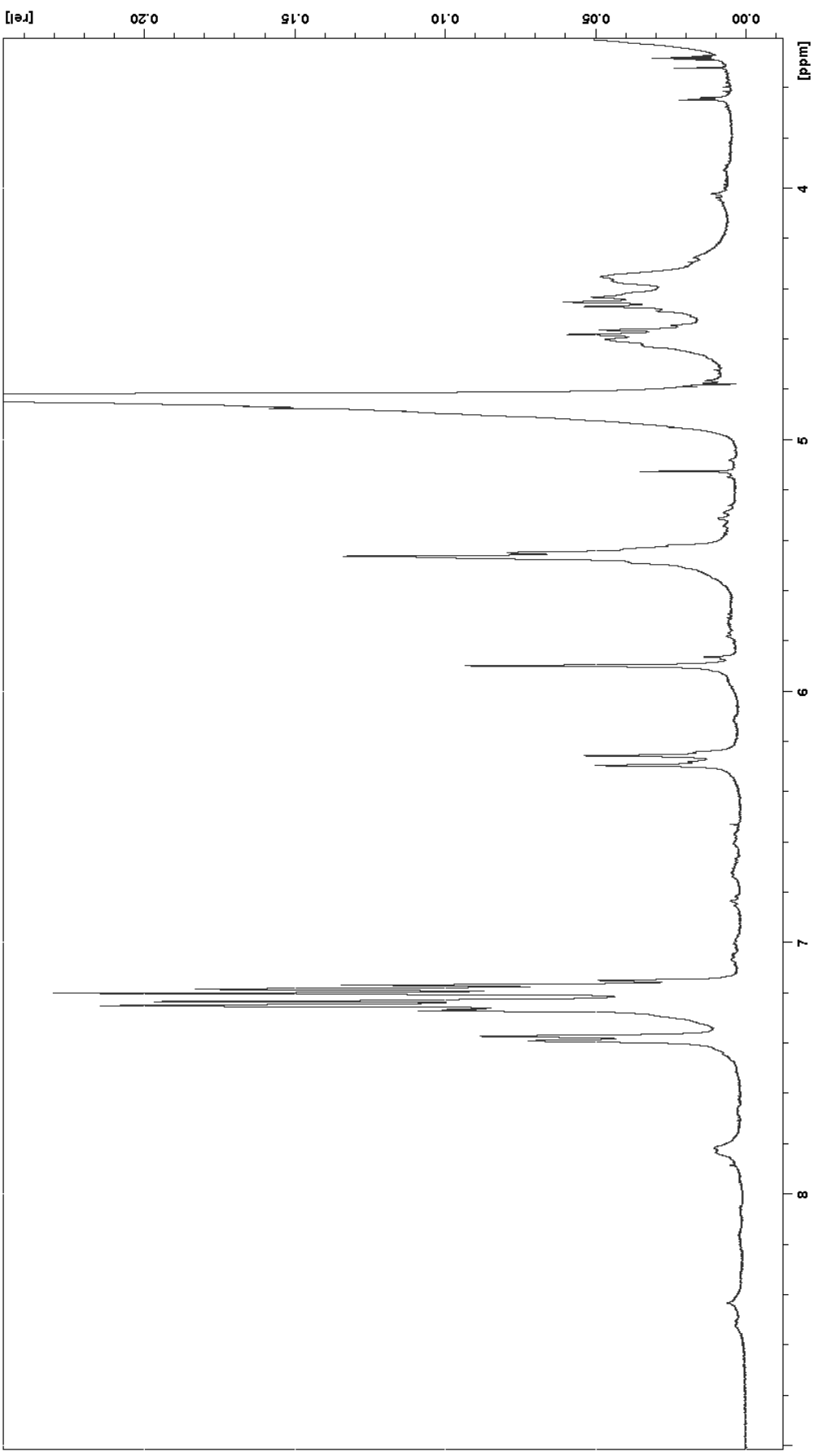

Appendix G.1: Downfield region for the ^{1}H NMR spectrum of MC-FA (**163**) in CD_3OD.

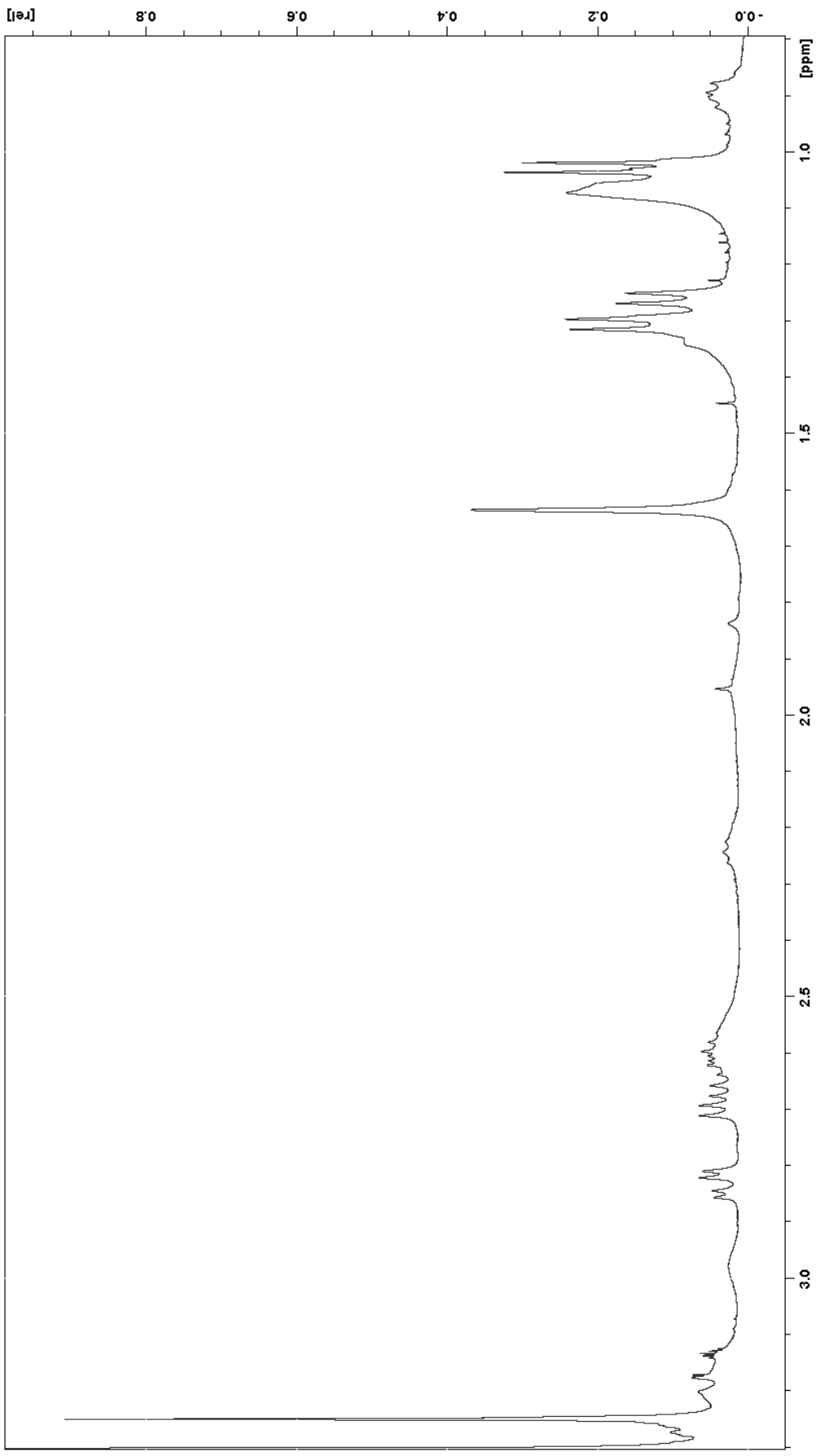

Appendix G.2: Upfield region for the ^{1}H NMR spectrum of MC-FA **(163)** in CD_3OD.

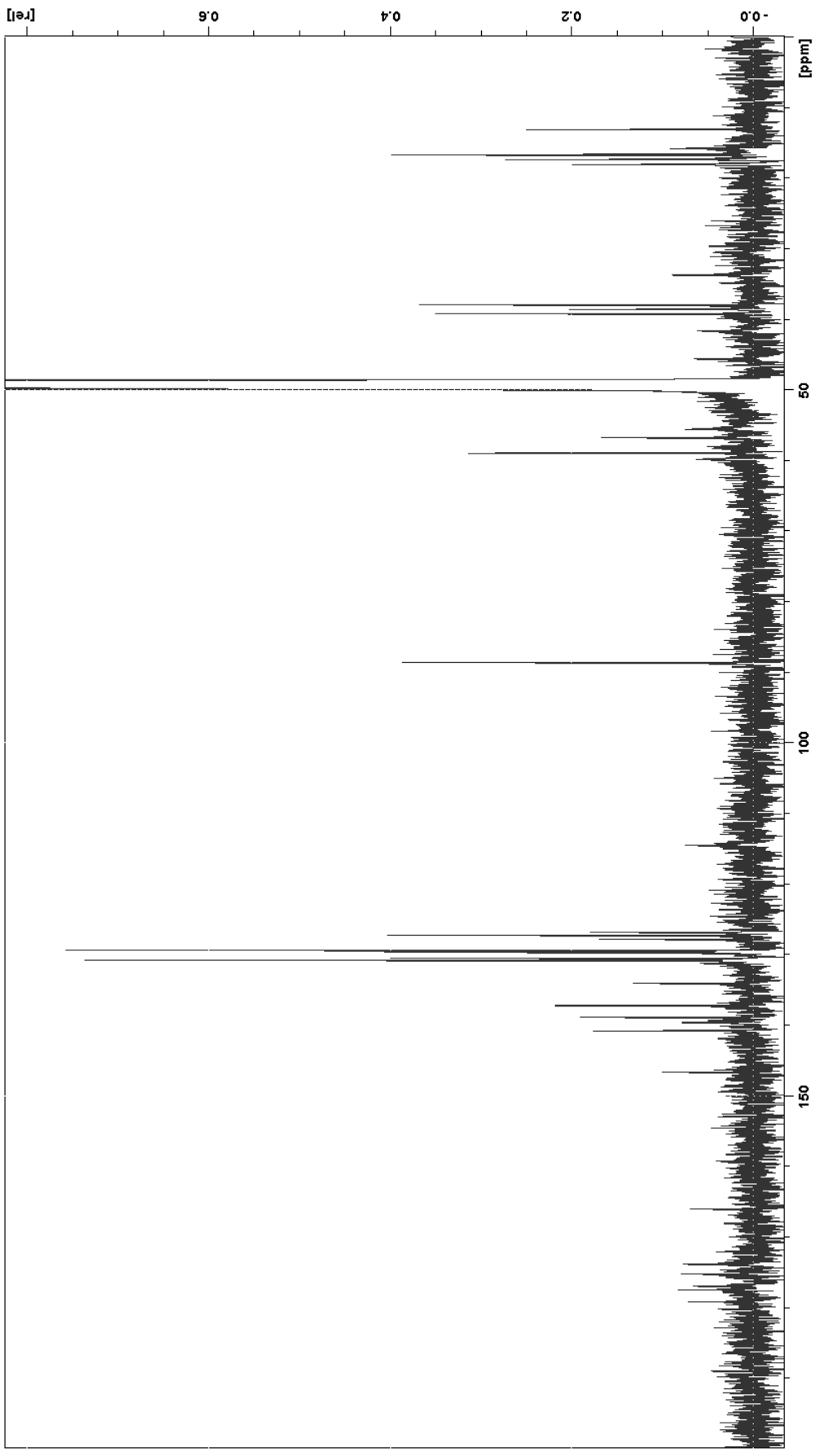

Appendix G.3: ^{13}C NMR spectrum of MC-FA **(163)** in CD_3OD.

Appendix G.4: ^{13}C DEPT NMR spectra of MC-FA (**163**) in CD_3OD; DEPT-135 **(A)**, DEPT-90 **(B)** and DEPT-45 **(C)**.

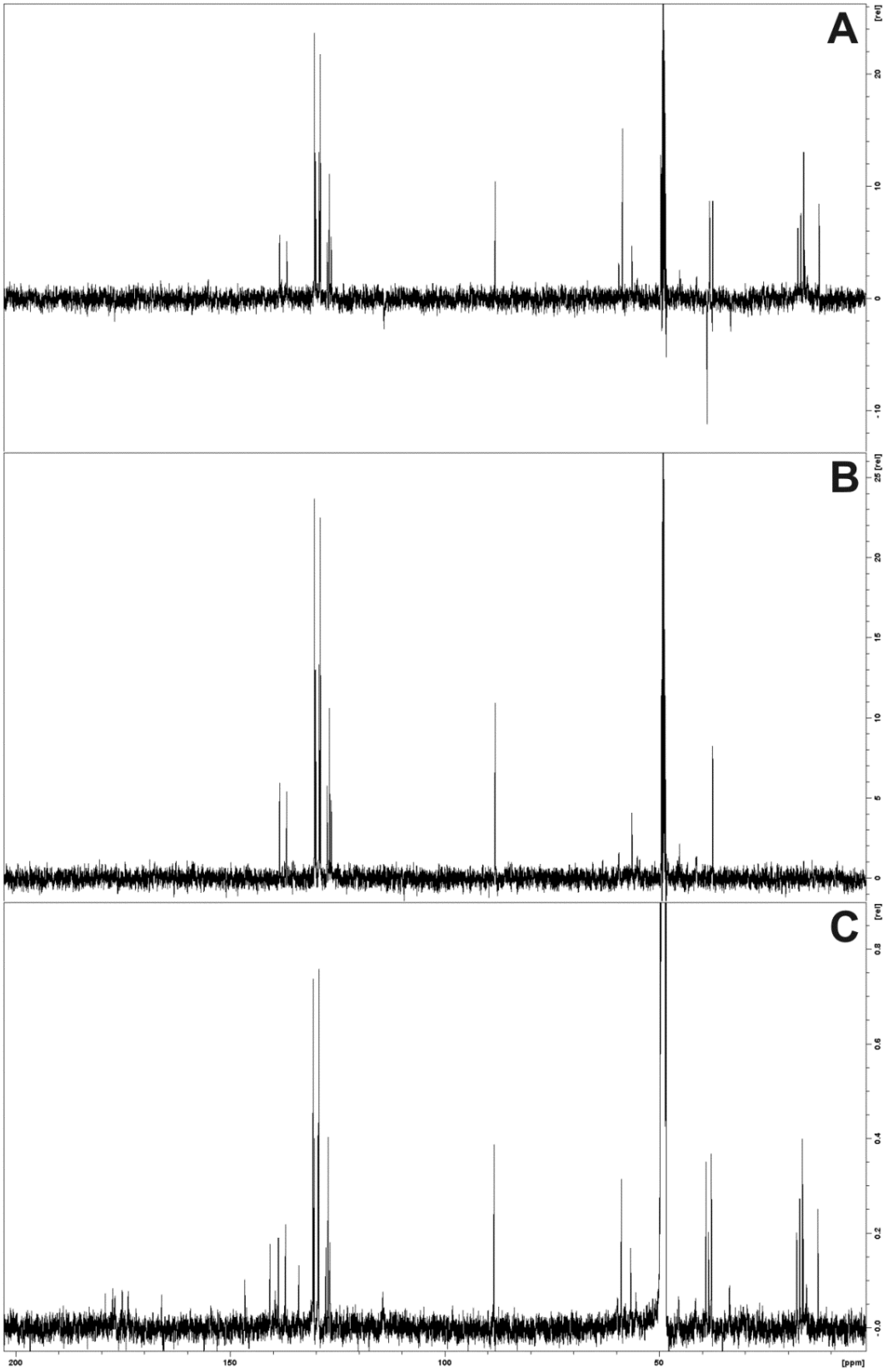

Appendix G

Appendix G.5: HSQC NMR spectrum of MC-FA (**163**) in CD_3OD.

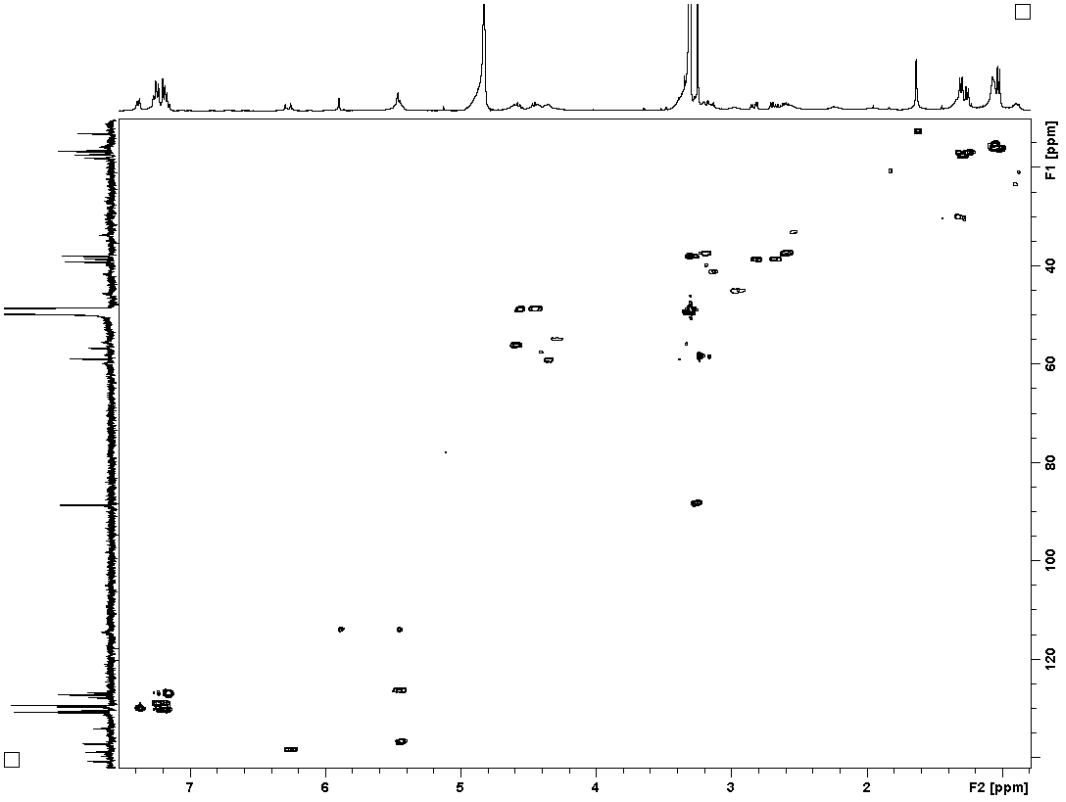

Appendix G.6: HMBC NMR spectrum of MC-FA (**163**) in CD_3OD.

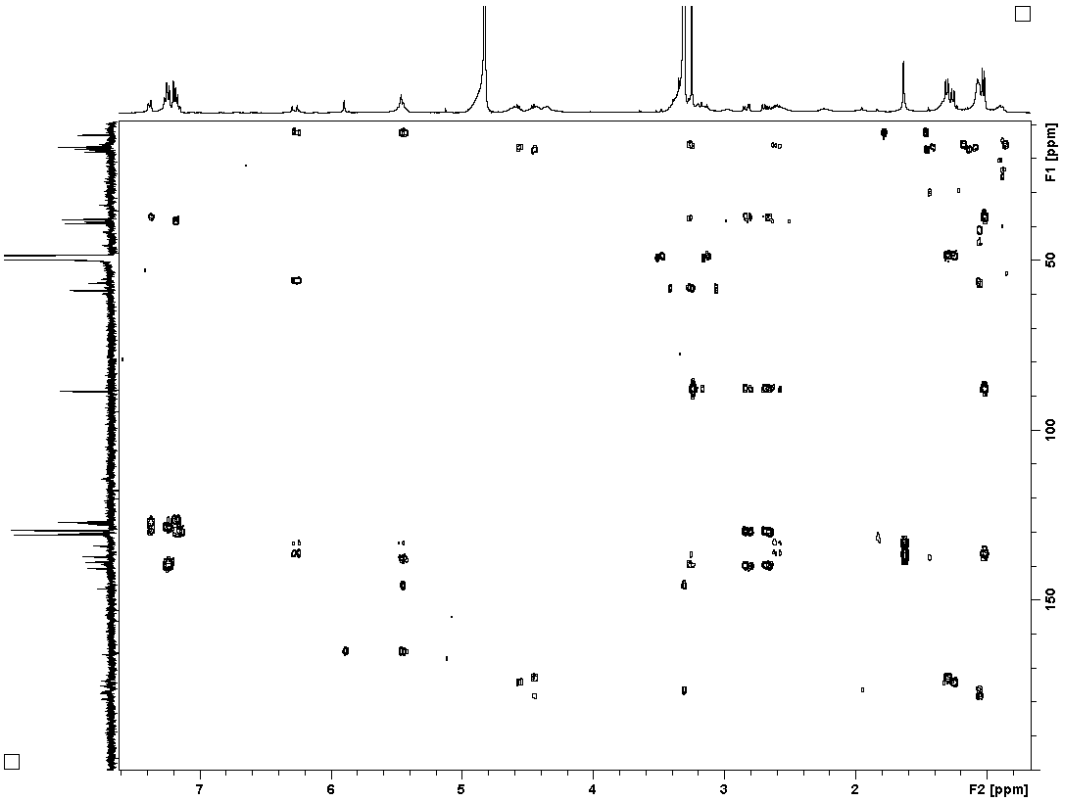

Appendix G.7: COSY NMR spectrum of MC-FA (**163**) in CD_3OD.

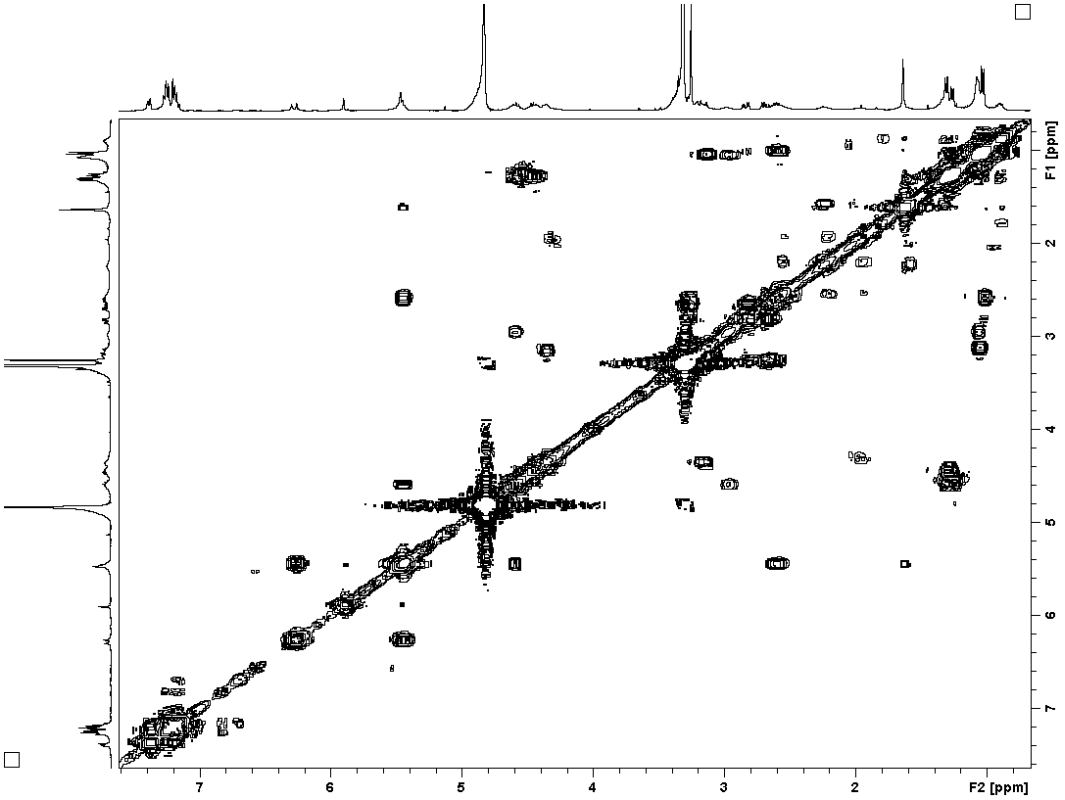

Appendix G.8: ROESY NMR spectrum of MC-FA (**163**) in CD_3OD.

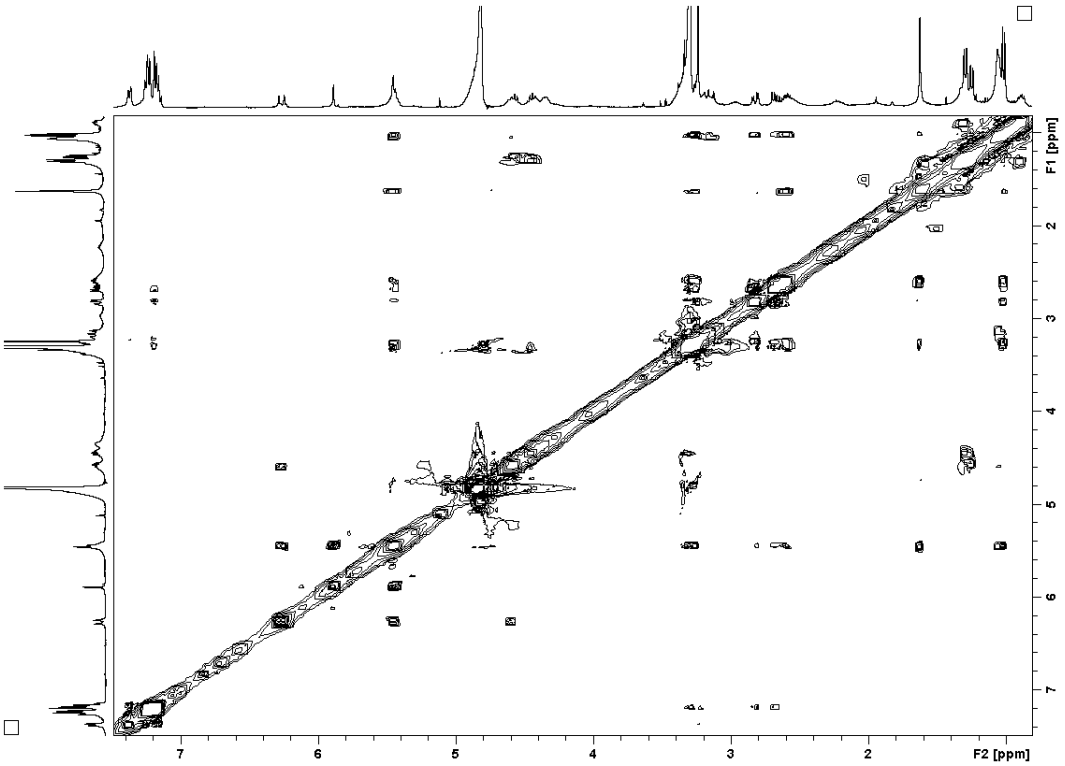

Appendix G

Appendix G.9: Selective TOCSY experiment to assign the aromatic signals from the phenylalanine residue of MC-FA (**163**) in CD_3OD. The 7.37 ppm proton signal was irradiated using a mixing time of 10 ms **(A)** and 50 ms **(B)**.

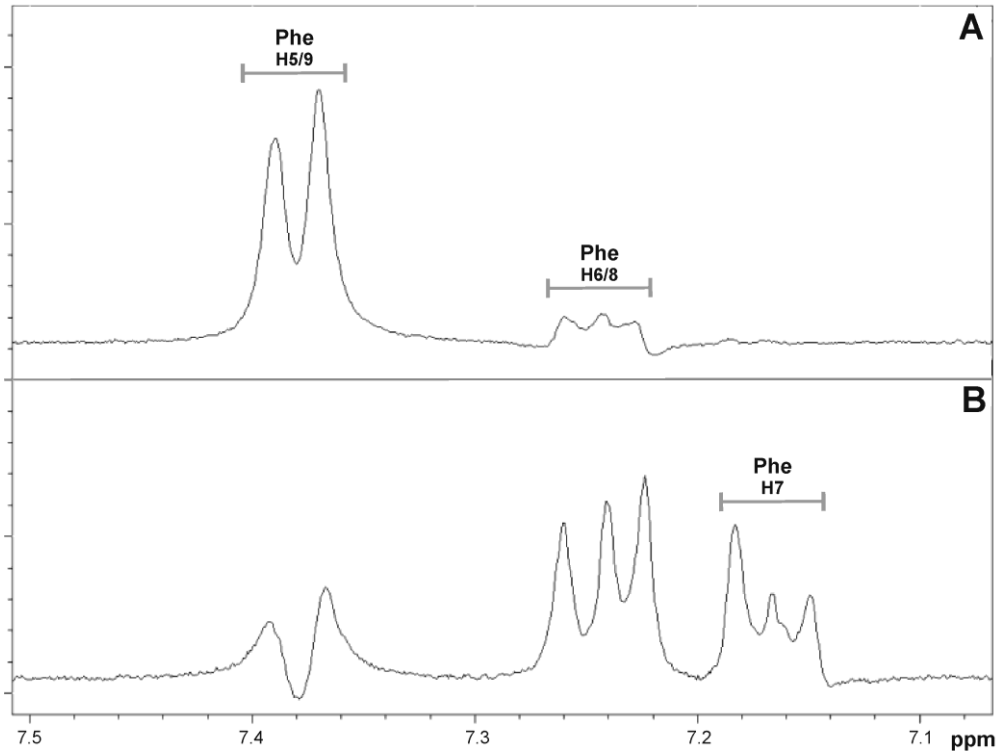

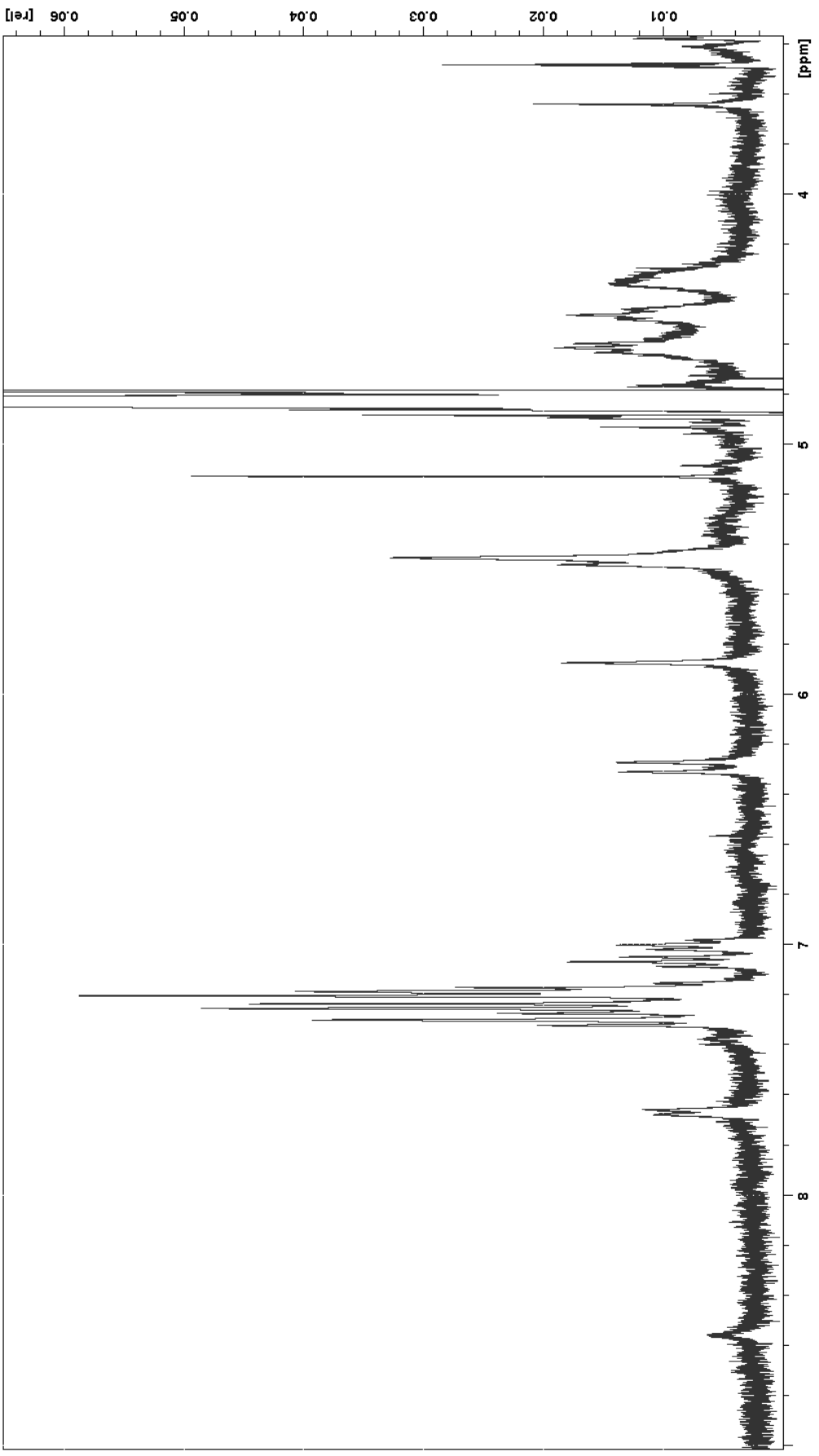

Appendix H.1: Downfield region for the ^{1}H NMR spectrum of MC-WA (**165**) in CD_3OD.

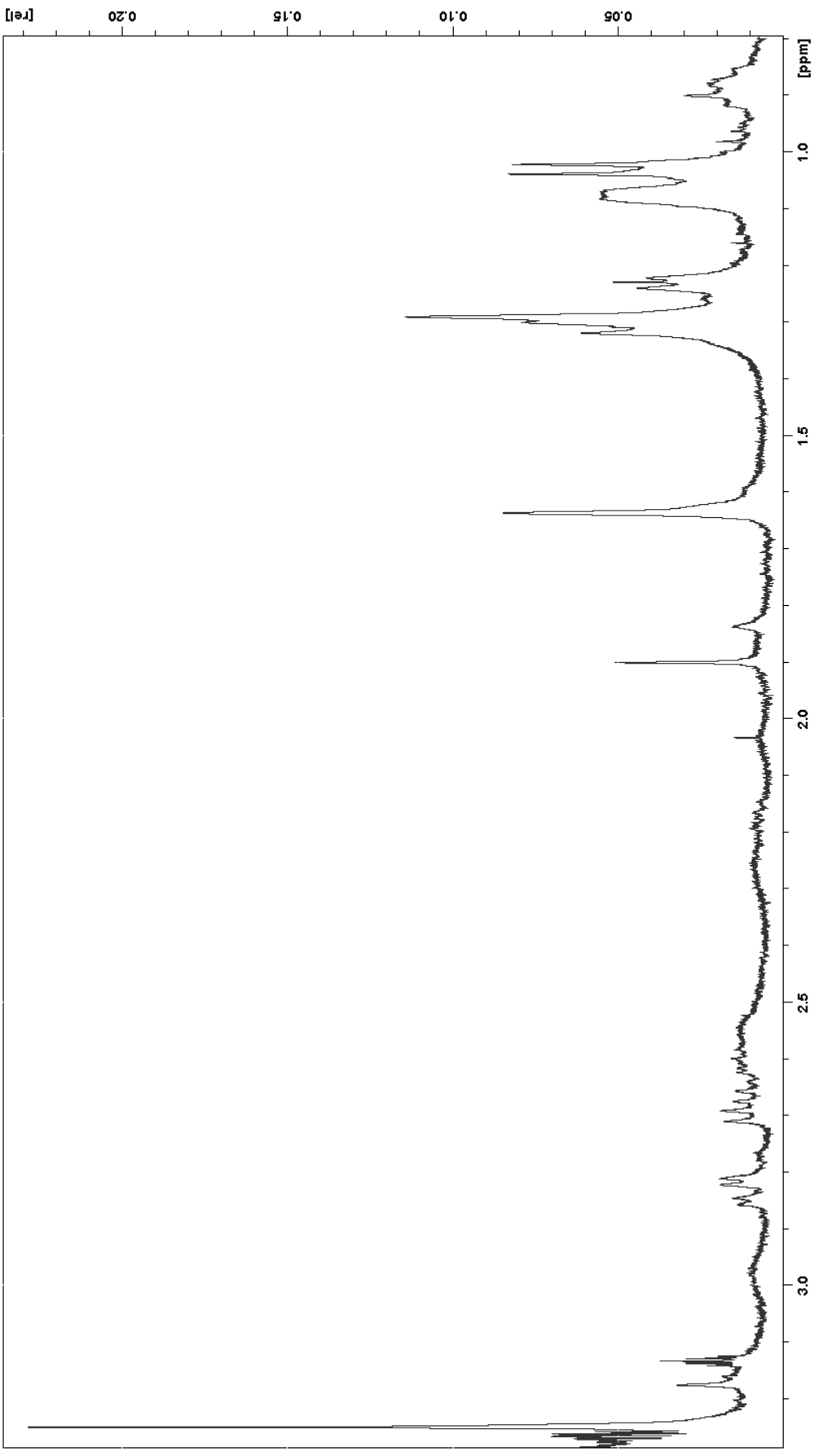

Appendix H.2: Upfield region for the ^{1}H NMR spectrum of MC-WA (**165**) in CD_3OD.

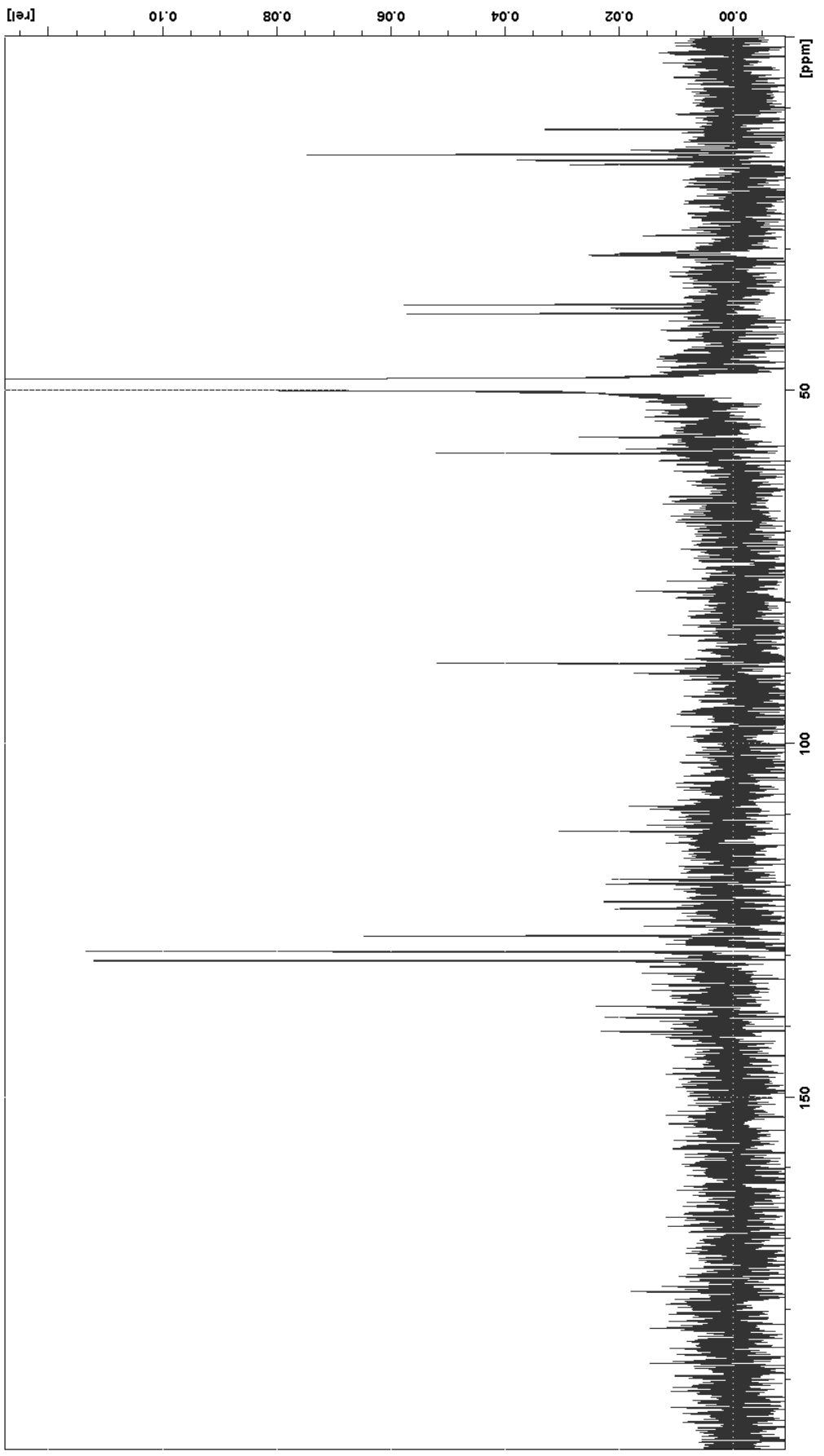

Appendix H.3: ^{13}C NMR spectrum of MC-WA (**165**) in CD_3OD.

Appendix H

Appendix H.4: ^{13}C DEPT NMR spectra of MC-WA (**165**) in CD_3OD; DEPT-135 **(A)**, DEPT-90 **(B)** and DEPT-45 **(C)**.

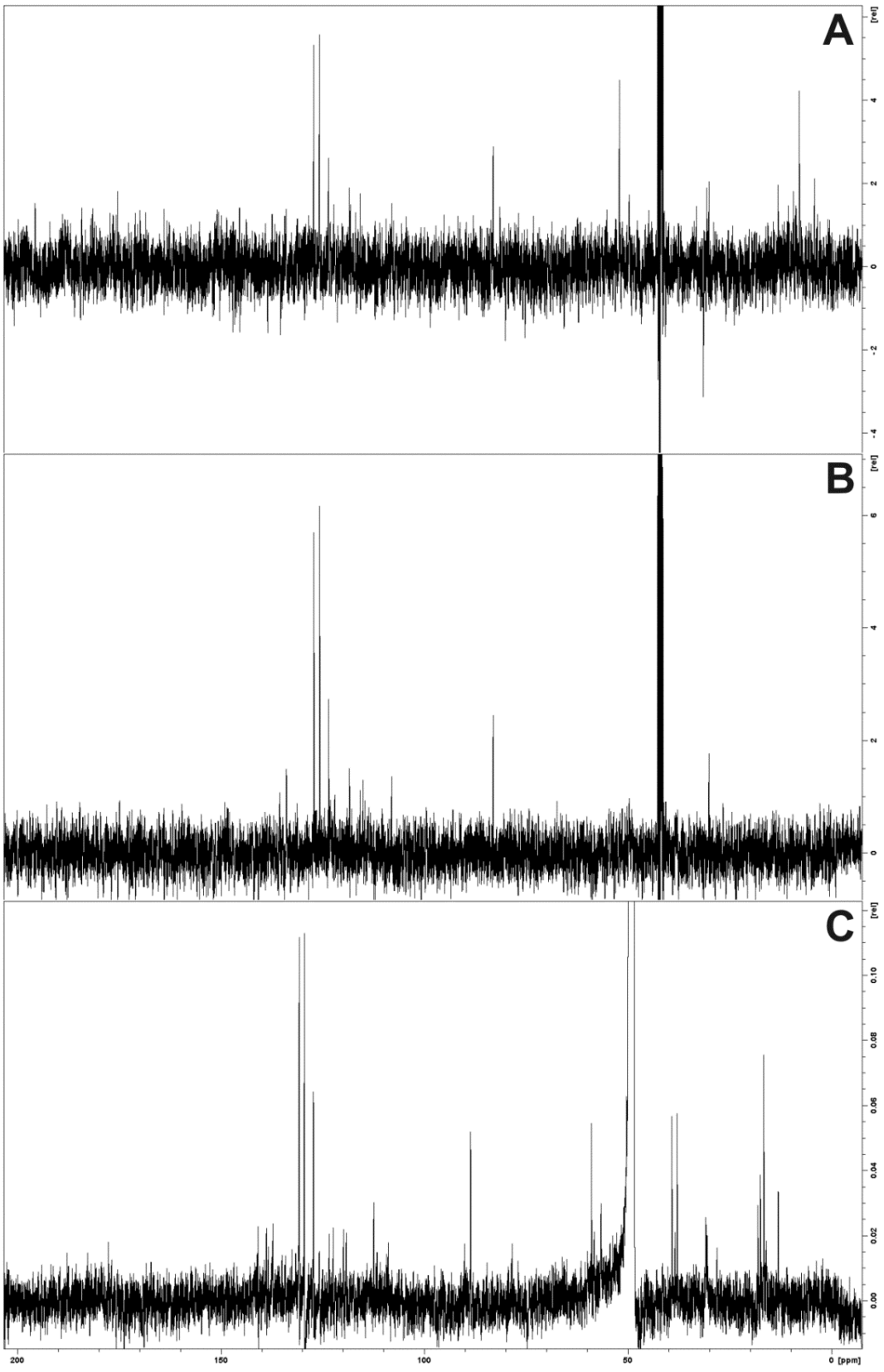

Appendix H.5: HSQC NMR spectrum of MC-WA (**165**) in CD_3OD.

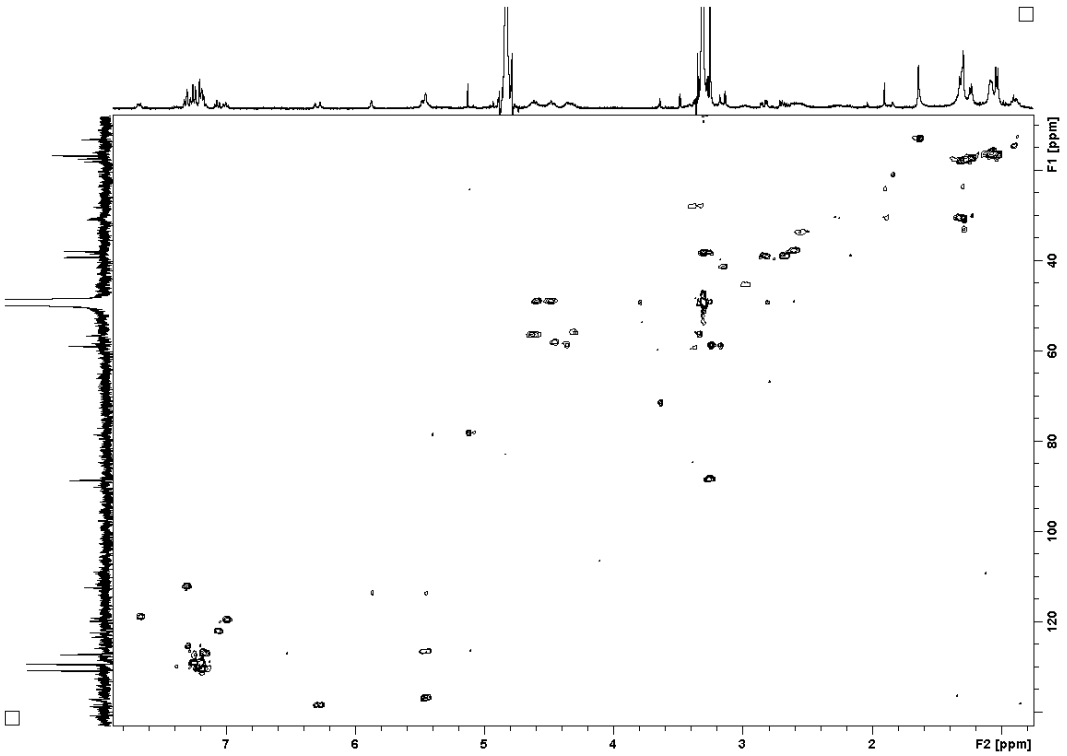

Appendix H.6: HMBC NMR spectrum of MC-WA (**165**) in CD_3OD.

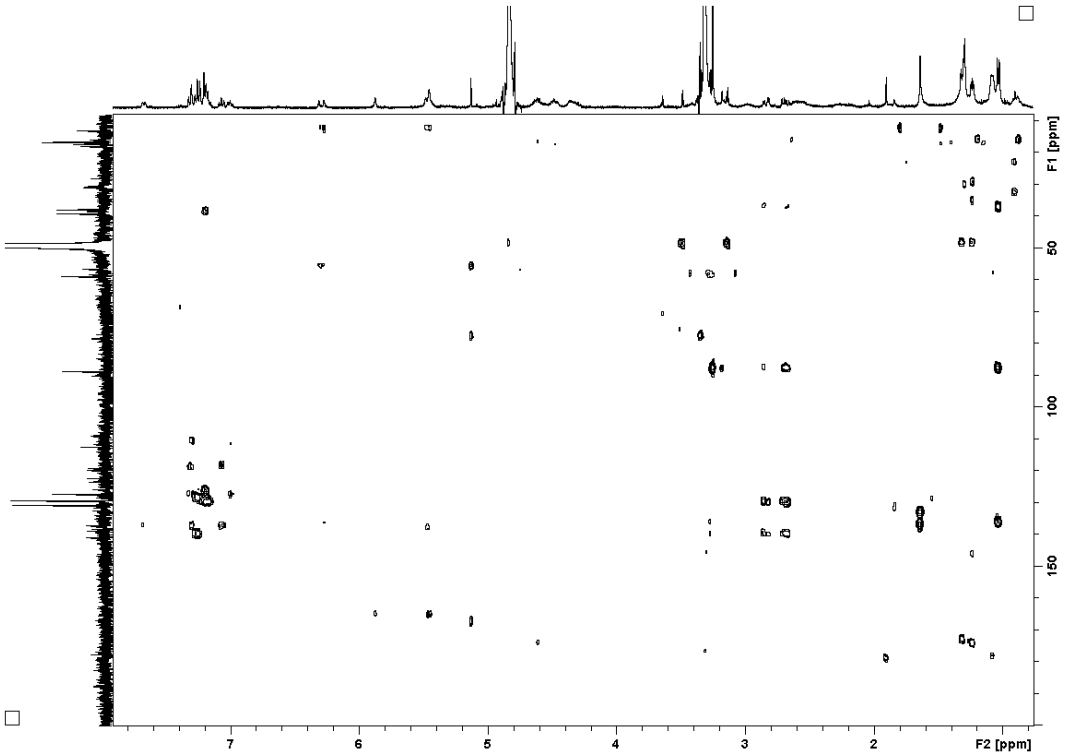

Appendix H.7: COSY NMR spectrum of MC-WA (**165**) in CD_3OD.

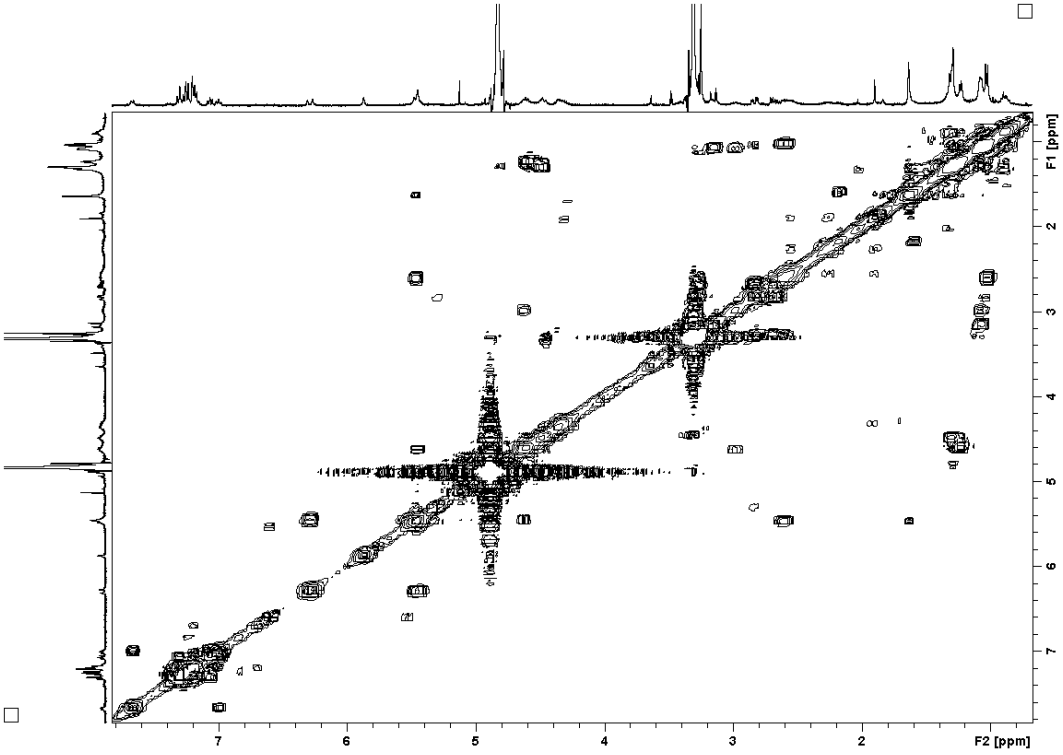

Appendix H.8: ROESY NMR spectrum of MC-WA (**165**) in CD_3OD, with continuous wave suppression of the O*H*/H_2O solvent peak.

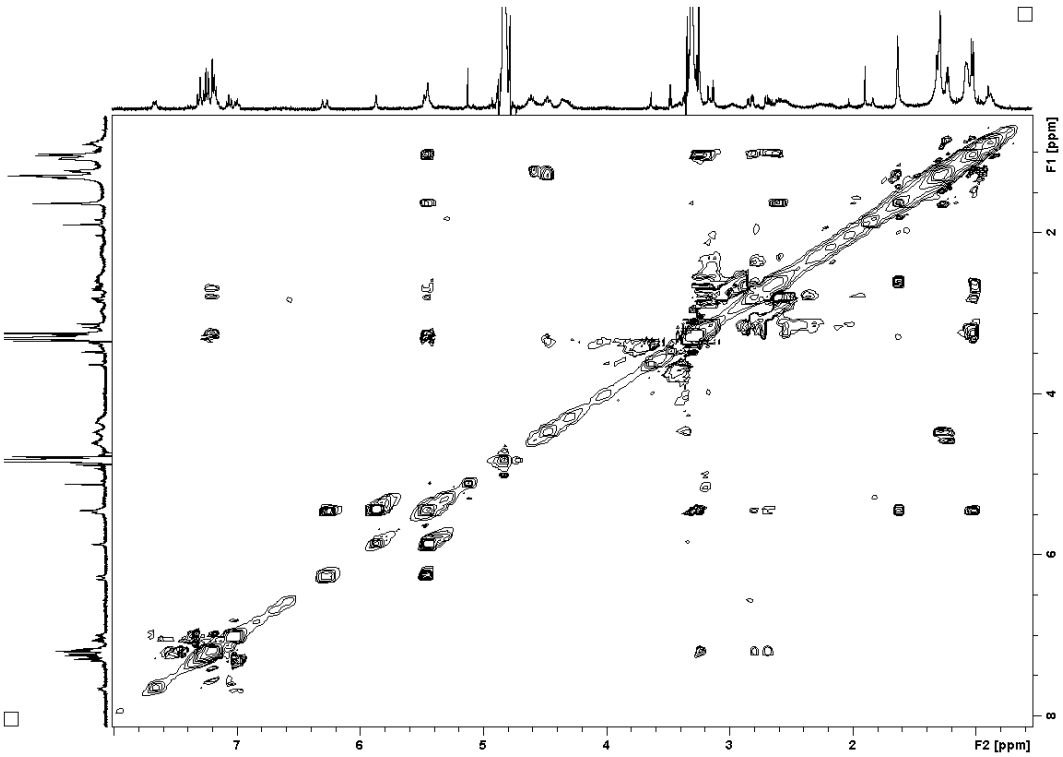

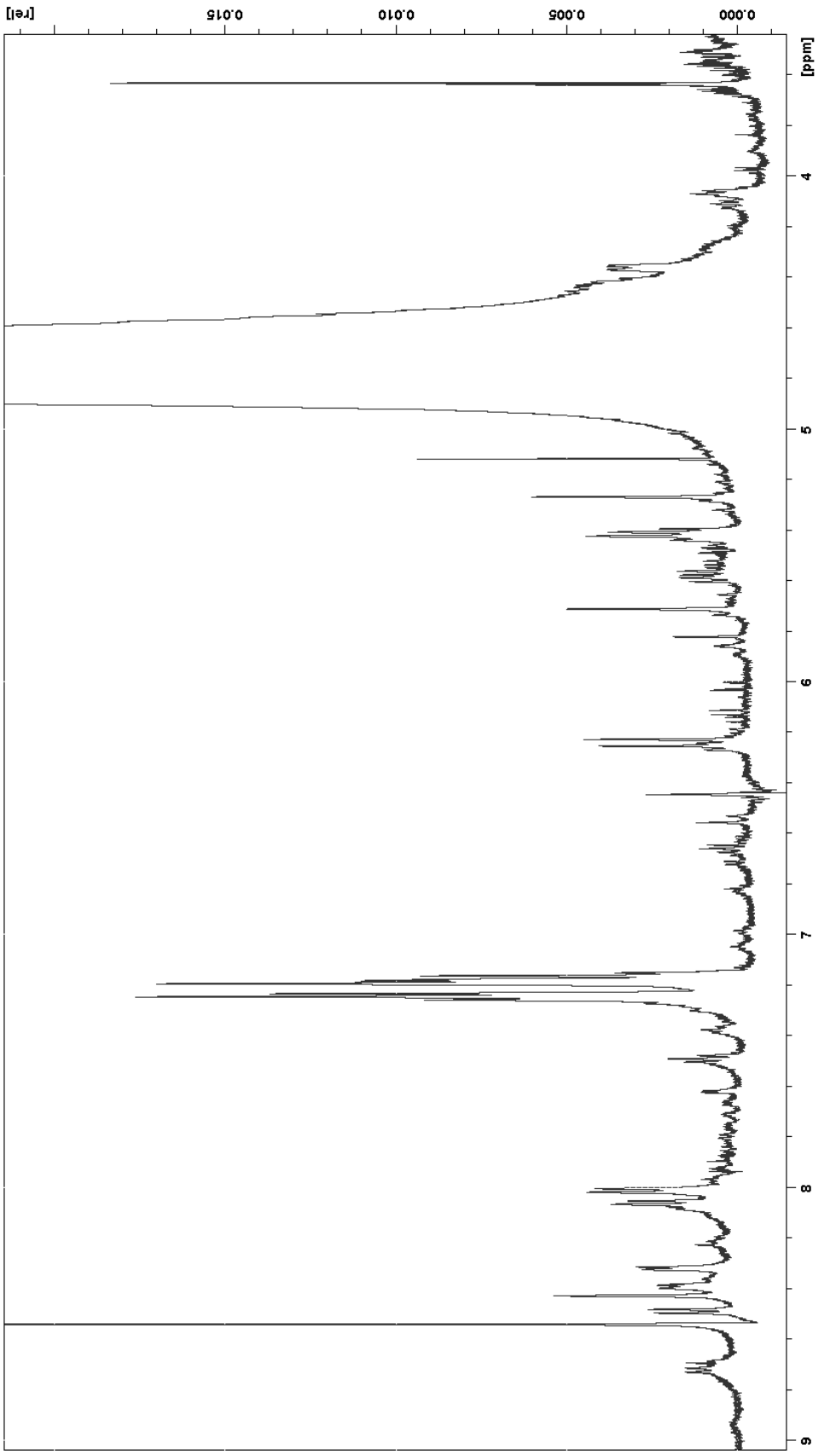

Appendix I.1: Downfield region for the ^{1}H NMR spectrum of MC-NflkA (**175**) in CD_3OH, with electronic sculpturing suppression of the OH/H_2O solvent peak and continuous wave suppression of the CHD_2OH solvent peak.

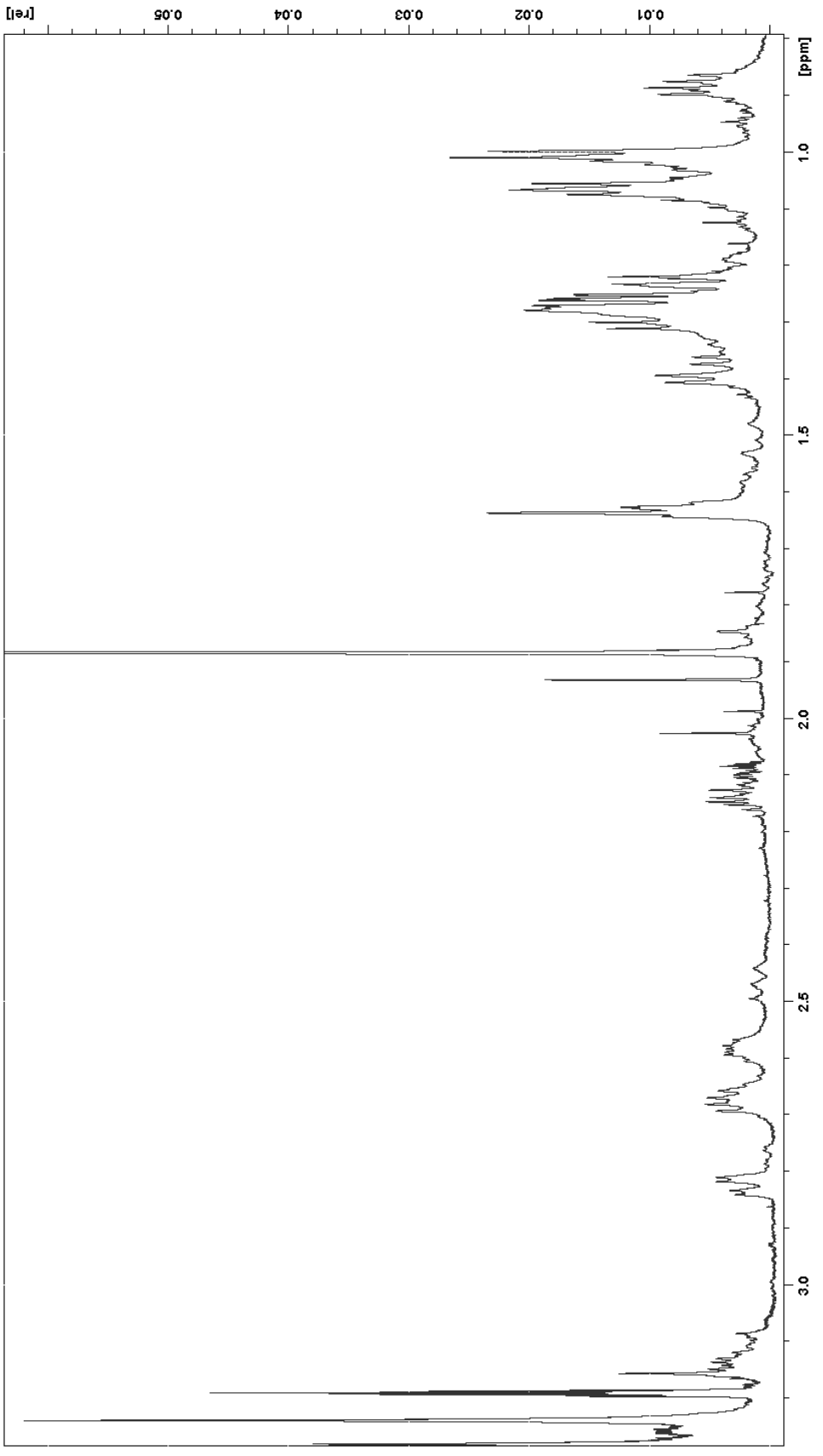

Appendix I.2: Upfield region for the ^{1}H NMR spectrum of MC-NfkA (**175**) in CD_3OH, with electronic sculpturing suppression of the OH/H_2O solvent peak and continuous wave suppression of the CHD_2OH solvent peak.

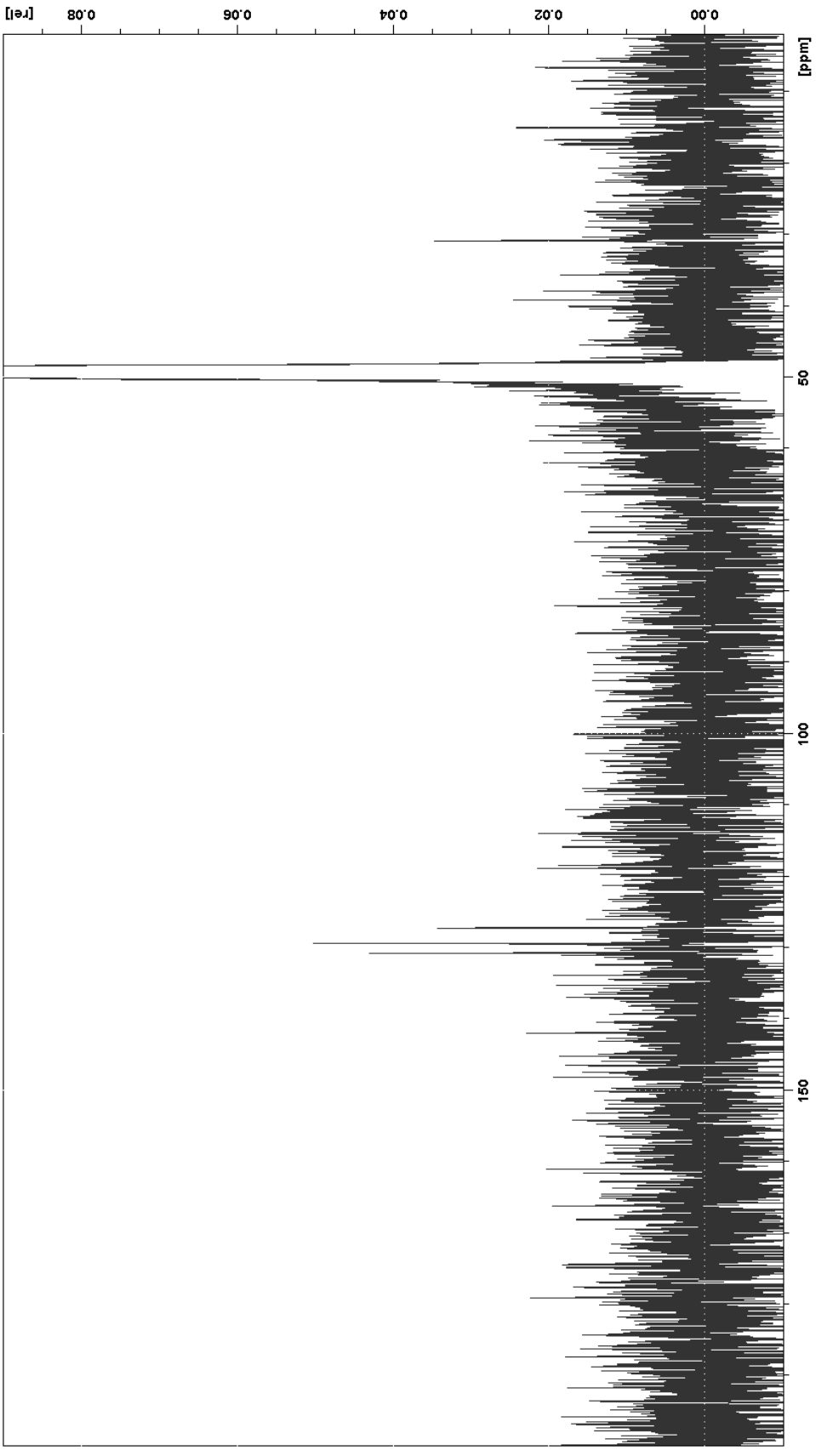

Appendix I.3: ^{13}C NMR spectrum of MC-NfkA (**175**) in CD_3OD.

Appendix I.4: Downfield region for the HSQC NMR spectrum of MC-NfkA (**175**) in CD_3OH, with continuous wave suppression of the O*H*/H_2O solvent peak.

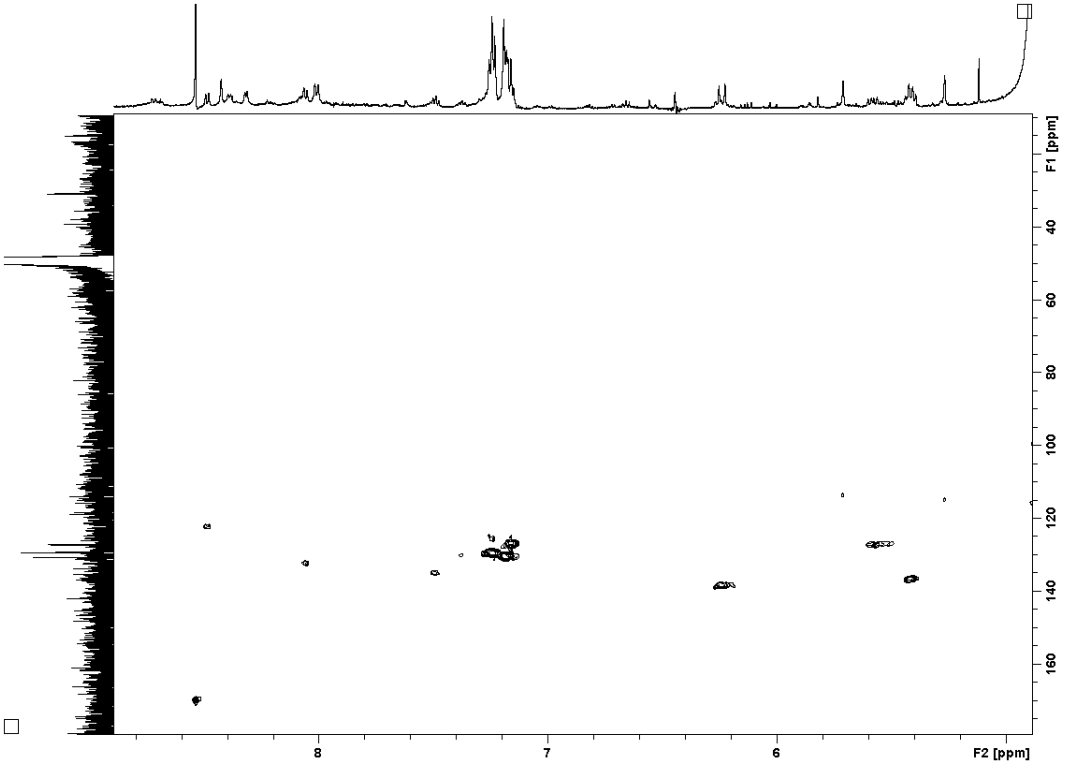

Appendix I.5: Upfield region for the HSQC NMR spectrum of MC-NfkA (**175**) in CD_3OH, with continuous wave suppression of the O*H*/H_2O solvent peak.

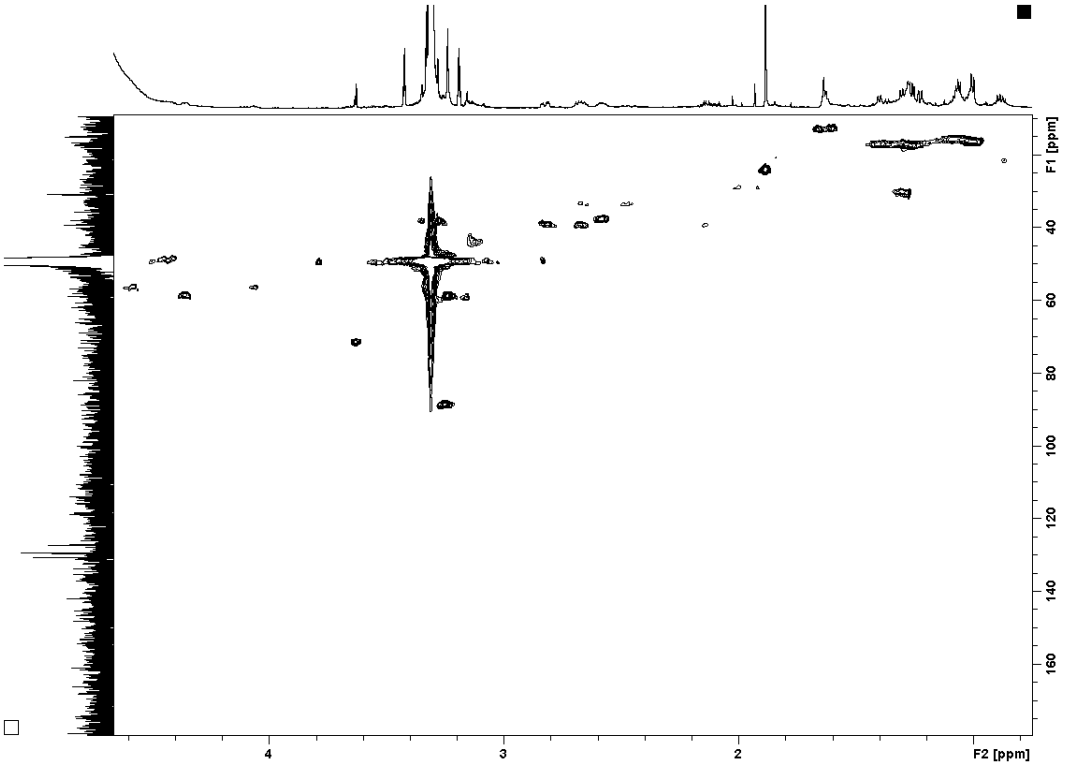

Appendix I.6: HMBC NMR spectrum of MC-NfkA (**175**) in CD_3OH.

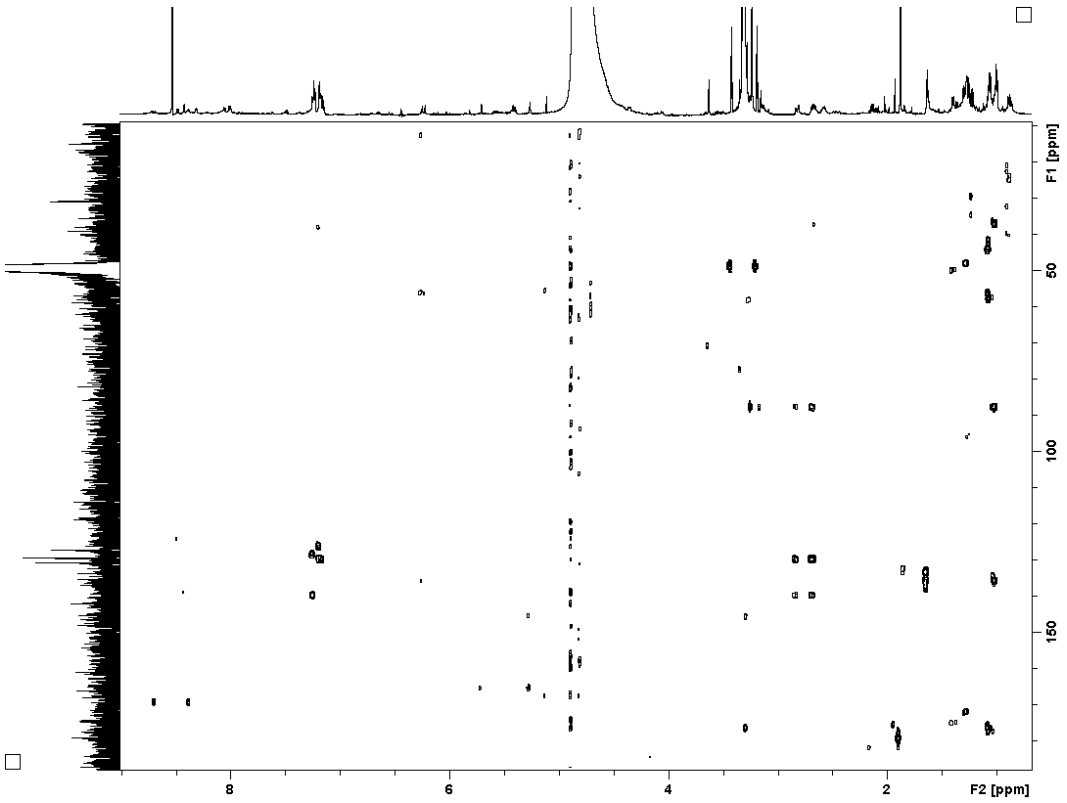

Appendix I.7: COSY NMR spectrum of MC-NfkA (**175**) in CD_3OH, with continuous wave suppression of the O*H*/H_2O solvent peak.

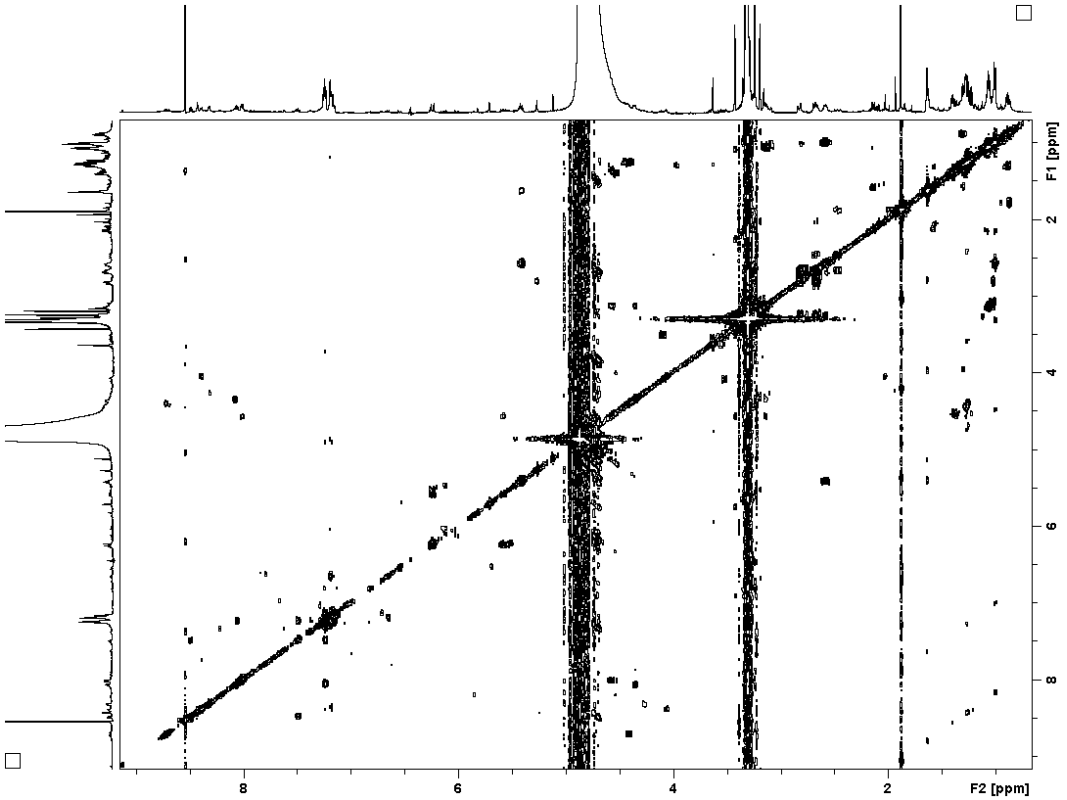

Appendix I.8: ROESY NMR spectrum of MC-NfkA (**175**) in CD_3OH, with continuous wave suppression of the O*H*/H_2O solvent peak.

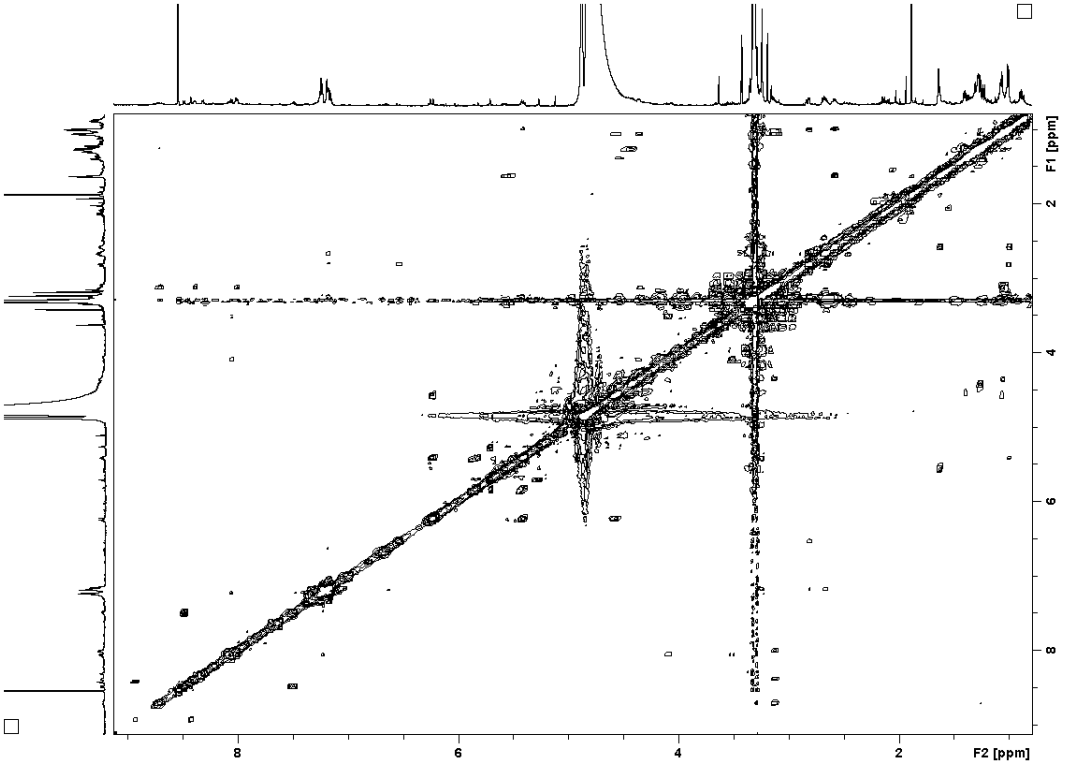

Appendix J.1: Tandem mass spectrometry fragment assignments for the -LR Antarctic microcystin congeners observed by ESI CID.

Fragment Assignment[a]	MC-LR[b]	[Gly^1, Asp^3, Dhb^7] MC-LR	[Gly^1, Asp^3, Dhb^7] MC-LHar	[Gly^1, Asp^3, ADMAdda^5, Dhb^7] MC-LR	[Gly^1, Asp^3, ADMAdda^5, Dhb^7] MC-LHar
M + H	995.6	967.6	981.6	995.6	1009.6
M – HOAc + H	-	-	-	935.5	949.3
(Me)Asp-Arg/Har-(ADM)Adda-Glu-Mdha/Dhb-Gly/Ala + H	882		868.6		896.9
Arg/Har-(ADM)Adda-Glu-Mdha/Dhb-Gly/Ala + H	753		753.3		781.4
(Me)Asp-Arg/Har-(ADM)Adda-Glu + H	728		728.4		756.4
Arg/Har-(ADM)Adda-Glu-Mdha/Dhb + H	682	682.5	696.1	710.3	724.3
Glu-Mdha/Dhb-Gly/Ala-Leu-(Me)Asp-Arg/Har + H	682		668.0		
Arg/Har-(ADM)Adda-Glu + H	599	599.3	613.2	627.2	641.4
(Me)Asp-Arg/Har-(ADM)Adda + H	599				627.3
(ADM)Adda'-Glu-Mdha/Dhb-Gly/Ala-Leu + H	559		545.4		
Mdha/Dhb-Gly/Ala-Leu-(Me)Asp-Arg/Har + H	553	525.2	539.4	525.2	539.3
Glu-Mdha/Dhb-Gly/Ala-Leu-(Me)Asp + H	526			498.2	
Arg/Har-(ADM)Adda + H	470				512.3
Gly/Ala-Leu-(Me)Asp-Arg/Har + H	470	442.3	456.2	442.1	456.1
(ADM)Adda'-Glu-Mdha/Dhb-Gly/Ala + H	446	432.2	432.1		
Leu-(Me)Asp-Arg/Har + H	399	385.1	399.1	385.4	
Glu-Mdha/Dhb-Gly/Ala-Leu + H	397			383.1	383.1
(ADM)Adda'-Glu-Mdha/Dhb + H	375	375.1	375.2	375.2	
Mdha/Dhb-Gly/Ala-Leu-(Me)Asp + H	397			369.2	
(ADM)Adda'-Glu + H	292	292.1	292.2	292.1	292.1
Gly/Ala-Leu-(Me)Asp + H	314		286.1	286.3	286.1
ADMAdda – HOAc + H	-	-	-	282.2	282.2
ADMAdda – HOAc – NH_3 + H	-	-	-	265.1	265.2
(Me)Asp-Arg/Har + H	286	272.1	286.1	272.1	286.1
Glu-Mdha/Dhb-Gly/Ala + H	284	270.2	270.2	270.1	270.2
Mdha/Dhb-Gly/Ala-Leu + H	268	254.3	254.1	254.1	254.1
Leu-(Me)Asp + H	243		229.2	229.0	229.1
Glu-Mdha/Dhb + H	213	213.1	213.1	213.1	213.1
Gly/Ala-Leu + H	185	171.0	171.1	171.0	171.1
(ADM)Adda' + H	163	163.1	163.1	163.1	163.0
Arg/Har + H	157	157.0	171.1	157.1	171.1
Mdha/Dhb-Gly/Ala + H	155	141.0	141.0	141.1	141.1
(ADM)Adda sidechain	135	135.1	135.1	163.1	163.0
Arg/Har immonium	129	129.2	143.1	129.1	143.1
Arg/Har fragment	112	112.1	112.0/126.1	112.0	111.9/126.1

[a] Fragments containing CO losses and NH_4^+ adducts were not included; Adda' = Adda minus NH_2 and the sidechain ($C_9H_{11}O$ or $C_{10}H_{11}O_2$). [b] *m/z* values for MC-LR fragments are theorised nominal values.[45,75,78]

Appendix J.2: Tandem mass spectrometry fragment assignments for the -RR Antarctic microcystin congeners observed by ESI CID.

Fragment Assignment[a]	MC-RR [b]	[Gly^1, Asp^3, Dhb^7] MC-RR	[Gly^1, Asp^3, Dhb^7] MC-RHar	[Gly^1, Asp^3, ADMAdda^5, Dhb^7] MC-RR	[Gly^1, Asp^3, ADMAdda^5, Dhb^7] MC-RHar
M + H	1024.7	1010.7	1024.7	1038.7	1052.7
M – CN_2H_2 + H	982	968.9	982.5	996.5	1010.8
M – HOAc + H	-	-	-	978.6	992.5
Arg/Har-(ADM)Adda-Glu-Mdha/Dhb-Gly/Ala-Arg + H	909	895.3	909.6		
(Me)Asp-Arg/Har-(ADM)Adda-Glu-Mdha/Dhb-Gly/Ala + H	882		868.6		896.4
(Me)Asp-Arg/Har-(ADM)Adda-Glu-Mdha/Dhb + H	811		811.5	825.1	839.8
Arg/Har-(ADM)Adda-Glu-Mdha/Dhb-Gly/Ala + H	753	739.2	753.4		781.0
(Me)Asp-Arg/Har-(ADM)Adda-Glu + H	728	714.3	728.3	742.1	756.2
Arg/Har-(ADM)Adda-Glu-Mdha/Dhb + H	682	682.2		710.2	724.2
Glu-Mdha/Dhb-Gly/Ala-Arg-(Me)Asp-Arg + H	725	697.5		697.3	
Arg/Har-(ADM)Adda-Glu + H	599		613.5		641.2
(Me)Asp-Arg/Har-(ADM)Adda + H	599	585.2	599.2	613.4	627.9
Mdha/Dhb-Gly/Ala-Arg-(Me)Asp-Arg/Har + H	596		582.4	568.7	
Har-ADMAdda – HOAC + H	-	-	-		452.5
(ADM)Adda'-Glu-Mdha/Dhb-Gly/Ala + H	446	432.2			
Glu-Mdha/Dhb-Gly/Ala-Arg + H	440	426.4		426.2	
Mdha/Dhb-Gly/Ala-Arg-(Me)Asp + H	440	412.1	412.3	412.2	412.3
(ADM)Adda'-Glu-Mdha/Dhb + H	375	375.1	375.2		
Gly/Ala-Arg-(Me)Asp + H	357	329.1		329.1	329.1
Mdha/Dhb-Gly/Ala-Arg + H	311	297.1	296.9	297.0	297.0
(ADM)Adda'-Glu + H	292			292.1	
ADMAdda – HOAc + H	-	-	-	282.3	282.1
ADMAdda – HOAc – NH_3 + H	-	-	-	265.4	265.3
(Me)Asp-Arg/Har + H	286	272.3	286.2		286.1
Arg-(Me)Asp + H	286	272.3	272.1	272.2	272.5
Glu-Mdha/Dhb-Gly/Ala + H	284	270.0		270.1	
Gly/Ala-Arg + H	228	214.1	214.0	214.1	214.2
Glu-Mdha/Dhb + H	213	213.1	212.9	213.1	213.2
(ADM)Adda'+ H	163	163.0	162.9	163.0	
Har + H	-	-		-	171.0
Arg + H	157	157.0	157.1	156.6	156.9
Mdha/Dhb-Gly/Ala + H	155	141.5	140.9	141.2	140.7
(ADM)Adda sidechain	135	135.1	135.1	163.0	
Har immonium	-	-	143.1	-	143.1
Arg immonium	129	129.5	129.1	129.1	
Har fragment	-	-	112.0/126.0	-	111.8/125.8
Arg fragment	112	112.2	112.0	112.1	111.8

[a] Fragments containing CO losses and NH_4^+ adducts were not included; Adda' = Adda minus NH_2 and the sidechain ($C_9H_{11}O$ or $C_{10}H_{11}O_2$). [b] *m/z* values for MC-RR fragments are theorised nominal values.[78,265]

Appendix J.3: Tandem mass spectrometry fragment assignments for the Antarctic linear peptides observed by MALDI PSD and/or ESI CID.

Fragment Assignment [a]	**Peptide 800** X = MePhe	**Peptide 816** X = MeTyr	**Peptide 830A** X = MeTyr(*O*Me)	**Peptide 814** X = MePhe	**Peptide 830B** X = MeTyr	**Peptide 844** X = MeTyr(*O*Me)
M + H	801	817	831	815	831	845
$C_9H_{14}NO_2$-Ile-X-MeTyr + H	620	636	650	620	636	650
$C_9H_{14}NO_2$-Ile-X + H	443	459	473	443	459	473
$C_9H_{14}NO_2$-Ile + H	282	282	282	282	282	282
$C_9H_{14}NO_2$ + H	169	169	169	169	169	169
X-MeTyr-(Me)Hpla + H	520	536	550	534	550	564
MeTyr-(Me)Hpla + H	359	359	359	373	373	373
Ile-X + H	275	291	305	275	291	305
$C_9H_{14}NO_2 - H_2O + H$	151	151	151	151	151	151
$C_9H_{14}NO_2 - CO + H$	141		141	141		
Fragment of $C_9H_{14}NO_2$	113		113	113		
MeTyr/Hpla sidechain	107		107	107		
X sidechain	91		121	91		
Mass of X (Da)	161	177	191	161	177	191

[a] X = Position three amino acid; $C_9H_{14}NO_2$ is the unidentified 168 Da N-terminus.

Appendix K

Appendix K.1: The relative abundance of eleven microcystin congeners during a 40-day batch culture of *Microcystis* CYN06. Graphs focussing on the -XR and -XA congeners **(A)** and on the -RR, -RZ and -XL congeners **(B)**.

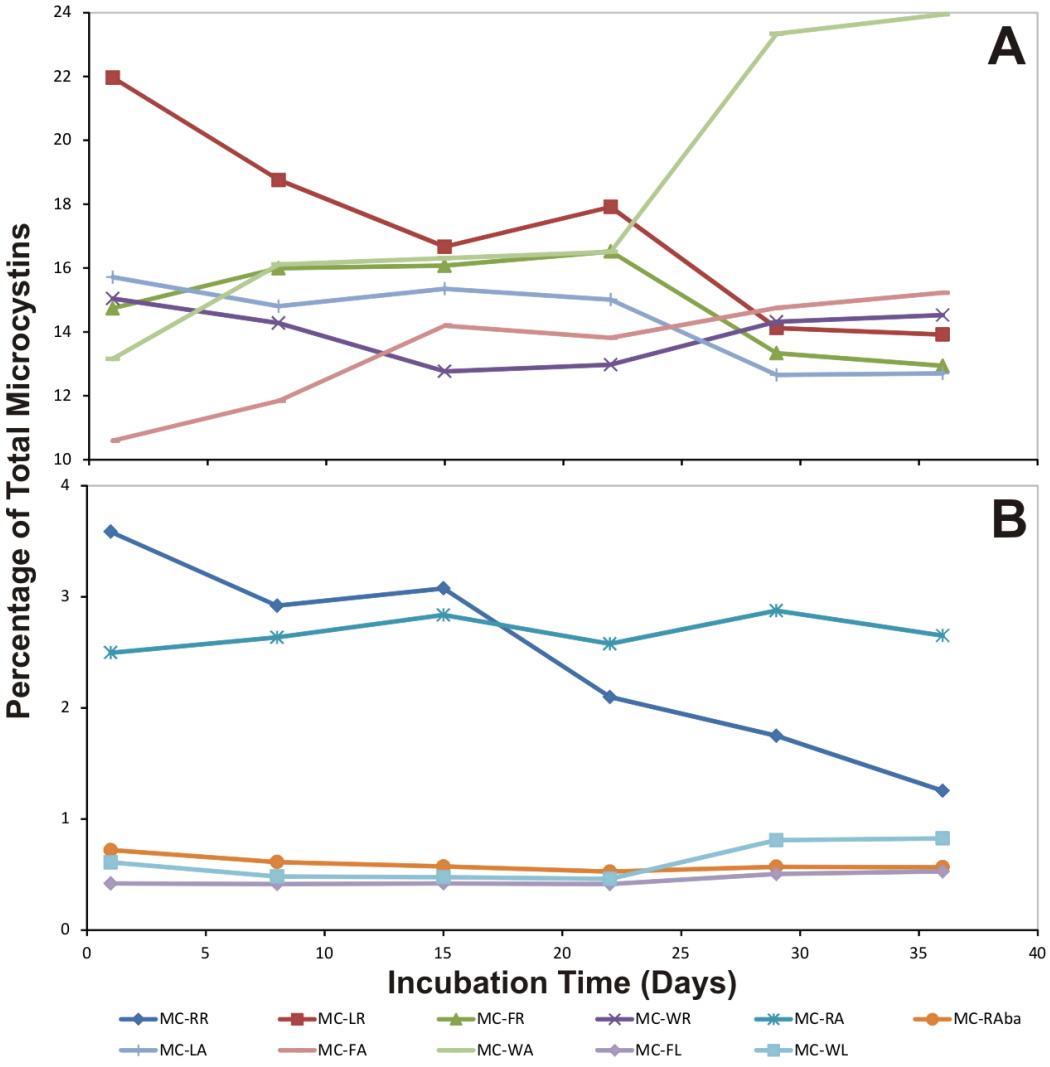

Appendix K.2: Correlation matrices showing the statistical significance of the changes in microcystin congener abundance a batch culture of *Microcystis* CYN06. Matrix was constructed using the *p*-values from a one-tailed Student's t-test; statistically significant changes are indicated by grey shading ($p \leq 0.05$). No statistically significant differences were observed for the -RZ microcystin congeners ($p > 0.05$).

MC-RR	Day 1	Day 8	Day 15	Day 22	Day 29	Day 36
Day 1		0.009	0.134	0.007	0.010	<0.001
Day 8	0.009		0.635	0.060	0.039	<0.001
Day 15	0.134	0.635		0.060	0.036	0.002
Day 22	0.007	0.060	0.060		0.306	0.056
Day 29	0.010	0.039	0.036	0.306		0.202
Day 36	<0.001	<0.001	0.002	0.056	0.202	

MC-XRs	Day 1	Day 8	Day 15	Day 22	Day 29	Day 36
Day 1		0.043	0.002	0.008	<0.001	<0.001
Day 8	0.043		0.029	0.139	0.002	<0.001
Day 15	0.002	0.029		0.856	0.036	0.022
Day 22	0.008	0.139	0.856		0.007	0.002
Day 29	<0.001	0.002	0.036	0.007		0.544
Day 36	<0.001	<0.001	0.022	0.002	0.544	

MC-XAs	Day 1	Day 8	Day 15	Day 22	Day 29	Day 36
Day 1		0.012	0.005	0.004	0.004	<0.001
Day 8	0.012		0.068	0.081	0.020	<0.001
Day 15	0.005	0.068		0.592	0.083	0.010
Day 22	0.004	0.081	0.592		0.063	0.005
Day 29	0.004	0.020	0.083	0.063		0.362
Day 36	<0.001	<0.001	0.010	0.005	0.362	

MC-XLs	Day 1	Day 8	Day 15	Day 22	Day 29	Day 36
Day 1		0.996	0.998	0.998	0.014	<0.001
Day 8	0.996		0.499	0.707	0.003	<0.001
Day 15	0.998	0.499		0.725	0.003	<0.001
Day 22	0.998	0.707	0.725		0.003	<0.001
Day 29	0.014	0.003	0.003	0.003		0.351
Day 36	<0.001	<0.001	<0.001	<0.001	0.351	

Appendix K.3: Scatter-plots of $\log_{10}$ microcystin content against nitrate concentration.

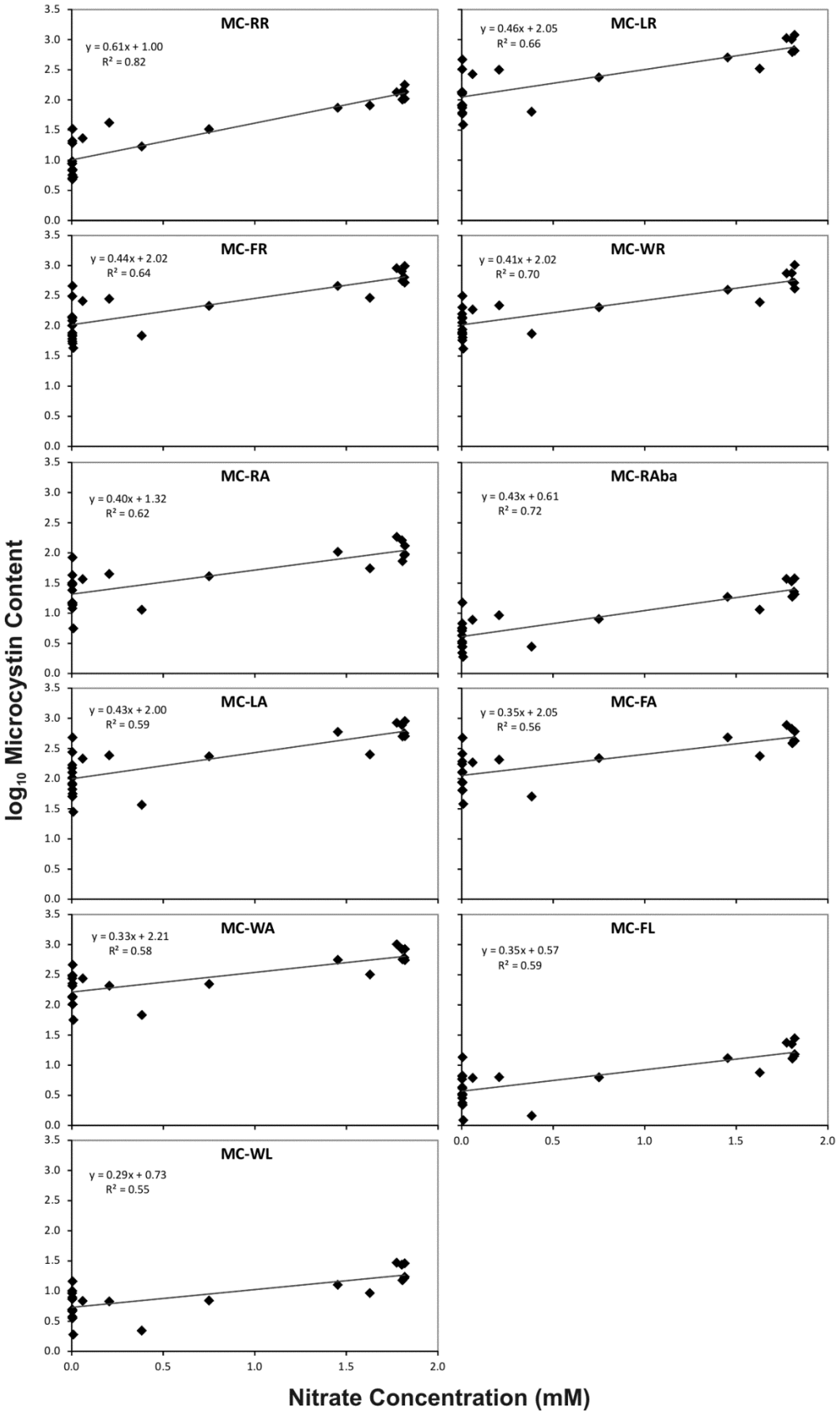

Appendix K.4: Scatter-plots of $\log_{10}$ microcystin content against incubation time for the time-points with nitrate concentrations less than 0.005 mM.

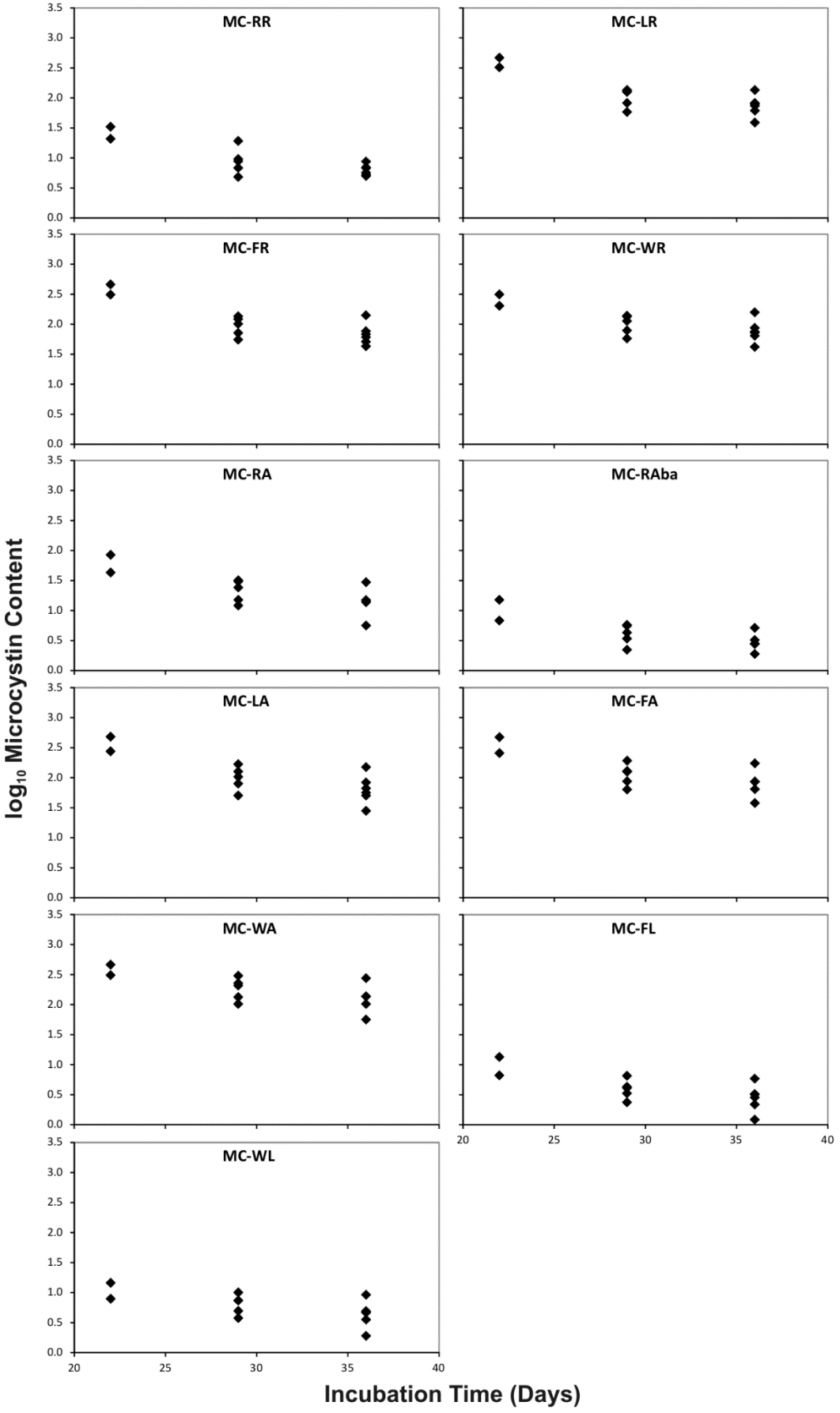

Appendix K.5: Correlation matrix showing the statistical significance of the differences between the gradients for the relationship of $\log_{10}$ microcystin content against incubation time. Matrix was constructed using the *p*-values from a two-tailed Student's t-test; statistically significant changes are indicated by grey shading ($p \leq 0.05$).

	MC-RR	**MC-XRs**	**MC-RZs**	**MC-XAs**	**MC-XLs**
MC-RR		0.001	<0.001	<0.001	<0.001
MC-XRs	0.001		0.427	0.117	0.010
MC-RZs	<0.001	0.427		0.332	0.030
MC-XAs	<0.001	0.117	0.332		0.189
MC-XLs	<0.001	0.010	0.030	0.189	

Appendix K.6: Correlation matrix showing the statistical significance of the differences between the gradients for the relationship of $\log_{10}$ microcystin content against nitrate concentration. Matrix was constructed using the *p*-values from a two-tailed Student's t-test; statistically significant changes are indicated by grey shading ($p \leq 0.05$).

	MC-RR	**MC-XRs**	**MC-RZs**	**MC-XAs**	**MC-XLs**
MC-RR		<0.001	<0.001	<0.001	<0.001
MC-XRs	<0.001		0.490	0.129	0.008
MC-RZs	<0.001	0.490		0.315	0.021
MC-XAs	<0.001	0.129	0.315		0.174
MC-XLs	<0.001	0.008	0.021	0.174	

Appendix L.1: Purification scheme for the fractionation of the CYN06 microcystins (Chapters 3 and 4).

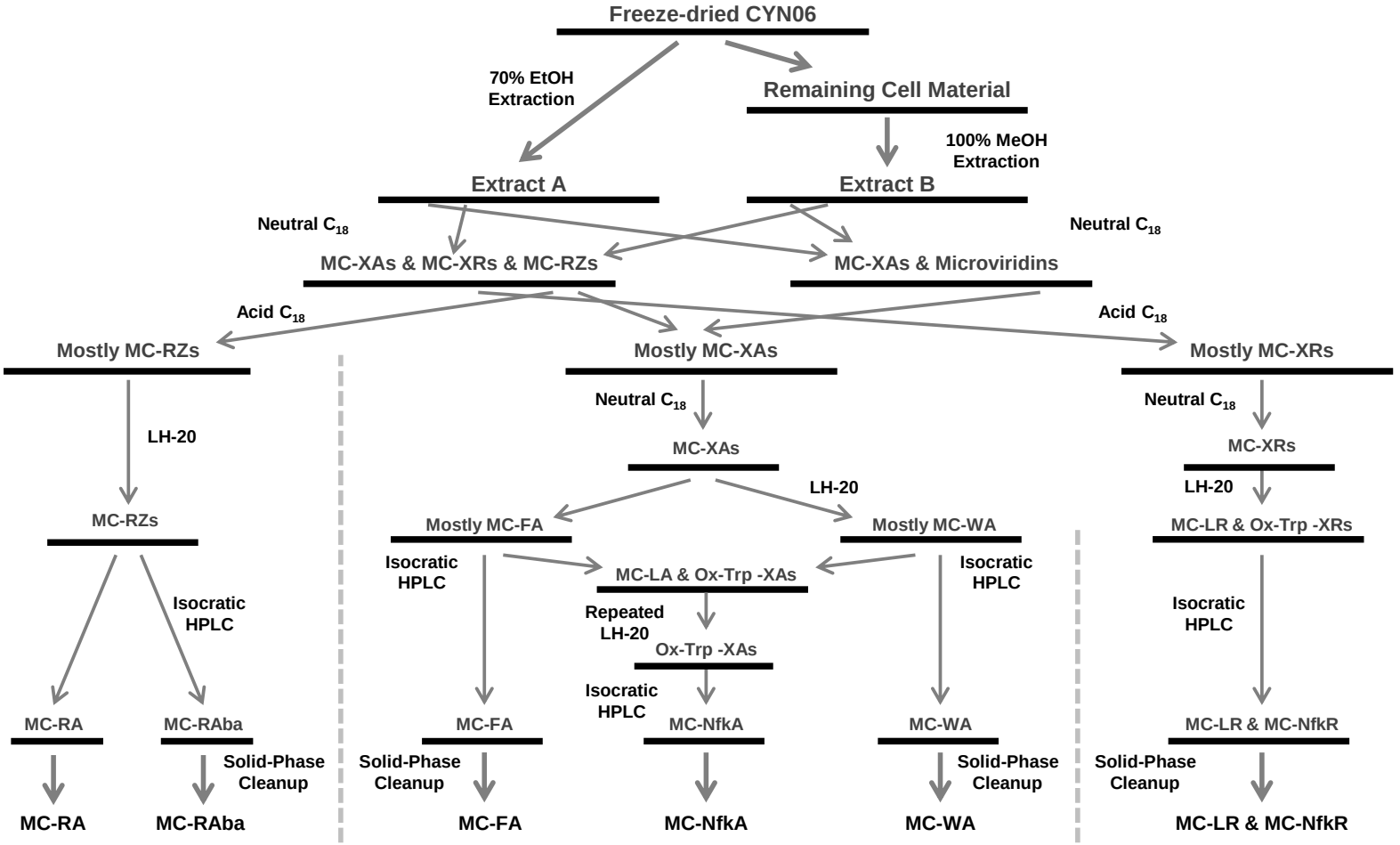

Appendix L

Appendix L.2: Purification scheme for the fractionation of the Antarctic oligopeptides (Chapter 5).

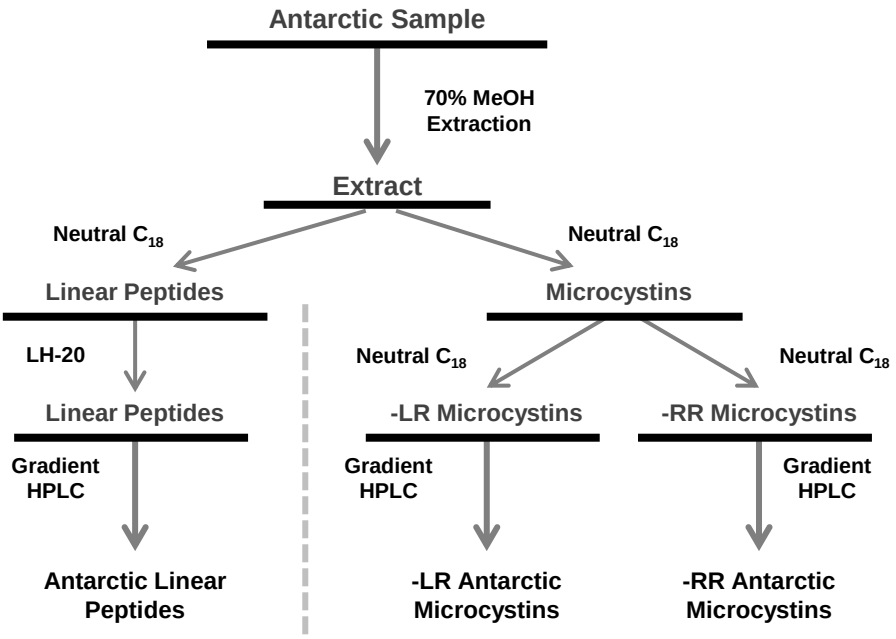

Appendix M: List of the compounds referred to in this thesis.

1. Aeruginosin 103 A
2. Anabaenopeptin A
3. Cyanopeptolin A
4. Aerucyclamide B
5. Microginin FR1
6. Microviridin A
7. MC-LR
8. [Asp^{3}] MC-LA
9. MC-LA
10. [Asp^{3}, Glu(OMe)^{6}] MC-LAba
11. MC-LAba
12. MC-LV
13. [Asp^{3}] MC-LL
14. MC-LL
15. MC-AR
16. MC-RA
17. MC-YA
18. MC-AHar
19. MC-RAba
20. [Asp^{3}, Dha^{7}] MC-LR
21. [Asp^{3}, Dha^{7}] MC-EE(OMe)
22. MC-LM
23. [Asp^{3}] MC-LF
24. MC-VF
25. [Asp^{3}, Dha^{7}] MC-LY
26. MC-YAba
27. MC-VR
28. MC-RV
29. MC-RApa
30. [Asp^{3}] MC-LR
31. [Asp^{3}, Dhb^{7}] MC-LR
32. [DMAdda^{5}] MC-LR
33. [Dha^{7}] MC-LR
34. MC-AW
35. [Dha^{7}] MC-EE(OMe)
36. [Asp^{3}, Dha^{7}] MC-E(OMe)E(OMe)
37. MC-LF
38. [Asp^{3}] MC-LY
39. [Asp^{3}, Dhb^{7}] MC-HilR
40. [Asp^{3}, Glu(OMe)^{6}] MC-LR
41. MC-RL
42. [(6*Z*)Adda^{5}] MC-LR
43. [Dha^{7}] MC-E(OMe)E(OMe)
44. [Ser^{7}] MC-LR
45. [Asp^{3}] MC-HilY
46. [Asp^{3}, Ser^{7}] MC-E(OMe)E(OMe)
47. [Ser^{7}] MC-EE(OMe)
48. MC-LY
49. MC-YL
50. [Asp^{3}, MeSer^{7}] MC-LY
51. [Asp^{3}, ADMAdda^{5}, Dhb^{7}] MC-LR
52. [Asp^{3}, ADMAdda^{5}] MC-LR
53. [Glu(OMe)^{6}] MC-LR
54. [Mdhb^{7}] MC-LR
55. MC-HilR
56. [Asp^{3}, Dha^{7}] MC-RR
57. [Asp^{3}] MC-LW
58. [MeSer^{7}] MC-LR
59. [Asp^{3}] MC-FR
60. [Dha^{7}] MC-FR
61. [Asp^{3}] MC-RF
62. [Ser^{7}] MC-E(OMe)E(OMe)
63. [Asp^{3}, Dha^{7}] MC-RY
64. MC-YM
65. [Asp^{3}, ADMAdda^{5}] MC-LHar
66. [ADMAdda^{5}] MC-LR
67. [Asp^{3}] MC-RR
68. [Asp^{3}, Dhb^{7}] MC-RR
69. [Dha^{7}] MC-RR
70. MC-LW
71. MC-M(O)R
72. MC-FR
73. MC-RF
74. [Dha^{7}] MC-HphR
75. [Asp^{3}] MC-YR
76. [Dha^{7}] MC-YR
77. [Asp^{3}, Dha^{7}] MC-HtyR
78. [Asp^{3}] MC-RY
79. [Dha^{7}] MC-RY
80. MC-LY(OMe)
81. MC-YM(O)
82. [Leu^{1}] MC-LR
83. [ADMAdda^{5}] MC-HilR
84. [ADMAdda^{5}] MC-LHar
85. MC-RR
86. [Asp^{3}] MC-YY
87. [Asp^{3}, Glu(OMe)^{6}] MC-RR
88. [(6*Z*)Adda^{5}] MC-RR
89. [Ser^{1}, ADMAdda^{5}] MC-LR
90. [ADMAdda^{5}, MeSer^{7}] MC-LR
91. [Asp^{3}, MeSer^{7}] MC-RR
92. [Ser^{7}] MC-RR
93. [Asp^{3}, Dhb^{7}] MC-HtyR
94. [Dha^{7}] MC-HtyR
95. [Asp^{3}] MC-HtyR
96. MC-YR
97. MC-RY
98. [Asp^{3}, MeSer^{7}] MC-RY
99. [Ser^{7}] MC-YR
100. MC-(H_4)YR
101. [Asp^{3}, Dhb^{7}] MC-HtyY
102. [Asp^{3}, ADMAdda^{5}, Dhb^{7}] MC-RR
103. [Glu(OC_3H_6OH)^{6}] MC-LR
104. [Asp^{3}] MC-WR
105. MC-HtyR
106. [Ser^{7}] MC-HtyR
107. [MeSer^{7}] MC-YR
108. [MeSer^{7}] MC-RY
119. MC-HarHar
110. [Asp^{3}, Dhb^{7}] MC-HtyHty
111. [ADMAdda^{5}] MC-RR
112. MC-WR
113. [Asp^{3}, ADMAdda^{5}] MC-HtyR
114. [Asp^{3}, ADMAdda^{5}, Dhb^{7}] MC-HtyR
115. MC-RY(OMe)
116. [ADMAdda^{5}] MC-(H_4)YR

Appendix M

117. [MeLan^{7}] MC-LR
118. Nodularin-R
119. seco[Asp^{3}] MC-RR
120. Anabaenopeptin B
121. Anabaenopeptin B1
122. Anabaenopeptin C
123. Anabaenopeptin D
124. Anabaenopeptin E
125. Anabaenopeptin F
126. Anabaenopeptin F1
127. Anabaenopeptin G
128. Anabaenopeptin G*
129. Anabaenopeptin H
130. Anabaenopeptin I
131. Anabaenopeptin J
132. Anabaenopeptin T
133. Anabaenopeptin HU892
134. Anabaenopeptin KT864
135. Anabaenopeptin MM823
136. Anabaenopeptin MM850
137. Anabaenopeptin MM913
138. Anabaenopeptin NZ825
139. Anabaenopeptin NZ841
140. Anabaenopeptin NZ857
141. Anabaenopeptin 820
142. Anabaenopeptin 908
143. Anabaenopeptin 915
144. Ferintoic Acid A
145. Ferintoic Acid B
146. Lyngbyaureidamide A
147. Lyngbyaureidamide B
148. Nodulapeptin A
149. Nodulapeptin B
150. Nodulapeptin 899
151. Nodulapeptin 901
152. Nodulapeptin 917
153. Oscillamide B
154. Oscillamide C
155. Oscillamide H
156. Oscillamide Y
157. Schizopeptin 791
158. Mozamide A
159. Anabaenopeptin 906
160. [Asp^{3}] MC-RA
161. [Asp^{3}] MC-RAba
162. [Asp^{3}] MC-FA
163. MC-FA
164. [Asp^{3}] MC-WA
165. MC-WA
166. MC-FAba
167. MC-WAba
168. MC-FL
169. MC-WL
170. MC-KynR
171. MC-OiaR
172. MC-NfkR
173. MC-KynA
174. MC-OiaA
175. MC-NfkA
176. MC-KynAba
177. MC-OiaAba
178. MC-NfkAba
179. [Gly^{1}, Asp^{3}, Dhb^{7}] MC-LR
180. [Gly^{1}, Asp^{3}, Dhb^{7}] MC-LHar
181. [Gly^{1}, Asp^{3}, ADMAdda^{5}, Dhb^{7}] MC-LR
182. [Gly^{1}, Asp^{3}, ADMAdda^{5}, Dhb^{7}] MC-LHar
183. [Gly^{1}, Asp^{3}, Dhb^{7}] MC-RR
184. [Gly^{1}, Asp^{3}, Dhb^{7}] MC-RHar
185. [Gly^{1}, Asp^{3}, ADMAdda^{5}, Dhb^{7}] MC-RR
186. [Gly^{1}, Asp^{3}, ADMAdda^{5}, Dhb^{7}] MC-RHar
187. Antarctic peptide 800
188. Antarctic peptide 816
189. Antarctic peptide 830A
190. Antarctic peptide 814
191. Antarctic peptide 830B
192. Antarctic peptide 844

References

1. Schopf, J.W. & Packer, B.M. *Science*, **1987**, *237*, 70-73.
2. Holt, J.G.; Krieg, N.R.; Sneath, P.H.A.; Staley, J.T. & Williams, S.T. Oxygenic photosynthetic bacteria. In *Bergey's manual of determinative bacteriology*, 9th ed.; Lippincott Williams and Wilkins: Philadelphia, **2000**, pp 377-426.
3. Whitton, B.A. & Potts, M. *The ecology of cyanobacteria, their diversity in time and space*. Kluwer Academic Publishers: Dordrecht, **2000**.
4. Chorus, I. & Bartram, J. *Toxic cyanobacteria in water: A guide to their public health consequences, monitoring and management*. E & FN Spon: London, **1999**.
5. Baker, P.D. *Marine and Freshwater Research*, **1999**, *50*, 265-279.
6. Jones, G.J. & Korth, W. *Water Sci. Technol.*, **1995**, *31*, 145-151.
7. Aráoz, R.; Molgo, J. & Tandeau de Marsac, N. *Toxicon*, **2010**, *56*, 813-828.
8. Kato, Y. & Scheuer, P.J. *J. Pure Appl. Chem.*, **1975**, *41*, 1-14.
9. Griffiths, D.J. & Saker, M.L. *Environ. Toxicol.*, **2003**, *18*, 78-93.
10. Stewart, I.; Schluter, P. & Shaw, G. *Environmental Health: A Global Access Science Source*, **2006**, *5*, 7.
11. van Apeldoorn, M.E.; van Egmond, H.P.; Speijers, G.J.A. & Bakker, G.J.I. *Mol. Nutr. Food Res.*, **2007**, *51*, 7-60.
12. Sivonen, K. & Jones, G. Cyanobacterial toxins. In *Toxic cyanobacteria in water: A guide to their public health consequences, monitoring and management*, Chorus, I. & Bartram, J., Eds. E & FN Spon: London, **1999**, pp 55-124.
13. Namikoshi, M. & Rinehart, K.L. *J. Ind. Microbiol. Biotechnol.*, **1996**, *17*, 373-384.
14. Welker, M. & von Döhren, H. *FEMS Microbiol. Rev.*, **2006**, *30*, 530-563.
15. Kodani, S.; Ishida, K. & Murakami, M. *J. Nat. Prod.*, **1998**, *61*, 1046-1048.
16. Shin, H.J.; Matsuda, H.; Murakami, M. & Yamaguchi, K. *J. Org. Chem.*, **1997**, *62*, 1810-1813.
17. Murakami, M.; Okita, Y.; Matsuda, H.; Okino, T. & Yamaguchi, K. *Tetrahedron Lett.*, **1994**, *35*, 3129-3132.
18. Ishida, K.; Okita, Y.; Matsuda, H.; Okino, T. & Murakami, M. *Tetrahedron*, **1999**, *55*, 10971-10988.
19. Murakami, M.; Ishida, K.; Okino, T.; Okita, Y.; Matsuda, H. & Yamaguchi, K. *Tetrahedron Lett.*, **1995**, *36*, 2785-2788.
20. Matsuda, H.; Okino, T.; Murakami, M. & Yamaguchi, K. *Tetrahedron*, **1996**, *52*, 14501-14506.
21. Harada, K.-I.; Fujii, K.; Shimada, T.; Suzuki, M.; Sano, H.; Adachi, K. & Carmichael, W.W. *Tetrahedron Lett.*, **1995**, *36*, 1511-1514.
22. Zi, J.; Lantvit, D.D.; Swanson, S.M. & Orjala, J. *Phytochemistry*, **2012**, *74*, 173-177.
23. Martin, C.; Oberer, L.; Ino, T.; Konig, W.A.; Busch, M. & Weckesser, J. *The Journal of antibiotics*, **1993**, *46*, 1550-6.

24. Portmann, C.; Blom, J.F.; Gademann, K. & Jüttner, F. *J. Nat. Prod.*, **2008**, *71*, 1193-1196.

25. Neumann, U.; Forchert, A.; Flury, T. & Weckesser, J. *FEMS Microbiol. Lett.*, **1997**, *153*, 475-478.

26. Ishida, K.; Matsuda, H. & Murakami, M. *Tetrahedron*, **1998**, *54*, 13475-13484.

27. Ishida, K.; Kato, T.; Murakami, M.; Watanabe, M. & Watanabe, M.F. *Tetrahedron*, **2000**, *56*, 8643-8656.

28. Ishitsuka, M.O.; Kusumi, T.; Kakisawa, H.; Kaya, K. & Watanabe, M.M. *J. Am. Chem. Soc.*, **1990**, *112*, 8180-8182.

29. Rounge, T.; Rohrlack, T.; Nederbragt, A.; Kristensen, T. & Jakobsen, K. *BMC Genomics*, **2009**, *10*, 396.

30. Philmus, B.; Christiansen, G.; Yoshida, W.Y. & Hemscheidt, T.K. *ChemBioChem*, **2008**, *9*, 3066-3073.

31. Botes, D.P.; Wessels, P.L.; Kruger, H.; Runnegar, M.T.C.; Santikarn, S.; Smith, R.J.; Barna, J.C.J. & Williams, D.H. *Org. Bioorg. Chem.*, **1985**, *12*, 2747-2748.

32. Botes, D.P.; Tuinman, A.A.; Wessels, P.L.; Viljoen, C.C.; Kruger, H.; Williams, D.H.; Santikarn, S.; Smith, R.J. & Hammond, S.J. *Org. Bioorg. Chem.*, **1984**, *10*, 2311-2318.

33. Rinehart, K.; Namikoshi, M. & Choi, B. *J. Appl. Phycol.*, **1994**, *6*, 159-176.

34. Diehnelt, C.W.; Dugan, N.R.; Peterman, S.M. & Budde, W.L. *Anal. Chem.*, **2006**, *78*, 501-512.

35. del Campo, F.F. & Ouahid, Y. *Environ. Pollut.*, **2010**, *158*, 2906-2914.

36. Mahakhant, A.; Sano, T.; Ratanachot, P.; Tong-a-ram, T.; Srivastava, V.C.; Watanabe, M.M. & Kaya, K. *Phycol. Res.*, **1998**, *46*, 25.

37. Craig, M.; McCready, T.L.; Luu, H.A.; Smillie, M.A.; Dubord, P. & Holmes, C.F.B. *Toxicon*, **1993**, *31*, 1541-1549.

38. Namikoshi, M.; Rinehart, K.L.; Sakai, R.; Stotts, R.R.; Dahlem, A.M.; Beasley, V.R.; Carmichael, W.W. & Evans, W.R. *J. Org. Chem.*, **1992**, *57*, 866-872.

39. Lee, T.-H.; Chen, Y.-M. & Chou, H.-N. *Toxicon*, **1998**, *36*, 247-255.

40. Prakash, S.; Lawton, L.A. & Edwards, C. *Harmful Algae*, **2009**, *8*, 377-384.

41. Miles, C.O.; Sandvik, M.; Nonga, H.E.; Rundberget, T.; Wilkins, A.L.; Rise, F. & Ballot, A. *Environ. Toxicol.*, **2012**, *46*, 8937–8944.

42. Harada, K.-I.; Ogawa, K.; Matsuura, K.; Nagai, H.; Murata, H.; Suzuki, M.; Itezono, Y.; Nakayama, N.; Shirai, M. & Nakano, M. *Toxicon*, **1991**, *29*, 479-489.

43. Namikoshi, M.; Yuan, M.; Sivonen, K.; Carmichael, W.W.; Rinehart, K.L.; Rouhiainen, L.; Sun, F.; Brittain, S. & Otsuki, A. *Chem. Res. Toxicol.*, **1998**, *11*, 143-149.

44. Robillot, C.; Vinh, J.; Puiseux-Dao, S. & Hennion, M.-C. *Environ. Sci. Technol.*, **2000**, *34*, 3372-3378.

45. Bateman, K.P.; Thibault, P.; Douglas, D.J. & White, R.L. *J. Chromatogr. A*, **1995**, *712*, 253-268.

46. Mazur-Marzec, H.; Browarczyk-Matusiak, G.; Forycka, K.; Kobos, J. & Plinski, M. *Oceanologia*, **2010**, *52*, 127-146.

47. Krishnamurthy, T.; Szafraniec, L.; Hunt, D.F.; Shabanowitz, J.; Yates, J.R.; Hauer, C.R.; Carmichael, W.W.; Skulberg, O.; Codd, G.A. & Missler, S. *Proc. Natl. Acad. Sci. USA*, **1989**, *86*, 770-774.

48. Sano, T.; Beattie, K.A.; Codd, G.A. & Kaya, K. *J. Nat. Prod.*, **1998**, *61*, 851-853.

49. Sano, T. & Kaya, K. In *Microcystin-AW, a new microcystin variant isolated from cyanobacterial waterbloom in Thailand*, 9th International Conference on Harmful Algal Blooms, Tasmania, Australia, Location, **2000**.

50. Sano, T.; Takagi, H. & Kaya, K. *Phytochemistry*, **2004**, *65*, 2159-2162.

51. Sivonen, K.; Skulberg, O.M.; Namikoshi, M.; Evans, W.R.; Carmichael, W.W. & Rinehart, K.L. *Toxicon*, **1992**, *30*, 1465-1471.

52. Harada, K.; Ogawa, K.; Matsuura, K.; Murata, H.; Suzuki, M.; Watanabe, M.F.; Itezono, Y. & Nakayama, N. *Chem. Res. Toxicol.*, **1990**, *3*, 473-481.

53. Namikoshi, M.; Sivonen, K.; Evans, W.R.; Carmichael, W.W.; Sun, F.; Rouhiainen, L.; Luukkainen, R. & Rinehart, K.L. *Toxicon*, **1992**, *30*, 1457-1464.

54. Beattie, K.A.; Kaya, K.; Sano, T. & Codd, G.A. *Phytochemistry*, **1998**, *47*, 1289-1292.

55. Namikoshi, M.; Rinehart, K.L.; Sakai, R.; Sivonen, K. & Carmichael, W.W. *J. Org. Chem.*, **1990**, *55*, 6135-6139.

56. Sivonen, K.; Carmichael, W.W.; Namikoshi, M.; Rinehart, K.L.; Dahlem, A.M. & Niemela, S.I. *Appl. Environ. Microbiol.*, **1990**, *56*, 2650-2657.

57. Namikoshi, M.; Sun, F.; Choi, B.W.; Rinehart, K.L.; Carmichael, W.W.; Evans, W.R. & Beasley, V.R. *J. Org. Chem.*, **1995**, *60*, 3671-3679.

58. Lee, T.-H. & Chou, H.-N. *Bot. Bull. Academ. Sinica*, **2000**, *41*, 197-202.

59. Luukkainen, R.; Namikoshi, M.; Sivonen, K.; Rinehart, K.L. & Niemelä, S.I. *Toxicon*, **1994**, *32*, 133-139.

60. Meriluoto, J.A.O.; Sandström, A.; Eriksson, J.E.; Remaud, G.; Grey Graig, A. & Chattopadhyaya, J. *Toxicon*, **1989**, *27*, 1021-1034.

61. Sano, T. & Kaya, K. *Tetrahedron*, **1998**, *54*, 463-470.

62. Kiviranta, J.; Namikoshi, M.; Sivonen, K.; Evans, W.R.; Carmichael, W.W. & Rinehart, K.L. *Toxicon*, **1992**, *30*, 1093-1098.

63. Namikoshi, M.; Sivonen, K.; Evans, W.R.; Carmichael, W.W.; Rouhiainen, L.; Luukkainen, R. & Rinehart, K.L. *Chem. Res. Toxicol.*, **1992**, *5*, 661-666.

64. Namikoshi, M.; Sivonen, K.; Evans, W.R.; Sun, F.; Carmichael, W.W. & Rinehart, K.L. *Toxicon*, **1992**, *30*, 1473-1479.

65. Sivonen, K.; Namikoshi, M.; Evans, W.R.; Gromov, B.V.; Carmichael, W.W. & Rinehart, K.L. *Toxicon*, **1992**, *30*, 1481-1485.

66. Okello, W.; Portmann, C.; Erhard, M.; Gademann, K. & Kurmayer, R. *Environ. Toxicol.*, **2010**, *25*, 367-380.

67. Elleman, T.C.; Falconer, I.R.; Jackson, A.R.B. & Runnegar, M.T. *Aust. J. Biol. Sci.*, **1978**, *31*, 209-218.

68. Matthiensen, A.; Beattie, K.A.; Yunes, J.S.; Kaya, K. & Codd, G.A. *Phytochemistry*, **2000**, *55*, 383-387.

69. Kaasalainen, U.; Jokela, J.; Fewer, D.P.; Sivonen, K. & Rikkinen, J. *Mol. Plant-Microbe Interact.*, **2009**, *22*, 695-702.

70. Kusumi, T.; Ooi, T.; Watanabe, M.M.; Takahashi, H. & Kakisawa, H. *Tetrahedron Lett.*, **1987**, *28*, 4695-4698.

71. Grach-Pogrebinsky, O.; Sedmak, B. & Carmeli, S. *J. Nat. Prod.*, **2004**, *67*, 337-342.

72. Sivonen, K.; Namikoshi, M.; Evans, W.R.; Fardig, M.; Carmichael, W.W. & Rinehart, K.L. *Chem. Res. Toxicol.*, **1992**, *5*, 464-469.

73. Luukkainen, R.; Sivonen, K.; Namikoshi, M.; Fardig, M.; Rinehart, K.L. & Niemela, S.I. *Appl. Environ. Microbiol.*, **1993**, *59*, 2204-2209.

74. Harada, K.-I.; Ogawa, K.; Kimura, Y.; Murata, H.; Suzuki, M.; Thorn, P.M.; Evans, W.R. & Carmichael, W.W. *Chem. Res. Toxicol.*, **1991**, *4*, 535-540.

75. Mayumi, T.; Kato, H.; Imanishi, S.; Kawasaki, Y.; Hasegawa, M. & Harada, K.-I. *J. Antibiot.*, **2006**, *59*, 710-719.

76. Christiansen, G.; Yoshida, W.Y.; Blom, J.F.; Portmann, C.; Gademann, K.; Hemscheidt, T. & Kurmayer, R. *J. Nat. Prod.*, **2008**, *71*, 1881-1886.

77. Okello, W.; Ostermaier, V.; Portmann, C.; Gademann, K. & Kurmayer, R. *Water Res.*, **2010**, *44*, 2803-2814.

78. Frias, H.V.; Mendes, M.A.; Cardozo, K.H.M.; Carvalho, V.M.; Tomazela, D.; Colepicolo, P. & Pinto, E. *Biochem. Biophys. Res. Commun.*, **2006**, *344*, 741-746.

79. Ferranti, P.; Fabbrocino, S.; Nasi, A.; Caira, S.; Bruno, M.; Serpe, L. & Gallo, P. *Rapid Commun. Mass Spectrom.*, **2009**, *23*, 1328-1336.

80. Laub, J.; Henriksen, P.; Brittain, S.M.; Wang, J.; Carmichael, W.W.; Rinehart, K.L. & Moestrup, Ø. *Environ. Toxicol.*, **2002**, *17*, 351-357.

81. Rinehart, K.L.; Harada, K.; Namikoshi, M.; Chen, C.; Harvis, C.A.; Munro, M.H.G.; Blunt, J.W.; Mulligan, P.E.; Beasley, V.R. & et al. *J. Am. Chem. Soc.*, **1988**, *110*, 8557-8558.

82. An, J. & Carmichael, W.W. *Toxicon*, **1994**, *32*, 1495-1507.

83. Runnegar, M.T.; Falconer, I.R. & Silver, J. *Naunyn-Schmiedeberg's Arch. Pharmacol.*, **1981**, *317*, 268-272.

84. Falconer, I.R. & Yeung, D.S.K. *Chem. Biol. Interact.*, **1992**, *81*, 181-196.

85. Fujiki, H. & Suganuma, M. *Adv. Cancer Res.*, **1993**, *61*, 143-194.

86. Ohta, T.; Sueoka, E.; Iida, N.; Komori, A.; Suganuma, M.; Nishiwaki, R.; Tatematsu, M.; Kim, S.-J.; Carmichael, W.W. & Fujiki, H. *Cancer Res.*, **1994**, *54*, 6402-6406.

87. Eriksson, J.E.; Meriluoto, J.A.O.; Kujari, H.P.; Österlund, K.; Fagerlund, K. & Hällbom, L. *Toxicon*, **1988**, *26*, 161-166.

88. Mohamed, Z.A. & Al Shehri, A.M. *FEMS Microbiol. Ecol.*, **2009**, *69*, 98-105.

89. Saker, M.L.; Jungblut, A.D.; Neilan, B.A.; Rawn, D.F.K. & Vasconcelos, V.M. *Toxicon*, **2005**, *46*, 555-562.

90. Domingos, P.; Rubim, T.K.; Molica, R.J.R.; Azevedo, S.M.F.O. & Carmichael, W.W. *Environ. Toxicol.*, **1999**, *14*, 31-35.

91. Ballot, A.; Krienitz, L.; Kotut, K.; Wiegand, C. & Pflugmacher, S. *Harmful Algae*, **2005**, *4*, 139-150.

92. Silva-Stenico, M.E.; Silva, C.S.P.; Lorenzi, A.S.; Shishido, T.K.; Etchegaray, A.; Lira, S.P.; Moraes, L.A.B. & Fiore, M.F. *Microbiol. Res.*, **2011**, *166*, 161-175.

93. Fiore, M.F.; Genuário, D.B.; da Silva, C.S.P.; Shishido, T.K.; Moraes, L.A.B.; Neto, R.C. & Silva-Stenico, M.E. *Toxicon*, **2009**, *53*, 754-761.

94. Prinsep, M.R.; Caplan, F.R.; Moore, R.E.; Patterson, G.M.L.; Honkanen, R.E. & Boynton, A.L. *Phytochemistry*, **1992**, *31*, 1247-1248.

95. Izaguirre, G.; Jungblut, A.-D. & Neilan, B.A. *Water Res.*, **2007**, *41*, 492-498.

96. Vieira, J.M.d.S.; Azevedo, M.T.P.; Azevedo, S.M.F.O.; Honda, R.Y. & Corrêa, B. *Toxicon*, **2003**, *42*, 709-713.

97. Nascimento, S.M. & Azevedo, S.M.F.O. *Environ. Toxicol.*, **1999**, *14*, 37-44.

98. Willame, R.; Jurczak, T.; Iffly, J.-F.; Kull, T.; Meriluoto, J. & Hoffmann, L. *Hydrobiologia*, **2005**, *551*, 99-117.

99. Tillett, D.; Dittmann, E.; Erhard, M.; von Döhren, H.; Börner, T. & Neilan, B.A. *Chem. Biol.*, **2000**, *7*, 753-764.

100. Nishizawa, T.; Asayama, M.; Fujii, K.; Harada, K.-I. & Shirai, M. *J. Biochem.*, **1999**, *126*, 520-529.

101. Nishizawa, T.; Ueda, A.; Asayama, M.; Fujii, K.; Harada, K.-I.; Ochi, K. & Shirai, M. *J. Biochem.*, **2000**, *127*, 779-789.

102. Rouhiainen, L. *Characterization of Anabaena cyanobacteria: repeated sequences and genes involved in biosynthesis of microcystins and anabaenopeptilides*. Ph.D. Thesis, University of Helsinki, Helsinki, **2004**.

103. Christiansen, G.; Fastner, J.; Erhard, M.; Börner, T. & Dittmann, E. *J. Bacteriol.*, **2003**, *185*, 564-572.

104. Dittmann, E.; Neilan, B.A.; Erhard, M.; Von Döhren, H. & Börner, T. *Mol. Microbiol.*, **1997**, *26*, 779-787.

105. Moore, R.E.; Chen, J.L.; Moore, B.S.; Patterson, G.M.L. & Carmichael, W.W. *J. Am. Chem. Soc.*, **1991**, *113*, 5083-5084.

106. Arment, A.R. & Carmichael, W.W. *J. Phycol.*, **1996**, *32*, 591-597.

107. Sielaff, H.; Dittmann, E.; De Marsac, N.T.; Bouchier, C.; von Döhren, H.; Börner, T. & Schwecke, T. *Biochem. J.*, **2003**, *373*.

108. Hartrampf, G. & Buckel, W. *FEBS Lett.*, **1984**, *171*, 73.

109. Pearson, L.A.; Hisbergues, M.; Borner, T.; Dittmann, E. & Neilan, B.A. *Appl. Environ. Microbiol.*, **2004**, *70*, 6370-6378.

110. Börner, T. & Dittmann, E. Molecular biology of cyanobacterial toxins. In *Harmful Cyanobacteria*, Huisman, J.; Matthijs, H.C.P. & Visser, P.M., Eds. Springer: Dordrecht, **2005**, pp 25-40.

111. Park, H.; Namikoshi, M.; Brittain, S.M.; Carmichael, W.W. & Murphy, T. *Toxicon*, **2001**, *39*, 855-862.

112. Fujii, K.; Sivonen, K.; Nakano, T. & Harada, K.-I. *Tetrahedron*, **2002**, *58*, 6863-6871.

113. Kaya, K. & Sano, T. *Chem. Res. Toxicol.*, **1998**, *11*, 159-163.

114. Mikalsen, B.; Boison, G.; Skulberg, O.M.; Fastner, J.; Davies, W.; Gabrielsen, T.M.; Rudi, K. & Jakobsen, K.S. *J. Bacteriol.*, **2003**, *185*, 2774-2785.

115. Krishnamurthy, T.; Carmichael, W.W. & Sarver, E.W. *Toxicon*, **1986**, *24*, 865-873.

116. Xing, Y.; Xu, Y.; Chen, Y.; Jeffrey, P.D.; Chao, Y.; Lin, Z.; Li, Z.; Strack, S.; Stock, J.B. & Shi, Y. *Cell*, **2006**, *127*, 341-353.

117. MacKintosh, R.W.; Dalby, K.N.; Campbell, D.G.; Cohen, P.T.W.; Cohen, P. & MacKintosh, C. *FEBS Lett.*, **1995**, *371*, 236-240.

118. Horn, M.J.; Jones, D.B. & Ringel, S.J. *J. Biol. Chem.*, **1941**, *138*, 141-149.

119. Painuly, P.; Perez, R.; Fukai, T. & Shimizu, Y. *Tetrahedron Lett.*, **1988**, *29*, 11-14.

120. Watanabe, M.F.; Oishi, S.; Harada, K.-I.; Matsuura, K.; Kawai, H. & Suzuki, M. *Toxicon*, **1988**, *26*, 1017-1025.

121. Harada, K.-I.; Matsuura, K.; Suzuki, M.; Watanabe, M.F.; Oishi, S.; Dahlem, A.M.; Beasley, V.R. & Carmichael, W.W. *Toxicon*, **1990**, *28*, 55-64.

122. Jang, M.-H.; Ha, K.; Joo, G.-J. & Takamura, N. *Freshwater Biol.*, **2003**, *48*, 1540-1550.

123. Jang, M.-H.; Ha, K.; Lucas, M.C.; Joo, G.-J. & Takamura, N. *Aquat. Toxicol.*, **2004**, *68*, 51-59.

124. Rantala, A.; Fewer, D.P.; Hisbergues, M.; Rouhiainen, L.; Vaitomaa, J.; Börner, T. & Sivonen, K. *Proc. Natl. Acad. Sci. USA*, **2004**, *101*, 568-573.

125. Rohrlack, T. & Utkilen, H. *Hydrobiologia*, **2007**, *583*, 231-240.

126. Repka, S.; Koivula, M.; Harjunpa, V.; Rouhiainen, L. & Sivonen, K. *Appl. Environ. Microbiol.*, **2004**, *70*, 4551-4560.

127. Tonk, L.; Welker, M.; Huisman, J. & Visser, P.M. *Harmful Algae*, **2009**, *8*, 219-224.

128. Babica, P.; Bláha, L. & Marsálek, B. *J. Phycol.*, **2006**, *42*, 9-20.

129. Orr, P.T. & Jones, G.J. *Limnol. Oceanogr.*, **1998**, *43*, 1604-1614.

130. Rapala, J. & Sivonen, K. *Microb. Ecol.*, **1998**, *36*, 181-192.

131. Codd, G.A. & Poon, G.K. Cyanobacterial toxins. In *Proceedings of the Phytochemical Society of Europe*, Gallon, J.G. & Rogers, L.J., Eds. Oxford University Press: Oxford, **1988**, Vol. 23, pp 283-296.

132. van der Westhuizen, A.J. & Eloff, J.N. *Planta*, **1985**, *163*, 55-59.

133. van der Westhuizen, A.J.; Eloff, J.N. & Krüger, G.H.J. *Arch. Hydrobiol.*, **1986**, *108*, 145-154.

134. Watanabe, M.F. & Oishi, S. *Appl. Environ. Microbiol.*, **1985**, *49*, 1342-1344.

135. Amé, M. & Wunderlin, D. *Water, Air, Soil Pollut.*, **2005**, *168*, 235-248.

136. Sivonen, K. *Appl. Environ. Microbiol.*, **1990**, *56*, 2658-2666.

137. Rapala, J.; Sivonen, K.; Lyra, C. & Niemelä, S.I. *Appl. Environ. Microbiol.*, **1997**, *63*, 2206-12.

138. Utkilen, H. & Gjølme, N. *Appl. Environ. Microbiol.*, **1992**, *58*, 1321-1325.

139. Utkilen, H. & Gjølme, N. *Appl. Environ. Microbiol.*, **1995**, *61*, 797-800.

140. Lukac, M. & Aegerter, R. *Toxicon*, **1993**, *31*, 293-305.

141. Lyck, S.; Gjølme, N. & Utkilen, H. *Phycologia*, **1996**, *35*, 120-124.

142. Hesse, K.; Dittmann, E. & Börner, T. *FEMS Microbiol. Ecol.*, **2001**, *37*, 39-43.

143. Lyck, S. *J. Plankton Res.*, **2004**, *26*, 727-736.

144. Long, B.M.; Jones, G.J. & Orr, P.T. *Appl. Environ. Microbiol.*, **2001**, *67*, 278-283.

145. Shi, L.; Carmichael, W.W. & Miller, I. *Arch. Microbiol.*, **1995**, *163*, 7-15.

146. Kameyama, K.; Sugiura, N.; Inamori, Y. & Maekawa, T. *Environ. Toxicol.*, **2004**, *19*, 20-25.

147. Kaya, K. & Watanabe, M.M. *J. Appl. Phycol.*, **1990**, *2*, 173-178.

148. Tonk, L.; Visser, P.M.; Christiansen, G.; Dittmann, E.; Snelder, E.O.F.M.; Wiedner, C.; Mur, L.R. & Huisman, J. *Appl. Environ. Microbiol.*, **2005**, *71*, 5177-5181.

149. Song, L.; Sano, T.; Li, R.; Watanabe, M.M.; Liu, Y. & Kaya, K. *Phycol. Res.*, **1998**, *46*, 19-23.

150. Tonk, L.; van de Waal, D.B.; Slot, P.; Huisman, J.; Matthijs, H.C. & Visser, P.M. *FEMS Microbiol. Ecol.*, **2008**, *65*, 383-390.

151. van de Waal, D.B.; Verspagen, J.M.H.; Lürling, M.; van Donk, E.; Visser, P.M. & Huisman, J. *Ecol. Lett.*, **2009**, *12*, 1326-1335.

152. World Health Organisation *Guidelines for drinking-water quality*. World Health Organisation: Geneva, **2008**.

153. Meriluoto, J.; Lawton, L.A. & Harada, K.-I. Isolation and detection of microcystins and nodularins, cyanobacterial peptide hepatotoxins. In *Bacterial toxins: Methods and protocols*, Holst, O., Ed. Humana Press: Totowa, **2000**, pp 65-87.

154. Metcalf, J.S. & Codd, G.A. The status and potential of cyanobacteria and their toxins as agents of bioterrorism. In *Handbook on cyanobacteria: Biochemistry, biotechnology and applications*, Gault, P.M. & Marler, H.J., Eds. Nova Science Publishers: New York, **2009**.

155. Msagati, T.A.M.; Siame, B.A. & Shushu, D.D. *Aquat. Toxicol.*, **2006**, *78*, 382-397.

156. Spoof, L. Microcystins and nodularins. In *TOXIC: Cyanobacterial monitoring and cyanotoxin analysis*, Meriluoto, J. & Codd, G.A., Eds. Åbo Akademi University Press: Turku, **2005**.

157. Mountfort, D.O.; Holland, P. & Sprosen, J. *Toxicon*, **2005**, *45*, 199-206.

158. Bialojan, C. & Takai, A. *Biochem. J.*, **1988**, *256*, 283-290.

159. Butler, J.E. *J. Immunoassay*, **2000**, *21*, 165-209.

160. Kfir, R.; Johannsen, E. & Botes, D.P. *Toxicon*, **1986**, *24*, 543-552.

161. Brooks, W.P. & Codd, G.A. *Br. Phycol. J.*, **1987**, *22*, 301.

162. Young, F.M.; Metcalf, J.S.; Meriluoto, J.A.O.; Spoof, L.; Morrison, L.F. & Codd, G.A. *Toxicon*, **2006**, *48*, 295-306.

163. Chu, F.S.; Huang, X.; Wei, R.D. & Carmichael, W.W. *Appl. Environ. Microbiol.*, **1989**, *55*, 1928-1933.

164. Fischer, W.J.; Garthwaite, I.; Miles, C.O.; Ross, K.M.; Aggen, J.B.; Chamberlin, A.R.; Towers, N.R. & Dietrich, D.R. *Environ. Sci. Technol.*, **2001**, *35*, 4849-4856.

165. Carmichael, W.W. & An, J. *Nat. Toxins*, **1999**, *7*, 377-385.

166. Meriluoto, J. *Anal. Chim. Acta*, **1997**, *352*, 277-298.

167. Lawton, L.A.; Edwards, C. & Codd, G.A. *Analyst*, **1994**, *119*, 1525-1530.

168. Purdie, E.L.; Young, F.M.; Menzel, D. & Codd, G.A. *Toxicon*, **2009**, *54*, 887-890.

169. Moollan, R.W.; Rae, B. & Verbeek, A. *Analyst*, **1996**, *121*, 233–238.

170. Ikawa, M.; Phillips, N.; Haney, J.F. & Sasner, J.J. *Toxicon*, **1999**, *37*, 923-929.

171. Li, C.-M.; Chu, R.Y.-Y. & Hsientang Hsieh, D.P. *J. Mass Spectrom.*, **2006**, *41*, 169-174.

172. Bruno, M.; Melchiorre, S.; Messineo, V.; Volpi, F.; Di Corcia, A.; Aragona, I.; Guglielmone, G.; Di Paolo, C.; M., C.; Ferranti, P. & Gallo, P. Microcystin detection in contaminated fish from Italian lakes using ELISA immunoassays and LC-MS/MS analysis. In *Handbook on cyanobacteria: Biochemistry, biotechnology and applications*, Gault, P.M. & Marler, H.J., Eds. Nova Science Publishers: New York, **2009**.

173. Neffling, M.-R.; Spoof, L. & Meriluoto, J. *Anal. Chim. Acta*, **2009**, *653*, 234-241.

174. Xu, W.; Chen, Q.; Zhang, T.; Cai, Z.; Jia, X.; Xie, Q. & Ren, Y. *Anal. Chim. Acta*, **2008**, *626*, 28-36.

175. Karas, M.; Bachmann, D.; Bahr, U. & Hillenkamp, F. *Int. J. Mass Spectrom. Ion Processes*, **1987**, *78*, 53-68.

176. Welker, M.; Fastner, J.; Erhard, M. & von Döhren, H. *Environ. Toxicol.*, **2002**, *17*, 367-374.

177. Duncan, M.W.; Roder, H. & Hunsucker, S.W. *Brief. Funct. Genomic. Proteomic.*, **2008**, *7*, 355-370.

178. Saker, M.L.; Fastner, J.; Dittmann, E.; Christiansen, G. & Vasconcelos, V.M. *J. Appl. Microbiol.*, **2005**, *99*, 749-757.

179. Neumann, U.; Campos, V.; Cantarero, S.; Urrutia, H.; Heinze, R.; Weckesser, J. & Erhard, M. *Syst. Appl. Microbiol.*, **2000**, *23*, 191-197.

180. Fastner, J.; Erhard, M. & von Döhren, H. *Appl. Environ. Microbiol.*, **2001**, *67*, 5069-5076.

181. Erhard, M.; von Döhren, H. & Jungblut, P.R. *Rapid Commun. Mass Spectrom.*, **1999**, *13*, 337-343.

182. Erhard, M.; von Döhren, H. & Jungblut, P.R. *Nat. Biotechnol.*, **1997**, *15*, 906-909.

183. Welker, M.; Marsálek, B.; Sejnohová, L. & von Döhren, H. *Peptides*, **2006**, *27*, 2090-2103.

184. Howard, K.L. & Boyer, G.L. *Anal. Chem.*, **2007**, *79*, 5980-5986.

185. Tholey, A. & Heinzle, E. *Anal. Bioanal. Chem.*, **2006**, *386*, 24-37.

186. Horneffer, V.; Forsmann, A.; Strupat, K.; Hillenkamp, F. & Kubitscheck, U. *Anal. Chem.*, **2001**, *73*, 1016-1022.

187. Kang, M.-J.; Tholey, A. & Heinzle, E. *Rapid Commun. Mass Spectrom.*, **2000**, *14*, 1972-1978.

188. Persike, M.; Zimmermann, M.; Klein, J. & Karas, M. *Anal. Chem.*, **2010**, *82*, 922-929.

189. Persike, M. & Karas, M. *Rapid Commun. Mass Spectrom.*, **2009**, *23*, 3555-3562.

190. Simm, R.; Morr, M.; Remminghorst, U.; Andersson, M. & Römling, U. *Anal. Biochem.*, **2009**, *386*, 53-58.

191. Amini, A. & Nilsson, E. *J. Pharm. Biomed. Anal.*, **2008**, *46*, 411-417.

192. Marczak, L.; Kachlicki, P.; Kozaniewski, P.; Skirycz, A.; Krajewski, P. & Stobiecki, M. *Rapid Commun. Mass Spectrom.*, **2008**, *22*, 3949-3956.

193. Wilkinson, W.; Gusev, A.; Proctor, A.; Houalla, M. & Hercules, D. *Fresenius J. Anal. Chem.*, **1997**, *357*, 241-248.

194. Bungert, D.; Heinzle, E. & Tholey, A. *Anal. Biochem.*, **2004**, *326*, 167-175.

195. Bucknall, M.; Fung, K.Y.C. & Duncan, M.W. *J. Am. Soc. Mass. Spectrom.*, **2002**, *13*, 1015-1027.

196. Ekman, R.; Silberring, J.; Westman-Brinkmalm, A.M. & Kraj, A. *Mass spectrometry: Instrumentation, interpretation, and applications*. John Wiley & Sons: Hoboken, **2009**.

197. Domon, B. & Aebersold, R. *Science*, **2006**, *312*, 212-217.

198. Aebersold, R. & Mann, M. *Nature*, **2003**, *422*, 198-207.

199. Kebarle, P. & Ho, Y. On the mechanism of electrospray mass spectrometry. In *Electrospray ionization mass spectrometry: Fundamentals instrumentation and applications*, Cole, R.B., Ed. John Wiley & Sons: New York, **1997**, pp 3-64.

200. Loo, J.A. & Ogorzalek-Loo, R.R. Electrospray ionization mass spectrometry of peptides and proteins. In *Electrospray ionization mass spectrometry: Fundamentals instrumentation and applications*, Cole, R.B., Ed. John Wiley & Sons: New York, **1997**, pp 385-420.

201. Marfey, P. *Carlsberg Res. Commun.*, **1984**, *49*, 591-596.

202. Harada, K.-I.; Fujii, K.; Mayumi, T.; Hibino, Y.; Suzuki, M.; Ikai, Y. & Oka, H. *Tetrahedron Lett.*, **1995**, *36*, 1515-1518.

203. Harada, K.-I.; Fujii, K.; Hayashi, K.; Suzuki, M.; Ikai, Y. & Oka, H. *Tetrahedron Lett.*, **1996**, *37*, 3001-3004.

204. Fujii, K.; Ikai, Y.; Mayumi, T.; Oka, H.; Suzuki, M. & Harada, K.-I. *Anal. Chem.*, **1997**, *69*, 3346-3352.

205. Fujii, K.; Ikai, Y.; Oka, H.; Suzuki, M. & Harada, K.-I. *Anal. Chem.*, **1997**, *69*, 5146-5151.

206. Silverstein, R.M.; Webster, F.X. & Kiemle, D.J. *Spectrometric identification of organic compounds*. 7 ed.; John Wiley and Sons: Hoboken, **2005**.

207. Jameson, C.J. & Mason, J. The parameters of NMR spectroscopy. In *Multinuclear NMR*, Mason, J., Ed. Plenum Press: New York, **1987**, pp 3-50.

208. Jameson, C.J. & Mason, J. The chemical shift. In *Multinuclear NMR*, Mason, J., Ed. Plenum Press: New York, **1987**, pp 51-88.

209. Jameson, C.J. Spin-spin coupling. In *Multinuclear NMR*, Mason, J., Ed. Plenum Press: New York, **1987**, pp 89-131.

210. Rouhiainen, L.; Jokela, J.; Fewer, D.P.; Urmann, M. & Sivonen, K. *Chem. Biol.*, **2010**, *17*, 265-273.

211. Murakami, M.; Shin, H.J.; Matsuda, H.; Ishida, K. & Yamaguchi, K. *Phytochemistry*, **1997**, *44*, 449-452.

212. Murakami, M.; Suzuki, S.; Itou, Y.; Kodani, S. & Ishida, K. *J. Nat. Prod.*, **2000**, *63*, 1280-1282.

213. Ferranti, P.; Nasi, A.; Bruno, M.; Basile, A.; Serpe, L. & Gallo, P. *Rapid Commun. Mass Spectrom.*, **2011**, *25*, 1173-1183.

214. Fujii, K.; Harada, K.-I.; Suzuki, M.; Kondo, F.; Ikai, Y.; Oka, H. & Sivonen, K. *Tennen Yuki Kagobutsu Toronkai Koen Yoshishu*, **1995**, *37*, 445-450.

215. Shin, H.J.; Matsuda, H.; Murakami, M. & Yamaguchi, K. *J. Nat. Prod.*, **1997**, *60*, 139-141.

216. Sano, T.; Usui, T.; Ueda, K.; Osada, H. & Kaya, K. *J. Nat. Prod.*, **2001**, *64*, 1052-1055.

217. Itou, Y.; Suzuki, S.; Ishida, K. & Murakami, M. *Bioorg. Med. Chem. Lett.*, **1999**, *9*, 1243-1246.

218. Kodani, S.; Suzuki, S.; Ishida, K. & Murakami, M. *FEMS Microbiol. Lett.*, **1999**, *178*, 343-348.

219. Gesner-Apter, S. & Carmeli, S. *J. Nat. Prod.*, **2009**, *72*, 1429-1436.

220. Beresovsky, D.; Hadas, O.; Livne, A.; Sukenik, A.; Kaplan, A. & Carmeli, S. *Isr. J. Chem.*, **2006**, *46*, 79-87.

221. Zafrir-Ilan, E. & Carmeli, S. *Tetrahedron*, **2010**, *66*, 9194-9202.

222. Grach-Pogrebinsky, O. & Carmeli, S. *Tetrahedron*, **2008**, *64*, 10233-10238.

223. Okumura, H.S.; Philmus, B.; Portmann, C. & Hemscheidt, T.K. *J. Nat. Prod.*, **2009**, *72*, 172-176.

224. Williams, D.E.; Craig, M.; Holmes, C.F.B. & Andersen, R.J. *J. Nat. Prod.*, **1996**, *59*, 570-575.

225. Fujii, K.; Sivonen, K.; Adachi, K.; Noguchi, K.; Sano, H.; Hirayama, K.; Suzuki, M. & Harada, K.-I. *Tetrahedron Lett.*, **1997**, *38*, 5525-5528.

226. Schumacher, M.; Wilson, N.; Tabudravu, J.N.; Edwards, C.; Lawton, L.A.; Motti, C.; Wright, A.D.; Diederich, M. & Jaspars, M. *Tetrahedron*, **2012**, *68*, 1622-1628.

227. Sano, T.; Srivastava, V.C. & Kaya, K. *Tennen Yuki Kagobutsu Toronkai Koen Yoshishu*, **1996**, *38*, 433-438.

228. Sano, T. & Kaya, K. *Tetrahedron Lett.*, **1995**, *36*, 5933-5936.

229. Reshef, V. & Carmeli, S. *J. Nat. Prod.*, **2002**, *65*, 1187-1189.

230. Matthew, S.; Ross, C.; Paul, V.J. & Luesch, H. *Tetrahedron*, **2008**, *64*, 4081-4089.

231. Robinson, S.J.; Tenney, K.; Yee, D.F.; Martinez, L.; Media, J.E.; Valeriote, F.A.; van Soest, R.W.M. & Crews, P. *J. Nat. Prod.*, **2007**, *70*, 1002-1009.

232. Uemoto, H.; Yahiro, Y.; Shigemori, H.; Tsuda, M.; Takao, T.; Shimonishi, Y. & Kobayashi, J. *Tetrahedron*, **1998**, *54*, 6719-6724.

233. Schmidt, E.W.; Harper, M.K. & Faulkner, D.J. *J. Nat. Prod.*, **1997**, *60*, 779-782.

234. Kobayashi, J.-I.; Sato, M.; Murayama, T.; Ishibashi, M.; Walchi, M.R.; Kanai, M.; Shoji, J. & Ohizumi, Y. *J. Chem. Soc., Chem. Commun.*, **1991**, 1050-1052.

235. Kobayashi, J.-I.; Sato, M.; Ishibashi, M.; Shigemori, H.; Nakamura, T. & Ohizumi, Y. *J. Chem. Soc., Perkin Trans. 1*, **1991**, 2609-2611.

236. Müller, D.; Krick, A.; Kehraus, S.; Mehner, C.; Hart, M.; Küpper, F.C.; Saxena, K.; Prinz, H.; Schwalbe, H.; Janning, P.; Waldmann, H. & König, G.M. *J. Med. Chem.*, **2006**, *49*, 4871-4878.

237. Schmidt, E.W.; Nelson, J.T.; Rasko, D.A.; Sudek, S.; Eisen, J.A.; Haygood, M.G.; Ravel, J. & Haselkorn, R. *Proc. Natl. Acad. Sci. USA*, **2005**, *102*, 7315-7320.

238. Ploutno, A. & Carmeli, S. *Tetrahedron*, **2002**, *58*, 9949-9957.

239. Ishida, K.; Matsuda, H.; Murakami, M. & Yamaguchi, K. *Tetrahedron*, **1997**, *53*, 10281-10288.

240. Okino, T.; Murakami, M.; Haraguchi, R.; Munekata, H.; Matsuda, H. & Yamaguchi, K. *Tetrahedron Lett.*, **1993**, *34*, 8131-8134.

241. Fujii, K.; Nishizawa, T.; Asayama, M.; Sivonen, K.; Shirai, M. & Harada, K.-I. *Symposium on the Chemistry of Natural Products*, **2000**, *42*, 265-270.

242. Papayannopoulos, I.A. *Mass Spectrom. Rev.*, **1995**, *14*, 49-73.

243. Stults, J.T. & Watson, J.T. *Biol. Mass Spectrom.*, **1987**, *14*, 583-586.

244. Dawson, R.M. *Toxicon*, **1998**, *36*, 953-962.

245. Fewer, D.; Rouhiainen, L.; Jokela, J.; Wahlsten, M.; Laakso, K.; Wang, H. & Sivonen, K. *BMC Evol. Biol.*, **2007**, *7*, 183.

246. Rueckert, A.; Wood, S.A. & Cary, S.C. *Limnol. Oceanogr. Methods*, **2007**, *5*, 474-483.

247. Fujii, K.; Sivonen, K.; Naganawa, E. & Harada, K.-I. *Tetrahedron*, **2000**, *56*, 725-733.

248. Miles, C.O.; Sandvik, M.; Haande, S.; Nonga, H. & Ballot, A. Submitted to *Environmental Science and Technology* on 19 Dec 2012, **2012**.

249. Gathercole, P.S. & Thiel, P.G. *J. Chromatogr. A*, **1987**, *408*, 435-440.

250. Kruger, T.; Christian, B. & Luckas, B. *Toxicon*, **2009**, *54*, 302-312.

251. Ooi, T.; Kusumi, T.; Kakisawa, H. & Watanabe, M. *J. Appl. Phycol.*, **1989**, *1*, 31-38.

252. Gademann, K.; Portmann, C.; Blom, J.F.; Zeder, M. & Jüttner, F. *J. Nat. Prod.*, **2010**, *73*, 980-984.

253. Hopkins, F.G. & Cole, S.W. *J. Physiol.*, **1903**, *29*, 451-466.

254. Kotake, Y. & Iwao, J. *Z. Physiol. Chem.*, **1931**, *195*, 139-145.

255. Schwarcz, R. *Curr. Opin. Pharmacol.*, **2004**, *4*, 12-17.

256. Taylor, S.W.; Fahy, E.; Murray, J.; Capaldi, R.A. & Ghosh, S.S. *J. Biol. Chem.*, **2003**, *278*, 19587-19590.

257. Simat, T.J. & Steinhart, H. *J. Agric. Food. Chem.*, **1998**, *46*, 490-498.

258. Finley, E.L.; Dillon, J.; Crouch, R.K. & Schey, K.L. *Protein Sci.*, **1998**, *7*, 2391-2397.

259. Bienvenut, W.V.; Déon, C.; Pasquarello, C.; Campbell, J.M.; Sanchez, J.-C.; Vestal, M.L. & Hochstrasser, D.F. *Proteomics*, **2002**, *2*, 868-876.

260. Lushchak, V. *Biochemistry (Moscow)*, **2007**, *72*, 809-827.

261. Berlett, B.S. & Stadtman, E.R. *J. Biol. Chem.*, **1997**, *272*, 20313-20316.

262. Kuroda, M.; Sakiyama, F. & Narita, K. *J. Biochem.*, **1975**, *78*, 641-651.

263. Stadtman, E.R.; Moskovitz, J. & Levine, R.L. *Antioxidants & Redox Signaling*, **2003**, *5*, 577-582.

264. Levine, R.L.; Moskovitz, J. & Stadtman, E.R. *IUBMB Life*, **2000**, *50*, 301-307.

265. Hummert, C.; Dahlmann, J.; Reinhardt, K.; Dang, H.; Dang, D. & Luckas, B. *Chromatographia*, **2001**, *54*, 569-575.

266. Itakura, K.; Uchida, K. & Kawakishi, S. *Tetrahedron Lett.*, **1992**, *33*, 2567-2570.

267. Quintanilla-Licea, R.; Colunga-Valladares, J.; Caballero-Quintero, A.; Rodríguez-Padilla, C.; Tamez-Guerra, R.; Gómez-Flores, R. & Waksman, N. *Molecules*, **2002**, *7*, 662-673.

268. Doran, P.T.; McKay, C.P.; Clow, G.D.; Dana, G.L.; Fountain, A.G.; Nylen, T. & Lyons, W.B. *J. Geophys. Res.*, **2002**, *107*, 4772.

269. Claridge, G.G.C. & Campbell, I.B. *Soil Sci.*, **1977**, *123*, 377-384.

270. Cowan, D.; Russell, N.; Mamais, A. & Sheppard, D. *Extremophiles*, **2002**, *6*, 431-436.

271. Wynn-Williams, D.D. *Adv. Microb. Ecol.*, **1990**, *11*, 71-146.

272. Vishniac, H.S. The microbiology of Antarctic soils. In *Antarctic microbiology*, Friedmann, I.E., Ed. Wiley-Liss: New York, **1993**, pp 297-341.

273. Taton, A.; Grubisic, S.; Balthasart, P.; Hodgson, D.A.; Laybourn-Parry, J. & Wilmotte, A. *FEMS Microbiol. Ecol.*, **2006**, *57*, 272-289.

274. Cavacini, P. *Polar Biosci.*, **2001**, *14*, 45-60.

275. Fumanti, B.; Cavacini, P. & Alfinito, S. *Polar Biol.*, **1996**, *17*, 25-30.

276. Hitzfeld, B.C.; Lampert, C.S.; Spaeth, N.; Mountfort, D.; Kaspar, H. & Dietrich, D.R. *Toxicon*, **2000**, *38*, 1731-1748.

277. Jungblut, A.-D.; Hawes, I.; Mountfort, D.; Hitzfeld, B.; Dietrich, D.R.; Burns, B.P. & Neilan, B., A. *Environ. Microbiol.*, **2005**, *7*, 519-529.

278. Jungblut, A.-D.; Hoeger, S.J.; Mountfort, D.; Hitzfeld, B.C.; Dietrich, D.R. & Neilan, B.A. *Toxicon*, **2006**, *47*, 271-278.

279. Wood, S.A.; Mountfort, D.; Selwood, A.I.; Holland, P.T.; Puddick, J. & Cary, S.C. *Appl. Environ. Microbiol.*, **2008**, *74*, 7243-7251.

280. Oksanen, I.; Jokela, J.; Fewer, D.P.; Wahlsten, M.; Rikkinen, J. & Sivonen, K. *Appl. Environ. Microbiol.*, **2004**, *70*, 5756-5763.

281. Yuan, M.; Namikoshi, M.; Otsuki, A. & Sivonen, K. *Eur. J. Mass Spectrom.*, **1998**, *4*, 287-298.

282. Yuan, M.; Namikoshi, M.; Otsuki, A.; Rinehart, K.L.; Sivonen, K. & Watanabe, M.F. *J. Mass Spectrom.*, **1999**, *34*, 33-43.

283. Knochenmuss, R.; Stortelder, A.; Breuker, K. & Zenobi, R. *J. Mass Spectrom.*, **2000**, *35*, 1237-1245.

284. Mayumi, T.; Kato, H.; Kawasaki, Y. & Harada, K.-I. *Rapid Commun. Mass Spectrom.*, **2007**, *21*, 1025-1033.

285. Ambihapathy, K.; Yalcin, T.; Leung, H.-W. & Harrison, A.G. *J. Mass Spectrom.*, **1997**, *32*, 209-215.

286. Raith, K.; Neubert, R.; Poeaknapo, C.; Boettcher, C.; Zenk, M.H. & Schmidt, J. *J. Am. Soc. Mass. Spectrom.*, **2003**, *14*, 1262-1269.

287. Challis, G.L.; Ravel, J. & Townsend, C.A. *Chem. Biol.*, **2000**, *7*, 211-224.

288. Rouhiainen, L.; Paulin, L.; Suomalainen, S.; Hyytiäinen, H.; Buikema, W.; Haselkorn, R. & Sivonen, K. *Mol. Microbiol.*, **2000**, *37*, 156-167.

289. Schuerenberg, M.; Luebbert, C.; Eickhoff, H.; Kalkum, M.; Lehrach, H. & Nordhoff, E. *Anal. Chem.*, **2000**, *72*, 3436-3442.

290. Vorm, O.; Roepstorff, P. & Mann, M. *Anal. Chem.*, **1994**, *66*, 3281-3287.

291. Cañas, B.; Piñeiro, C.; Calvo, E.; López-Ferrer, D. & Gallardo, J.M. *J. Chromatogr. A*, **2007**, *1153*, 235-258.

292. Neilan, B.A.; Pearson, L.A.; Muenchhoff, J.; Moffitt, M.C. & Dittmann, E. *Environ. Microbiol.*, **2012**, DOI: 10.1111/j.1462-2920.2012.02729.x.

293. Sanmartín, P.; Aira, N.; Devesa-Rey, R.; Silva, B. & Prieto, B. *Biofouling*, **2010**, *26*, 499-509.

294. Collier, J.L. & Grossman, A.R. *J. Bacteriol.*, **1992**, *174*, 4718-4726.

295. Berner, T. *Ultrastructure of microalgae*. CRC Press: Boca Raton, U.S.A, **1993**.

296. Bolch, C. & Blackburn, S. *J. Appl. Phycol.*, **1996**, *8*, 5-13.

297. Howard, K.L. & Boyer, G.L. *Rapid Commun. Mass Spectrom.*, **2007**, *21*, 699-706.

298. Nelson, R.W.; McLean, M.A. & Hutchens, T.W. *Anal. Chem.*, **1994**, *66*, 1408-1415.

299. Utermöhl, H. *Mitteilungen der Internationale Vereinigung für Theoretische und Angewandte Limnologie*, **1958**, *9*, 1-38.

300. van der Westhuizen, A.J. & Eloff, J.N. *Zeit. Planzenphysiol.*, **1983**, *110*, 157-163.

301. Wood, S.A.; Dietrich, D.R.; Cary, S.C. & Hamilton, D.P. *Inland Waters*, **2012**, *2*, 17-22.

302. Sivonen, K.; Namikoshi, M.; Evans, W.R.; Carmichael, W.W.; Sun, F.; Rouhiainen, L.; Luukkainen, R. & Rinehart, K.L. *Appl. Environ. Microbiol.*, **1992**, *58*, 2495-2500.

303. Dai, R.; Liu, H.; Qu, J.; Zhao, X. & Hou, Y. *J. Hazard. Mater.*, **2009**, *161*, 730-736.

304. Li, H.; Murphy, T.; Guo, J.; Parr, T. & Nalewajko, C. *Limnologica - Ecology and Management of Inland Waters*, **2009**, *39*, 255-259.

305. Welker, M.; Christiansen, G. & von Döhren, H. *Arch. Microbiol.*, **2004**, *182*, 288-298.